Universitat Autònoma de Barcelona

# Exploring the regulatory mechanisms of the S. cerevisiae Ppz1 protein phosphatase and the molecular basis for its toxicity

**Diego Velázquez Sánchez**

**DOCTORAL THESIS**

# Exploring the regulatory mechanisms of the *S. cerevisiae* Ppz1 protein phosphatase and the molecular basis for its toxicity.

**Diego Velázquez Sánchez**

**September 2019**

**Departament de Bioquímica i Biologia Molecular**

**Institut de Biotecnologia I Biomedicina**


# Exploring the regulatory mechanisms of the *S. cerevisiae* Ppz1 protein phosphatase and the molecular basis for its toxicity.


Doctoral thesis presented by

**DIEGO VELÁZQUEZ SÁNCHEZ**

Graduated in Biochemistry


For the degree of PhD in Biochemistry, Molecular Biology and Biomedicine from the Universitat Autònoma de Barcelona


Thesis performed at the Departament de Bioquímica i Biología Molecular and the Institut de Biotecnología i Biomedicina of the Universitat Autònoma de Barcelona

Thesis supervised by **Dr. Joaquín Ariño Carmona**

**Diego Velázquez Sánchez** **Dr. Joaquín Ariño Carmona**


Cerdanyola del Vallès, September 2019

*"Cada mentira que contamos es una deuda con la verdad. Más tarde o más temprano hay que pagarla. Así es como explota el núcleo de un reactor RBMK: por las mentiras"*

*Dr. Valery Legasov*

*Chernobyl HBO Temporada 1; Episodio 5*

# AGRADECIMIENTOS

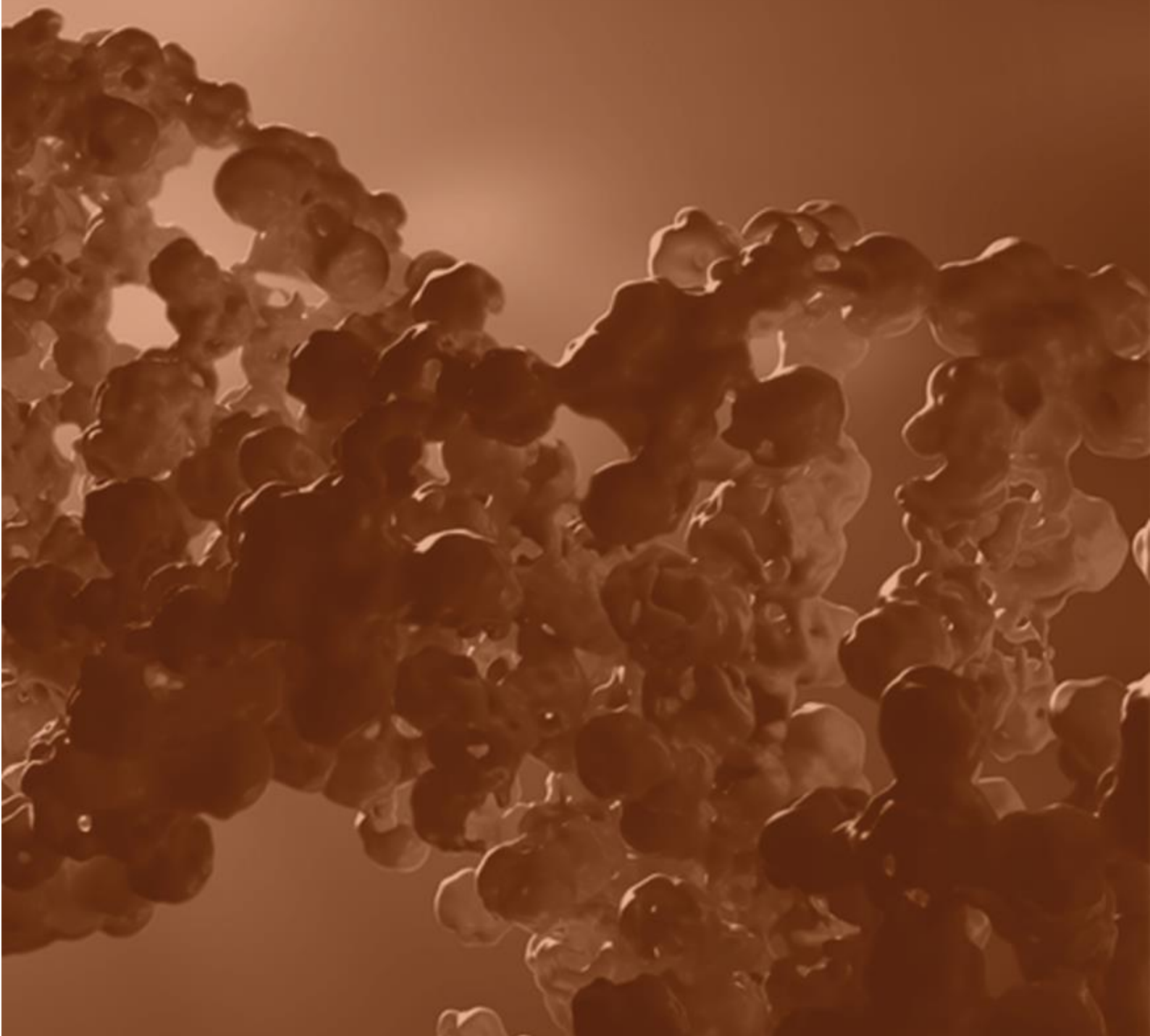

Posiblemente esta sea la parte más fácil de escribir por lo que al idioma respecta, pero quizás sea complicado resumir sin olvidar a nada ni a nadie, que directa o indirectamente me ha ayudado a conseguir escribir esta tesis. Hace algo menos de 5 años que estoy en este laboratorio trabajando con levaduras, pero esta historia para mí empieza un poco antes, concretamente en 2009. Cuando un Diego joven y algo inmaduro, dejó Calatayud ("el pueblo") y vino hasta Barcelona para estudiar bioquímica; con el corazón en la mano y citando la canción de José Antonio Labordeta que más hace que se me salten las lágrimas: "Albada"; diciendo *"Adiós a los que se quedan y a los que se van también"*.

En esta parte voy a utilizar una palabra del castellano que me encanta, y es GRACIAS, tengo muchas gracias que dar y repartir.

Para empezar, quiero darle las gracias al Dr. Joaquín Ariño, quien me ha dado posiblemente una de las mejores noticias que hasta ahora he recibido, que es la posibilidad de hacer un doctorado. Recuerdo perfectamente el día, y el lugar donde estaba (eran las 3 de la tarde aproximadamente del 18 de Junio de 2014, estaba tomándome una cerveza en el césped de la Villa) cuando recibí un mail en el que me indicaba si podía acercarme a comentar un asunto. Allí me dijo que me daba la oportunidad de hacer el doctorado en su grupo. La alegría fue inmensa y lo primero que hice tras darle las gracias y salir del IBB fue llamar a mi madre corriendo. Mil gracias Joaquín por esa oportunidad, por la dirección, el trabajo y el tiempo que has dedicado a esta tesis. Gracias por la paciencia que has tenido conmigo, en especial en las correcciones de este trabajo, gracias por escucharme y apoyarme. He aprendido muchas cosas de ti, pero especialmente la rigurosidad y la perseverancia en la ciencia, hechos que hacen que uno pueda estar orgulloso de su trabajo. Espero haber aprovechado la oportunidad y haber estado a la altura.

También quiero agradecer enormemente al Dr. Antonio Casamayor quien, con sus risas, sus chistes, sus bromas y sus charlas de ciencia, ha contribuido a que mis días en el laboratorio fueran mucho mejor, y de quien he aprendido un montón de cosas. Gracias por echarme una mano con el *review*, y por escucharme en los momentos más pesimistas en la escritura de la tesis.

Por descontado, si hay un grupo de personas a las que les debo muchísimo más que mucho, es a ese maravilloso equipo humano que forman o han formado parte del grupo de "Llevats".

Me gustaría empezar con los que ya no están.En primer lugar gracias al Dr. David Canadell, gracias por perder tiempo cuando más agobiado estabas para enseñarme más que algún truquillo para trabajar con las levaduras. También gracias por acompañarme en las risas, en la búsqueda de "chocobombs" y por tu "perret". También quiero agradecer al Dr. Albert Serra, quien desde un primer momento confío en mis posibilidades haciendo el doctorado, y quien me ha animado en muchas ocasiones. Muchísimas gracias también a la Dra. Laura Tatjer, de quien he heredado ese título de "gossip", y quien desde los primero días hemos hecho muy buenas migas y, a quien sigo

considerando una muy buena amiga. Gracias por apoyarme desde los primeros y temblorosos pasos en el laboratorio, hasta los últimos ánimos en la escritura desde la distancia. Recuerdo que perdiste muchísimos ratos conmigo enseñándome a hacer y cargar geles, yo no paraba de darte las gracias y me dijiste: “no te preocupes, esto es parte de nuestro trabajo, es muy importante enseñar lo que hacemos y como lo hacemos”. Esta frase me ha calado hondo, y como tú; he considerado muy importante enseñar a la gente que ha pasado por el laboratorio y he tenido a mi cargo. Gracias también por esas cervezas en Odense, gracias por venir a verme y por tu cariño.

Una de las personas que ya no está en el grupo, pero con la que más buenos momentos y alguno que otro malo he pasado, es la Dra. María López Malo, pero para mí siempre serás Merrypú. Sé que si te tengo que dar gracias por todo no acabo, pero sí que quiero decirte que eres un ejemplo como científica, y por ello soy un afortunado por haber podido trabajar contigo. Espero llegar algún día a ser la mitad de buen científico que tú. Pero si como científica eres increíble, lo superas con creces como ser humano. En serio Merry, gracias; gracias por todo; esto sin ti no habría sido posible. Una de las cosas que más quiero hacer cuando acabe esta etapa, es tomarme una paella contigo y con unas cervezas de por medio. Por supuesto que esa paella nos la haga Guillem, a quien también quiero agradecer el haberme abierto la puerta de su casa desde el principio, y de quien su humildad, sus “jajas” y su buen hacer me han aportado muchísimo. Espero que nos veamos pronto, y nos pongas unos guisantes en la paella.

Ahora me toca agradecer con quien más tiempo he compartido, con los que heredaran algunas cosas que he empezado, y los que más me han sufrido.

Muchas gracias a Carlos, por esas charlas sobre ciencia, por esos momentos compartidos y sobre todo por esos “puñitos”. Ha sido un placer conocerte y haber pasado juntos por esta aventura de la tesis doctoral, te deseo lo mejor en tu escritura y en lo que sigue. Muchas gracias a Ana-Chunyi, espero no haberte asustado mucho con mi forma de ser y no haberte enseñado demasiadas palabras malsonantes. Eres una persona alucinante, doy muchas gracias por haberte conocido, por qué te hayas apuntado siempre a un bombardeo con nosotros; pero le pido a la vida que en algún momento nos podamos volver a ver, quien sabe si en vez de en España es en China.

Incontables gracias a Marcel, nos conocemos desde el principio de esta aventura en 2009 y luego hemos tenido la suerte de compartir laboratorio. Muchas gracias por apoyarme y por valorarme como nadie, siempre a tu manera, con pocas palabras, con más gestos, pero siempre tú; haz lo que te de la real gana, pero no cambies. Gracias por esa súper ayuda desinteresada con el inglés y por “perder el culo” con cada cosa que te he pedido. Te deseo lo mejor con la tesis, pero por favor acaba a ese hijo que he dejado a medio crecer en el laboratorio que es el FRET.

Santo, si tengo que resumir todo lo que hemos pasado juntos durante esta aventura no podría escribirlo en menos de 50 páginas. Me has aguantado en el labo, dirigiéndote la tesina, enseñándote todo lo que sé del trabajo en el laboratorio y además me has tenido cada día en casa dándote la brasa. Gracias por aguantarme, gracias por

soportar mi mal humor, gracias ayudarme, por tomarte una cerveza cuando más lo he necesitado, gracias por venir a verme a Dinamarca, gracias por tu forma de ser, gracias por absolutamente todas las comas que he escrito en esta tesis, pero sobre todo gracias por tu amistad. Te he enseñado lo mejor que he sabido, y no sólo te deseo lo mejor, sé de sobras que te lo mereces. Sólo sé un poco más organizado pero no pierdas jamás esa pasión silenciosa que tú tienes. A pesar de ser tan diferentes, creo que hemos congeniado muy bien. Gracias de nuevo hijo, jamás me cansaré de repetírtelo. Gracias también a Monche Chimonche (Montse), por tus diez mil cuatrocientas treinta y cuatro placas, por tus cuarenta y cinco mil litros de medios, por tus enseñanzas, tu apoyo, tu ayuda y tu cariño, y por hacer que nunca tirase la toalla. También quiero agradecer a esos chicos y chicas que he tenido de prácticas/Máster: Bernat, Luís, Natalia, Elisa y otros tantos que han pasado por el Laboratorio.

Gracias a Lourdes por tu ayuda con los contratos, documentos, envíos a Dinamarca, y por sonreír siempre. Gracias al "Servei" a Anna y a Roger, por las secuencias, y por el buen trato.

Gracias al Dr. Miguel Ángel Peñalva, quien tanto me ha enseñado sobre el maravilloso mundo de la microscopía. Gracias por adoptarme esas dos semanas en Madrid.

I want to extend my heartfelt gratitude to my supervisor in Odense, Dr. Ole Norregard Jensen. Thanks for your time, your teachings about proteomics, and your smile. One part of this thesis would have been impossible without your help. Thanks too to all people of PD group in SDU. Thanks so much to my dear friend Efthy, for being incredible and to do my stay in Denmark much better. Gracias a Vale y a Gra, dos chicas italianas que me ayudaron muchísimo a que Odense no fuese tan aburrido.

Muchas gracias a toda esa gente del IBB que han hecho que estos casi 5 años aquí hayan sido inolvidables. Gracias a esos organizadores de la Fondue 2017, Sergi, Laura y Carlos. Extiendo mi agradecimiento a todo "molekitos", quienes siempre han estado ahí para tomarse un café conmigo y charlar, a Marina, a Lucía, a Carlos y a Sergi, y a la molekito adoptiva Jara, quien también me ha escuchado alguna vez que otra cuando he necesitado desahogarme con la escritura. Gracias también por esas partidas de padel que tanto me han ayudado a evadirme. Y a ti Sergi, por tu ejemplo y tu ayuda con el inglés desde la distancia, no cambies por favor.

Gracias a esa sonrisa del IBB, que es Araís. Gracias también a Manu, a Marcos, a Paolo, a Mireia, a Montpeyó... Y Gracias a todos esas personas que me saludáis y charláis conmigo cada día.

Mil gracias "Mitos" y "Chucki" por esos Wimpis, por esos vermuts, por vuestra compañía y vuestro cariño. Espero que Sabadell haya sido un poco más entretenido para vosotros gracias a mis ganas de sacaros de casa. Prometo un buen vermuteo pronto.

Gracias a esa gente del máster increíble, al Capitán Hadock, a Martus, a Aída y a Tere. Gracias por vuestro tiempo vuestro apoyo y vuestro cariño. A ti Tere, mil gracias

por esas llamadas, por venir a verme y por valorarme tantísimo. A todos vosotros os deseo todo lo mejor, y a Tere le mando un apoyo extra, para que acabe de escribir la tesis.

Muchas gracias a la gente de la Vila, con quien he madurado, crecido, reído, pero sobre todo me lo he pasado genial. Gracias a Muchá y a Saioa, aunque la vida nos haya separado os guardo un cariño enorme. Gracias Jorge, un persona un pelín loquilla, pero que desde el día uno en Barcelona ha hecho que mi estancia fuera mejor, a Anna Mur, a Aine, a Dume, a Setillas, a Guille y a otros tantos. Gracias a esa gente de Tortosa, que hace demasiado que no veo, a Carlos, a Pepis, a Fran… Gracias Otero, por todo lo anterior, y por hacer que vuelva a tener ganas de competir, haber ganado la liga de pádel contigo me ha ayudado muchísimo y ha permitido que te conozca mejor. Gracias a Antonio, por compartir 3 años de vivencias en casa, por las "chervechas" y por las cenas desestresantes. Gracias a Calitos, mi barman favorito. A Lorenzo, por sus arrocitos, y sus cenas en casa.

Gracias a Jordi, por pasar tantos buenos ratos conmigo, por aguantarme en momentos no tan buenos, y por regalarme su amistad desde el primer día que nos escuchó en clase jugando a los "barquitos". Es una suerte contar contigo. El día que seas algo más organizado y no vayas a última hora, serás imparable.

Gracias a Milito y a Calros, juntos hemos formado una unidad envidiable, os debo mucho, vosotros lo sabéis. Milito fue un honor dedicarte aquellas palabras en tu boda, sigo pensando lo mismo. Calros, gracias por enseñarme a usar la lógica como tú la usas. Os aprecio un montón.

Por supuestísimo que muchísimas gracias a Fullería, a mis amigos de toda la vida, con quienes deseo celebrar San Roque este año con más ganas si cabe. Gracias por aguantar todas mis "chapas" sobre ciencia, que aunque no tuvierais ni idea, me poníais buena cara. Gracias a Visan por venir a verme a Dinamarca y por incitarme a la maldad. A Sierra, quien aparte de venir a verme a 2K Km de casa, siempre me ha aguantado por teléfono soportando las ganas de fiesta. A Monreal, amigos de toda la vida, a quien veo menos de lo que me gustaría. A Nacho por abrirme las puertas de su casa en Madrid durante dos semanas que trabajé allí. A Josseff, por llevarme de cañas por Madrid, a quien le deseo una buena tesis. A Sada, amigo desde crío, que siempre le ha parecido muy raro lo que hacía, y me ha echado una mano con la informática. A Miguel por esas cervecitas en el Wimpi en esta última etapa de la tesis. A Pablito por todo el apoyo legal de Clavogado. A Moji, un tío muy especial al que le deseo que se nos centre un poco más pero que tiene un corazón enorme el canalla. Y a Gonzalo, que aparte de ser un McFreelance alucinante, me ha ayudado un montón; tanto, que la portada de esta tesis lleva el sello de la ardilla. Me joroba un montón haberme perdido momentos con vosotros, pero espero que nos queden muchos que vivir. Sois la leche. Os quiero hijos

Creo que la parte final de esta tesis la he llevado mejor gracias a haber recuperado un *hobby* hace tiempo olvidado, y que he retomado con más pasión que nunca: la lectura. Esto ha sido posible gracias a "Macondo". Diría que Macondo es una librería,

pero para mí es mucho más que eso, es una referencia cultural inigualable; es un sitio donde desde la primera vez que fui y me lleve *Mi planta de naranja lima*, me he sentido como en casa. Este pequeño rincón de Sabadell existe gracias a Tefi y Anna, dos mujeres, dos madres, dos compañeras y sobre todo tengo la suerte de poder decir dos amigas, increíbles. Gracias por escucharme, recomendarme libros, esas charlas cuando salía de escribir para cambiar el mundo, que tanto me han ayudado. Gracias por esa pasión que ponéis en todo y gracias por este granito de arena que habéis aportado a mi tesis. Gracias de corazón. Os deseo lo mejor de lo mejor y que yo pueda verlo durante mucho tiempo.

Quiero agradecer también a mi Padre, por echarme una mano en algunos momentos complicados durante el desarrollo de la tesis. Espero que esto sirva en el futuro para estar más unidos.

Para acabar, si hay personas a las que dar GRACIAS, de una forma infinita, es a tres mujeres increíbles, impresionantes. Ellas han confiado lo inimaginable en mí, os lo debo todo.

Pero si a alguna de ellas le debo todo esa es mi madre, Irene; que aparte de darme la vida, ha desarrollado un amor incondicional hacia mí que crece con los años. Fue muy duro separarme de ti con 18 años, se lo que nos echamos de menos, pero creo que con perspectiva ha sido positivo para mí haber salido de casa y venirme tan lejos a estudiar. Sabes lo nervioso que he pasado esta última etapa de la tesis, y has respetado ese espacio que necesitaba. Te quiero por encima de todas las cosas, espero no haberte defraudado. Cómo ya te he dicho en alguna ocasión esto no hubiera tenido sentido sin ti. Espero verte sonreír más, tanto en cantidad como en proximidad. No olvides jamás, que soy lo que soy gracias a ti.

Gracias a alguien que conocía de hace tiempo, pero que desde hace casi cuatro años ha tomado la decisión de acompañarme en esta aventura de vivir. Para ella soy mucho mejor de lo que realmente soy, pero quizás eso sea el amor. Patri, Du, bicho; gracias, por quererme sin esperar nada a cambio, gracias por aguantar mis berrinches, mis malas caras y mis cambios de humor. Decirte cosas que ya no te haya dicho es difícil, es increíble que estés tan orgullos de mí, eres la suerte de mi vida. Gracias por ser alguien en quien apoyarme de forma incondicional. Gracias por en contra de todo, volar hasta Dinamarca, sentarte a mi lado con una cerveza, mirarnos y contarnos como nos habían ido esas últimas semanas separados. Eres mucho más increíble de lo que piensas. Te quiero

Y finalmente gracias al amor de mi vida, a mi hermana, a mi tata, a Andrea. Es espectacular como alguien a quien tanto echas de menos, que has sacrificado verla crecer, te idolatra, te apoya, te sigue y te venera sin pedir absolutamente nada. Eres de sobra la persona que más ilusión le hace todo esto. Quiero decirte que este trabajo no es ni mejor, ni peor que lo que tú haces cada día. Tú eres increíble, tú eres maravillosa, tú eres una mujer que llegarás donde tú quieras llegar. Eres la persona con más potencial que he conocido. Desde el día que naciste eres una parte irrompible de mí. Gracias por

todo esto. No pienso olvidar jamás tus llamadas de apoyo, tú serenidad y tú confianza. Espero algún día en estar a tú altura. Te quiero. Juntas habéis conseguido que ese Diego que tengo dentro no desista nunca.

A vosotras y a todos los demás aparte de haberos dado las gracias, os quiero pedir perdón, en especial por las ausencias. Este trabajo ha dedicado muchas horas y mucha pasión, y por ello no he estado a vuestro lado cuando lo habéis necesitado. Disculpas de todo corazón y gracias de nuevo.

# TABLE OF CONTENTS

# ABBREVIATIONS

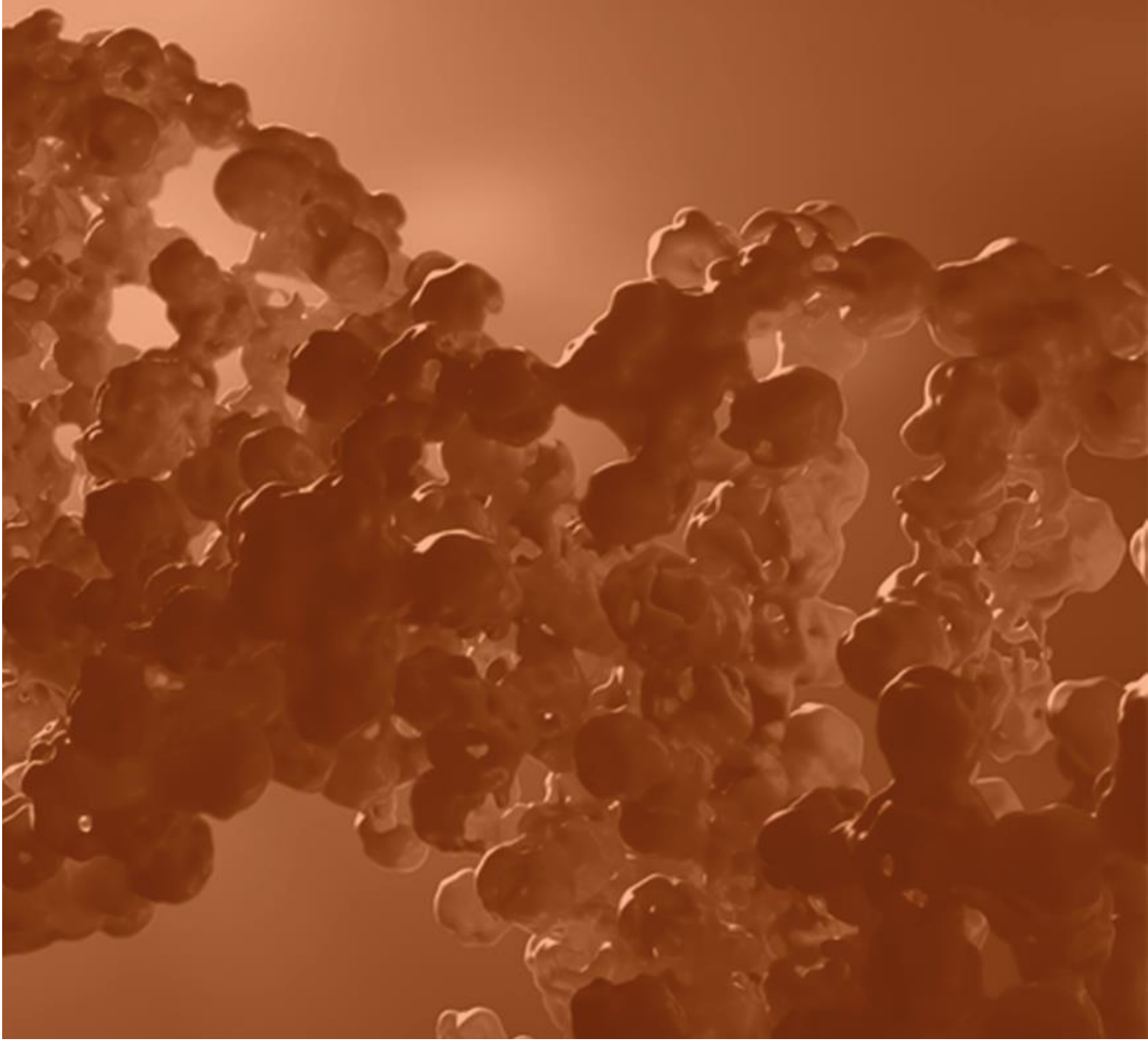

# Abbreviations

| | |
|---|---|
| **aa** | **a**mino **a**cids |
| **ACN** | **Ac**eto**n**itrile |
| **AICAR** | 5’-phosphoribosyl-5-**a**mino-4-**i**midazole **car**boxamide |
| **AMP** | **A**denosine **m**ono**p**hosphate |
| **AMPK** | **AMP**- activated protein **k**inase |
| **APS** | **A**denylyl **p**er**s**ulfate |
| **ATP** | **A**denosine **t**ri**p**hosphate |
| **BCA** | **Bic**inchonic **a**cid |
| **CAA** | **c**hloro**a**cet**a**mide |
| ***C. albicans*** | ***C****andida* ***albicans*** |
| **CDK** | **C**yclin **d**ependent **k**inase |
| **CFP** | **C**yan **f**luorescent **p**rotein |
| **CoA** | **Co**enzyme **A** |
| **CPF** | **C**leavage and **p**olyadenylation **f**actor |
| **C-terminal** | **C**arboxyl **terminal** |
| **DNA** | **D**eoxyribo**n**ucleic **a**cid |
| **DTT** | **Di**thio**t**reitol |
| ***E. coli*** | ***E****scherichia* ***C****oli* |
| **EDTA** | **Et**hylene**d**iamine**t**etraacetic **a**cid |
| **ER** | **E**ndoplasmic **r**eticulum |

| | |
|---|---|
| **ESR** | **E**nvironmental **s**tress **r**esponse |
| **FACS** | **F**luorescence-**a**ctivated **c**ell **s**orting |
| **fmol** | **f**emto**mol** |
| **GAAC** | **G**eneral **a**mino **a**cid **c**ontrol |
| **GFP** | **G**reen **f**luorescent **p**rotein |
| **GSH** | Reduced **G**lutathione |
| **GST** | **G**lutathione **S**-**t**ransferasa |
| **GTP** | **G**uanosine **t**ri**p**hosphate |
| **H** | **H**ours |
| **HOG** | **H**igh **o**smolarity **g**lycerol |
| **IMAC** | **I**mmobilized **M**etal **A**ffinity **C**hromaography |
| **IAA** | **I**odo**a**cet**a**mide |
| **IP** | **I**nositol **p**hosphate |
| **IPTG** | **I**so**p**ropyl-ß-**t**hio**g**alactopyranoside |
| **kDa** | **K**ilo **D**altons |
| **$K_m$** | **M**ichaelis constant |
| **LC-MS** | **L**iquid **c**hromatography–**m**ass **s**pectrometry |
| **M** | **M**olar concentration |
| **MAP** | **M**itogen-**a**ctivated **p**rotein |
| **Mbp** | **M**ega **b**ase **p**airs |
| **MCM** | **M**ini**c**hromosome **M**aintenance |
| **min** | **Min**utes |
| **mM** | **m**illi**m**olar |

| | |
|---|---|
| **ms** | **m**illi**s**econds |
| **NAD** | **N**icotinamide **a**denine **d**inucleotide |
| **NAMN** | **N**icotinic **a**cid **m**ononucleotide |
| **NCE** | **N**ormalised **c**ollision **e**nergy |
| **NCR** | **N**itrogen **c**atabolite **r**epression |
| **nmol** | **n**ano**mol** |
| **NmR** | **N**icotina**m**ide **r**iboside |
| **mg** | **m**illi**g**ram |
| **N-terminal** | Amino **terminal** |
| **OD** | **O**ptical **d**ensity |
| **ORF** | **O**pen **R**eading **F**rame |
| **PHO** | **Pho**sphate-responsive signaling |
| **$P_i$** | **I**norganic **p**hosphate |
| **pI** | **I**soelectric **p**oint |
| **PIC** | **P**re**i**nitiation **c**omplex |
| **PKA** | **P**rotein **k**inase **A** (cAMP-dependent protein kinase) |
| **PMSF** | **p**henyl**m**ethyl**s**ulfonyl **f**luoride |
| **PNPP** | **P**-**n**itro**p**henyl **p**hosphate |
| **PTMs** | **P**ost-**t**ranslational **m**odifications |
| **RiBi** | **Ri**bosome **Bi**ogenesis |
| **RNA** | **R**ibo**n**ucleic **a**cid |
| **ROS** | **R**eactive **o**xygen **s**pecies |
| **RTG** | **R**e**t**ro**g**rade signalling |

| | |
|---|---|
| ***S. cerevisiae*** | ***S****accharomyces* ***cerevisiae*** |
| **SAM** | **S**-**a**denosyl-**m**ethionine |
| **SAP** | **S**it4 **A**ssociated **P**rotein |
| **SMM** | **S**-**m**ethyl**m**ethionine |
| **SPS** | **S**sy1-**P**tr3-**S**sy5 |
| **SR** | **S**/**R**-rich (Ser/Arg-rich) |
| **TAF** | **T**BP-**a**ssociated **f**actor |
| **TBP** | **T**ATA-box **b**inding **p**rotein |
| **TCA** | **T**ri**c**hloroacetic **a**cid |
| **TFA** | **T**ri**f**luoroacetic **a**cid |
| **TCEP** | **T**ris (2-**C**arboxy**e**thyl) **P**hosphine |
| **TMT** | **T**andem **M**ass **T**ag |
| **TOR** | **T**arget **o**f **r**apamycin |
| **TORC1** | **T**arget **o**f **r**apamycin **c**omplex **1** |
| **UTR** | **U**n**t**ranslated **r**egion |
| $\mathbf{V_{max}}$ | **Max**imum rate in Michaelis–Menten kinetics |
| **WT** | **W**ild **t**ype |
| **XL-MS** | **Crossl**ink follow by **m**ass **s**pectrometry |
| **YFP** | **Y**ellow **f**luorescent **p**rotein |
| **µM** | **microm**olar |

# SUMMARIES

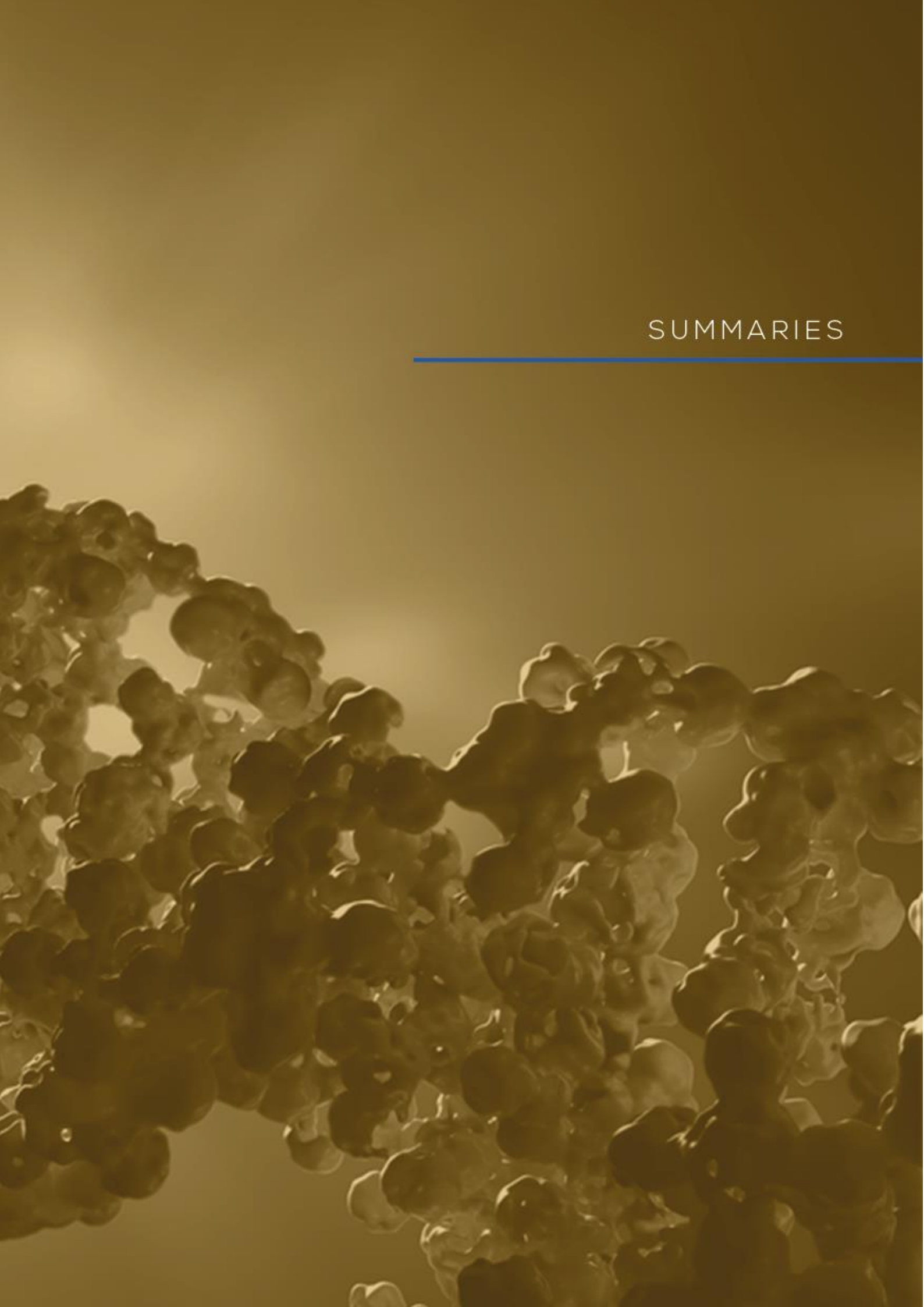

Uno de los más notables componentes en la homeostasis de cationes en levaduras es la proteína fosfatasa Ppz1. El papel de Ppz1 es doble: por un lado, inhibe la entrada de potasio mediante el control de la actividad de los transportadores Trk1 y Trk2 y, por otro lado, atenúa la expresión del gen de la $Na^+$-ATPasa *ENA1*. Ppz1, a su vez, está controlada negativamente por dos subunidades reguladoras estructuralmente relacionadas, Hal3 y Vhs3, siendo la primera la más relevante funcionalmente. A parte de esto se ha demostrado hace tiempo que niveles altos de Ppz1 son extremadamente perjudiciales para la célula.

El primer objetivo de este trabajo ha sido estudiar la interacción entre Ppz1 y Hal3. A pesar de las numerosas evidencias de que ambas proteínas interaccionan físicamente, se desconoce las regiones de cada proteína que están involucradas en dicha interacción y hasta qué punto es un proceso dinámico. Para ello se han diseñado dos aproximaciones experimentales, por un lado se han creado una serie de cepas con etiquetas fluorescentes en Ppz1 y Hal3, para seguir su interacción *in vivo* gracias al fenómeno de la transferencia de energía por resonancia de fluorescencia (FRET) mediante citometría de flujo. Estas fusiones de Hal3 y Ppz1 con proteínas fluorescentes, además de ser completamente funcionales, han demostrado la interacción *in vivo* de ambas proteínas y permiten estudiar posibles variaciones en la interacción. Por otro lado, mediante experimentos de *crosslinking in vitro* de ambas proteínas y un posterior análisis por LC-MS/MS se han mostrado dos regiones del dominio C-terminal de Ppz1 y tres regiones de Hal3, que podrían ser las responsables de llevar a cabo esta interacción.

Si bien Ppz1 es regulada negativamente por Hal3 y Vhs3, es evidente que la región más N-terminal de Ppz1 es muy rica en residuos fosforilables. De hecho, el 30% de este dominio son serinas o treoninas, y algunas de ellas han sido identificadas como fosforiladas en diversos estudios. Sin embargo, apenas ha sido estudiado que efectos funcionales pueden dar lugar cambios en el estado de fosforilación de Ppz1. En este trabajo hemos conseguido demostrar que la MAPK Hog1 fosforila a Ppz1 en la posición S265, pero este hecho no es suficiente para alterar el comportamiento de la fosfatasa. Además, hemos conseguido demostrar que el estado de fosforilación de Ppz1 puede variar dependiendo de factores externos como alta concentración de sal o deficiencia de potasio.

Se ha demostrado que Ppz1 es la proteína más tóxica de levadura cuando se sobredosifica. Recientemente, en nuestro laboratorio se ha verificado que la actividad fosfatasa de Ppz1 es necesaria para causar dicha toxicidad, ya que la sobreexpresión de una versión catalíticamente inactiva no causa problemas de crecimiento en las células. Sin embargo, las bases moleculares de esta toxicidad son desconocidas. En nuestro caso hemos realizado experimentos para conocer el estado del proteoma y del fosfoproteoma de *S. cerevisiae* cuando se sobreexpresa Ppz1, y hemos descrito una variación en el estado de fosforilación en numerosas proteínas de la levadura. De hecho, se han identificado cambios importantes en proteínas relacionadas con la traducción, polarización celular, la transición G1/S del ciclo celular o con el metabolismo de carbohidratos. Además, algunos experimentos paralelos han reforzado los resultados obtenidos mediante espectrometría de masas, como la defosforilación de Mig1 y Rps6, o una hiperfosforilación de eIF2α en la Ser-51, indicando una posible inhibición en la iniciación de la traducción.

En resumen, los resultados obtenidos en esta tesis han puesto a punto herramientas para conocer más sobre el dinamismo de la interacción Ppz1-Hal3, han aportado datos sobre la fosforilación de Ppz1, y han generado una gran cantidad de datos de fosfoproteómica cuyo estudio detallado podría llevar a esclarecer bases moleculares de la toxicidad de Ppz1 en *S. cerevisiae.*

The protein phosphatase Ppz1 is one of the most relevant components in cation homeostasis in yeast. It has two major roles: on one hand, it inhibits potassium influx by controlling the activity of the Trk1 and Trk2 potassium transporters and, on the other hand, it represses the expression of the *ENA1* gene, coding for a $Na^+$-ATPase. Ppz1 is negatively regulated by two structurally related subunits, Hal3 and Vhs3, being Hal3 the most functionally relevant. Previous studies have shown that high levels of Ppz1 are extremely detrimental for yeast cell growth.

The first objective of this work has been to study the interaction between Ppz1 and Hal3. Although there is evidence of both proteins interacting physically, the regions of each protein involved in the interaction, as well as the dynamics of the interaction, are still unknown. Therefore, two different experimental approaches have been designed. The first approach is based on the detection of fluorescence resonance energy transfer (FRET) by flow-cytometry. Several strains have been constructed with fluorescent tags on Ppz1 and Hal3, to monitor the interaction *in vivo*. These tagged versions of Ppz1 and Hal3, in addition to be fully functional, were suitable to demonstrate the interaction between both proteins *in vivo* and to allow the study of possible variations on the interaction. The second approach, based on *in vitro* crosslinking of both proteins, followed by LC-MS/MS analysis, has shown two regions of the Ppz1 C-terminal region and three from Hal3 that could be involved in the interaction.

Even though Ppz1 is negatively regulated by Hal3 and Vhs3, the most N-terminal region of Ppz1 is very rich in phosphorylatable residues (in fact, 30 % of the N-terminal residues are serine or threonine) and some of them have been identified as phosphorylated in several studies. However, how phosphorylation could affect Ppz1 function remains unknown. In this work we show that the MAPK Hog1 phosphorylates Ppz1 at S265, but this is not enough to alter the behavior of the phosphatase. Moreover, we demonstrate that the phosphorylation state of Ppz1 can change depending on external factors, such as high salt or low potassium concentrations.

It has been recently demonstrated that Ppz1, when over-expressed, is the most toxic protein for yeast cells. We described shortly ago in our laboratory that the phosphatase activity of Ppz1 is crucial for this toxicity, since over-expression of a catalytically inactive version does not negatively affect cell growth. However, the molecular basis of this toxicity is still unknown. To address this question our approach was to characterize the proteomic and phosphoproteomic landscape of *S. cerevisiae* cells overexpressing Ppz1. We have found changes in the phosphorylation state of numerous proteins, including proteins related to translation, polarized cell growth, G1/S transition and carbon metabolism. Moreover, we provide additional evidence that reinforce or complement the results obtained by mass-spectrometry, such in the case of Mig1 and Rps6 dephosphorylation, or hyperphosphorylation of eiF2α at Ser-51, pointing to a possible inhibition of translation initiation.

Overall, the results obtained in this thesis have set tools to dynamically study the Ppz1-Hal3 interaction *in vivo*, have provide information on the phosphorylation of Ppz1, and have generated a large database of proteomic and phosphoproteomic data whose future analysis might provide the clues to understand the toxicity of Ppz1 over-expression.

# OBJECTIVES

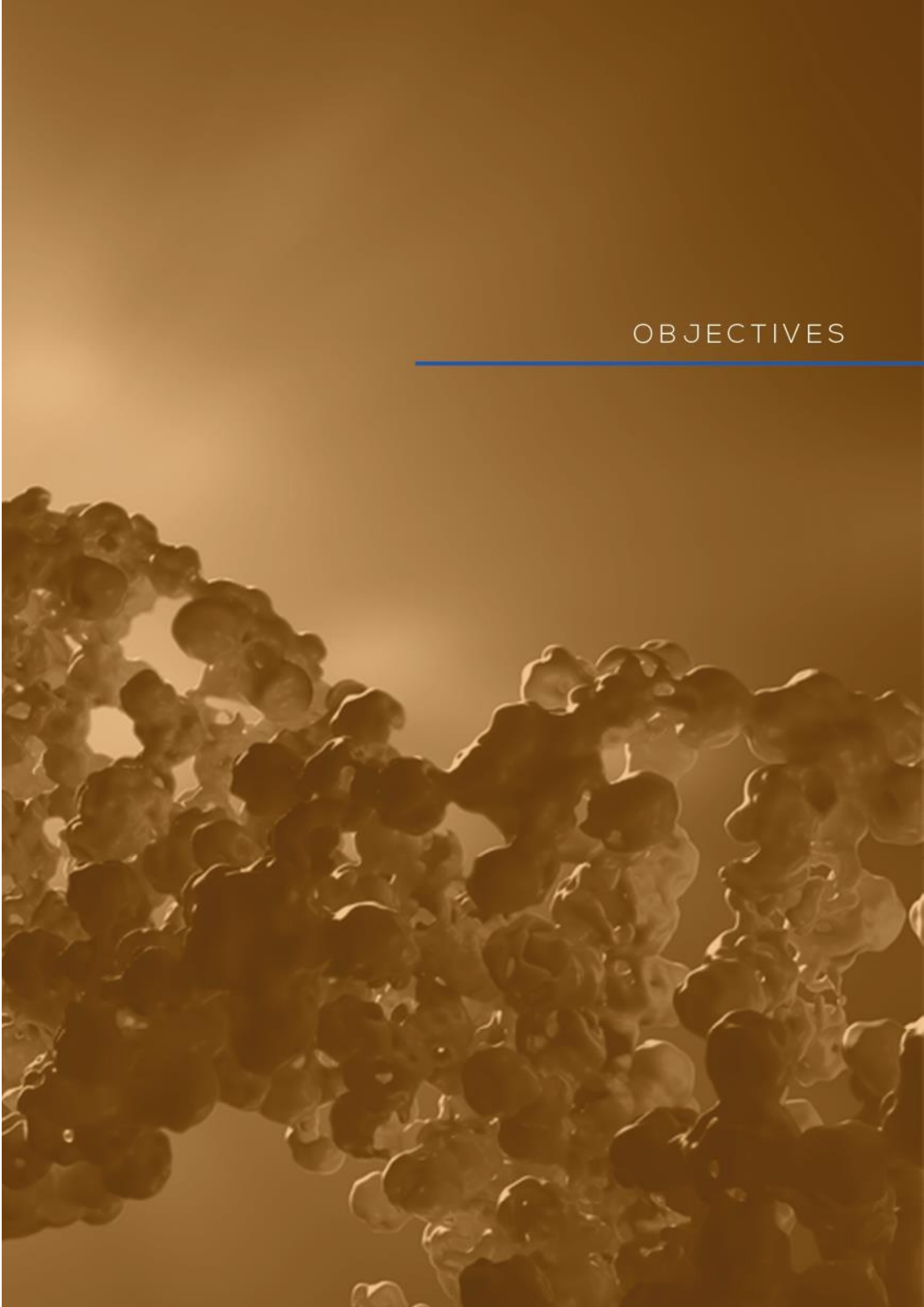

# Objectives

The aims of this work have been:

1.- To generate tools to demonstrate the Ppz1-Hal3 interaction *in vivo* and to study its dynamism.

2.-To decipher the crucial regions in the Ppz1-Hal3 interaction.

3.-To understand the possible regulation of Ppz1 by phosphorylation, and how it could be altered by environmental changes.

4.-To unveil the molecular basis of Ppz1 toxicity using a phosphoproteomic approach.

# INTRODUCTION

# 1.- *Saccharomyces cerevisiae* as a model organism

The budding yeast *Saccharomyces cerevisiae* is a unicellular fungus belonging to the Ascomycota phylum and to the *Saccaromycetaceae* family. In nature, it is often found on the skin of ripe fruits such as grapes and has an optimum temperature for growth around 30ºC. *S. cerevisiae* laboratory strains exist in two stable forms: haploid and diploid. Haploid cells proliferate through mitosis and are sexually differentiated as mating type ***a*** or **α**. Two opposite mating types can mate to generate a diploid cell, which can proliferate via mitosis or, under nutrient starvation, undergoes meiosis producing four haploid spores. This budding yeast can grow aerobically and anaerobically utilizing different sugars as carbon source, although glucose is the preferred one. Its genome was sequenced in 1996 (the first eukaryotic organism to be sequenced) and it is composed of 16 chromosomes accounting for 12.1 Mbp. It encodes 6000 genes approximately, of which 85% have an annotated biological role (Botstein & Fink, 2011).

*S. cerevisiae* is responsible for the alcoholic fermentation associated with the production of bread or alcoholic beverages like beer or wine. Apart from its obvious importance in the food industry, it is used to produce various compounds with commercial interest and for heterologous protein expression. Because it is an organism easy to cultivate and manipulate and it is not a pathogen, it began to be used as a model for genetic and metabolic studies. Since the sequencing of its genome in 1996, it has become an invaluable tool for research in molecular genetics and metabolism. Because cellular mechanisms that govern basic functions, such as replication or cell division, are well conserved between yeast and higher eukaryotes, *S. cerevisiae* serves as the perfect model to unravel the secrets behind eukaryotic life.

# 2.-The regulation by protein phosphorylation

## 2.1.- General view of protein phosphorylation

Reversible protein phosphorylation is one of the most important and widespread mechanisms of regulation of many biological process such as metabolism, gene transcription, cell cycle and responses to a plethora of either internal or external stimuli. The phosphorylation state of any protein depends on the specific and opposite action of protein kinases (PK) and protein phosphatases (PP). Phosphorylation changes the net charge of the protein leading to an alteration of its functional properties, such as modification of its biological activity (by increasing or decreasing it) or its subcellular localization; alteration of the protein half-life, and initiation or elimination of interactions with other proteins (Cohen, 2002). Nowadays, reversible phosphorylation of proteins is defined as the most common post-translational modification and plays an important role in all known signal transduction pathways. Approximately 50% of the *S. cerevisiae* proteome can be phosphorylated [(Sadowski *et al*, 2013) and phosphoGRID database (https://thebiogrid.org/)].

The importance of this regulatory mechanism is evident if one considers that the number of genes encoding phosphatases and kinases represents 2-4% of the total number of genes in a typical eukaryotic genome (Manning *et al*, 2002). Moreover, the number of PKs is much greater than the number of PPs. For instance, in *S. cerevisiae*, 127 kinases are found while only 43 phosphatases have been identified (Offley & Schmidt, 2019). This kinase/phosphatase ratio is conserved in higher eukaryotes. For example, the human genome is thought to encode 518 potential protein kinases (Johnson & Hunter, 2004), of which 428 are Ser/Thr kinases, but only contains approximately 150 genes encoding PPs, where approximately 30 of them are Ser/Thr-specific phosphatases. Another example is the ratio between Ser/Thr-specific kinases and Ser/Thr-specific phosphatases in *Drosophila melanogaster,* higher than 6:1 (Morrison *et al*, 2000).

Proteins can be phosphorylated on nine aminoacids: tyrosine, serine, threonine, cysteine, arginine, lysine, aspartate, glutamate and histidine. Serine, threonine and

tyrosine phosphorylation is predominant in eukaryotic cells, where it plays key regulatory roles (Moorhead *et al*, 2009). Specifically, studies on the human proteome shows that the phosphorylation of serine, threonine and tyrosine residues represents approximately 86.4, 11.8 and 1.8%, respectively, of the total number of phosphorylated amino acids (Olsen *et al*, 2006).

According to the dephosphorylated residue, protein phosphatases have historically been grouped into three main families: the group of Ser/Thr phosphatases, the superfamily of protein tyrosine phosphatases (PTP) and the set of dual phosphatases, which are able to dephosphorylate both Ser/Thr as well as Tyr residues.

## 2.2.- Properties of Ser/Thr phosphatases

The Ser/Thr phosphatases constitute the most abundant group of phosphatases. Based on biochemical assays the Ser/Thr phosphatases were originally classified as type1 (PP1) or type 2 (PP2). An early classification, based on biochemical and functional differences, established criteria to subdivide them into four major classes (PP1, PP2A, PP2B and P2C) (Cohen, 1989).

Nowadays, based on their sequence, structure and enzymatic properties, Ser/Thr phosphatases are divided into three major families: phosphoprotein phosphatases, (PPPs), metal-dependent protein phosphatases (PPM) and aspartate-based phosphatases (Cohen, 1997) (Figure 1).

### 2.2.1.- Phosphoprotein phosphatases (PPPs)

The members of the PPP family are PP1, PP2A, PP2B, PP4, PP5, PP6 and PP7. Biochemical characterization of the first purified members indicated that type 1 protein phosphatase (PP1) preferably dephosphorylates the ß-subunit of the phosphorylase kinase, whereas type 2 (PP2A) acts on the α-subunit of this specific PK. In addition, PPPs have distinct regulatory subunits. PP1 activity is sensitive to the polypeptides Inhibitor-1 and -2 and, whereas PP2 does not respond to any of those inhibitors. PP1 depends on

the presence of $Mn^{2+}$ to catalyze *in vitro* the reaction, while PP2A does not require these ions. Type 2B protein phosphatase (PP2B), also called calcineurin, depends on $Ca^{2+}$ to carry out its function (Ingebritsen & Cohen, 1983). Structurally, all PPPs share a high degree of similarity, especially in a region of 150 amino acids, which is considered the catalytic core of the enzyme (Cohen, 1991). Moreover, the family of PPP phosphatases includes a set of enzymes structurally related but functionally different to those of type 1 and 2A. Most of these protein phosphatases (with the exception of PP7) are represented in the yeast *S. cerevisiae* (Ariño, 2002). As shown in Figure 1, PP4 is represented by Pph3 in *S. cerevisiae*. The PP5 protein phosphatase, Ppt1 in *S. cerevisiae*, possesses a fused N-terminal domain that contains four tetratricopeptide (TPR) motifs which are essential for substrate targeting. Sit4 encodes the PP6 type in *S. cerevisiae* (Stark, 1996).

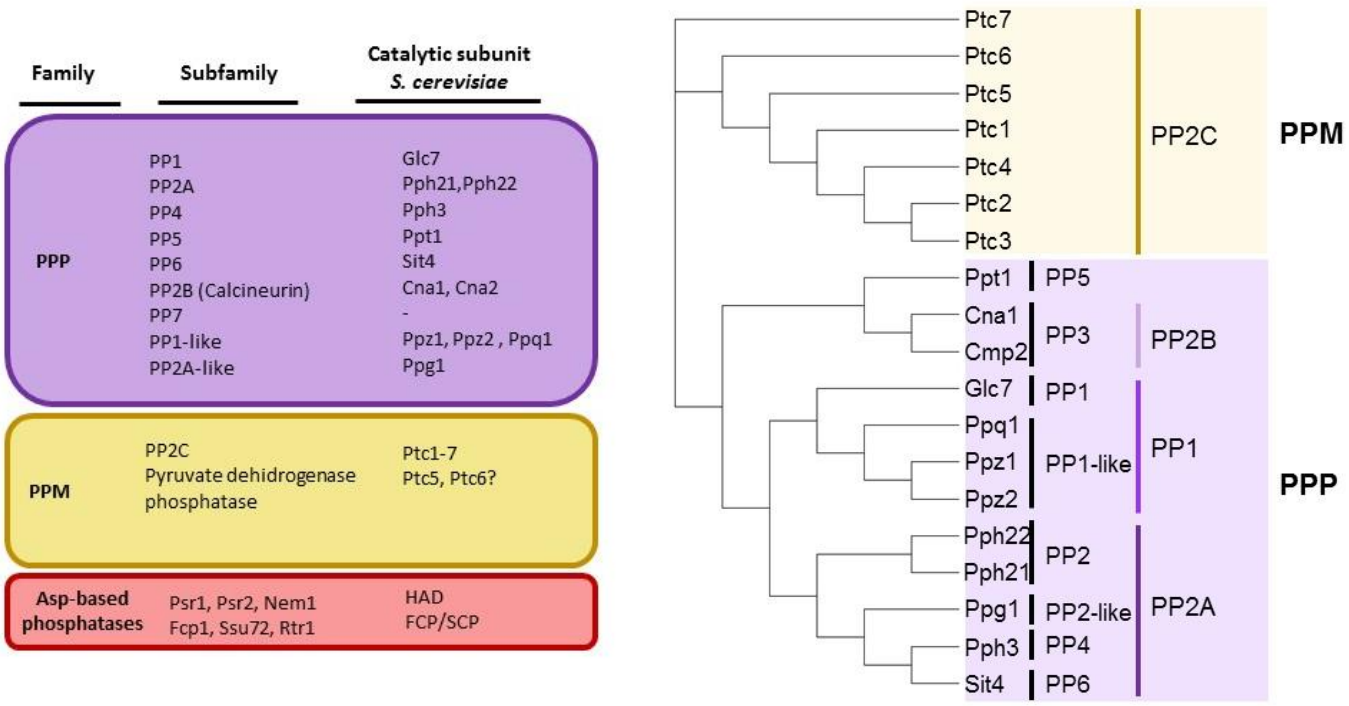


**Figure 1. Classification of Ser/Thr phosphatases. A)** The three main families and the corresponding subfamilies of catalytic subunits of Ser/Thr protein phosphatases are shown. The *S. cerevisiae* catalytic subunits of each subfamily are shown in the right column. **B)** Tree alignment of PPP and PPM, adapted from [19].

### 2.2.2.- Metal-dependent Protein Phosphatase (PPMs)

This family consist of PP2C and pyruvate dehydrogenase phosphatases. PP2C shares the typical PP2 common characteristics such as acting on the α-subunit of the phosphorylase kinases and not responding to inhibitors 1 and 2, but this family is unrelated in sequence to the PPP family and is characterized by its dependency on manganese/magnesium ions. Catalytic subunits of PP2C are implicated in diverse pathways such as the High Osmolarity Glycerol (HOG), Cell Wall Integrity (CWI) and pheromone response, among others, by dephosphorylating several MAPKs (reviewed in (Ariño *et al*, 2011)). In contrast to PPPs, members of the PPM family do not have regulatory subunits but they contain instead additional domains and conserved

sequence motif that may help to determine substrate specificity (Lammers & Lavi, 2007).

### 2.2.3.- Aspartate-based phosphatases: FCP/SCP

The members of this group, using the aspartate-based catalysis mechanism, are represented by the FCP/SCP proteins (TFIIF-associating component of RNA polymerase II CTD phosphatase/small CTD phosphatase). Only one substrate has been described for this family members, the C-terminal domain (CTD) of RNA polymerase II, which contains diversetandem repeats of a serine-rich heptapeptide (Shi, 2009b). The FCP homology (FCPH) is the conserved structural core of FCP/SCP enzymes, whereas FCPs have and extra BRCT (BRCA1 C-terminal)-like domain (Ghosh *et al*, 2008). Moreover, these family members are magnesium dependent.

## 3.- The Type 1 Ser/Thr protein phosphatase

Among PPPs family, protein phosphatase-1 (PP1) was one of the first members biochemically characterized and it is probably the most extensively studied.

In eukaryotes, PP1 is involved in many cellular functions including the regulation of glycogen metabolism, muscle physiology, RNA processing, protein synthesis, transmission of nerve signals, induction of apoptosis and control of multiple checkpoints and events that occur throughout the cell cycle (Cohen, 2002; Ceulemans & Bollen, 2004; Cannon, 2010). To fulfill these roles, each functional PP1 enzyme consists of a catalytic subunit (PP1c) which binds to different proteins called regulatory subunits. These regulators are needed either to target the PP1 catalytic subunit to specific subcellular localizations, to modulate substrate specificity or to serve as substrates themselves.

The catalytic subunit of PP1 (PP1c) is highly conserved among all eukaryotes, with approximately 70% or greater sequence identity. Moreover, the number of genes

encoding the PP1 varying from 1 gene in the flagellated protozoan parasite *Giardia lambdia* to 9 isoforms in the plant *Arabidopsis thaliana*.

In mammals, for example, PP1c is encoded by three genes (PP1α, PP1β/δ and PP1γ). PP1γ produces two isoforms (PP1γ1 and PP1γ2) as a result of alternative splicing. In the yeast *S. cerevisiae*, however, this enzyme is the product of a single gene, termed *GLC7* (aliases are *DIS2S1* and *CID1)* (Ohkura *et al*, 1989; Feng *et al*, 1991). The name *GLC7* derives from the reduction in glycogen content identified in specific mutant strains (Clotet *et al*, 1991; Feng *et al*, 1991; Cannon *et al*, 1994). As its mammals counterpart, the functions of Glc7 are regulated by the interaction with different regulatory subunits affecting their substrate specificity and/or subcellular localization (Cohen, 2002; Cannon, 2010).

## 3.1.- Structure

*GLC7* encodes a protein of 312 amino acids that is 85% identical to the four human PP1 proteins. The central section of Glc7 is also similar to the related yeast protein phosphatases PP2A, PP2B and Ppz1,2. Orthology of human PP1 isoenzymes with Glc7 has been verified by complementation of the *glc7* mutant with human PP1c cDNAs (Gibbons *et al*, 2007).

Several 3D-structures are available for the mammalian PP1 catalytic subunit. This is an example of the interest on using the structural information in order to design new inhibitors of PP1. The structure of these PP1s is nearly identical despite the difference in PP1 isoforms, crystallizations conditions and crystals packing contact. The catalytic subunit PP1 adopts a compact α/ß fold, with a ß sandwich wedged between two α-helical domains, which are the C-terminus, and the extreme N-terminus of the protein (Egloff *et al*, 1995; Goldberg *et al*, 1995). The ß sandwich and the two helical domains form a "Y"-shaped cleft where the active site is located. There, an invariant number of residues (three histidine, two aspartic acids and one asparagine) coordinate two metal ions, $Mn^{2+}$ and $Fe^{2+}$, which are needed to contribute to catalysis. These residues are highly conserved in all members of the PPP family suggesting a common mechanism of metal-catalyzed reaction (Shi, 2009a). Through that cleft, there are three grooves called hydrophobic, acidic and C-terminal (Figure 2).

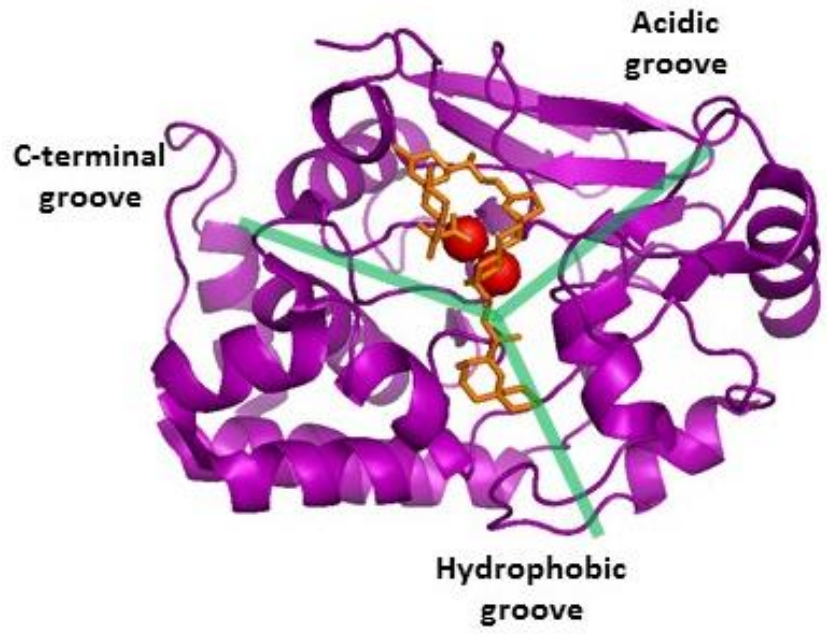


**Figure 2. The crystal structure of the PP1c**. Structure of the catalytic subunit (**purple**) of protein phosphatase 1 (PP1c) bound to okadaic acid (OA) (**orange**), a Y-shaped surface groove (**green**) is defined by the three domains of PP1. The two metal ions (**red spheres**) are $Fe^{2+}$ and $Mn^{2+}$ (modified from [34] PDB code: 1JK7).

## 3.2.- Regulation and binding motifs

PP1c does not exist freely in the cell and it has been described that the large functional diversity of PP1c depends on which regulatory subunit is interacting. These regulators are not structurally related and produce distinct effects on the activity, localization and substrate specificity of the phosphatase. More than 100 putative PP1 regulatory subunits have been described in mammals (Moorhead *et al*, 2007), and around 30 for the yeast Glc7 phosphatase (Cannon, 2010; Offley & Schmidt, 2018).

In spite of their differences in sequence, most of these subunits bind to PP1c in the same manner. The binding of regulatory subunits to PP1c is mediated by Short Linear Motifs (SLiMs), that is, short sequences of about 4-8 residues present in the regulatory subunits that are combined to create a larger interaction surface for PP1c. Despite the

conservation of motifs during evolution, they are somewhat degenerated, displaying variants of the consensus sequence that differ in affinity for PP1c.

There are about 10 known distinct PP1-SLiMs identified in the regulatory subunits in mammals, although not all of them are found in yeast. Most regulatory subunits bind to PP1c by the identifiable RVxF consensus sequence using the hydrophobic groove as PP1c interface (Egloff *et al*, 1997; Terrak *et al*, 2004; Ewald *et al*, 2012). Mutation of residues in this hydrophobic groove reduced affinity to some regulatory subunits and resulted in traits due to reduced Glc7 activity (Wu & Tatchell, 2001). Several variants affecting the hydrophobic groove could not complement the essential functions of Glc7 to allow viability in a *glc7Δ* strain (Cannon, 2010). Among the regulatory subunits for which the RVxF motif is key for interaction are Ref2, Gip2, Afr1, Reg1, Reg2, Sla1, Bud14, Bni4 and Gac1. In some cases more than a putative consensus is found (i. e. in Scd5, Gip1 or Fin1), although not necessarily all of them are required for interaction (Chang *et al*, 2002; Nakamura *et al*, 2017). In contrast, Sds22 interacts with Glc7 at a region different from the hydrophobic groove and using a different motif that is based, similarly to its mammalian counterpart, in the characteristic leucine-rich repeats (Ceulemans *et al*, 2002; Ghosh & Cannon, 2013). In the case of Pti1, an essential component of the CPF (cleavage and polyadenylation factor) that interacts with Glc7, the interaction motifs are unknown, but likely are not based on the RxVF consensus (He & Moore, 2005). Finally, certain regulatory subunits can associate to form larger complexes. For instance, formation of a trimeric complex involving Glc7 together with Sds22 and Ypi1 been reported as necessary for translocation of the phosphatase to the nucleus (Pedelini *et al*, 2007). In this complex both regulatory subunits interact with Glc7 at different sites and the formation of the trimeric complex reinforces bipartite interactions.

## 3.3.- Functions

Glc7 can play a large number of roles in different cellular localizations in yeast cells. On the one hand, cytosolic functions for Glc7 related to glucose repression, regulation of septin assembly and chitin synthesis, bud site selection or endocytosis and

actin organization. On the other hand, nuclear tasks related to transcriptional regulation, microtube attachment to kinetochores, and diverse cell cycle checkpoints (Cannon, 2010).

*GLC7* was initially identified as a gene involved in carbohydrate metabolism, playing a role in the accumulation of intracellular glycogen (Feng *et al*, 1991; Ohkura *et al*, 1989; Clotet *et al*, 1991). As in mammals, the yeast PP1c is responsible of the dephosphorylation and the activation of glycogen synthase, whose major isoform in *S. cerevisiae* is encoded by *GSY2*. This process appears to be regulated by the binding to Gac1, a regulatory subunit which contains a glycogen synthase binding region and the RVxF motif needed to interact with Glc7 (Wu & Tatchell, 2001).

The phosphatase activity of Glc7 plays a crucial role in the phenomenon of repression by glucose. Reg1 and its paralog Reg2, also assisted by Sip5, regulate the dephosphorylation of the protein kinase Snf1 in the presence of high glucose concentrations (Sanz *et al*, 2000; Maziarz *et al*, 2016). Although, Reg1-Glc7 dephosphorylates Snf1 when in complex with of all its subunits (Gal83 and Snf4), it preferentially associates with the one containing the Gal83 subunit (Zhang *et al*, 2011), the only one capable of nuclear localization upon glucose limitation. Moreover, the tandem Glc7-Reg1 may also be important for inactivation of genes dispensable for growth in high glucose, such as *HXK2*, *PDA1* and *HSP60* (Alms *et al*, 1999; Gancedo, 2008). Although Reg1-Glc7 plays the major role in the Snf1-mediated signaling pathway, other phosphatases like Ptc1 or Sit4 contribute to maintenance of the Snf1 activation loop in the dephosphorylated state during growth on high glucose (Ruiz *et al*, 2011, 2013). A major target for Snf1 is the Mig1 repressor, whose phosphorylation promotes its eviction from the nucleus. A possible role for the Glc7-Reg1 phosphatase in the direct dephosphorylation of Mig1 was also suggested several years ago (Rubenstein *et al*, 2008). More recently, the possibility of the existence of an additional glucose and Glc7-Reg1 independent mechanism for dephosphorylating Mig1 (Figure 3), perhaps involving Tyr phospho-dephosphorylation, has been suggested (Shashkova *et al*, 2017).

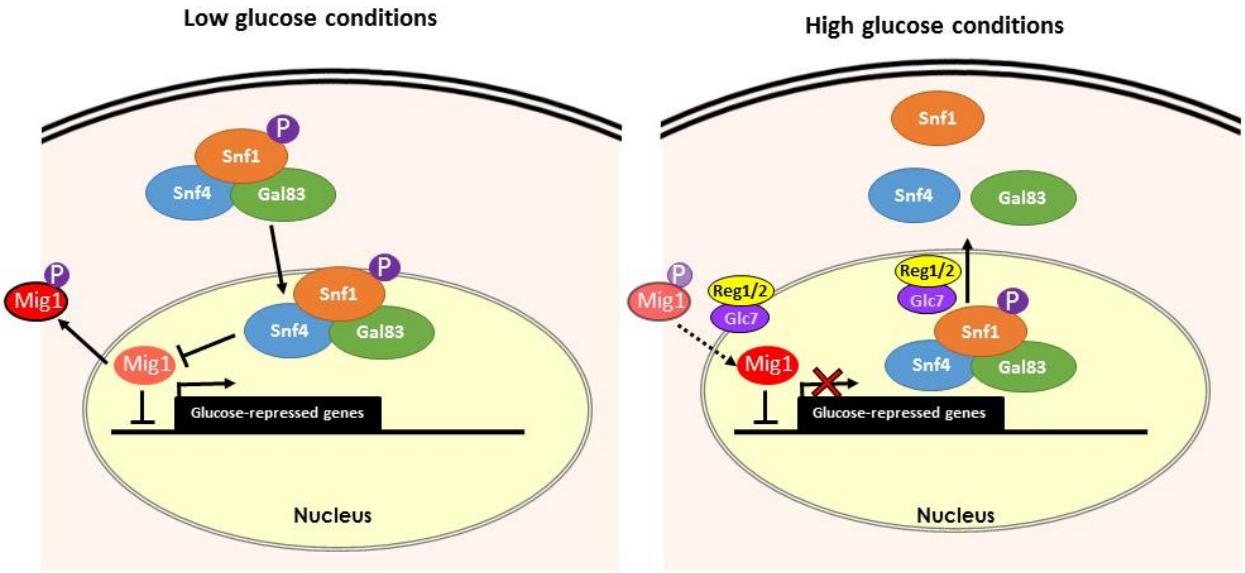


**Figure 3. Schematic representation of the Mig1 pathway**. Snf1 is phosphorylated in low glucose conditions and enters the nucleus where it phosphorylates the transcriptional repressor Mig1 prompting its nuclear exclusion. In high glucose conditions, Gcl7-Reg1 dephosphorylate Mig1 and Snf1. Kinases upstream Snf1 are not represented.

Glc7 also has relevance in the unfolded protein response (UPR). It has been reported that lack of Reg1 causes hypersensitivity to unfolded protein response (UPR)-inducers, which is concomitant with an augmented UPR element-dependent transcriptional response. This effects are attributable to the inappropriate activation of Snf1 (Ferrer-Dalmau *et al*, 2015; Kimura *et al*, 2017).

Glc7 is important in several cell cycle check-points. The lack of the essential regulatory subunit Ypi1, the yeast homologue of mammalian inhibitor 3, activates the morphogenetic checkpoint. Depletion of Ypi1 results in stabilization of the Pds1 securin, suggesting the activation of a G2/M checkpoint (Marquina *et al*, 2012b). Since under normal conditions most of the Glc7 protein is found in the nucleus, in particular in the nucleolus (Bloecher & Tatchell, 2000), it is possible that these defects could be due to the alteration of nuclear localization previously reported for Ypi1-depleted cells (Pedelini *et al*, 2007). Shp1, a protein involved in shmoo formation and bipolar bud site selection, could also be a positive regulator of Glc7, working in a complex with the AAA-

ATPase Cdc48 and promoting cell cycle progression (Böhm & Buchberger, 2013). Nuclear localization of Glc7 requires the Cdc48-Sph1 complex, which possibly functions as a molecular chaperone for the structural integrity of the PP1 complex, and specifically promotes the assembly of Glc7-Sds22-Ypi1 for nuclear import (Cheng & Chen, 2015, 2010).

The subunits Bni4, Afr1 and Gip1 mediate different septin localization activities. Specifically, the Glc7-Bni4 holoenzyme regulates the targeting of chitin synthase III (Chs3) to the incipient bud sites when Bni4 is phosphorylated by Pho85-Pcl1,2 (Kozubowski *et al*, 2002). It is worth noting that depletion of Ypi1 also causes depletion of the Cdc11 septin, which possibly explains the failure to form properly assembled septin rings at the bud necks (Marquina *et al*, 2012b).

Recently, it has been postulated that Ref2-Glc7 would be required for dephosphorylation of the formin Bni1, thus playing a role in defining the subcellular localization of formins during cytokinesis (Orii *et al*, 2016).

Early work linked Glc7 to maintenance of monovalent cation homeostasis (Williams-Hart *et al*, 2002), More recently, two Glc7 subunits have been found relevant for tolerance to toxic cations. Thus, lack of Ref2 is additive to blockage of the calcineurin pathway and might disrupt multiple mechanisms controlling expression of the *ENA1* $Na^+$-ATPase-encoding gene in a way dependent on Glc7 but independent of its previously known function in the formation of mRNA via the APT (for associated with Pta1) subcomplex of the large CPF complex (Ferrer-Dalmau *et al*, 2010). Remarkably, partial depletion of the subunit Ypi1 render cells sensitive to $Li^+$ , whereas high levels of this protein confer a lithium-tolerant phenotype to yeast cells. This phenotype is independent of the role of Ypi1 as a Glc7 regulatory subunit and, instead, the increased $Li^+$ tolerance and *ENA1* expression are abolished in a *cnb1* mutant, indicating that the effect of Ypi1 on cation homeostasis is essentially mediated by calcineurin (Marquina *et al*, 2012a).

The eukaryotic translation initiation factor 2 (eIF2) is required for initiation of translation. eIF2 is composed of α, β, and γ subunits and translation initiation requires dephosphorylation of the α subunit at Ser51. Although Glc7 was identified long ago as a major eIF2α phosphatase, in *S. cerevisiae* it was not evident which regulatory subunits are relevant for targeting the phosphatase to eIF2α, given the lack of knowledge about

the subunits playing this role in mammalian cells. Only recently, Rojas and coworkers (Rojas *et al*, 2014) nicely demonstrated that, in fact, such subunit might not exist, and that it would be replaced by the eIF2γ component of the complex, by means of a RVxF-like motif (KKVAF) present in its N-terminal extension. Such motif would be rather unique to certain yeast species, which would rely on the recruitment of PP1 in *cis* to the eIF2 complex to maintain eIF2α phosphorylation at the appropriate levels.

Besides, *GLC7* is one of the genes that are deleterious for yeast cells when are over-expressed (Liu *et al*, 1992). In fact, *GLC7* over-expression increases the chromosome missegregation, similar to what happen in *ipl1* mutations (Francisco *et al*, 1994). It is described that the lethality of *GLC7* over-expression requires the function of Sds22, Reg2 and phosphorylated Glc8, suggesting a relationship between the toxicity of Glc7 and its nuclear import (Ghosh & Cannon, 2013).

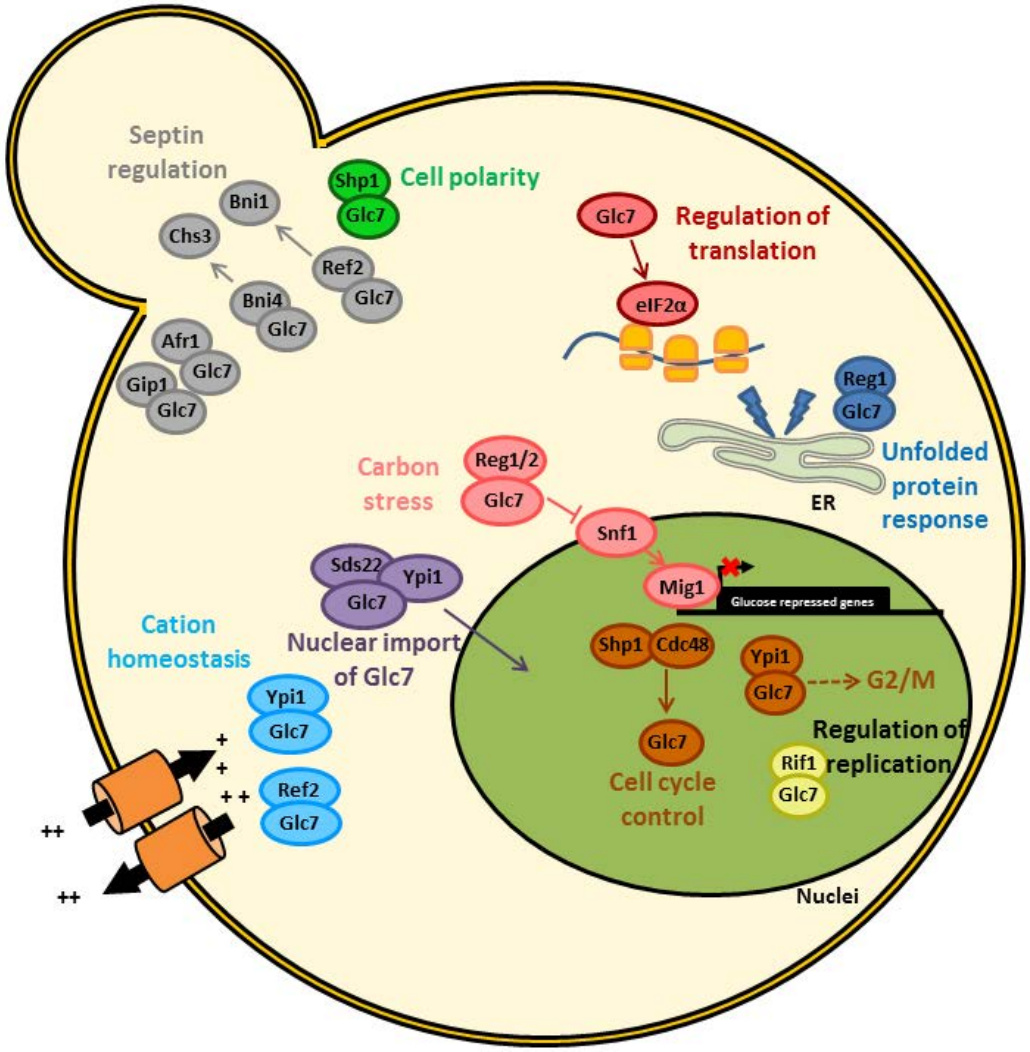


**Figure 4. Simplified representation of the different regulatory subunits of Glc7 and their functions**

## 4.- Ppz Ser/Thr phosphatases in *S. cerevisiae*: Ppz1 and Ppz2

The Ppz phosphatase are type 1-related enzymes found only in fungi. They are characterized by a well-conserved carboxy-terminal catalytic domain, related to type 1 PPases, and an N-terminal domain that largely differs in sequence and size among fungi. These enzymes were first identified in *S. cerevisiae*, were two paralogs, *PPZ1* and *PPZ2* are found (Lee *et al*, 1993; Clotet *et al*, 1996). These genes encode proteins of 692 and 710 amino acids, respectively, showing 67% identity over their full length and 93% in its

catalytic domain. *PPZ1* and *PPZ2*, in contrast to *GLC7*, are not essential. Thus, these phosphatases do not perform the same functions that yeast PP1.

In *S. cerevisiae* the C-terminal half of *PPZ1* and *PPZ2* (about 350 residues), comprises the catalytic domain and shows more than 60% sequence identity to the catalytic subunit of proteins phosphatase 1 (PP1c) from a large variety of species, including mammals. These N-terminal halves are of roughly the same size (350 residues approximately, but much less closely related in sequence) and are largely unstructured, rich in basic residues, as well as in Ser, Thr and Asn amino acids (in fact 30% of the N-terminal residues are Ser or Thr) and show no close similarities to other protein phosphatase sequences (Posas *et al*, 1992; Hughes *et al*, 1993). One of the most relevant aspects of the N-terminal region is the presence of a conserved Gly in position 2 within a consensus sequence for N-myristoylation. It has been shown that Ppz1 is myristoylated *in vivo* (Clotet *et al*, 1996), and the initial octapeptides from Ppz1 and Ppz2 have been shown to be excellent substrates *in vitro* for the Nmt1 N-myristoil transferase (Johnson *et al*, 1994). The myristoyl group attached to the proteins is important in subcellular location of proteins, mediating protein-membrane interaction or increasing its stability (Yonemoto *et al*, 1993). In addition, a relatively conserved sequence near of the N-terminus of Ppz1 and Ppz2 ($^{43}$SSRSRRSLPS$^{52}$ and $^{43}$SSRSLRSLRS$^{52}$, respectively) can be found in many fungi in the form of a SxRSxRxxS consensus(Minhas *et al*, 2012). Such sequence seems to have a functional relevance, being important in regulation of cationic homeostasis (Minhas *et al*, 2012).

In *S. cerevisiae* deletion of *PPZ1* results in a large number of phenotypic traits, whereas that of *PPZ2* is hardly noticeable, suggesting that the former enzyme has a more prominent cellular role. However, deletion of *PPZ2* in a *ppz1Δ* background usually potentiates the phenotype.

Besides, PPZ phosphatases have been also characterized in other fungi such as *Schizosaccharomyces pombe* (Pzh1), *Neurospora crassa* (Pzl-1) or *Candida albicans* (CaPpz1), with similar structural and functional characteristics (Balcells *et al*, 1997; Szöőr *et al*, 1998; Vissi *et al*, 2001; Leiter *et al*, 2012).

# 5.- Cellular roles of Ppz1 in *S. cerevisiae*

The catalytic properties of Ppz1 are quite similar to that of protein phosphatases PP1 and PP2A. The Ppz1 C-terminal domain displays activity against several substrates, such as myelin basic protein, histone 2A, casein (Posas *et al*, 1995a) or myosin light chain (Petrényi *et al*, 2016), and it is also active towards *p*-nitrophenyl phosphate. This activity is dependent on the presence of $Mn^{2+}$ ions, as it has been reported for PP1c. Ppz1 is also sensitive to some inhibitory toxin that bind to the PP1c active site (okadaic acid, microcystin-LR). This resemblance may be due to the sequence GEFD present in the C-terminal region of PP1c, which is also found in residues from 629 to 632 of Ppz1 (Posas *et al*, 1995a). The main difference with both PP1 and PP2A, is that Ppz1 is unable to dephosphorylate *in vitro* glycogen phosphorylase (Posas *et al*, 1995a). The phosphatase activity of Ppz1 is completely necessary for the function of this protein and the catalytic activity is largely lost by the mutation of Arg-451, a highly conserved residue in many eukaryotic Ser/Thr protein phosphatases that corresponds to Arg-95 in the catalytic subunit of PP1 (Clotet *et al*, 1996).

Ppz1 was initially characterized in *S. cerevisiae* by playing a role in the maintenance of cell integrity (Posas *et al*, 1993). However, the activity of this phosphatase is a key determinant in cation homeostasis, a function that was postulated long time ago (Yenush *et al*, 2002; Posas *et al*, 1995b). It should be noted that this involvement in $Na^+$, $K^+$ and pH homeostasis could have important consequences for other cellular processes such as the establishment of membrane potential, cell cycle regulation, cell wall integrity or protein translation.

## 5.1.- Ppz1 and regulation of cation homeostasis in *S. cerevisiae*

An important characteristic of the physiology of living cells is the maintenance of ionic homeostasis, on which a whole series of fundamental parameters, such as cellular size, concentration of intracellular cations, turgor, internal pH and membrane potential,

depends. To reach the internal equilibrium, and in response to changes in the external environment, cells carefully regulate the pass of ions across their plasma membrane. The intracellular concentrations of the major monovalent cations ($H^+$, $K^+$ and $Na^+$) must be tightly regulated to avoid damage to the cell (Serrano, 1996).

Yeast are free living organisms that exhibit a rapid adaptation to the large variation in the external medium to which they are exposed. These organisms maintain correct ion homeostasis because of the presence of a cell wall and a membrane transport strategy, which is different from mammals. In *S. cerevisiae*, many of these ion transporters and their regulators have been identified and characterized. Their differences with that of mammals has boosted their study as a possible antifungal targets (Ariño *et al*, 2010).

Sodium can be abundant cation in the environment and can enters yeast cells through several low-affinity cation transport systems. *S. cerevisiae* is able to maintain a suitable intracellular concentration of $Na^+$, even in the presence of relatively high concentrations of this cation in the extracellular ambient, through the coordinate regulation of uptake and efflux systems. In addition to the $Na^+/H^+$ antiporter Nha1 in the plasma membrane (Prior *et al*, 1996; Kinclova-Zimmermannova *et al*, 2006), the P-type ATPase encoded by the gene *ENA1* constitutes the second significant system for sodium and lithium efflux in budding yeast cells. This pump is able to actively extrude sodium and lithium, but also potassium cations, in reactions coupled to ATP hydrolysis. In *S. cerevisiae* until five *ENA* genes are disposed in an unusual tandem repeat. Deletion of the entire *ENA* cluster results in a dramatic phenotype of sensitivity to high salinity environments as well as to alkaline pH (Haro *et al*, 1991; Garciadeblas *et al*, 1993; Rodríguez-Navarro *et al*, 1994; Vasicek *et al*, 2014; Wieland *et al*, 1995). *ENA1* was the first member of this tandem to be identified and it is widely accepted to be the functionally relevant component of the cluster (Haro *et al*, 1991; Wieland *et al*, 1995; Martinez *et al*, 1991; Yenush *et al*, 2005).

Under normal growth conditions, expression of *ENA* genes is very low, but when cells are exposed to elevated sodium and/or lithium levels, or to alkaline pH, the expression of *ENA1*, but not that of other members of the cluster, is potently induced (Garciadeblas *et al*, 1993; Mendoza *et al*, 1994). In addition, a transcriptional response

of *ENA1* is observed under glucose starvation growth conditions (Alepuz *et al*, 1997), showing that the expression could be repressed by the presence of glucose in the medium. The transcriptional regulation of *ENA1* requires the intervention of multiple pathways (calcineurin, Snf1, PKA, Hog1, etc.) that transmit signals to its promoter, which contains diverse regulatory elements recognized by specific transcription factors (Crz1, Sko1, Mig1, Nrg1,..) that activate or inhibit transcription according to the signal.

The phosphatase Ppz1 and Ppz2 in *S. cerevisiae* play an important role in cationic homeostasis, in part because these phosphatases affect the expression level of *ENA1* (Ariño, 2002; Posas *et al*, 1995b). Ppz1 has a major role in salt tolerance, and strains lacking Ppz1 display a strong phenotype of hypertolerance to sodium or lithium cations, which is enhanced by additional deletion of *PPZ2* (Posas *et al*, 1995b). Thus, the effect of Ppz1 on *ENA1* expression is opposite to the effect described for the Ser/Thr phosphatase calcineurin, a positive effector of the ATPase gene (Mendoza *et al*, 1994). In fact, it has been shown that the effect of the absence of Ppz1 on *ENA1* expression requires an intact calcineurin pathway (Ruiz *et al*, 2003), thus suggesting that Ppz1 negatively regulate calcineurin activity. Nevertheless, Ppz1 also influences salt tolerance in an *ENA1*-independent way. Early evidence came from the observation that over-expression of the Sky1 protein kinase increases sensitivity to LiCl in a way that requires the function of *PPZ1* but not that of *ENA1* (Erez & Kahana, 2001).

Moreover, Ppz phosphatases are involved in the proper regulation of intracellular potassium concentration, which is important because $K^+$ is the major intracellular cation responsible for cellular volume, turgor, and electrical membrane potential and ionic strength. In *S. cerevisiae*, potassium is the only alkali cation specifically transported under normal growth conditions. Through the uptake potassium, the cell is able to reduce its membrane potential and thus prevents the entry of toxic cations such as sodium or lithium. *S. cerevisiae* has a dual mode for potassium transport, consisting of a high-affinity and low-affinity transport systems (Rodríguez-Navarro & Ramos, 1984). High-affinity potassium uptake is mediated by the transporters Trk1 and Trk2 (Ko *et al*, 1990; Ko & Gaber, 1991; Gaber *et al*, 1988), where Trk1 is the most physiologically relevant. Trk1 is a 180 kDa plasma membrane protein, with an initially predicted structure of 12 transmembrane domains, exclusively present in

plasma membrane lipids rafts (Yenush *et al*, 2005). The deletion of both *TRKs* results in a significant defect in potassium transport and slow growth phenotype under limiting concentrations of potassium, which is restored by the addition of this cation to the media. The defect in $K^+$ transport produces a hyperpolarization of the plasma membrane and consequently, an increase in sensitivity to sodium, lithium, as well as other toxic cations such as spermine, hygromicine or tetramethylammonium (TMA) (Ko *et al*, 1990; Ko & Gaber, 1991).

The Trk transporters are probably regulated at the post-translational level by phosphorylation mechanisms, and this regulation is crucial due to the effect that the influx of potassium produces on the membrane potential. Several protein kinases and phosphatases control the activity and/or stability of Trk1 and Trk2. For instance, the protein kinases Hal4 and Hal5 are required to stabilize the Trk proteins at the plasma membrane, especially under low potassium conditions. However, no direct phosphorylation of Trks by Hal4 and Hal5 kinases has been reported. Despite that, Trk1 could be phosphorylated *in vitro* and *in vivo* by protein (Yenush *et al*, 2005; Holt *et al*, 2009; Swaney *et al*, 2013).

The phosphatases Ppz1 and Ppz2 play an important role in the regulation of Trk activity. It is not known how the Ppz phosphatases influence Trk-mediated $K^+$ transport, but it has been shown that Trk1 physically interacts with Ppz1, and that the *in vivo* phosphorylation level of Trk1 increases in a Ppz-deficient strain (Yenush *et al*, 2005). However, no proof for direct dephosphorylation of Trk1 by Ppz1 has been obtained. In addition, the Ppz phosphatases also regulate potassium influx in a Trk-independent way, which involves calcium signaling but not calcineurin activation (Ruiz *et al*, 2004b). Interestingly, it has been shown that Ppz1 could down-regulate the contribution to $K^+$ influx of an heterogously expressed barley HvHak1 transporter (a kind of $K^+$ transporter also present in some fungi but not in *S. cerevisiae* (Ramos *et al*, 2011)), thus raising the possibility that the regulatory network controlling $K^+$ homeostasis in fungi could be conserved.

Therefore, an appropriate Trk regulation by Ppz phosphatases is essential for maintenance of $K^+$ and pH homeostasis. The deletion or overproduction of *PPZ1* and *PPZ2* leads to diverse Trk-mediated cellular effects caused by alterations of the internal potassium concentration. An increase in $K^+$ triggers proton efflux to maintain electrical balance and the consequent internal alkalinization. The increase of intracellular pH could signal on the *ENA1* promoter, which is responsive to high pH. Besides, the turgor pressure increment causes constant stress on the cell wall, activating the Slt2/Mpk1 pathway as is detailed below. In fact, an increased activity of the Slt2 pathway is observed in *ppz1 ppz2* mutant cells (Yenush *et al*, 2002; Merchan *et al*, 2004).

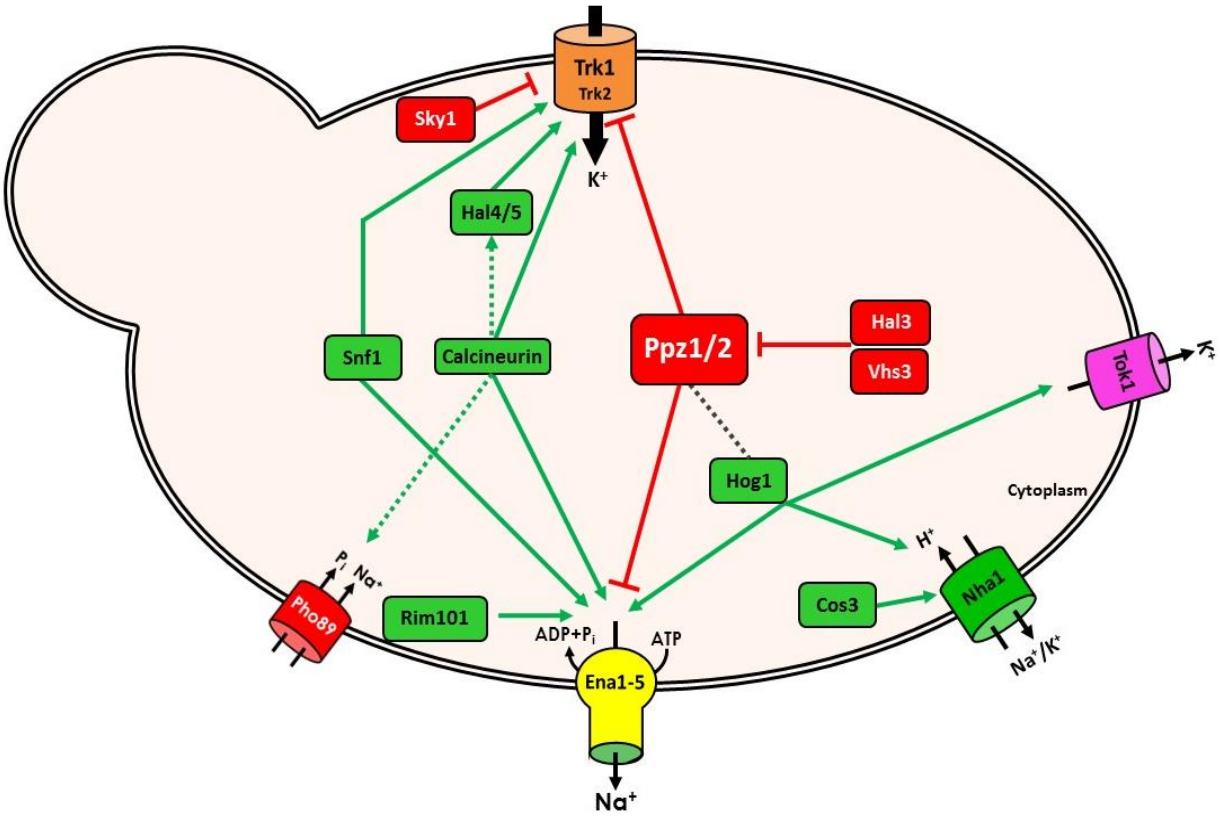


**Figure 6. Principal transporters and their regulatory components involved in the homeostasis of monovalent cations in *S. cerevisiae* and the role of Ppz1 in cation homeostasis**. Only the main transporters located at the plasma membrane and their functional regulators are shown. Other elements involved in this process, such as vacuoles are obviated for simplicity. Modified from [90].

## 5.2.- The Ppz phosphatases and the maintenance of the cell-wall integrity in *S. cerevisiae*

*S. cerevisiae* spends a considerable amount of metabolic energy in cell wall construction, whose mass may account for about 10-25% of the total cell mass (dry weight), depending on growth conditions (Aguilar-Uscanga & François, 2003). The main function of the cell wall in *S. cerevisiae* is to maintain cell shape and to act as a shield against physical or chemical external stresses, such as osmotic changes (Klis *et al*, 2006). In this way, a correct maintenance of the integrity of this structure is necessary for survival. For this reason, it is under the thigh control of a regulatory mechanism known as the Cell Wall Integrity (CWI) pathway. This pathway consists of several plasma membrane proteins, such as Wsc1 and Mid2 that act as sensors for the pathway. Their signal results in activation of a small GTPase (Rho1), which is a signal transducer that binds and activates the protein kinase C (Pkc1). The protein kinase C, is a member of the Mitogen Activated Protein (MAP) kinase pathway, that consist of several protein kinases (Bck1, Mkk1, Mkk2 and Slt2), which in response to certain stimuli and through a phosphorylation cascade, results in the final activation of the Slt2/Mpk1 (suppressor of the lytic phenotype) MAP kinase. Activation of Slt2 results in phosphorylation of several nuclear (as the transcriptional factor Rlm1) and cytosolic targets that activate specific transcription in response to aggressions of the cell wall (Levin, 2005).

The CWI pathway is active during vegetative growth and pheromone-induced morphogenesis on yeast cells. In fact, Wsc1 acts as a sensor during vegetative growth and Mid2 does so in the case of pheromone-induced morphogenesis. The CWI pathway also mediates the response triggered by cell wall damage provoked by agents (e.g. Congo red, calcofluor white, zymolyase or caffeine) or environmental conditions (e.g. heat shock, hypoosmotic shock or alkaline pH) (Levin, 2005). Mutations in any of the elements that compose this pathway, such as deletion of the MAP kinase Slt2, result in cells prone to lysis under conditions that compromise cell wall integrity, as salt exposure or high temperature (37-40°C). Besides, *slt2* mutants are particularly sensitive to caffeine or calcofluor white. The lytic phenotype of this mutant is rescued by addition of 1 M sorbitol to the medium as osmotic stabilizer.

The Ppz phosphatases were initially related to the maintenance of cell wall integrity in *S. cerevisiae*, because the *PPZ2* gene was isolated as a dosage dependent suppressor of the lytic defect associated with the disruption of *SLT2/MPK1* (Lee *et al*, 1993). Similar lytic phenotypes observed in strains lacking components of the Slt2/Mpk1 pathway (*bck1*, *mkk1*/*mkk2* or *slt2* mutants) were described for *ppz* phosphatase mutants, such as increased size (elongated morphology), and temperature or caffeine sensitivity, leading to cell lysis. Moreover, the effects due to *PPZ1* and/or *PPZ2* deletion are additive to those caused by the absence of Slt2. Similarly to the *slt2* mutant, these defects can be suppressed in the presence of 1 M sorbitol (Hughes *et al*, 1993; Posas *et al*, 1993). The link between the Slt2/Mpk1 pathway and the Ppz phosphatases can be explained by the relationship of these phosphatases with the regulation of potassium uptake. Indeed, cells lacking *ppz1* and *ppz2* showed increased potassium uptake, leading to augmented intracellular turgor. Therefore, these cells require a reinforcement of the cell wall mediated by the Pkc1-Slt2/Mpk1 pathway, and for that reason the activity of this pathway increases (Yenush *et al*, 2002; Merchan *et al*, 2004). In absence of Slt2, which leads to weakened cell wall, this situation produces a lytic phenotype. This effect could explain the impact of Ppz1 on the CWI pathway and provided the basis to understand earlier findings pointing to the involvement of Ppz1 and Ppz2 in the maintenance of the CWI**.**

## 5.3.- The role of Ppz1 phosphatase in cell cycle progression

In *Saccharomyces cerevisiae*, as in any eukaryotic cell, the cell cycle consists of a succession of phases: DNA replication (phase S) and it separation into two complete genomes (mitosis, phase M), which are separated by the intervals G1 and G2. The regulation of the eukaryotic cell cycle is a complex process that involves two major control points (checkpoints); at G1/S, which determines DNA replication because it controls that external conditions are appropriate, that the size of the cell is adequate to start a new cycle, and ensures that any DNA damage caused by the previous replication is already repaired; and at G2/M, which regulates entry into mitosis after supervision that the DNA has been correctly duplicated during the S phase (Tyson *et al*, 2002). In *S.*

*cerevisiae* a new round of the cell cycle is committed at a control point called Start in the G1/S transition (Figure 7). It demands a sufficient level of G1 cyclin/Cdc28 protein kinase activity for the DNA synthesis, bud formation, and replication of the spindle pole body. *CDC28* encodes a cyclin dependent kinase (CDK) that, in contrast to mammals, it is the only CDK responsible for cell cycle control. Thus, the activity of Cdc28 is regulated mainly by the binding of proteins denominated cyclins. Towards the end of mitosis, the complex formed by Cdc28 and Cln3 is responsible for the control of cell size. When the cell has reached the proper dimensions, Cln3-Cdc28 activates transcriptional complexes that induce genes specific for the G1 phase, which include cyclins *CLN1*, *CLN2*, *CLB5* and *CLB6*. Transcription of genes specific for the G1/S transition also requires the activity of some phosphatases, such as Sit4 or Glc7.

The *S. cerevisiae* gene *SIT4* (also known as *PPH1*) encodes a type 2A-related protein phosphatase of 311 residues that was initially cloned in an screen for restoration of *HIS4* expression in strains lacking Bas1, Bas2 and Gcn4 (Arndt *et al*, 1989). Two years later it was found necessary for progression for the G1/S cell cycle transition (Sutton *et al*, 1991). Sit4 is required for expression of *CLN1* and *CLN2* G1-cyclins, as well as of the transcription factor *SWI4*, and cells lacking the phosphatase do show defects in bud emergence (Fernandez-Sarabia *et al*, 1992; Di Como *et al*, 1995). Deletion of *SIT4* in some genetic backgrounds (cells lacking *SSD1* or harboring defective *ssd1*-d alleles) is lethal, whereas in others cells are viable but display a noticeable slow-growth phenotype (Sutton *et al*, 1991; Doseff & Arndt, 1995).

Ppz1 has been proposed also as a regulatory component of the G1/S transition in the yeast cell cycle, since its regulatory subunit, Hal3 (see section 6), was identify by its capacity, when over-expressed, to recover the growth defect of *sit4Δ* cells (Di Como *et al*, 1995). In agreement, over-expression of *PPZ1* causes blockage of cell growth, decreased expression level of *CLN2* and *CLB5* cyclins and results in an increased number of unbudded cells, all these features characteristics of a delay in G1/S transition (Clotet *et al*, 1999; Merchan *et al*, 2004). By contrast, deletion of *PPZ1* accelerates the slow growth phenotype of *sit4* mutants and results in an earlier expression of *CNL2* and *CLB5* to favor entry in S phase. The link between the functions of Ppz1 and Sit4 phosphatases evidences that Ppz1 exerts an important effect in the G1/S transition that it is opposed

to some of the functions attributed to the Sit4 phosphatase, negatively regulating G1 cyclin transcription, through a mechanism that would not be mediated by Sit4, Bck2 or Cln3. In addition, Ppz1 should negatively regulate certain processes that affect proper budding (Clotet *et al*, 1999).

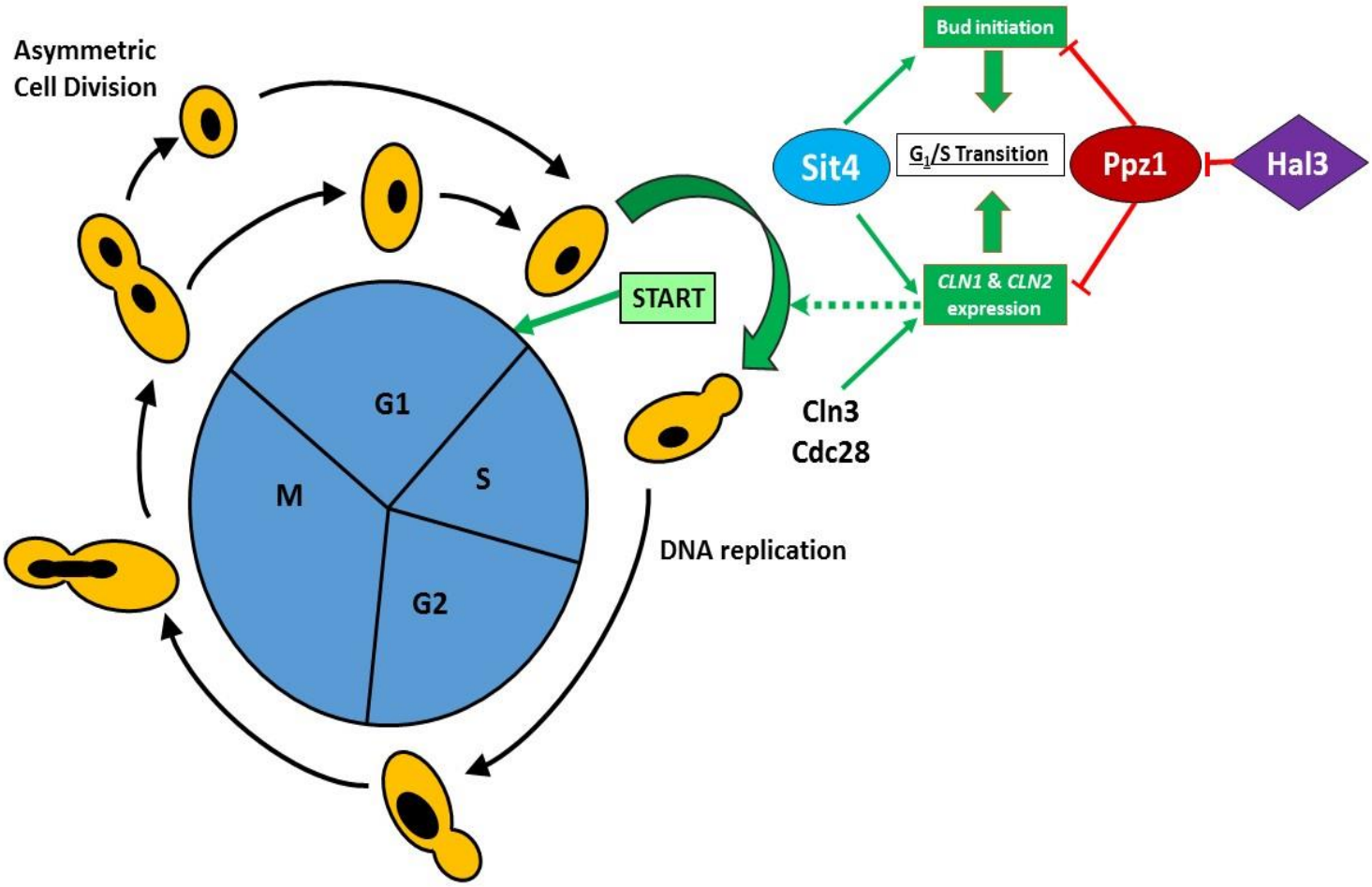


**Figure 7. Sketch of the yeast mitotic cell cycle, which is subdivided into the G1, S, G2, and M phases.** DNA replication occurs during S phase and at the end of M phase the cell divides asymmetrically into a larger mother and a smaller daughter cell. The proposed role of the phosphatases Sit4 and Ppz1 in the regulation of G1/S transition is also depicted. Adaptation from [122].

### 5.4.- Ppz1 involvement in protein translation

Protein translation is the process by which messenger RNA (mRNA) is decoded by ribosomes in the cytoplasm to produce specific polypeptides. The Ppz phosphatases are likely influencing protein translation. Thus, it was demonstrated that Ppz1 interacts *in vivo* with the translation elongation factor 1Bα (Tef5), the GTP / GDP exchanging factor for translation elongation factor 1, and that in *ppz1Δ ppz2Δ* cells the conserved Ser86 of Tef5 was hyperphosphorylated. Indeed, lack of Ppz phosphatases resulted in enhanced read-through at all three nonsense codons, suggesting that translational fidelity might be affected (De Nadal *et al*, 2001). A role of Ppz1 (and possibly Ppz2) on protein translation accuracy has been reinforced by a series of publications on the regulation of read-through efficiency and manifestation of non-Mendelian anti-suppressor determinant [ISP(+)], and on the phenotypic expression of various mutant alleles of genes *SUP35* and *SUP45*, and the yeast prion [PSI+] (Aksenova *et al*, 2007; Ivanov *et al*, 2008, 2010).

## 6. Regulatory subunits of Ppz phosphatases: Hal3 and Vhs3

In contrast to the PP1 phosphatase, for which many regulatory subunits related to different cellular functions have been identified, only two regulatory subunits have been described for Ppz phosphatases. These subunits are negative regulators and are named Hal3 and Vhs3. As it will be described below, Hal3 and Vhs3 are able to regulate all the functions mediated by the phosphatases.

The gene *HAL3/SIS2* was identified by two laboratories independently, as a multicopy suppressor of the growth defect in a *sit4Δ* background, in which normalizes the expression of the G1 phase cyclins *CLN1* and *CLN2* (and was named *SIS2*) (Di Como *et al*, 1995), and as a gene that confers salt tolerance when over-expressed in wild type cells (named *HAL3*) (Ferrando *et al*, 1995). *HAL3* encodes a protein of 562 amino acids located in the cytoplasm and is constitutively expressed. Besides, the protein Hal3

contains a characteristic C-terminal tail of around 80 amino acids which is very rich in acidic residues, especially in aspartic.

The over-expression of *HAL3* confers tolerance to high concentrations of sodium and lithium cations due to increased *ENA1* expression (Ferrando *et al*, 1995; de Nadal *et al*, 1998). Moreover, Hal3 over-expression increase $K^+$ influx via Trks transporters and it allows growth at potassium limiting conditions. These are phenotypes similar to those found in a *ppz1Δ* background. In fact, the phenotypes found in a *ppz1Δ* mutant are completely opposite to *hal3Δ* phenotypes (de Nadal *et al*, 1998). De Nadal and coworkers demonstrated that the effects of over-expression of Hal3 on salt tolerance could be explained through the inhibition of Ppz1. It was also demonstrated that Hal3 binds to the C-terminal catalytic moiety of the PPase and, in fact, binding is more intense when the N-terminal domain of Ppz1 is eliminated (De Nadal *et al*, 1998). In keeping with the negative role of Hal3 on Ppz1, the over-expression of Hal3 aggravates the lytic phenotype of the *slt2Δ* mutant and this combination is only viable in the presence of osmotic support (i.e. 1 M sorbitol) (de Nadal *et al*, 1998).

On the other hand, as mentioned above, the over-expression of *HAL3* induces the synthesis of G1 cyclins that accelerate the release from a halt in G1 phase and increases the rate of budding in cells lacking *sit4Δ*, suppressing, at least in part, the characteristic growth defect of *sit4Δ* cells (Di Como *et al*, 1995; de Nadal *et al*, 1998; Clotet *et al*, 1999). Besides, it is known that the *sit4Δ* and *hal3Δ* double mutations are synthetically lethal because of a G1/S blockade (Di Como *et al*, 1995; Simon *et al*, 2001) and this phenotype is suppressed by deletion of *PPZ1* (Clotet *et al*, 1999). Finally, cells with excess of Hal3 show an increase in the phosphorylation of Tef5 (elongation factor 1Bα) (De Nadal *et al*, 2001b). Therefore, Hal3 appears to negatively regulate all known Ppz1 cellular functions (Table 1).

This general effect of the regulatory subunit Hal3 on Ppz1 function appears rather different from the situation described for the Glc7 gene, the only catalytic subunit of type 1 protein phosphatase (PP1) in *S. cerevisiae*. In the latter case, deletion of *GLC7* results in lethality (Feng *et al*, 1991; Clotet *et al*, 1991) whereas the absence of regulatory components yields less dramatic phenotypes (only three of them, Scd5, Sds22 and Ypi1 are also essential), suggesting that the diverse cellular roles attributed

to Glc7 are the result of specific interactions of the catalytic subunit with different regulatory subunits (Cannon, 2010). It must be noted, however, that Ppz1 and Glc7 might not be fully insulated with respect to some specific functions or to modulation by their counterpart regulators. For instance, *PPZ1* and *PPZ2* display genetic interactions with *GLC7*, as deduced from the different growth defects observed in cells carrying certain mutant alleles of *GLC7* in combination with null alleles of the PPZ phosphatases (Venturi *et al*, 2000). As explained above, many PP1c regulatory subunits are proteins containing a consensus RVxF SLiM (Bollen *et al*, 2010), which binds to a hydrophobic groove that is strongly conserved in Ppz1. It is worth noting that *in vivo* interactions between Ppz1 and two Glc7 regulatory subunits displaying RVxF motifs (Glc8 and Ypi1), has been reported by 2-hybrid analysis (Venturi *et al*, 2000). Interaction between Ppz1 and Ypi1 has been also documented by pull-down assays (although Ypi1 barely affects Ppz1 activity), and it was shown that a W53A mutation in its $^{48}$RHNVRW$^{53}$ motif abolished binding to both the Glc7 and Ppz1 phosphatases (Garcia-Gimeno *et al*, 2003). In addition, both *S. cerevisiae* and *C. albicans* Ppz1 are sensitive *in vitro* to mammalian Inhibitor-2 (Chen *et al*, 2016b; Posas *et al*, 1995a), a PP1c regulatory subunit that contains a $^{44}$RKLHY$^{148}$ sequence functionally replacing the RVxF SLiM(Wakula *et al*, 2003). These observations suggested that the structural elements required for binding to the RVxF motif is functionally conserved in Ppz1.

The Ppz1 inhibitor Hal3 contains a $^{263}$KLHVLF$^{268}$ sequence alike to the RVxF motif. However, mutation of H$^{265}$ or F$^{268}$ does not affect binding nor the inhibitory capacity of Hal3 upon Ppz1 (Munoz *et al*, 2004), suggesting that this RVxF-like motif is not relevant for the interaction with Ppz1. Sequence comparisons and recent experimental evidence on the *C. albicans* Ppz1 C-terminal domain (Chen *et al*, 2016a) indicate that diverse SLiMs found in PP1c, such as PNUTS or spinophilin, are likely not relevant for yeast Ppz1. The structural determinants for interaction between Ppz1 and Hal3 are still unknown, but they should differ substantially from those used by PP1c-regulatory subunits to bind to PP1c, since it has been shown that Hal3 does not bind to Glc7 *in vitro* (De Nadal *et al*, 1998; Garcia-Gimeno *et al*, 2003).

In any case, Ppz1 and Hal3 can be co-expressed in *E. coli* and purified as a complex with an apparent 1:1 stoichiometry (Abrie *et al*, 2015), and a recent study has suggested that inhibition of Ppz1 by Hal3 could happen by occlusion of the catalytic site,

in a way similar to that used by inhibitor-2 to inhibit PP1c (Molero *et al*, 2017). The ability of ScHal3 to bind to and inhibit Ppz1 phosphatases has been demonstrated in the past for diverse fungal species, suggesting that this is a relatively well conserved mechanism (Ádám *et al*, 2012; Petrényi *et al*, 2016; Molero *et al*, 2013; Minhas *et al*, 2012). In *S. cerevisiae* is has been postulated that the interaction between Ppz1 and Hal3 is dependent on the internal pH and serves to maintain intracellular pH homeostasis (Yenush *et al*, 2005).

The second regulatory subunit of Ppz phosphatase is Vhs3 (YOR054c). The YOR054c gene was identified (among others) in our laboratory as a multicopy suppressor of the G1 phase blockage in a *sit4Δ hal3Δ* conditional mutant, from which its name *VHS3* (***v***iable in ***h***al3 ***s***it4) derives (Muñoz *et al*, 2003). *VHS3* encodes a 674 residues protein structurally close to Hal3 (49% identity) and maintains the characteristic acidic-rich tail.

Over-expression of *VHS3* improves the slow growth phenotype in cells lacking *SIT4*; in a *slt2Δ* background it produces a growth defect and increases sensitivity to caffeine. In terms of cations homeostasis, *VHS3* over-expression also improves salt tolerance, increasing slightly the levels of *ENA1* expression. Then, all phenotypes resulting from deletion or excess of *VHS3* are similar to those derived from that of *HAL3*, although the effect is usually less noticeable. This suggested that *VHS3* functionally mimics Hal3. Therefore, Vhs3 acts as a negative regulatory subunit of the Ppz1 but with lesser effective biological role that its paralog Hal3, which could be explained due to lower *VHS3* mRNA levels (Ruiz *et al*, 2004a).

| Cellular Process | Strain | *PPZ1* | | *HAL3* | |
|---|---|---|---|---|---|
| | | **Over-expression** | **Deletion** | **Over-expression** | **Deletion** |
| **Saline Homeostasis** | Wild Type | NA | $Na^+$/ $Li^+$ tolerance | $Na^+$/ $Li^+$ tolerance | $Na^+$/ $Li^+$ sensitivity |
| | *ppz1Δ* | - | - | $Na^+$/ $Li^+$ tolerance | NP |
| | *ppz1Δ ppz2Δ* | - | - | NP | NP |
| **Cell Cycle Progression** | Wild type | No/slow Growth | NP | NP | NP |
| | *sit4Δ* | Lethal | Improves Growth | Improves Growth | Lethal |
| **Cell Integrity** | Wild type | NA | Caffeine sensitivity | NP | NP |
| | *slt2Δ* | Improves Growth | Lethal | Lethal | Improves Growth |
| **Protein translation** | Wild type | NP | Tolerance to translational inhibitors and decrease translational fidelity | Tolerance to translational inhibitors and decrease translational fidelity | Induces allosupression |

**Table 1. Phenotypic comparison between the overexpression or deletion of Ppz1 and its negative regulate subunit Hal3.** The phenotypes are grouped according to the cell processes. NA: not analyzed; NP: no phenotype. Modified from (Zhang, 2019).

The *hal3Δ vhs3Δ* double mutation is synthetically lethal, but this phenotype, contrary to that expected, is not caused by excess of Ppz1 phosphatase activity, because deletion of *PPZ1* and *PPZ2* cannot rescue the lethal phenotype produced by the absence of their regulatory subunits (Ruiz *et al*, 2004a). This observation suggested for the first time that Vhs3 and/or Hal3 could be acting in other functions, independently of their inhibitory role of Ppz phosphatases.

The *S. cerevisiae* genome contains another structurally Hal3-related protein, named Cab3. Cab3 is characterized as an essential protein showing a 28% sequence

identity to Hal3. Moreover, Cab3 contains a C-terminal acidic tail as Hal3 and Vhs3. However, it has been demonstrated that Cab3 is not able to inhibit the phosphatase activity of Ppz1 (Ruiz *et al*, 2009a).

Published studies demonstrated that Hal3 and Vhs3 are moonlight proteins that associate with Cab3 (also a Hal3 and Vhs3 paralog) to form an active, heterotrimeric phosphopantothenoylcysteine decarboxylase (PPCDC) enzyme (Ruiz *et al*, 2009). While in most organisms PPCDC is an homotrimer with three catalytic sites, each formed at the interface of two monomers; in budding yeast a single catalytic site is formed at the interface of Cab3 and either Hal3 or Vhs3, thus explaining the essential nature of *CAB3* and the synthetically lethal phenotype of the *hal3Δ vhs3Δ* mutations (Ruiz *et al*, 2009). It has been proposed that Vhs3 has a higher tendency to form heterotrimers, whereas Hal3 can be easily released and undergo monomer exchange, thus becoming able to interact with Ppz1 (Abrie *et al*, 2015).

The subunit composition of *S. cerevisiae* PPCDC is rather exceptional, not only because in most eukaryotic organisms, such as humans and plants, PPCDC is an homotrimer, but also because this unique component subunit is a much shorter polypeptide ( ~250 residues), lacking the N-terminal extension and the large acidic C-terminal tail also found in certain fungal orthologs, such as in *C. albicans* (Petrényi *et al*, 2016).

Previous studies have shown that this central domain, denoted as Hal3 PD, is required for Ppz1 binding and regulation, although the acidic C-terminal tail also plays an important functional role (Abrie *et al*, 2012). Full-length Hal3 (as well as the PD domain) can form trimers itself. This ability is altered by mutation of L405 to Glu, which would disrupt a possible hydrophobic core in the trimer, although the change does not abolish the ability to interact with Cab3 and to generate a functional PPCDC *in vivo*. Remarkably, this mutation also decreases binding with Ppz1 *in vitro* and causes partial loss of Ppz1-mediated Hal3 functions *in vivo* (Santolaria *et al*, 2018).

A coarse functional mapping of Hal3 has been carried out (Abrie *et al*, 2012). As shown in Figure 8, the conserved central domain (PD) plays a key role in the PPCDC activity. Instead, neither the N-terminal extension nor the acidic C-terminal tail appear necessary for PPCDC function. Besides, the Hal3 PD domain itself did not show inhibitory capacity to the Ppz1 phosphatase activity, although it is essential in Ppz1 binding and

regulation. The C-terminal acidic tail is required for the Ppz1 inhibition. Moreover, previous studies showed that mutation of several amino acids at the PD domain affected the capacity to bind or inhibit Ppz1 without interference with the PPCDC activity (Muñoz *et al*, 2004; Santolaria *et al*, 2018). In conclusion, the Hal3 structural determinants required for Ppz1 regulation and PPCDC function are independent.

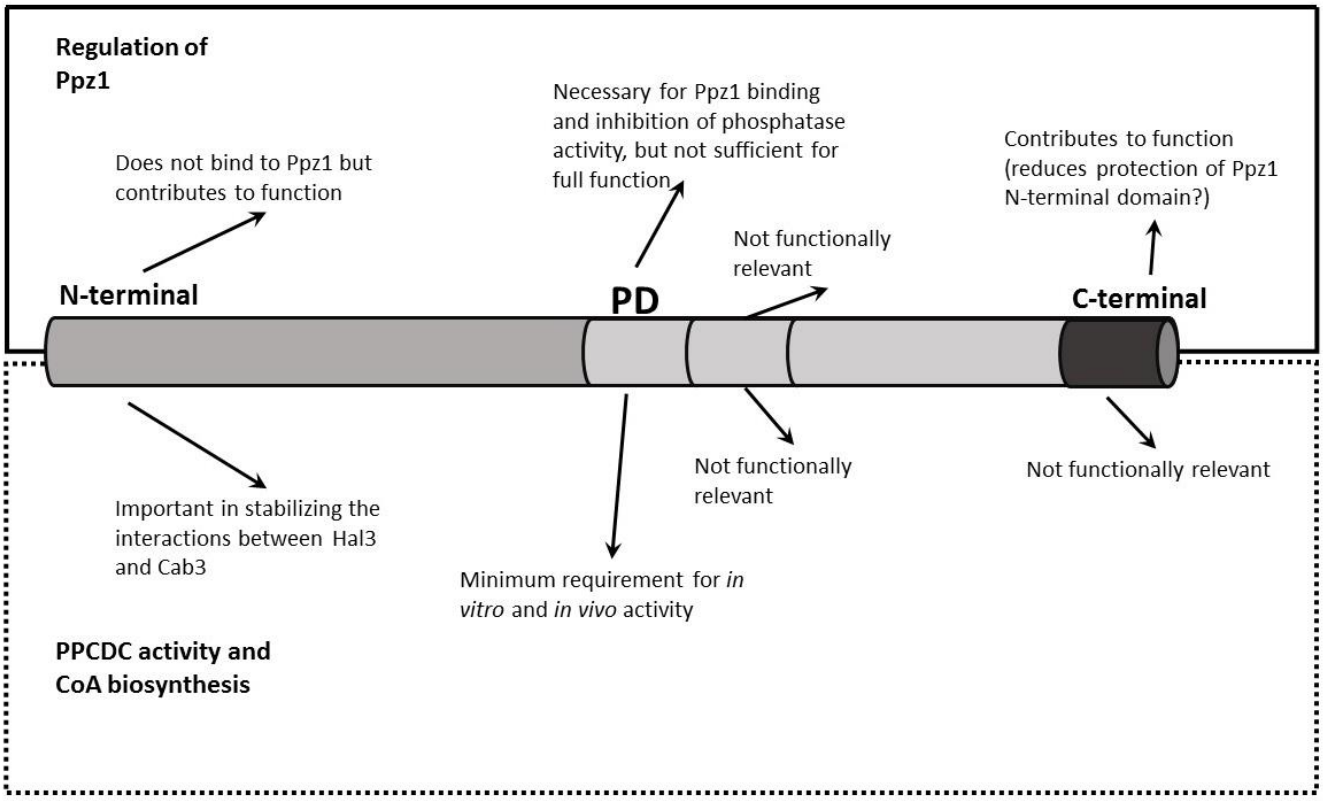


**Figure 8.- Schematic representation of the functional domains of Hal3.** PD: Core domain, which contains the essential residues for PPCDC activity. (Adapted from (Abrie *et al*, 2012)).

## 7.- Characteristics of the N-terminal half of Ppz1

The N-terminal half contains multiple potential phosphorylation sites for a number of known protein kinases, including PKA, PKC and Ck-2 (Posas *et al*, 1995b). It is conceivable that phosphorylation might occur *in vivo* under certain conditions and, perhaps, regulate the intracellular localization of the protein. However, it does not seem

to be necessary for the enzyme activity, as deduced from the evaluation of the recombinant enzyme expressed in *E. coli* (Posas *et al*, 1995a). Although the function of the Ppz1 N-terminal extension is unknown, it has been reported that it might be relevant for specificity, and contains some regions that are required for specific Ppz1 functions. In addition, it was suggested that the N-terminal domain may have a regulatory role for the C-terminal domain, protecting thereby the phosphatase activity (Clotet *et al*, 1996), and interfering with the binding of the C-terminal Ppz1 domain and the regulatory subunits Hal3 and Vhs3.

As shown in Figure 9, some studies where specific deletions of the N-terminal region are analyzed, shows that this region is important for the function of Ppz1 and could affect the interaction with Hal3. For example, the change of Gly2 to Ala, preventing the myristoylation of the phosphatase, abolished the complementation of the lithium tolerant phenotype (Clotet *et al*, 1996). Deletion of residues 17-193 does not affect normal activity of Ppz1 in salt tolerance, but this version does not complement the caffeine sensitivity of the *ppz1* mutant (Clotet *et al*, 1996). Also this deletion increases binding with Hal3, in comparison with Ppz1 full-length (de Nadal *et al*, 1998). In contrast, a deletion comprising residues 241 and 318 does complement the caffeine sensitivity of the mutant, but does not normalize the salt tolerance of a *ppz1* mutant (Clotet *et al*, 1996). Deleting residues 241-318 slightly increased the binding with Hal3 (De Nadal *et al*, 1998). It has been also shown that a deletion of residues 43-52 is not functional in complementing the salt tolerant phenotype. These amino acids constitute a Ser/Arg rich motif that is conserved in many *PPZ1* orthologues. When tested for Hal3 interaction, this version did not differ from the native phosphatase (Minhas *et al*, 2012).

In conclusion, the function of the N-terminal Ppz1 domain is unknown, but it seems important for Ppz1 function, both playing roles in Ppz1 localization and the interaction with Hal3.

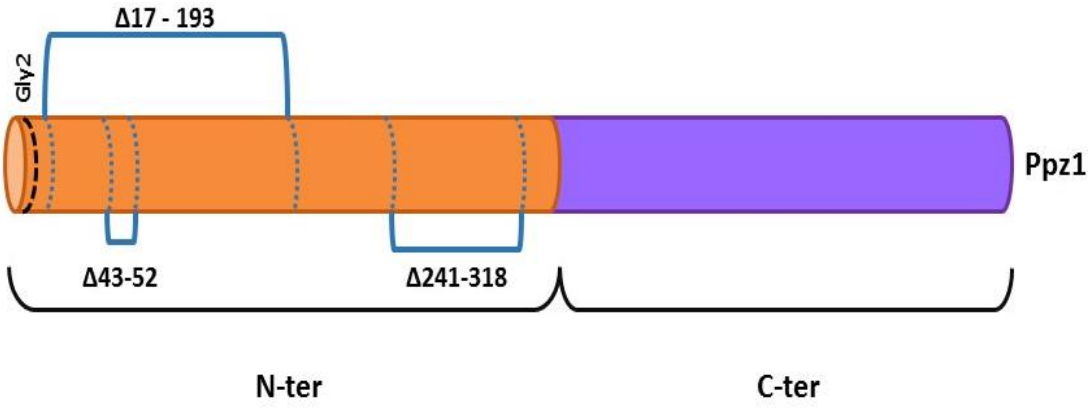


**Figure 9. Schematic representation of Ppz1 protein**. Different studied deletions is marked in blue showing the positions.

## 8.- Toxicity of Ppz1 over-expression

As for PP1, the activity of Ppz1 must be tightly regulated. One of the reasons is that the over-expression of Ppz1 has been shown to be detrimental for yeast cell growth (Clotet *et al*, 1996; De Nadal *et al*, 1998). The expression of *PPZ1* from its own promoter in episomal plasmids already reduces growth rate, compared with wild type cells. In fact, the over-expression of *PPZ1* using a strong inducible promoter, such as *GAL1*, shows a dramatic decrease in growth both in liquid cultures and in plates. It has been demonstrated that the over-expression of the C-terminal half of *PPZ1* results in an equivalent phenotype, whereas the over-expression of the N-terminal half does not affect growth (Clotet *et al*, 1996). It has been demonstrated too, that the over-expression of *HAL3* improves growth of cells overexpressing *PPZ1* (De Nadal *et al*, 1998).

Remarkably, a genome-wide study in *S. cerevisiae*, in which the tolerance limit of gene over-expression from the strong inducible *GAL1-10* promoter is measured, has identified Ppz1 as one of the most toxic proteins in over-expression (Makanae *et al*, 2013).

Work in our laboratory has demonstrated that the toxic effect of the over-expression of Ppz1 is due to the increase in phosphatase catalytic activity. In fact, the over-expression of the catalytically impaired version $Ppz1^{R451L}$ shows a growth rate almost equal than that of wild type cells. This indicate that the toxicity is not due to a possible titration of the Hal3 and Vhs3 regulatory subunits, which are essential in the CoA biosynthetic pathway (Zhang, 2019).

## 9.- Ribosome biogenesis and translation in *S. cerevisiae*

Ribosomes are the highly conserved cellular machinery that catalyze protein synthesis. Ribosomes are formed by complexes between RNA and RNA-biding proteins named ribonucleoprotein particles (RNP). In eukaryotes, the ribosome is formed by of a large 60S subunit and a small 40S subunit. In *S. cerevisiae*, hundreds of copies of rRNAs (5S, 5.8S, 18S, and 25S) are encoded in the rDNA locus located in chromosome 12. The rRNAs are produced in two separate transcripts, the 5S and the 35S transcript, which contains rRNAs 5.8S, 18S and 25S (Venema & Tollervey, 1999; Jenner *et al*, 2012).

In an exponential culture of *S. cerevisiae* in a rich medium, 60 % of total transcription is devoted to ribosomal RNA and 90 % of mRNA splicing is focused on the production of mRNAs for ribosomal proteins, consuming an enormous amount of cell resources. Coordinated regulation of the expression of rRNA and ribosomal protein genes is affected by nutritional changes *via* a number of signal transduction pathways that can quickly induce or silence these genes (Li *et al*, 1999; Zhao *et al*, 2003).

Both subunits of the ribosome need to assemble, and this process occurs in different parts of the cell and through a very complex mechanism. Ribosomal protein encoding genes are transcribed in the nucleus, and the mRNA is transported to the cytoplasm for translation. The “novo” synthesized ribosomal proteins will then enter the nucleus and they will associate in the nucleolus with the two rRNA transcripts, the 35S is methylated, and then cleaved into three individual rRNAs (18S, 5.8S and 25S) as part of the assembly process (Venema & Tollervey, 1999). After that, separated ribosomal subunits are transported from the nucleolus to the cytoplasm, where they assemble into mature ribosomes before functioning in translation (Moritz *et al*, 1990; Milgrom *et al*, 2007).

## 9.1.- Initiation of translation and its regulation

Translation is the process in which ribosomes perform the synthesis proteins in the cytoplasm or endoplasmic reticle (ER).Translation is divided in three stages: 1) initiation, 2) elongation and 3) finalization.

Translation initiation is the process by which the ribosomal subunits are properly assembled forming a 80s competent ribosome, in which the initiation codon is paired with the anticodon of the initiator tRNA (Met-tRNA$^{met}$) in the ribosomal P-site (Jackson *et al*, 2010).

The translation initiation mechanism is mediated by a set of highly conserved proteins named eIFs (eukaryotic initiation factors) and associated proteins. This process comprises two steps: first, the formation of 48S initiation complexes with the correct codon-anticodon base-pairing in the P-site of the 40S ribosomal subunits and second, the binding of 48S complexes with the 60S subunit to form the final 80S ribosome.

To assemble the 48S complexes is necessary first to form a 43S preinitiation complex, which is formed by a 40S ribosomal subunit, the eIF2-GTP-Met-tRNA$^{met}$ Ternary complex (TC), eIF3, eIF1A and eIF5 (Hinnebusch, 2005). Besides, it is also necessary the correct formation of the Closed Loop Complex, constituted by a loop between the CAP and the poly-(A) of the mRNA, and several proteins (as eIF4G, eIF4A , eIF4E, and Pab1) (Tomek & Wollenhaupt, 2012). Once this happens, the 43S complex and Closed loop Complex form the 48S complex, and together with the 60S ribosomal subunit and eIF5B finally assemble to form the 80S initiation complex (Jackson *et al*, 2010).

These processes are strictly regulated and this is of vital importance in order to survive environmental changes. Translational initiation regulation involves modification of protein activities, changes in protein interactions and stabilities, and post-translational modifications. Two known regulatory pathways are the GAAC (general amino acid control) and the TOR (target of rapamycin) pathway have a key role regulating translation initiation in front different stresses (Simpson & Ashe, 2012;

Sonenberg & Hinnebusch, 2009). As can be observed in Figure 11, this regulation affects both the Closed loop Complex and the Ternary Complex formation.

In case of amino acid depletion there is an increase in uncharged tRNAs. This activates the protein kinase Gcn2, responsible for the phosphorylation of the α-subunit of the initiation factor eIF2 at Ser 51 (Dey *et al*, 2011; Dever *et al*, 1992), encoded in *S. cerevisiae* by the gene *SUI2*. eIF2α phosphorylated at Ser51 acts as a competitive inhibitor of eIF2B (a guanine-nucleotide-exchange factor), triggering an accumulation of inactive eIF2-GDP, and a decrease in TC, thus decreasing the rate of translation initiation (Gordiyenko *et al*, 2019). Inhibition of translation can occur in response to other stresses as high salt, oxidative stress or by exposure to rapamycin, an antifungal and immunosuppressant macrolide that inhibits TORC1 (Hinnebusch, 2005; Simpson & Ashe, 2012).

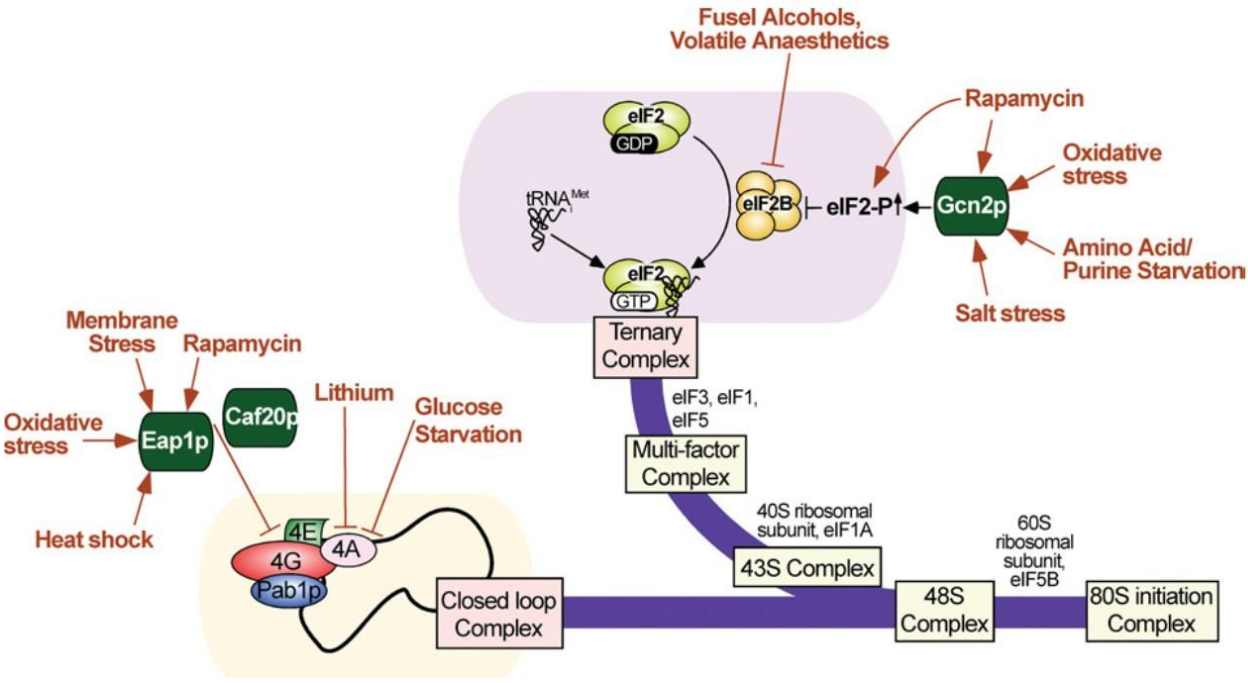


**Figure 1. Schematic representation of stress targets in the translation initiation process in *S. cerevisiae*.** Image from (Simpson & Ashe, 2012).

## 9.2.- Npl3 and its role in translation

The pre-60S complex requires the serine/arginine-rich (SR) protein Npl3 to be exported from the nucleus to the cytoplasm (Hackmann *et al*, 2011). This protein is also involved in mRNA export and in the early spliceosome recruitment (Kress *et al*, 2008). When Npl3 is dephosphorylated by Glc7 inside the nucleus, on the one hand it can bind to the Rpl10 protein to export the pre-60s to cytoplasm (Baierlein *et al*, 2013) and on the other hand Npl3 accompanies the pre-mRNA from the nucleus to the cytoplasm (Gilbert *et al*, 2001). After that, Npl3 is phosphorylated by the kinase Sky1, being the importin Mtr10 also necessary to return Npl3 to the nucleus (Windgassen *et al*, 2004). In fact, some mutants of interacting regions of Npl3 show an accumulation of ribosome 60S subunit in the nucleus and a decrease in translation (Windgassen *et al*, 2004; Baierlein *et al*, 2013). Npl3 binds to the pre-mRNA, interacting with the initiation factor eiF4G to inhibit translation. This factor plays an important role as a scaffolding protein for the recruitment of translation repressors (Rajyaguru *et al*, 2012). It is remarkable that Npl3 is toxic in over-expression due to its inhibitory role in translation and, in most strains, the deletion of *NPL3* is lethal (Russell & Tollervey, 1992; Lund *et al*, 2008).

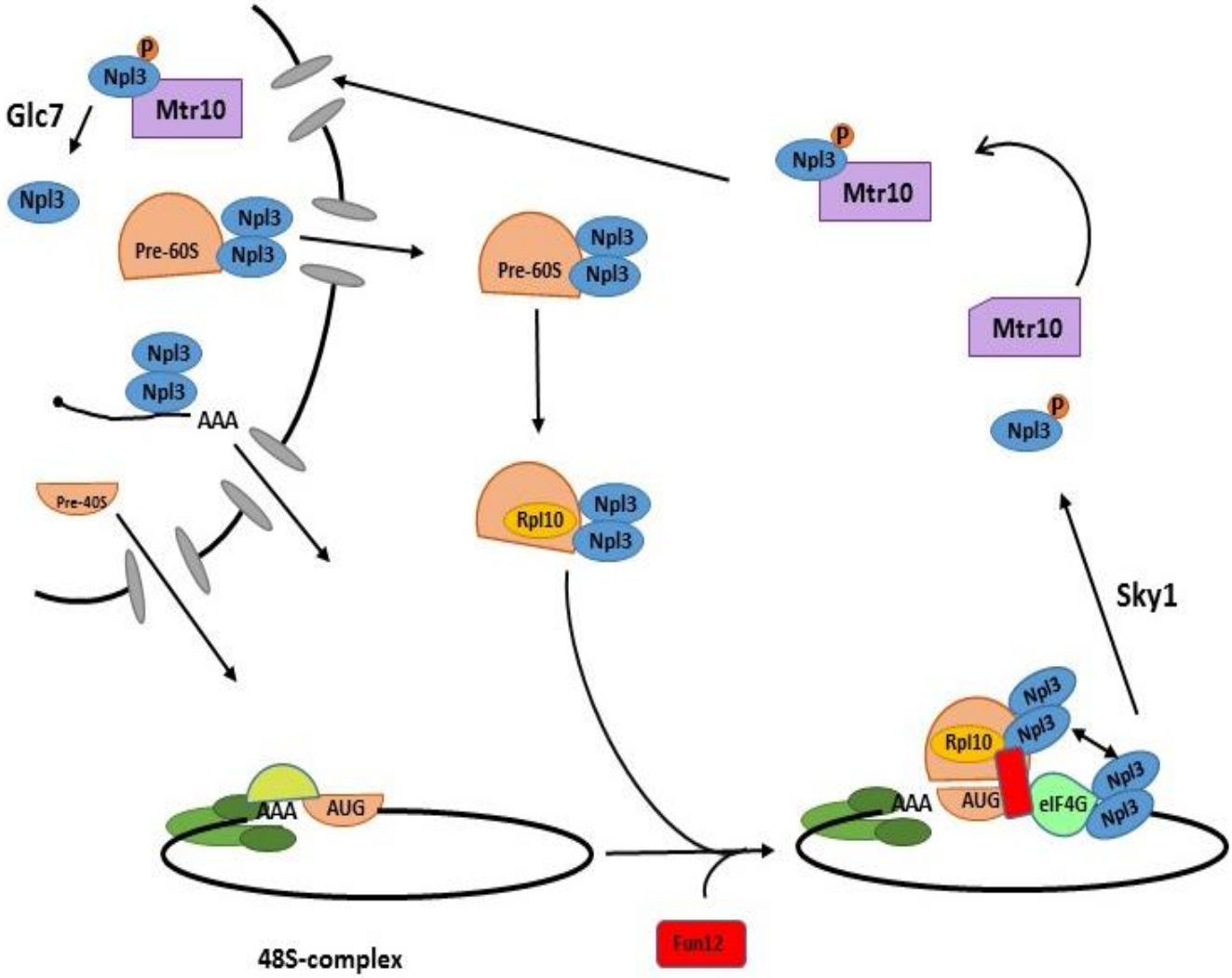


**Figure 11. Model for Npl3 function in translation initiation.** Npl3 executes the nuclear export of mRNA. Npl3 bound to mRNA interacts with the initiation complex after scanning and recognizing the AUG. The 40S ribosomal subunit will assemble with the mature 60S subunit. Besides, Npl3 is involved in the export of pre-60S particles and will remain bound to it through cytoplasmic maturation. Adapted from (Baierlein *et al*, 2013).

## 9.3.- The target of rapamycin (TOR) pathway and Rps6A

TOR (Target of Rapamycin) is a highly conserved kinase, and it plays important and central roles in the cell. As it was commented above, the TOR pathway can regulate the initiation of translation. Besides, the TOR pathway controls cell growth by regulating gene transcription, ribosome biogenesis, lipid synthesis, autophagy and actin polarization (Loewith & Hall, 2011). In *S. cerevisiae* there are two *TOR* genes, *TOR1* and *TOR2,* while in higher eukaryotes there is only one. The Tor proteins can be found in two functionally and distinct multiprotein complexes in yeast cells. These are named TOR complex 1 (TORC1) and TOR complex 2 (TORC 2). Rapamycin inhibits TORC1 but not TORC2 (Yerlikaya *et al*, 2016; Loewith & Hall, 2011).

One of the first ribosomal proteins found to undergo phosphorylation was the ribosomal protein S6 (Rps6) (Gressner & Wool, 1974). Rps6 is highly conserved from yeast to mammalian cells. In *S. cerevisiae* Rps6 is encoded by two genes, *RPS6A* and *RPS6B*. In its carboxy-terminus there are 2 sites of phosphorylation (Ser-232 and Ser-233), corresponding to Ser-235 and Ser-236 in higher eukaryotes, which have five sites of phosphorylation instead of two (Yerlikaya *et al*, 2016). Rps6 phosphorylation is sensitive to hormones, nutrients and to different stress conditions (Meyuhas, 2008). In yeast, on the one hand TORC1 regulate the phosphorylation state of of Rps6A via the AGC kinase Ypk3 and the PP1 phosphatase Glc7 of both serine residues (232 and 233). On the other hand TORC2 regulates phosphorylation of only Ser-232 via Ypk1 (Yerlikaya *et al*, 2016; González *et al*, 2015). For these reasons, Rps6 phosphorylation is usually used as readout of TOR pathway activation. However, the physiological role of Rps6 phosphorylation in yeast is unknown despite years of research.

# MATERIAL AND METHODS

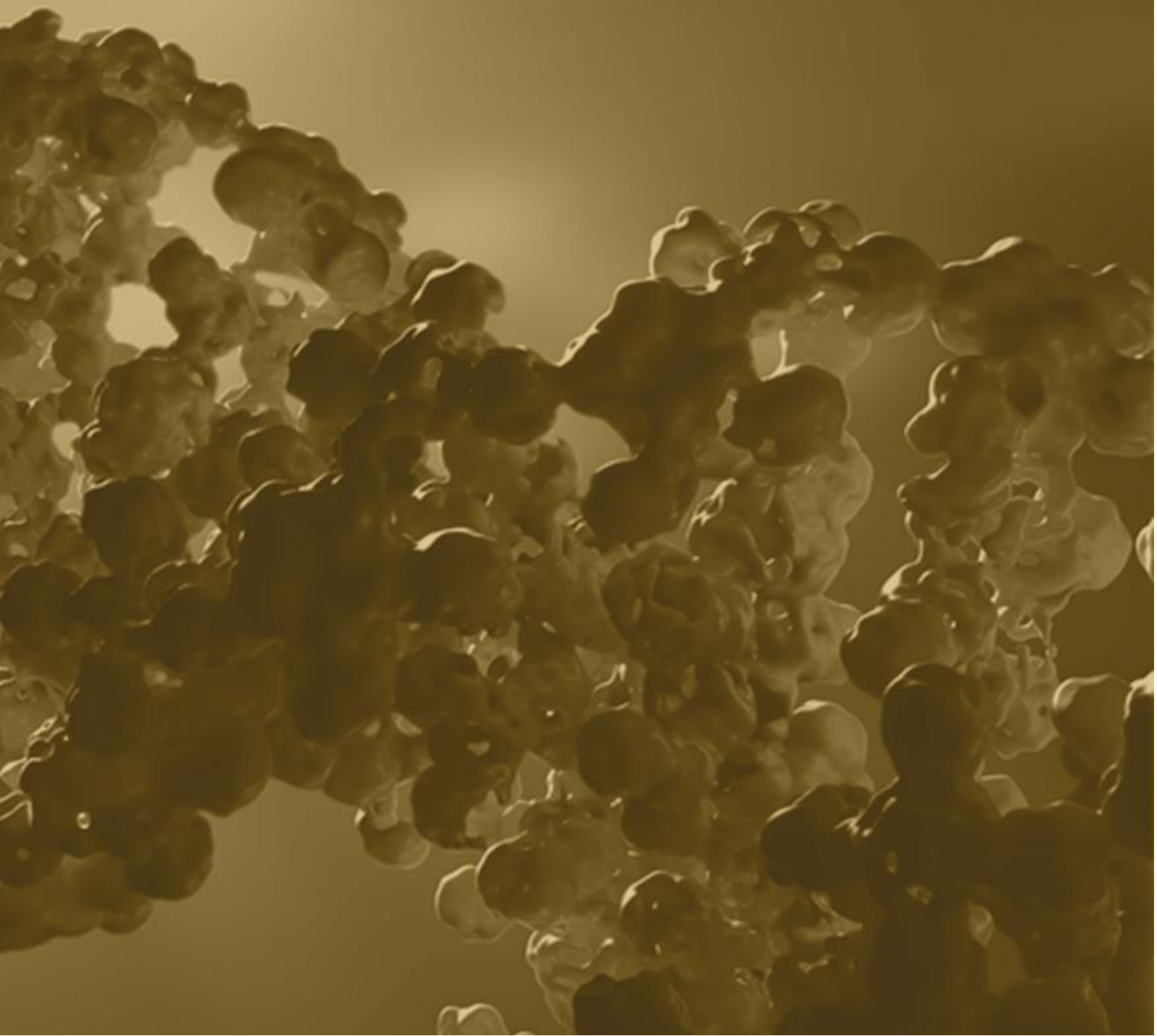

## 1.- Yeast strains and media

*S. cerevisiae* cells were grown at 28°C in YPD medium (10 g/L yeast extract, 20 g/L peptone and 20 g/L dextrose). For plasmid selection, cells were grown in synthetic medium composed of: 0.17% yeast nitrogen base (YNB) without ammonium sulfate and amino acids, 0.5% ammonium sulfate, 2% glucose and 0.13% drop-out mix (lacking the appropriate selection requirements)(Adams, A., gottschling, D.E.; Kaiser, C.A., and Stearns, 1997). When necessary, cells were grown in Translucent $K^+$-free medium (which carries only ≈ 15 µM $K^+$, ≈ 2 µM $Na^+$ and ≈ 70 mM ammonium) (CYN7505-Formedium) instead of YNB and containing in each case the specified concentration of KCl. These media were prepared with the proper carbon source and drop-out mix.

For fluorescence microscopy and flow cytometry, in order to reduce background fluorescence, the carbon source (glucose, raffinose or galactose) was sterilized separately and then added to the synthetic medium.

The yeast strains used in this work are listed in Table 1 of Annexes.

## 2.- Recombinant DNA techniques

*Escherichia coli* DH5α cells were used as a plasmid DNA host and were grown at 37°C in LB (Lysogeny Broth ), whose composition is 10 g/L of Tryptone, 5g/L of yeast extract, and 5g/L of NaCl, and supplemented, if necessary, with 100 µg/mL ampicillin for plasmid selection. Restriction reactions, DNA ligations, and other DNA recombinant techniques were performed as described in (Sambrook *et al*, 1989). In some cases, when *dam* methylation was a problem (e. g. for XbaI sites in *HAL3*), the GM2163 *E. coli* strain (*dam*- ) (Palmer & Marinus, 1994) was used for cloning. This strain was grown with 10 ug/ml chloramphenicol for selection.

DNA fragment purification, such as PCR products or restriction enzyme digestions, was done by isolation of the fragments by agarose gel electrophoresis. The bands of interest were purified using the NucleoSpin Gel and PCR Clean-Up kit (Macherey-Nagel)

*E. coli* cells were transformed by the standard calcium chloride procedure (Sambrook *et al*, 1989). *S. cerevisiae* cells were transformed following the lithium acetate method as described in (Ito *et al*, 1983). For heterologous transformation with disruption or tagging cassettes containing the genes *kanMX4* or *natNT2* (Goldstein & McCusker, 1999), after the heat shock, cells were resuspended in 0.5 mL of YPD and incubated at 28°C for 3 hours to allow the expression of resistance to G418 (Calbiochem) (Jimenez & Davies, 1980) o nourseothricin (Werner Bioagents) (Krügel *et al*, 1988). Cell were then plated on YPD plates containing G418 (200 μg/mL) or nourseothricin (200 μg/mL), respectively.

The correct insertion of the recombinant cassettes was verified by colony PCR (Illuxley *et al*, 1990). Yeast cells were deposited at the bottom of a 0.1 mL Eppendorf tube, incubated for 60 seconds at the microwave at maximal power, and immediately left at -20°C for 5 min before performing the PCR procedure.

## 2.1.- Quickchange PCR method

To perform point substitutions or deletions in genes as *PPZ1* or *HAL3*, a QuickChange site-directed mutagenesis method was used (Liu & Naismith, 2008). This procedure consist in the use of two pairs of complementary primers, both containing the mutations. The amplification of the entire template is carried out, with 1 min/kb of extension time. In our case, Q5 High-Fidelity DNA Polymerase (New England Biolabs) was used and the final volume of the reaction was 50 μL. The PCR product was purified with NucleoSpin Gel and PCR Clean-Up kit (Macherey-Nagel) and it was eluted in 30 μL. After that the PCR template is digested using DpnI (FastDigest, Thermo Scientific), an enzyme that recognizes the 5'-Gm6A^TC -3' sequence. To conclude, the digested product is use to transform *E. coli*.

## 3.- Deletion and tagging cassettes

Strains **DVS001**, **DVS002** and **DVS003**, carrying chromosomically integrated versions of *PPZ1* C-terminally tagged with different fluorescents proteins (Green fluorescent protein, GFP; Cyan fluorescent protein, CFP; and Yellow fluorescent protein, YFP), were constructed by transformation of the wild type strain DBY746 with cassettes (2.3 kb) amplified with primers S3_Ppz1_Ct_Fluo_Fw and S2_Ppz1_Ct_Fluo_Rev from vectors pYM28 (GFP), pYM31 (CFP) and pYM39 (YFP) following the protocol described in (Janke *et al*, 2004). The obtained cassettes were named *PPZ1-EGFP-HIS3MX6*, *PPZ1-CFP-HIS3MX6* and *PPZ1-YFP-kanMX4*.

Strains **DVS004**, **DVS005** and **DVS006**, carrying versions of *HAL3* C-terminally tagged with EGFP, CFP and YFP, respectively, were constructed as described above, but using primers S3_Hal3_Ct_Fluo_Fw and S2_Hal3_Ct_Fluo_Rev. The cassettes generated (HAL3-*EGFP-HIS3MX6*, *HAL3-CFP-HIS3MX6* and *HAL3-YFP-kanMX4*) were used to transform the DBY746 wild type strain.

Strains **DVS007** and **DVS008** were made by transformation of wild type strain DBY746 with PPZ1-mCherry-kanMX4 and HAL3-mCherry-kanMX4 cassettes obtained by PCR amplification from pFA6a-mCherry-kanMX4 plasmid using S3_Ppz1_Ct_Fluo_Fw and S2_Ppz1_Ct_Fluo_Rev primers for PPZ1-mCherry-kanMX4 and S3_Hal3_Ct_Fluo_Fw and S2_Hal3_Ct_Fluo_Rev primers for HAL3-mCherry-kanMX4.

Strain **DVS009** was constructed by transformation of strain DVS001 with the HAL3-mCherry-kanMX4 cassette. Similarly, strain **DVS010** was made by transformation of strain DVS004 with the PPZ1-mCherry-kanMX4 cassette. Strain **DVS011** was created by transformation of strain DVS003 with the *HAL3-CFP-HIS3MX6* cassette, whereas strain **DVS012** was obtained by transformation of DVS006 with the *PPZ1-CFP-HIS3MX6* cassette.

Strain **DVS013,** carrying a version of *PPZ1* encoding an N-terminal GFP-tag driven by the *GAL1-10* promoter, was created by transformation of wild type DBY746 with a 2.6-kbp NAT1-pGAL-GFP-PPZ1 cassette. This cassette was obtained by PCR amplification of plasmid pYM-N25 (Janke *et al*, 2004) with S1_Ppz1Nt_Fluo_Fw and

S4_Ppz1_Nt_Fluo_Rev primers, using the same conditions that in (Janke *et al*, 2004). To obtain the **DVS014** strain, we used the same method but changing the primers (S1_Hal3_Nt_Fluo_Fw and S4_Hal3Nt_Fluo_Rev) to obtain the NAT1-pGAL-GFP-HAL3 cassette.

The C-terminally tagged strains **DVS015** (PPZ1-YFP), **DVS016** (HAL3-YFP), **DVS017** (PPZ1-CFP), **DVS018** (HAL3-CFP), **DVS019** (PPZ1-YFP and HAL3-CFP) and **DVS020** (PPZ1-CFP and HAL3-YFP) were constructed following the same strategy, but using the BY4741 background.

In order to overexpress Ppz1 two BY4741 derivative strains were created. In strain ZCZ01, the *PPZ1* promoter was exchanged by the *GAL1-10* promoter (Zhang, 2019) whereas in strain in strain MLM004 it was replaced by the $tetO_7$-based tet-OFF promoter.

All yeast strains used in this work are listed in table 1 of Annexes.

## 4.- Plasmids

Yeast plasmids:

**-pBV215**: pNC160-based plasmid that includes the *PPZ1* gene with a GFP tag in the +54 bp position of the *PPZ1* ORF (Venturi *et al*, 2000).

**-pEGH**: yeast plasmid (*URA3* marker) for expression of GST N-terminally fused proteins from the *GAL1-10* promoter(Zhu *et al*, 2008).

**-pEGH-Ppz1**: plasmid for expression of the coding region of Ppz1 with GST N-terminal tag, inducible by galactose (Zhu *et al*, 2008).

**-pEGH-Ppz1 R451L**: similar to pEGH-Ppz1 but contains an catalytically inactive version of Ppz1. The Kpn2I-PacI (625 bp) fragment was removed and exchanged by the same fragment from YCp-$PPZ1^{R451L}$ (Clotet *et al*, 1996).

**-pHA-Mig1:** Episomal plasmid pRS426 (*bla*, *URA3*) containing the *MIG1* gene with a HA tag (Treitel *et al*, 1998).

**-pRS315 *GFP-NPL3***: Centromeric vector (*bla*, *URA3*) containing the *NPL3* gene with a GFP tag (Lund *et al*, 2008)

**-pRS316**: Centromeric vector containing the *URA3* gene for marker selection (Sikorski & Hieter, 1989).

-**pRS316-*PPZ1***: pRS316 plasmid (*bla*, *URA3*) containing the *PPZ1* gene (2750 bp) from plasmid YCp33-PPZ1 (Aksenova *et al*, 2007) cloned at BamHI/HindIII sites of pRS316 (Molero *et al*, 2017).

**-pRS316 GFP-PPZ1**: pRS316 plasmid containing a GFP-*PPZ1* gene (3450 bp) that derives from YEp195 GFP-PPZ1 (see below)cloned in the BamHI/HindIII sites.

**-pYES2**: episomal plasmid (*URA3* marker) for galactose-inducible expression in *S. cerevisiae* under the control of the *GAL1-10* promoter (Invitrogen).

**-pYES2 Ppz1**: pYES2 plasmid that contains the *PPZ1* ORF to overexpress the phosphatase in *S. cerevisiae* upon addition of galactose to the medium (Clotet *et al*, 1996).

-**YEplac181**: episomal plasmid carrying the *LEU2* marker. Used in the same way than YEplac195 (Gietz & Akio, 1988).

**-YEplac181 *HAL3***: YEp181 plasmid that contains the *HAL3* gene (2.4 Kpb) cloned at EcoRI/HindIII sites.

-**YEplac195:** episomal plasmid with *URA3* marker for high-copy number expression (Gietz & Akio, 1988).

**-YEplac195 *HAL3*:** YEp195 plasmid that contains the *HAL3* gene (2.4 Kbp) cloned at EcoRI/HindIII sites (Muñoz *et al*, 2004).

**-YEplac195 *NPL3*:** episomal plasmid that contains the *NPL3* gene, amplified from genomic DNA with primers BamHI_Npl3_prom_Fw and SacI_Npl3_term_Rev (2240 bp, from -437 respect the initiating ATG to 525 nt downstream the stop codon), and cloned in the BamHI/SacI sites of the YEplac195 plasmid.

**-YEplac195 *PPZ1*:** YEp195 plasmid containing the *PPZ1* gene (2750 bp) that was extracted from plasmid pRS316-PPZ1 (Molero *et al*, 2017) and cloned at BamHI/HindIII sites.

**-YEp195 GFP-PPZ1**: YEP195-PPZ1 plasmid that includes a GFP tag inserted in the +54 bp (XhoI site) position of the *PPZ1* ORF, recovered from pBV215 plasmid (fragment XhoI-XhoI).

**-YEplac195-SKY1:** episomal plasmid that contains the *SKY1* gene, amplified from genomic DNA with primers Sky1_Fw and Sky_Rev (3200bp, from -715 respect the initiating ATG to 397 nt downstream the stop codon), and cloned in the SalI/BamHI sites of the YEplac195 plasmid.

-**YEplac195 VHS2-6HA**: YEp195 plasmid carrying the *VHS2-6HA* gene amplified from strain RF1668 (Cassani *et al*, 2014) using SacI_Fw_vhs2_prom and KpnI_Rev_vhs2HA_term primers. The fragment (about 2.2 kbp) was cloned in YEp195 in the KpnI and SacI sites.

-**YEplac195 VHS2-6HA S314A**: YEplac195 *VHS2-6HA* mutagenized in Ser314 to Ala using the Quickchange PCR method.

-**YEplac195 VHS2-6HA S314D:** YEplac195 *VHS2-6HA* mutagenized in Ser314 to Asp using the Quickchange PCR method.

For *E. coli* heterologous expression:

**-pET-Duet-1:** Bacterial vector for the co-expression of two genes. The vector contains two multiple cloning sites (MCS), each of which preceded by a T7 promoter, *lac* operator and ribosome binding site (RBS). The plasmid contain the gene *bla* (Novagen).

**-pET-Duet-1-Ppz1Cter+Hal3**: pETDuet1 plasmid for the co-expression of the 6xHis-tagged catalytic domain of Ppz1 (Ppz1 C-ter, Δ1-344) and untagged Hal3 as recombinant proteins.

**-pGEX-6P-1**: plasmid for bacterial expression of GST (glutathione transferase) fusion proteins, with a PreScission protease site (Amersham Biosciencies).

**-pGEX-6P-1-Ppz1**: plasmid for expression in *E. coli* of the GST-fused coding region of Ppz1 (Ruiz *et al*, 2004a).

**-pGEX-6P-1-Hal3**: plasmid for expression of the *HAL3* coding region in *E. coli* as a recombinant protein fused to GST (Ruiz *et al*, 2004a).

## 5.-Mutations at the N-terminal region of Ppz1 and Hal3

In the case of Ppz1 we mutagenized some residues of the N-terminal region of the phosphatase, specifically Ser49, Thr261, Ser265 and Ser310 to Ala, and also generated the phosphomimetic change (to Asp or Glu). To accomplish these mutations we used different procedures.

To change Ppz1 T261 to Alanine a mutagenic PCR was done in 2-steps. First, two overlapping fragments were generated using the pairs of oligonucleotides Ppz1_HpaI_5/Ppz1_T261A_3 and Ppz1_BspEI_3/Ppz1_T261A_5 with plasmid pRS316 PPZ1 as template. A mixture of both fragments was subsequently amplified using Ppz1_HpaI_5 and Ppz1_BspEI_3. The final amplification fragment was cloned into the HpaI and BspEI sites of plasmid pRS316 PPZ1. The same method was used to generate the change of S265 to Ala, and the double mutant T261A and S265A using different pairs of primers (listed in Annex 3).

To create the pRS316 *PPZ1* T261E plasmid, a QuickChange site-directed mutagenesis method was employed. The pair of oligonucleotides Ppz1_T261E 5 and Ppz1_T261E 3 were used to amplify the plasmid pRS316 PPZ1. The same procedure was used to generate the S265D, T261E/S265D, S49A and S49D mutations, but changing the pairs of oligonucleotides for each specific mutagenesis.

To combine the S49A and S49D mutations in the pRS316 *PPZ1* plasmids bearing T261 and/or S265 versions, the relevant HpaI-BspEI fragments (731 bp) were cloned in pRS316 *PPZ1 S49A* or pRS216 *PPZ1 S49D.* To introduce the same mutation in the pGEX-6P-1-Ppz1 plasmid, a BglII-BglII fragment (937 bp) from the *PPZ1* ORF was extracted from

each specific pRS316-based *PPZ1* mutated version and cloned into pGEX-6P-1-Ppz1 digested with BglII.

The different versions of Hal3 were created by mutagenic PCRs in 2-steps using plasmid YEplac195 *HAL3* as template. The two overlapping fragments were generated using specific pairs of primers. For example, for the S47 to Ala change, 5'_HAL3-200/3-Hal3-S47A and 3'_HAL3+920/5-Hal3-S47A were used. A mixture of both fragments was subsequently amplified using 5'_HAL3-200/3'_HAL3+920. The amplification fragment was cloned into the XbaI and BamHI sites of plasmid YEplac195 HAL3. The same procedure was followed to create S47D S50A/D, S54A/D, S56A/D, S60D, S54+56A/D and Δ47-60 versions using the different pairs of primers that appear in Annex 2. It is worth noting that the YEplac195 plasmid used to clone the different mutations was extracted from the GM2163 *E. coli* strain, to avoid *dam* methylation in the position of the XbaI site (since XbaI is sensitive to *dam* methylation).

## 6.- Growth tests

The sensitivity of different yeast strains to several stresses such as saline (NaCl, LiCl), caffeine, Calcofluor white (CFW) or acetic acid was assayed by drop test on freshly prepared YPD or synthetic medium lacking uracil ($Ura^-$) plates containing different concentrations of the compounds (Posas *et al*, 1995b). Yeast saturated cultures were diluted to an $OD_{600}$ of 0.05 and 3 µL, plus serial 5-fold dilutions, were deposited on the plate. Growth was monitored usually after 3 days, unless otherwise indicated.

To study the toxicity of Ppz1 over-expression and the possible multicopy suppressor effect in strain MLM004, overnight cultures were prepared in media supplemented with 100 µg/mL of doxycycline to turn off the expression of *PPZ1*. Then the cultures were washed twice with 10 mL of the final medium (usually SD lacking uracil) and then the culture was diluted ½ and incubated at 28°C at least 5 hours. Cultures were then diluted to an $OD_{600}$ of 0.05 and 3 µL plus serial 5-fold dilutions were deposited on plates with different concentration of the carbon source in the presence or absence of doxycycline and growth was monitored after at least 2 days.

# 7.- Protein immunodetection

## 7.1.- Sample collection and preparation of extracts

Yeast extracts for protein extraction and immunodetection were prepared as follows.

To detect the expression of different Ppz1 versions carrying mutations at the N-terminal region, as well as Ppz1 and Hal3 tagged with fluorescent proteins at the C-terminus (DVS strains), 10 mL of cells were grown at 28°C in synthetic medium until $OD_{600}$ reached 0.8-0.9 and cells were collected by centrifugation (5 min at 1,300*xg*). Protein extracts were prepared as described in (Abrie *et al*, 2012). Briefly, the cell pellets were resuspended in 100 µL of Lysis Buffer A (50 mM Tris-HCl pH 7.5, 150 mM NaCl, 10 Glycerol, 0.1% Triton X-100, 2 mM dithiothreitol (DTT), and Complete™ protease inhibitor mixture (Roche)), and cell lysis was performed by adding 100 µL of Zirconia/Silica 0.5 mm beads (BioSpec) and vigorous shaking in a FastPrep cell breaker (FastPrep® 24, MP Biomedicals) at setting 5.0 for 45 seconds (5 repeats, placing on ice for one minute between repeats). Then, 25 µL of Lysis buffer A were added. Samples were centrifuged at 750x*g* for 10 min at 4°C and the cleared supernatants were transferred to new tubes. Protein quantification was performed by the Bradford method (Sigma Chemical Co.) and 40 µg of total protein were used for immunoblot analysis.

For monitoring Ppz1 levels in the ZCZ01 strain, cells were incubated at 28°C in YP Raffinose (2%) until $OD_{600}$, one sample of 10 mL was collected ($t_0$) and then galactose was added to the remaining culture up to 2% (final concentration). Further samples were collected after different times of over-expression. Then, samples were treated as described above. To follow the expression of Npl3 in the ZCZ01 strain, the procedure was identical but using a ZCZ01 strain transformed with the pRS315 NPL3-GFP plasmid.

To analyze the phosphorylation state of Rps6A in cells overexpressing Ppz1, cultures of wild type BY4741 and ZCZ01 strains were collected and processed as described above, except that Lysis Buffer B (50 mM Tris-HCl pH 7.5, 150 mM NaCl, 15% glycerol, 0.5% Tween-20, 1x phosphatase inhibitor cocktail Set V (Millipore), 1 mM PMSF and 1x EDTA-

free protease inhibitor cocktail (Roche)) was used. Protein quantification was performed by the Bradford method (Sigma Chemical Co.) and 25 µg of total protein were used for immunoblot analysis. The same procedure was used to detect phospho-eIF2α.

## 7.2.- SDS-PAGE and immunoblotting

Proteins extracts were mixed with 4xSDS-PAGE loading buffer (200 mM Tris-HCl pH 6.8, 40% glycerol, 8% SDS, 0.4% bromophenol blue) to yield a final concentration of 1x, heated for 5 minutes at 95°C, and resolved by SDS-PAGE at a concentration of 10% of acrylamide. Afterwards, proteins were transferred onto polyvinylidene difluoride (PVDF) membranes (Immobillon-P, Millipore). Membranes were then blocked with TBS-Tween 20 (20 mM Tris-HCl pH 7.6, 0.1% Tween-20, 150 mM NaCl) plus 5% of fat-free powdered milk for 1 hour with gentle agitation. In the case of eIF2α detection and Rps6A, membranes were blocked with TBST-Tween 20 plus 5% BSA (bovine serum albumin, Sigma). Incubation with the primary antibody was performed overnight at 4°C with gentle agitation. Membranes were then washed thrice with TBS-Tween 20 for 10 minutes and then incubated with the secondary antibody for 1 hour at room temperature and gentle agitation. Finally, membranes were washed thrice with TBS-Tween for 10 minutes.

HA-tagged proteins were detected by means of a mouse monoclonal Anti-HA antibody (Covance, MMS-101P-500) at a 1:1,000 dilution in TBS-Tween 20 plus 5% fat-free powdered milk, followed by a 1:20,000 dilution of the secondary anti-mouse IgG-horseradish peroxidase antibody (GE Healthcare) in TBS-Tween 20 plus 5% fat-free powdered milk . Npl3-GFP was monitored with anti-GFP antibody (Invitrogen, [9F9.F9]) at a 1:500 dilution, and the same secondary antibody that in the previous case.

To detect Ppz1 and Hal3, polyclonal antibodies anti GST-Ppz1 (Clotet *et al*, 1996) at a 1:250 dilution, or anti GST-Hal3 (De Nadal *et al*, 1998) at a 1:500 dilution in TBS-Tween 20 plus 5% fat-free powdered milk were used. Then a 1:20,000 dilution in TBS-Tween 20 plus 5% fat-free powdered milk of a secondary anti-rabbit IgG-horseradish peroxidase antibody (GE Healthcare) was employed.

To detect the phosphorylated Rps6A protein, anti-Phospho-S6 Ribosomal Protein (Ser235/236) (Cell Signaling®) was used at a 1:2000 dilution in TBS-Tween 20 plus 5% BSA (Sigma), followed by incubation with a 1:15,000 dilution in TBS-Tween 20 plus 5% fat-free powdered milk of a secondary anti-rabbit IgG-horseradish peroxidase antibody (GE Healthcare). A similar procedure was performed to detect eIF2α but using 1:1000 Anti-Phospho-eIF2α (Ser51) (Cell Signaling®)) as a primary antibody.

Immunoreactive proteins were visualized with the ECL Prime Western blotting detection kit (GE Healthcare) and chemiluminescence was detected in an Imaging-System-Versadoc 4000 MP (BioRad). Membranes were stained with Ponceau Red (prior of after antibody incubation) to evaluate loading and transfer efficiency.

# 8.- Protein purifications

## 8.1- Expression and purification of GST recombinants proteins

BL21 DE3 RIL *Escherichia coli* cells (Stratagene), were used to express GST-proteins from the plasmid pGEX-6P-1. Cells were grown in LB medium supplemented with 100 µg/mL ampicillin and 34 µg/mL chloramphemicol at 37°C. Five mL cultures, inoculated from single cell colonies or glycerinated stock, were grown overnight until saturation. A 1:10 dilution of these cultures was used to inoculate the appropriate volume for large cultures in TB (Terrific Broth) (Tartof & Hobbs, 1987) . Bacterial cultures were grown in a shaker at 37°C to an optical density of $OD_{600}$ 0.6-0.8. To induce protein expression, isopropyl-ß-D-thiogalactopyranoside (IPTG) was added (0.1 mM final concentration), and the culture was incubated 16 hours at 21°C to express the heterologous proteins in optimal conditions as described in (Ruiz *et al*, 2009; Muñoz *et al*, 2004). For Ppz1 and Ppz1 versions expression the medium was supplemented with 0.5 mM $MnCl_2$ to ensure catalytic activity.

Upon induction, cultures were centrifuged at 6500x*g* for 20 min at 4°C and pellets were resuspended in Lysis buffer C (25 mL/L of culture, approximately) that contained 50 mM Tris-HCl pH 7.5, 150 mM NaCl, 10% Glycerol, 0.1% Triton X-100, 2 mM

dithiothreitol (DTT), 0.5 phenylmethylsulfonyl fluoride (PMSF) and protease inhibitor cocktail (Roche). Then, samples were placed on ice and cells were sonicated using a Vibra-cell (Sonics and Materials Inc.) equipment for 5-6 minutes (10 seconds on, 10 seconds off) at up to 30% amplitude. The lysed cultures were centrifuged at 7800x*g* at 4°C for 15 minutes, and the supernatant was recollected. To purify GST fusion proteins, the bacterial crude lysates were incubated with Glutathione Sepharose 4B beads (GE Healthcare) at least for 4 hours at 4°C with mild rotation (350 µL of beads for 1 L culture, approximately). Afterwards, beads were spun down by centrifugation (750x*g*, 5 min) at 4°C, and a sample of the flow-through was collected for subsequent analysis. The beads were then washed at least 8 times with Lysis Buffer C using a MultiScreen® 96-well filter plates (Millipore), and twice with the same buffer without Triton X-100. When removal of the GST moiety was necessary, beads containing bound recombinant proteins were resuspended in PreScission Buffer (50 mM Tris-HCl pH 7, 150 mM NaCl, 1 mM EDTA and 1 mM DTT) and treated with PreScission protease (GE Healthcare) according to manufacturer's instructions. Incubation was performed at 4°C for 16 h in a rotating wheel (Abrie *et al*, 2012). Subsequently, samples were centrifuged at 750x*g* for 3 minutes at 4°C in a MultiScreen® 96-well filter plates (Millipore) to recover the eluate, which was made 10% glycerol and stored at -80°C. The amount of recombinant protein was determined by SDS-PAGE. To stain the proteins, the acrylamide gel was incubated with Coomassie Blue solution (10% acetic acid, 25% isopropanol and 0.25% of Coomassie brilliant Blue R250 (AMRESCO)). Then, the gel was unstained with a solution composed by 10% of acetic acid and 25% of isopropanol. the relevant proteins were then compared with different amounts of bovine serum albumin (BSA) used as standards (Laemmli, 1970). The gels were scanned with an Epson Perfection V500 Photo Scanner and the protein concentration of the specific proteins was estimated with Gel Analyzer software.

## 8.2.- Expression and co-purification of Hal3 and Ppz1 for crosslinking experiments

Co-purification of the Ppz1C-ter / Hal3 complex was accomplished upon co-expression in *E. coli* BL21 DE3 RIL cells transformed with a pET-Duet1-based plasmid. Culture and induction was carried out as described above (8.1). Upon induction, cultures were centrifuged at 6500x*g* for 20 min at 4°C, pellets were resuspended in Lysis buffer D (50 mM $NaH_2P0_4$ pH 7.5, 150 mM NaCl, 20 mM Imidazole, 0.1% Triton X-100) containing Complete EDTA-free protease inhibitor cocktail (Roche) plus 2 mM PMSF (approximately 3 mL of Lysis buffer D per gram of pellet). Samples were then sonicated as explained in section 8.1. The insoluble fraction was then removed by centrifugation at 12400x*g* for 30 min at 4°C, the soluble fraction was recovered and an aliquot taken for SDS-PAGE analysis. The soluble fraction was then incubated at least 1 hour at 4°C with Ni-NTA Agarose beads (Qiagen®) following the manufacturer's specifications. The mixture was loaded in an empty column (Pierce®Centrifuge columns 10 mL (RF: 99898)), and the flow-through was collected for SDS-PAGE analysis. The beads were washed with approximate 5 bed volumes of Lysis buffer D without Triton X-100 until the eluate was free of proteins (monitored by the Bradford's reagent). The elution of the Ppz1Cter-Hal3 complex was accomplished with 1.5 bed volume of Elution buffer (50 mM $NaH_2P0_4$ pH7.5, 150 mM NaCl, 150 mM Imidazole) and incubating the beads 10 minutes at RT in a roller. Finally, the elution buffer was exchanged with X-linking buffer (50 mM $NaH_2P0_4$ pH7.5, 150 mM NaCl) using an Amicon® Ultra Centrifugal filter (size 30 kDa, Millipore) to eliminate the imidazole, incompatible with crosslinking experiments. The amounts of protein complex (Ppz1C-ter / Hal3) were determined as previously explained in section 8.1.

# 9.- *In vitro* enzyme assays

## 9.1.- Phosphatase activity

*Saccharomyces cerevisiae* Ppz1 activity assays were performed in 96-wells plates as reported previously (Muñoz *et al*, 2004; Abrie *et al*, 2012) using *p*-nitrophenylphosphate (pNPP, Sigma) as substrate with a 50 mM Tris-HCl (pH7.5), 2 mM $MnCl_2$, 1 mM DTT buffer in a final volume of 300 µL. The amount of phosphatase in the assays was 1 µg (13 pmol). To test the inhibitory capacity on the diverse N-terminal Ppz1 variants, different amounts of Hal3 were added to the assay mixture and incubated at 30°C for 5 min. The reaction started with the addition of 10 mM of pNPP. The assays were carried out for 20 minutes by measuring the absorbance at 405 nm in an UV MultiSkan Ascent (Thermo Scientific). The absorbance of the mixture lacking the enzyme was measured as reaction blank, and the value was subtracted from the assay measurements.

## 9.2- Hog1 *in vitro* phosphorylation

To perform the *in vitro* phosphorylation of the different versions of Ppz1 by Hog1, one µg of GST1-Hog1 was activated with 0.5 µg of GST-Pbs2(EE) in the presence of kinase buffer and ATP as described in (Bilsland-Marchesan *et al*, 2000). Pbs2EE has a double phosphomimetic mutation at positions Ser514 and Thr518. This yields a hyperactive Pbs2 that can be used to phosphorylate and activate Hog1 *in vitro* (Warmka *et al*, 2001).

After 30 minutes of preactivation at 30°C, 1 µg of each Ppz1 version, purified from *E. coli*, were added to the previous mixture with [γ-$^{32}$P]ATP (0.2 µCi/µL). The mixture was incubated for 30 minutes at 30ºC and the reactions were terminated by the addition of 2xSDS loading buffer.

## 10.- Crosslinking assays

The interaction between Ppz1C-ter and Hal3 was analyzed by chemical crosslinking with BS3 (bis(sulfosuccinimidyl)suberate) (Covachem), BS2G (Bis-(sulfosuccinimidyl) glutarate) (Covachem) and DSBU (Disuccinimidyl Dibutyric Urea) (Thermo Scientific) as follows. The Ppz1C-ter /Hal3 protein complex was purified as described in section 8.2 and the protein concentration was adjusted to 0.2-1 µg/µL with X-linking buffer (50 mM $NaH_2P0_4$ pH 7.5, 150 mM NaCl). Forty µg of the complex were used for each crosslinking experiment. In the case of BS3 and BS2G, the proteins were incubated with 5, 10 and 20 weight excess of the crosslinker. In the case of the DSBU crosslinker, the proteins were treated with 20 and 100 molar excess of crosslinker.

The samples were incubated for 1 hour at room temperature, and the crosslinking reaction was quenched by adding $NH_4CO_3$ until a final concentration of 100 mM. Then, the samples were analyzed by SDS-PAGE in 6% acrylamide gels and stained. The different bands of the crosslinked protein complex were cut from the gel and send to Dr. Peter Hojrup (University of Southern Denmark) for LC-MS/MS analysis.

## 11.- Pull down experiments

### 11.1.- GST-pull down

With the objective to know which proteins interact with Ppz1 *in vivo*, we over-expressed in yeast a GST Ppz1 R451L version (lacking phosphatase activity) and GST as control. Yeast cells transformed with the relevant plasmids, were grown in 150 mL of synthetic medium lacking uracil and with raffinose as carbon source to a final $OD_{600}$ of 0.6-0.8 and galactose was then added to a final concentration of 2% to induce Ppz1 over-expression. After 60 min cells were filtered using 25 mm gn-6 (Pall Corporation) membranes, washed with cold water, and frozen at -80°C. Cells were then resuspended in 150 µL of Lysis buffer E (50 mM Tris-HCl pH 7.5, 10% Glycerol, 1% Triton, 0.1% SDS, 150 mM NaCl, 1 mM PMSF, protease inhibitors 1x (Complete EDTA-free Protease

Inhibitor Cocktail Tablets, Roche)). One hundred fifty µL of 0.5 mm Zirconia balls (BioSpec # 11079105z) were added and the cells were vortexed briefly and lysed using FastPrep cell broker (FastPrep 24, MP Biomedicals) at setting 5.5 for 25 seconds. This process was repeated five times, with intervals of one-minute incubation of the samples at -20°C. Finally, samples were centrifuged at 4°C, at 15700x*g* for 15 minutes.

To purify GST and GST Ppz1, protein extracts were incubated o/n at 4°C with 250 µL of Glutathione Sepharose 4B beads (GE Healthcare) with mild rotation. After that, beads was washed 8 times with Lysis buffer E using a Multi Screen 96-well filter plate (Millipore), and then twice with the same buffer without SDS and Triton-X-100. Finally, to recover the proteins bound to the glutathione-beads, these were mixed with 4x Loading buffer (200 mM Tris-HCl pH 6.8, 40% glycerol, 8% SDS, 0.4% bromophenol blue), plus 5% of ß-mercaptoethanol, heated for 5 minutes at 95°C, resolved by SDS-PAGE at a concentration of 8% of acrylamide, and stained as in section 8.1.

The bands corresponding to proteins that might interact specifically with Ppz1 were cut from the acrylamide gel and identified by MALDI-TOF at the "Servei de Proteòmica i Bioinformàtica (SePBio)".

## 11.2.- Detection of the phosphorylation state of Ppz1

The BY4741 *ppz1*::kanMX4 strain was transformed with plasmid pEGH-Ppz1 R451L and grown in synthetic medium lacking uracil with Raffinose as carbon source ($Ura^-$ Raff) until an $OD_{600}$ of 0.6-0.8. After that, galactose was added to a final concentration of 2% to induce expression of the protein. After 60 minutes of expression, the culture was separated in three identical aliquots that were filtered. Each aliquot of the original culture was resuspended in a different medium: Translucent medium with 50 mM KCl (as a control), Translucent medium with 50 µM KCl (low potassium stress), and in Translucent medium with 50 mM KCl + 0.8 M NaCl (sodium and osmotic stress). After that, the samples were collected by filtration (Whatman filter; 0.45 µm of pore size, Diamter 47mm (GE Healthcare)), after 5 and 20 minutes. Cells were resuspended in 150

µL of Lysis buffer E (50 mM Tris-HCl pH 7.5, 10% Glycerol, 1% Triton, 0.1% SDS, 150 mM NaCl, 1 mM PMSF, protease inhibitors 1x (Complete EDTA-free Protease Inhibitor Cocktail Tablets, Roche)), plus 1x phosphatase inhibitor cocktail Set V (Millipore)). One hundred fifty µL of 0.5 mm Zirconia balls (BioSpec # 11079105z) were added and the cells were vortexed briefly and lysed using Fast Prep cell baker (FastPrep 24, MP Biomedicals) at settings 5.5 for 25 seconds, this process was repeated five times, with intervals of one minute incubating the samples in -20°C. Later the samples were centrifuged at 4°C, 15700x*g* during 15 minutes.

Samples were analyzed by SDS-PAGE as described in section 11.1, and bands were analyzed by MALDI-TOF at the "Servei de Proteòmica i Bioinformàtica (SePBio)" and by LC-MS/MS in collaboration with Dr. Ole Jensen (Southern Denmark University).

### 11.2.1.- In gel digestion

To obtain the peptides from the protein bands resolved by SDS-PAGE, each band was placed in an Eppendorf tube and washed with a volume of water equivalent to 5-fold the gel band volume (≈80 µL) for 10 minutes in a centrifuge at 1000 xg. Water was then removed and 100 µL of 100% acetonitrile were added and incubated for 15 minutes at room temperature to shrink the bands and to remove the Coomassie Blue dye. Afterward, 100 µL of $H_2O$ were added and incubation continued in a shaker for 15 additional minutes, until gel bands turn white. After that, the liquid was removed and the bands were swelled with 50 µL of a 10 mM DTT, 0.1 M $NH_4HCO_3$ solution and incubated for 20 minutes at 56°C. The tubes were then cooled down at room temperature and the excess of liquid was removed and replaced with roughly the same volume of iodoacetamide solution (10 mg/mL (55 mM) of Iodoacetamide dissolved in 0.1 M $NH_4HCO_3$) and samples were incubated for 30 minutes in the dark at room temperature. Finally, the iodoacetamide solution was removed and the gel pieces were washed with 100 µL of 0.1 M $NH_4HCO_3$ and shrunk by addition of 80 µL of 100% of acetonitrile.

To rehydrate the gel pieces and fragment the proteins, 30 µL of a trypsin solution (6 ng/µL trypsin (Promega) in 50 mM $NH_4HCO_3$ was used. More trypsin solution was added if all initial volume had been absorbed by the gel bands. Samples were incubated on ice for 30 minutes, and then the remaining trypsin solution was removed, replaced with 30 µL of 50 mM $NH_4HCO_3$, and incubated at 37°C overnight. Then the supernatants were recovered.

### 11.2.2.- $TiO_2$ enrichment

The samples of peptides obtained in the previous step from the gel pieces were mixed with $Ti0_2$ loading buffer (80% Acetonitrile, 5% TFA and 1 M Glycolic Acid) up to 1 mL of final volume. The peptide solutions were transferred to low-binding tubes containing 0.3 mg $TiO_2$ beads (GL Sciences cat. No. 5020-75010) and incubated in a shaker (1500 rpm) at room temperature for 10 minutes. The tubes were centrifuged at 1000x*g* for 30 seconds, and the supernatants were transferred to another low-binding Eppendorf tube and subjected to a second round of $TiO_2$ beads but using half of the amount of beads used for the first incubation. The tubes were centrifuged, and the supernatants were transferred to fresh low binding tubes (these samples correspond to the unmodified peptides). The $TiO_2$ beads from the two incubations were pooled using 100 µL of $TiO_2$ loading buffer and were transferred to fresh low-binding tubes, this mixture was vortexed for 10 seconds, centrifuged for 30 seconds at 1000x*g* and the supernatant were removed and mixed with the non-modified peptides fraction. The beads were then washed with 100 µL of washing Buffer 1 (80% acetonitrile and 1% TFA) by vortexing for 10 seconds and centrifuging for 30 seconds at 1000x*g*, and supernatants were collected and added to the fraction of non-modified peptides. This process of washing was repeated changing the buffer to washing Buffer 2 (10% acetonitrile and 0.1% TFA) and the supernatant were also added to in the non-modified peptide fraction. Then the beads were dried for 5-10 minutes in the vacuum centrifuge.

To elute the phosphopeptides from the beads, 150 µL of Elution buffer (60 µL of ammonia solution (25%) in 940 µL $H_2O$, pH 11.3) were added and mixed by shaking (1000 rpm) 15 minutes to allow an efficient elution. After that, samples were centrifuged for

1 minute (highest speed) and the supernatant was passed over a filter (C8 stage tip, Thermo Scientific) to recover the liquid in a low-binding tube. The beads were washed with 30 µL of elution buffer and the supernatant was passed over the C8 filter and pooled with the previous filtered supernatant. To elute the peptides bound to the filter, 5 µL of 30% Acetonitrile were added at the end of the filter tip. The phosphopeptide samples were acidified by adding 3 µL of 100% TFA, until a pH below 2 was reached.

Finally, to purify the phosphorylated peptides, were used two p200 R3 microcolumns (1.5 cm long) (OLIGO™ R3 Reversed - Phase Resin, Thermo Scientific). The purification was carried out sequentially: the phosphopeptide samples are passed through the first R3 column and the flow-through goes directly onto the second R3 micro-column. Both columns are then washed with at least 60 µL of a 0.1 % TFA solution and the phosphopeptides are eluted using 60 µL of 60% acetonitril and 0.1% TFA solution for each column. One µL was taken for checking the quality of the phosphopeptides by MALDI-TOF, and the rest of the sample was analyzed by LC-MS/MS (Q Exactive™ HF Hybrid Quadrupole-Orbitrap™ Thermo Scientific).

# 12.- Cell-wide proteomic assays

## 12.1.- Sample collection

Yeast extracts for phosphoproteomic assays were prepared as follows. Two hundred fifty mL of cells (BY4741 and ZCZ001 strains) were grown from $OD_{600}$ 0.2 until $OD_{600}$ 0.6-0.8 in YP Raffinose (2%). At this point, one sample (50 mL) for each strain was collected and galactose was added to a final concentration of 2%. Then 50 mL samples were taken from each culture at 30, 60, 120 and 240 minutes. In each case, the cell suspension were mixed immediately with TCA (final concentration 6%) and put on ice for at least 10 minutes, before cells were pelleted at 1680x*g* for 5 minutes. The pellet was washed twice with 1 mL of cold acetone, dried at 37°C to eliminate de TCA and finally frozen at -80°C.

## 12.2.-Protein extraction and phosphopeptide sample preparation

To obtain the protein extracts for phosphoproteomic assays, one mL of the chilled (4°C) lysis Buffer F (3% SDS, 0.1 M ammonium bicarbonate, pH 7.5 ) with the addition of Complete protease inhibitor and PhosStop phosphatase inhibitor mixtures (Roche) was added to the cell pellet together with 200 μL of acid-washed glass-beads (Sigma). The yeast cells were broken in a BeadMill at 4°C with four cycles of 1 min shaking followed by 1 min vortexing. Then, the cell suspension was sonicated in a Bioruptor for 10 min (30 sec sonication followed by 30 sec break cycles) at 4°C, heated at 90°C for 10 min in a water bath and sonicated again in a Bioruptor for 10 additional min. Protein concentration was measured by BCA analysis (Thermo Scientific). The concentration of 100 μg aliquots was adjusted to 1 mg/mL with lysis buffer F, and TCEP (Tris (2-Carboxyethyl) Phosphine) and CAA (Chloroacetamide) were added to 10 mM and 40 mM, respectively. Samples were then heated at 80ºC to reduce and alkylate the proteins. Protein material was precipitated by the chloroform/methanol method (Friedman, 2007). Protein pellets were air dried and resuspended in 100 μl of 0.1 M TEAB (Triethylammonium bicarbonate buffer). Trypsin (Promega) was added at a 1/50 ratio and the digestion carried out at 37°C for 12 h. Then, an additional aliquot of trypsin (1/100) was added for 2 h at 37°C in order to improve the digestion.

Peptide solutions were labeled by TMT (Tandem Mass Tag labelling) according to the manufacturer recommendations (TMT11plex Thermo Scientific). The TMT label was dissolved in 50 μl of acetonitrile and mixed with the sample. After 1 h incubation at RT, 8 μL of 5% hydroxylamine were added to quench the reaction. Eighty per cent of the labeled samples were mixed and the relative amount of labeling deduced from the values of the MS2 reporter ion channels. Samples were then rectified, with the objective to equalize the amount of proteins. Twenty μg of the mixed TMT sample were taken to obtain data for total proteins (Proteome). The sample was fractionated with high pH RP (Reverse phase) chromatography into 10 fractions, which were concatenated into 5 fractions for LC-MS analysis (fraction 1 with fraction 6, fraction 2 with fraction 7 etc.). The rest of the TMT mixed sample (800-900 μg) was enriched for phosphopeptides on an IMAC column (Thingholm *et al*, 2007) or $TiO_2$ beads (GL Sciences, Tokyo, Japan)

(Jørgensen *et al*, 2005). The phosphopeptide fraction was similarly pre-fractionated with high pH RP into five final fractions.

## 12.3 LC-MS analysis

LC-MS analysis was carried out using an Ultimate 3000 RSLCnano HPLC system connected to a Q-Exactive HF mass spectrometer (ThermoFisher Scientific). The system was conditioned using a BSA tryptic digest (50 fmol) in a 15 min LC gradient that was run between each fraction. Samples were loaded on a PepMap 100 C18 5 µm 0.3 x 5 mm Trap Cartridge (ThermoScientific) in loading solvent (2% Acetonitrile, 98% $H_2O$, 0.1% TFA) at a flow of 10 µl/min and separated with an 1 h gradient starting at 99.9% Acetonitrile, 0.1% formic acid and ending with 99.9% $H_2O$, 0.1% formic acid on a 75 µm*30 cm column custom-packed with Reprosil Pur C18AQ 1.9 sorbent.

## 12.4 MaxQuant search

Raw data was analyzed using the MaxQuant software (v1.6.3.3) and its integrated search engine Andromeda (Tyanova *et al*, 2016a, 2015) with the following parameters: Reporter ion MS2 (TMT11plex search), PSM (peptide spectrum matches) FDR and protein FDR were set at 0.01; minimum peptide length was 7; minimum score for modified peptides was 40 and razor peptides (set to 1) were used for protein quantification. The search was executed against the *S. cerevisiae* orf_coding.fasta database (https://www.yeastgenome.org/). For protein abundance analysis, the ProteinGroups.txt MaxQuant file was used. For phosphoproteomic analysis the Phospho (STY) Sites.txt file was generated. To account for possible increases in specific proteins, the relevant data from the Phospho (STY) Sites.txt file was normalized with the protein abundance data extracted from the ProteinGroups.txt file. Only phosphopeptides with localization probability equal or higher than 0.5 were selected. and further processed with the Perseus software (v1.6.2.3) (Tyanova *et al*, 2016b).

To evaluate changes in protein abundance, data was loaded in the Perseus software, contaminants were removed and the Ppz1 over-expression/control ratios for each experiment were calculated. Categorical annotation and grouping of samples by experiments was done. Then, mean values and SEM valued were calculated and a 2-sample T-test ($p<0.05$) was performed to identify consistent changes. A similar process was carried out for phosphopeptide analysis, with a $p<0.05$ value set for significance.

## 13.- Microscopy

To investigate the localization of Npl3 or Mig1 upon Ppz1 over-expression, BY4741 and ZCZ01 strains were transformed with plasmid pRS315 *GFP-NPL3* or YEp195 GFP-MIG1, respectively. The transformed yeasts were grown in YP Raffinose to achieve an $OD_{600}$ of 0.6-0.8, one aliquot of each was taken, and galactose was added to a 2% of final concentration to start over-expression of the phosphatase. Additional samples were collected at 30, 60, 120 and 240 minutes after the induction. Yeast cells were fixed with a 3.7% formaldehyde solution at room temperature for 5 minutes, then centrifuged at 1000x*g* for 2 minutes, washed twice with 1x PBS, and finally resuspended in 1x PBS for microscopy analysis. Four µL of cells were deposited on a glass slide, covered with the coverslip and sealed with nail polish. The visualization of samples was done with a 100x objective using a Nikon Eclipse E-800 microscope, and a FIT-C filter (ex: 480/30 nm, em: 530/30 nm) was used to visualize green fluorescence protein.

## 14.- Flow cytometry

For flow cytometry analysis, cells were grown in selective media from a saturated culture until an $OD_{600}$ of 0.8 – 1 was achieved. At this point, two washing steps with Translucent medium were performed, cells were resuspended in one mL of Translucent medium supplemented with 50 µM KCl, or 50 mM KCl (with or without 0.8 M NaCl). The analyses were made using a FACSCalibur® (Becton Dickinson) and data were collected from 20000 cells per culture. Excitation was carried out using a 488 nm laser and the emission was detected using the FL1 and FL2 filters, for EGFP emission and mCherry emission, respectively.

# RESULTS

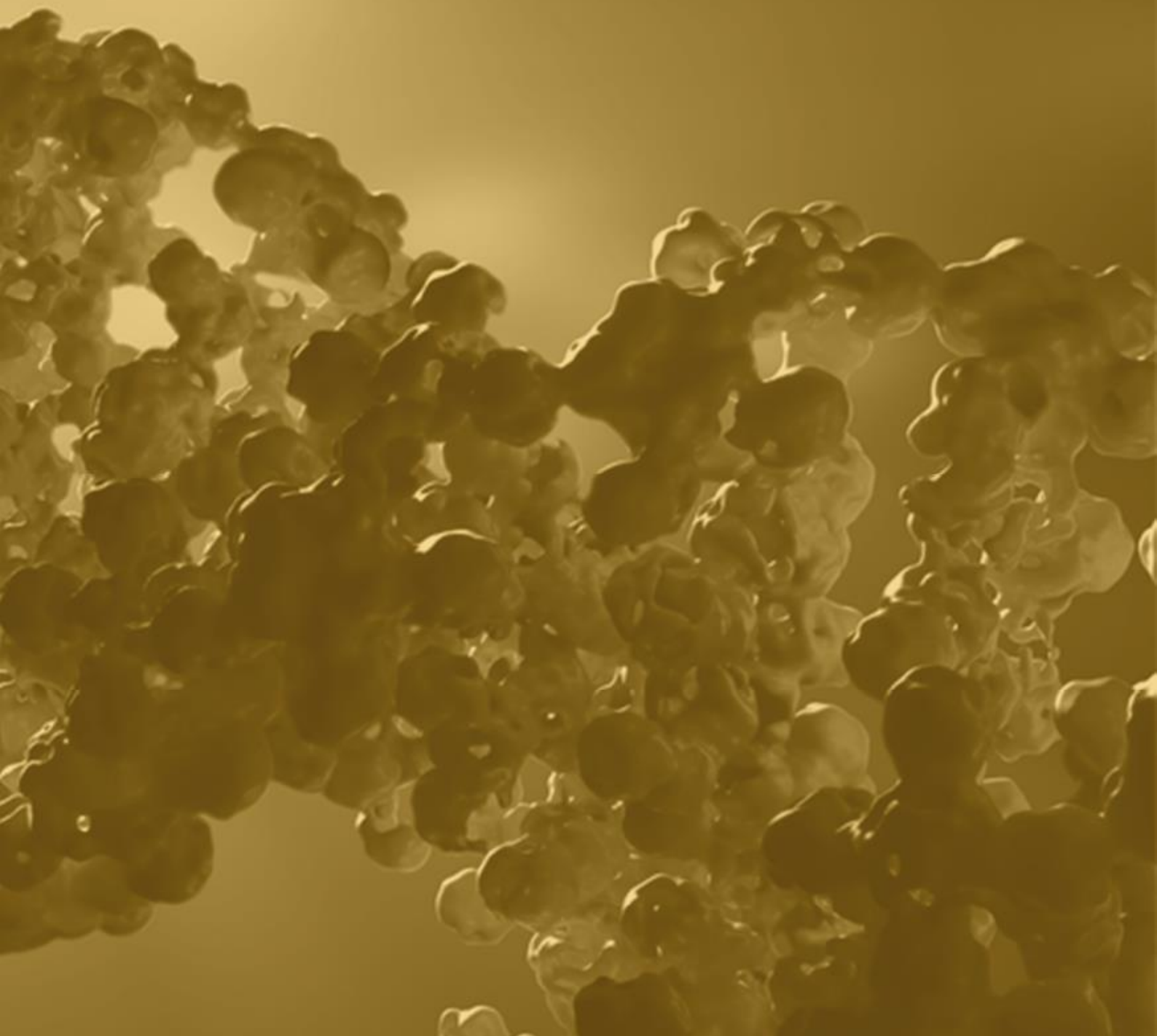

# CHAPTER1

## Study of the interaction between Ppz1 and Hal3 *in vivo* and *in vitro* approaches.

# Chapter 1.- Study of the interaction between Ppz1 an Hal3. *In vivo* and *in vitro* approaches

The Ser/Thr phosphatase Ppz1 is regulated by its subunit Hal3, which binds to the catalytic domain of the phosphatase and inhibits its activity. It is known that the PD domain of Hal3 is enough for binding to Ppz1, but cannot inhibit the phosphatase activity (Abrie *et al*, 2012). Despite the similarity between Ppz1 and PP1c, the regulatory subunit Hal3 is not similar in structure to other PP1c inhibitors characterized so far. Although Hal3 contains a sequence that resembles the RVxF motif, found in many regulators of PP1, previous work demonstrated that this motif in Hal3 is not relevant for the interaction with Ppz1 (Muñoz *et al*, 2004). Moreover, Hal3 does not bind to or inhibit yeast PP1c (Glc7). This indicates a strong specificity and suggests a unique regulatory mechanism towards Ppz1. However, the mechanism for *in vivo* regulation of Ppz1 through Hal3, or even the residues involved in the interaction, are still unknown.

In the following experiments we describe our attempts to understand how this interaction occurs, and to identify which residue/s make the interaction possible. To this end, we decided to create a tool that would allow the study of the dynamics of the *in vivo* interaction between Ppz1 and Hal3.

## 1.- *In vivo* interaction of Ppz1 and Hal3

Protein-protein interactions are necessary in virtually all cellular processes, from DNA replication, translation or transcription to cell cycle, metabolism or cell signaling. A large number of techniques can be used to study these interactions in yeast: two-hybrid system, pull-down assays, co-immunoprecipitation or chemical cross-linking, among others (Phizicky & Fields, 1995). Part of the aim of this work is to study the regulation *in vivo* of Ppz1 by Hal3, and how this interaction could change depending of the environment or cell requirements. To understand the dynamism of the Ppz1-Hal3 interaction, a Fluorescence Resonance Energy Transfer (FRET) approach was used. FRET is a physic event that occurs only when light energy that is emitted upon the excitation of a donor chromophore is transferred to and excites an acceptor chromophore (Figure 1A) provided both are properly oriented and sufficiently close (Dye *et al*, 2005). In FRET

approaches the pairs of fluorescent proteins CFP-YFP and GFP-mCherry are often used as donor and acceptor chromophores, respectively (Bajar *et al*, 2016).

The first experimental approach was the construction of strains containing versions of GFP and its derivatives (CFP, YFP…) fused to Ppz1 and/or Hal3 (Figure 12). GFP has been fused successfully to a myriad of proteins, without adversely affecting their location or function (opposite to what occurs in classic two-hybrid system, where the natural location of the protein of interest is often changed). Also, GFP and its derivatives are relatively inert, so their expression does not affect the normal performance of the cell (Tsien, 1998). Then, if the Ppz1 interacts with Hal3, chromophores tagged to each protein would be close to each other and, upon excitation of one the donor chromophore, its emission could excite the acceptor.

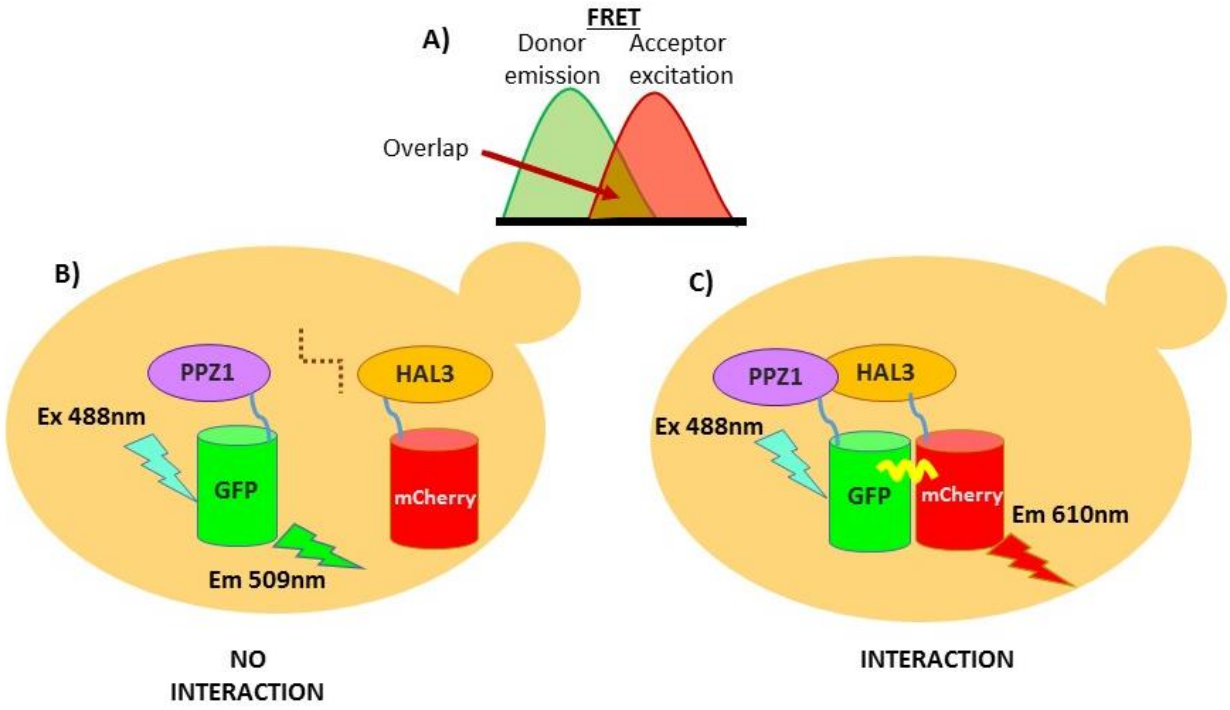


**Figure 12. FRET approach to study the interaction between Ppz1 and Hal3. A)** Representation of how donor emission can excite the acceptor, due to the overlap between the emission of the donor and the acceptor excitation. **B and C)** Cartoons showing no-interaction and interaction situations between Ppz1-GFP and Hal3-mCherry. Interaction allows FRET to occur.

Fluorescence microscopy and fluorometrics techniques is more often used to assess FRET. Previous results from versions of Ppz1 with different tags using fluorescence microscopy showed a low level of signal, possibly too low to detect FRET using this technique, so we considered that a more sensitive method would be necessary.

It is described in the literature that FRET can be evaluated by flow cytometry. This procedure has been done in mammalian cells (He *et al*, 2003) and, less frequently, also in yeast (Dye *et al*, 2005). Flow cytometry has some advantages: rapid collection of data, the possibility to analyze thousands of cells individually in seconds, cells can be tracked *in vivo* without any fixation, and data treatment and analysis is simpler that in fluorescence microscopy, where complex calculations and specialized software are necessary to analyze FRET data (Gordon *et al*, 1998). To do these experiments it is important to consider the autofluorescence of cells without fluorescence tags and, therefore, showing as false positives. For this reason, a special medium was prepared to decrease as much as possible autofluorescence.

## 1.1.- Fluorescent Ppz1 and Hal3 strains construction

Twenty different strains to use for FRET analysis were created with the help of the toolbox plasmids described in (Janke *et al*, 2004). The procedure to create these strains is described in the Material and Methods section. Ppz1 and Hal3 were tagged with 4 different fluorescent proteins: CFP, YFP, GFP and mCherry. Most of these strains have the fluorescent tag at its C-terminus, because introduction of the tag in the N-terminus would entail modification of the promoter, changing the native promoter for other as *ADH1* or *GAL1-10*.

The main objective was to analyze the interaction in standard conditions, as well as how it responded to changes in the cell environment. Therefore, this analysis requires Ppz1 and Hal3 to be active/functional, so that physiological conditions are conserved.

## 1.2.- Expression and functional analysis of the chromosomically encoded fusion fluorescent proteins

Different genetic backgrounds (BY4741, DBY746 and W303-1A) were tested at the beginning of this work in order to identify which of them would perform better in this experiment. The DBY746 strain showed the lower autofluorescence background and was considered the best option among the wild type strains tested. In addition, this strain is more sensitive to osmotic stress, a fact that might help to study the interaction in front this stress. We focused in 12 DBY746-based strains, named from DVS001 to DVS012. These strains have different C-terminal tags in Ppz1 and/or Hal3. In Figure 13.A can be observed a table with a schematic representation of each strain and its respective fluorescence tag.

To check if the different fusion proteins were properly expressed, an immunoblot assay was carried out. These assays were performed using anti-Ppz1 and anti-Hal3 antibodies. The size of native Ppz1 and Hal3 is 77.5 kDa and 62.5 kDa, respectively, which is increased in 25 kDa by fusion with GFP (and its derivatives, CFP and YFP) and 28.8 kDa in the case of mCherry. Results from immunoblots can be observed in Figure 13.B for Ppz1 and in 13.C for Hal3 detection, where black triangles show the wild type versions of Ppz1 and Hal3, whereas the white ones mark the tagged versions (approximately 110 kDa for Ppz1 and 95 kDa for Hal3). In all cases, the expressed Ppz1 and Hal3 tagged proteins matched the expected sizes.

A)

| Strain | Ppz1 | Hal3 |
|---|---|---|
| DVS001 | EGFP | wt |
| DVS002 | CFP | wt |
| DVS003 | YFP | wt |
| DVS004 | wt | EGFP |
| DVS005 | wt | CFP |
| DVS006 | wt | YFP |
| DVS007 | mCherry | wt |
| DVS008 | wt | mCherry |
| DVS009 | EGFP | mCherry |
| DVS010 | mCherry | EGFP |
| DVS011 | YFP | CFP |
| DVS012 | CFP | YFP |

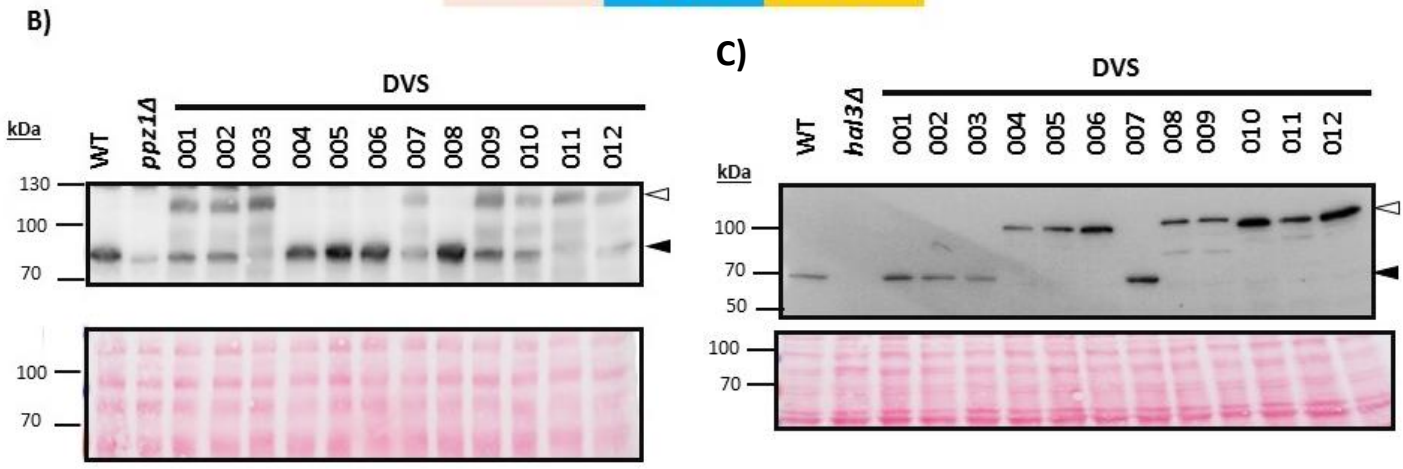


**Figure 13.Immuno detection of Ppz1 and Hal3 fluorescent derivates. A)** Table showing the different strains created. **B)** Strains DBY746, and its derivatives *ppz1Δ* and DVS001-DVS012 were grown and cells were collected in exponential phase. Protein extracts were prepared and subjected to SDS-PAGE. Proteins were transferred to PVDF membranes and the different Ppz1 versions were detected with anti GST-Ppz1 polyclonal antibodies [10]. The black triangle shows the size of native Ppz1 (77.5 kDa) and the white triangle denotes the Ppz1 tagged protein (~110 kDa, depending of the fluorescent tag). **C)** The same extracts that in **B)** were used, except that a *hal3Δ* strain was employed as negative control. After SDS-PAGE, Hal3 versions were detected using anti-GST-Hal3 antibodies. The black triangle shows native Hal3 (62.5 kDa) and the white one indicates the size of tagged Hal3 (~90 kDa). Ponceau staining of the membranes are shown for comparison of loading and transfer efficiency.

Once the correct expression of tagged proteins was verified, a phenotypic assay was carried out to check that tagged Ppz1 and Hal3 were still functional *in vivo*. Growth was carried out on plates containing LiCl and caffeine, where a functional defect in Hal3 or Ppz1 function could be easily detected. For example, strains lacking Ppz1 show tolerance to lithium (Posas *et al*, 1995b) and a lytic phenotype in the presence of caffeine (Posas *et al*, 1993). As it can be seen from Figure 14, the behavior of the different strains is the same as the wild type, indicating that the tagging procedure did not significantly alter the function of Ppz1 and Hal3. As in all cases both tagged proteins maintained their functionality *in vivo*, they were suitable for our interaction study.

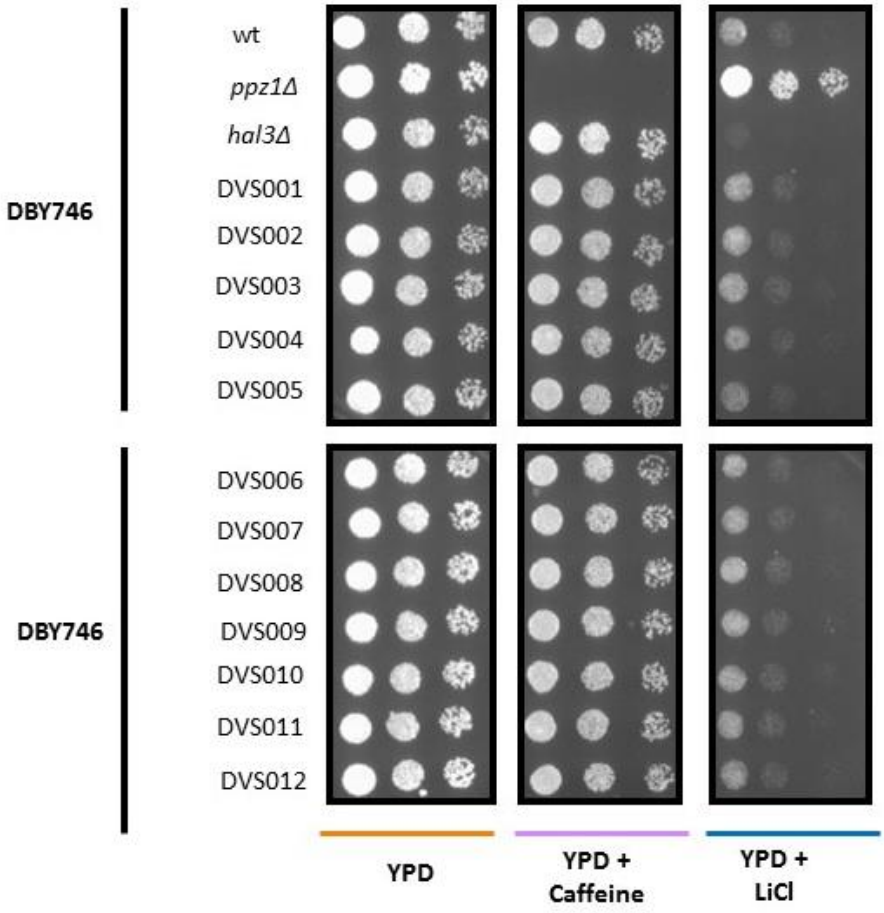


**Figure 14. Phenotypic analysis of fluorescent strains**. Strains were spotted at $OD_{600}$ =0.05 and 1/5 dilutions on YPD medium plates containing either caffeine (10 mM) or LiCl (30 mM). Plates were grown at 28°C for 72 h.

## 1.3.- Determination the interaction Ppz1-Hal3 by FRET detection using flow cytometry

Only four strains were analyzed using flow cytometry: DBY746 (no fluorescence tags), DVS001 (Ppz1-GFP), DVS008 (Hal3-mCherry) and DVS009 (Ppz1-GFP and Hal3-mCherry), because previous tests using Hal3-GFP as a donor and Ppz1-mCherry (DVS010) as acceptor showed too low FRET levels.

Due to the limitation of lasers and filters in the available cytometer (FACS Calibur), we could only excite at 488 nm (blue laser) and the emission was detected using FL1 (530/30) and FL2 (670LP) filters (green and red, respectively). Thus, the GFP signal was detected in the FL1 filter, and the interaction between Ppz1-GFP and Hal3-mCherry was detected with the FL2 filter upon excitation with the green laser.

As it can be observed in Figure 15, strains DBY746, DVS001, DVS008, and DVS009 were analyzed by flow cytometry, and excited with the 488 nm laser (blue laser). On the one hand it can be observed that DVS001 and DVS009 show stronger signal with the green filter (they express the Ppz1-GFP version) that DBY746 and DVS008. In fact, the mean of the signal in this filter is more than twice in these strains that in wild type or DVS008 cells. On the other hand, when filter FL2 is used, signal intensity is stronger in the DVS009 strain. As only the blue laser was used to excite the cells, a stronger FL2 signal in DVS009 could indicate that there was FRET between Ppz1-GFP and Hal3-mCherry, because the emission of GFP excite the mCherry tag. This result demonstrates the interaction of Ppz1 and Hal3 *in vivo*.

A)

| Strain | Ppz1 | Hal3 |
|---|---|---|
| DBY wt | wt | wt |
| DVS001 | EGFP | wt |
| DVS008 | wt | mCherry |
| DVS009 | EGFP | mCherry |

B)

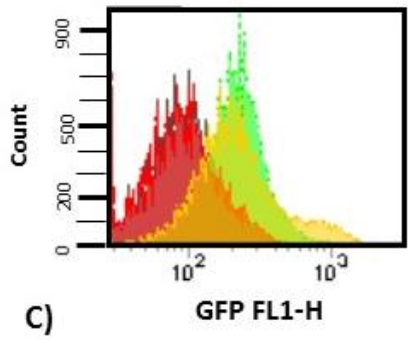


| Population | Events | %Parent | Mean |
|---|---|---|---|
| DBY wt | 20,006 | 99.0 | 99 |
| DVS001 | 20,000 | 98.7 | 232 |
| DVS008 | 20,002 | 98.6 | 102 |
| DVS009 | 20,043 | 96.7 | 273 |

C)

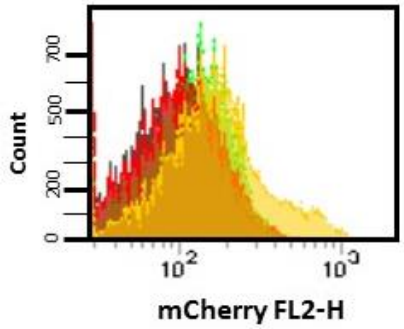


| Population | Events | %Parent | Mean |
|---|---|---|---|
| DBY wt | 20,006 | 99.0 | 106 |
| DVS001 | 20,000 | 98.7 | 131 |
| DVS008 | 20,002 | 98.6 | 111 |
| DVS009 | 20,043 | 96.7 | 206 |

**Figure 15. FRET results from flow cytometry**. **A)** Schematic table showing the different strains used and their tags. Four strains are represented, DBY746 wt (grey) DVS001 (green), DVS008 (red) and DVS009 (yellow). All samples were excited with the 488 nm wavelength laser, and detected using two channels, green **(B)** and red **(C)**. Twenty thousand cells of each strain where analyzed in low fluorescent medium in exponential phase ($OD_{600}$ =0.6-0.8). The mean indicates the signal of these strains in the specific channel.

Once the DVS009 strain (Ppz1-GFP Hal3-mCherry) was shown to yield measurable FRET by flow cytometry it was grown in low potassium (50 µM KCl) medium or in high concentration of salt (0.8 M NaCl) to test how these stresses could affect the interaction. In these conditions Ppz1 would supposedly be more inhibited, and therefore a greater interaction between Ppz1 and Hal3 would be expected. The main advantage with the flow cytometry technique is that we can follow FRET approximately ten seconds after changing the medium, and each measure could be easily performed every 30 seconds.

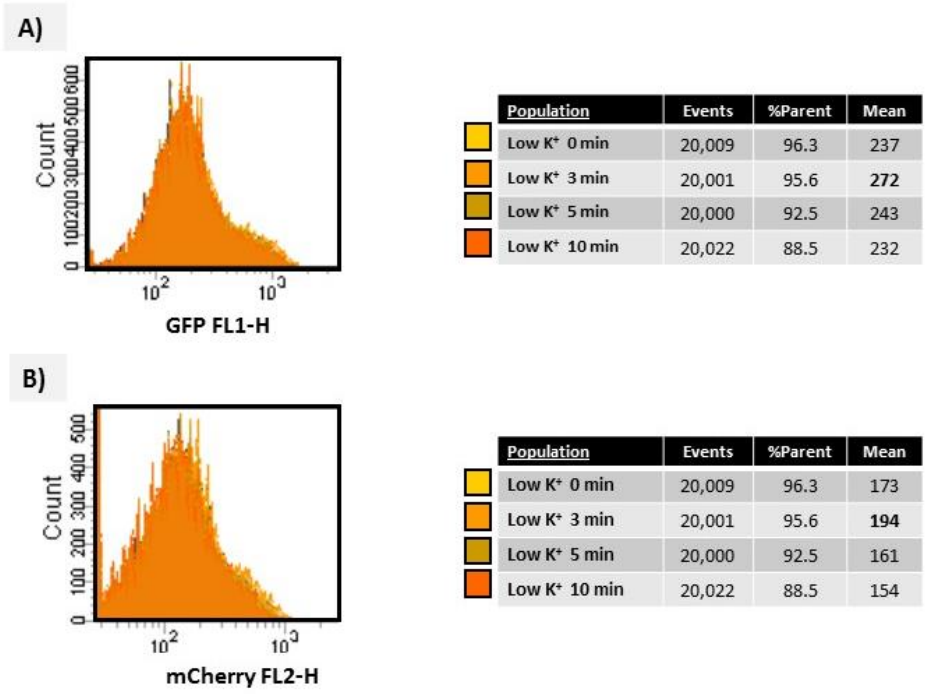


| Population | Events | %Parent | Mean |
|---|---|---|---|
| Low K⁺ 0 min | 20,009 | 96.3 | 237 |
| Low K⁺ 3 min | 20,001 | 95.6 | **272** |
| Low K⁺ 5 min | 20,000 | 92.5 | 243 |
| Low K⁺ 10 min | 20,022 | 88.5 | 232 |

| Population | Events | %Parent | Mean |
|---|---|---|---|
| Low K⁺ 0 min | 20,009 | 96.3 | 173 |
| Low K⁺ 3 min | 20,001 | 95.6 | **194** |
| Low K⁺ 5 min | 20,000 | 92.5 | 161 |
| Low K⁺ 10 min | 20,022 | 88.5 | 154 |

**Figure 16.- FRET results in low potassium.** DVS009 strain was exposed to low potassium stress, and 20,000 events were analyzed before changing the medium, and after 3, 5 and 10 minutes in low potassium medium. All samples were excited with the 488 nm wavelength laser, and detected using two channels, green **(A)** and red **(B)**.

These results were not completely satisfactory because, although some changes in the FRET levels were observed in low potassium and salt stress (not shown), they were not enough to determine the dynamism of this interaction *in vivo*. In Figure 16, where cells are exposed to a low potassium environment, we can observe an increase in FRET signal after three minutes. The problem was that these changes were too small and, in addition, the increment in FRET was accompanied by an increase in the signal in the green channel. For these reason we considered that a higher signal of FRET and consequently greater levels of expression of both tagged protein would be necessary.

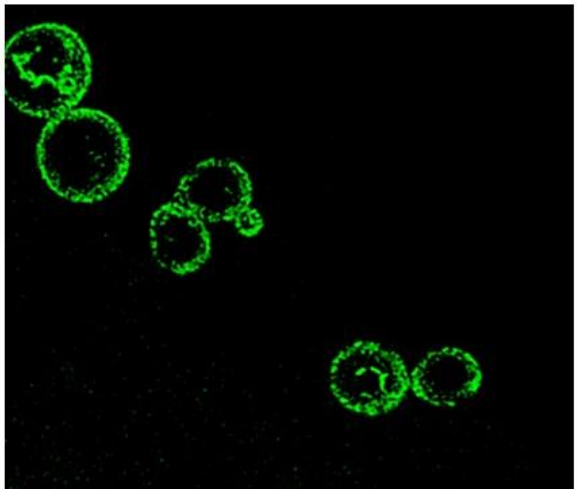

**Figure 17. Microscopy image of GFP-Ppz1.** DBY746 *ppz1*Δ were transformed with pRS316 GFP-Ppz1 and growth until exponential phase ($OD_{600}$ 0.6-0.8). The image was taken by confocal fluorescent microscopy.

To improve signal, we resorted to different strategies. One of them was to introduce in centromeric (pRS316) and multicopy plasmids (YEplac195) a *PPZ1* version with a GFP tag in the N-terminal region (position +54 bp), without modifying the myristoylation sequence, in order to do not affect the normal localization of Ppz1. Plasmid pRS316 *GFP-PPZ1* was introduced in DBY746 *ppz1Δ* cells, and observed by confocal microscopy in the *Servei de Microscopia UAB.* The result is shown in Figure 17. As it can be observed, the protein was largely detected at the cell periphery and possible internal endosomes. This result indicated that the GFP tag in the N-terminus of Ppz1 does not affect Ppz1 location.

In addition, the signal of this Ppz1 tagged version is higher than that detected in the chromosomically tagged strains, therefore being a good candidate to improve FRET.

Moreover, to increase the expression and consequently improve the FRET signal, we cloned in episomal plasmids (YEplac195 and YEplac181, marker URA3 and LEU2, respectively) the same constructs that were previously integrated in the chromosome. A FRET assay was performed by triplicate using a GFP tag in the N-terminal or C-terminal regions of Ppz1 and using a Hal3 version with the mCherry tag in the C-terminal part. Figure 18.A shows that when both tags are in the C-terminus of both proteins the percentage of FRET is higher than when a Ppz1 version with the GFP at the N-terminus was used. For this reason, hereinafter FRET experiments with Ppz1 and Hal3 were performed using these episomal plasmids with fluorescence tags at the C-terminal of both proteins.

It can be observed in Figure 18 that the results of preliminary tests were promising. The level of expression of both tagged proteins were higher than in Figure 16, as well as the signal in the FRET channel (approximately 10% of the cells are giving signal in the FRET channel). Nowadays, these experiments are being pursued in our laboratory by Marcel Albacar, another PhD student. This tool would be useful not only to analyze how Ppz1-Hal3 interaction changes in front of stresses as salt or low potassium, but also to map the regions of these proteins necessary for the interaction *in vivo*. In summary, these results show that flow cytometry analysis of FRET could be a powerful tool to study the *in vivo* interaction between Ppz1 and Hal3.

A)

YEp195 Ø + YEp181 Ø

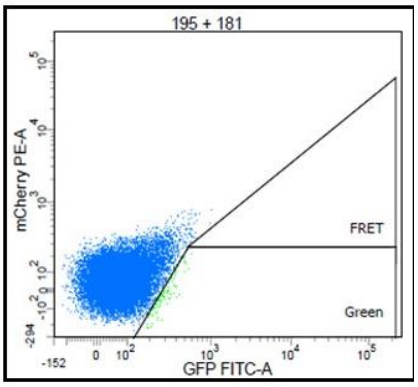


B)

YEp195 Ø + YEp181 *HAL3 mCherry*

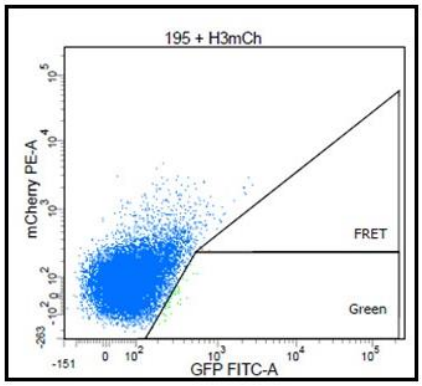


C)

YEp195 *PPZ1 GFP* + YEp181 *HAL3*

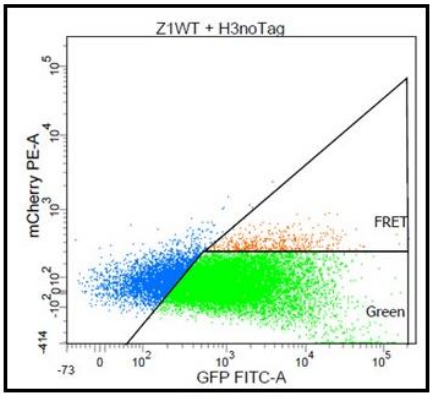


D)

YEp195 *PPZ1 GFP* + YEp181 *HAL3 mCherry*

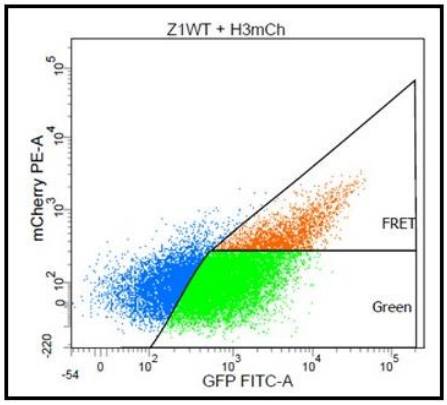


E)

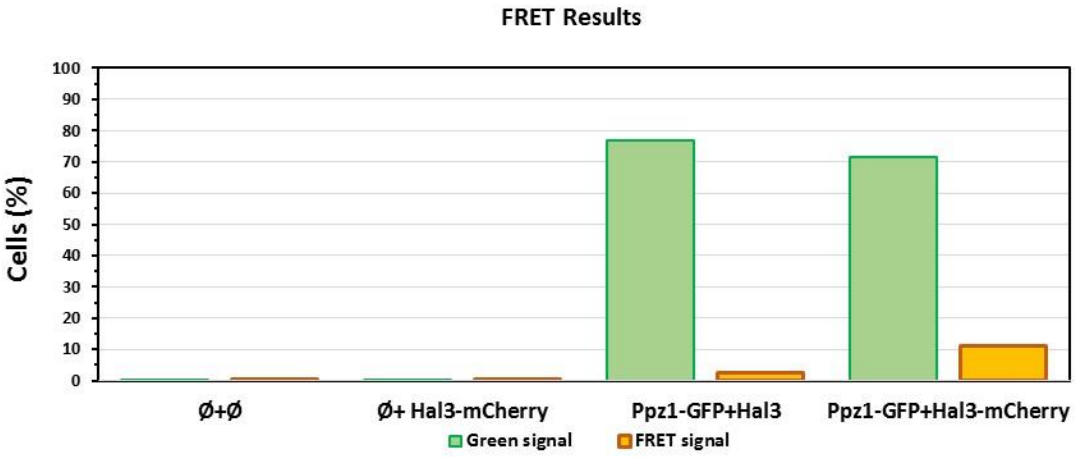

F)

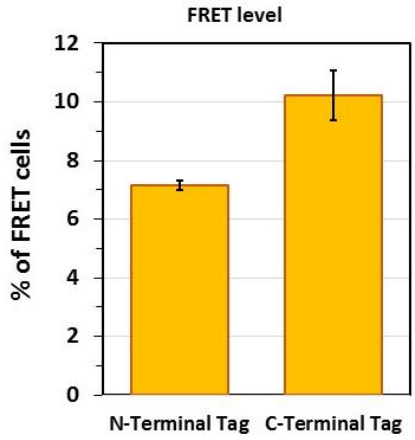


**Figure 18. Fluorescence signals and FRET analysis using episomal plasmids. A-D)** Fluorescence signal of DBY476 wild type strain transformed with empty vectors (showing little autofluorescence), mCherry-tagged Hal3 alone, a vector containing a GFP tagged version of Ppz1, plus a vector with an untagged version of Hal3, and with a vector containing a GFP tagged version of Ppz1 and a vector carrying an mCherry tagged version of Hal3. Approximately 20.000 events were counted at mid flow rate settings. **E)** The histogram shows the % of cells detected in the green and FRET channels. **F)** Histogram representing FRET percentage of the DBY476 wild type strain transformed with YEp181- Hal3-mCherry and YEp195 GFP-Ppz1 (N-terminal tag) or with YEp195 Ppz1-GFP (C-terminal tag). Data are mean ± SEM from three experiments.

## 2.- Identifying regions responsible for the Ppz1-Hal3 interaction

Numerous attempts to obtain crystals of the Ppz1-Hal3 protein complex, with the aim of obtain its 3D structure and elucidate which regions of these both proteins are involved in the interaction, were unsuccessful. Therefore, to circumvent this problem, we resorted to an approach based on chemical cross-linking *in vitro* followed by LC-MS/MS (XL-MS/MS).

XL-MS/MS consists in the binding of different proteins of interest *in vitro*, using a specific molecule denominated cross-linker, followed by proteolysis of the protein complex in order to obtain different cross-linked peptides for subsequent identification by LC-MS/MS. These crosslinkers are molecules that contain at least two reactive ends, connected through a spacer or linker, with the capacity to attach chemically functional groups as primary amines or sulfhydryl groups (lysine in the case of proteins) that are spatially close. With this procedure, intra and inter protein crosslinks can be obtained. This technique has been used to determine the interaction between more of two proteins, and to elucidate possible 3D-structures due to the intra-protein crosslinking (Hofmann *et al*, 2015; De Graaf *et al*, 2019).

After the *in vitro* crosslinking reaction, the samples were run and analyzed by acrylamide gels, although it is possible to analyze them without this step. To obtain the peptides, samples were digested using different proteases and enriched by separation of the non-crosslinked peptides. Later these samples were analyzed by LC-MS/MS, and peptides were identified by computational analysis (Leitner *et al*, 2010, 2016). Figure 19 shows an overview of the crosslinking workflow.

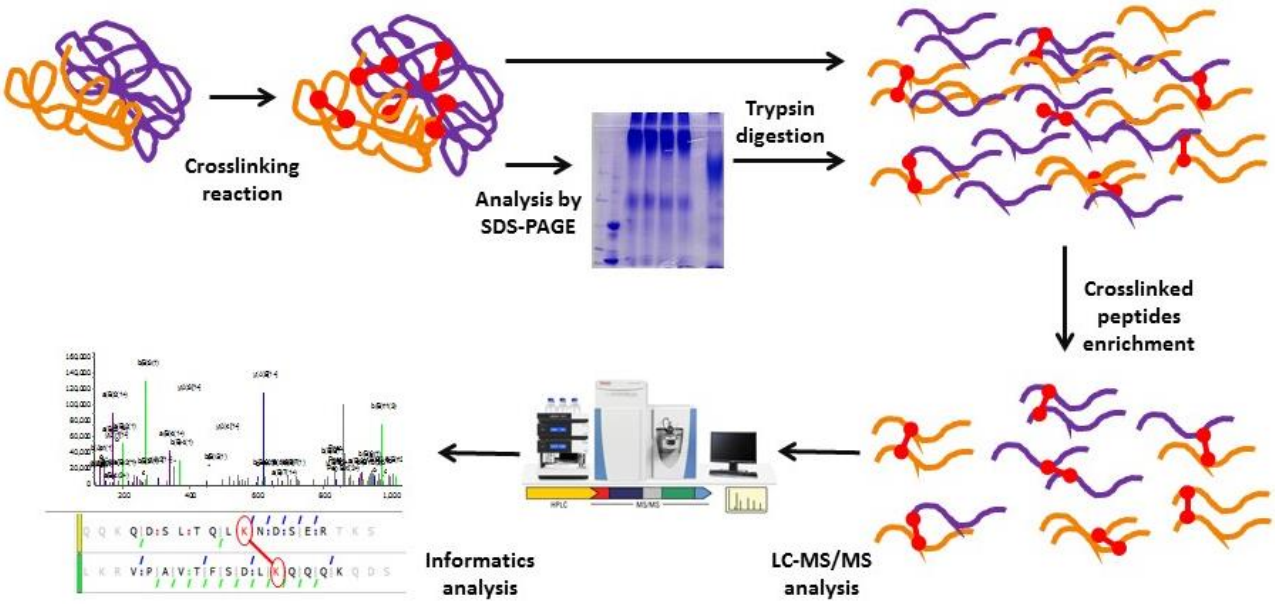


**Figure 19. Schematic representation of the crosslinking workflow.**

Recent advances in proteomics software, in crosslinked peptide enrichment and new crosslinkers that allow their own fragmentation, results in great improvement of the identification of peptides linked with the crosslinker.

In this work different crosslinkers were used (Figure 20); the main difference among them is the spacer arm (distance between the reactive parts of the molecule), i.e. BS3 is near 4 Å larger than BS2G, and could give rise to different crosslinked peptides involving different lysines. DSBU is the largest crosslinker used in this work. In addition, DSBU is a cleavable and membrane-permeable crosslinker, incorporating a urea linker in the middle of the spacer arms that can be cleaved in the gas phase during MS/MS tandem, facilitating peptide sequencing and posterior identification.

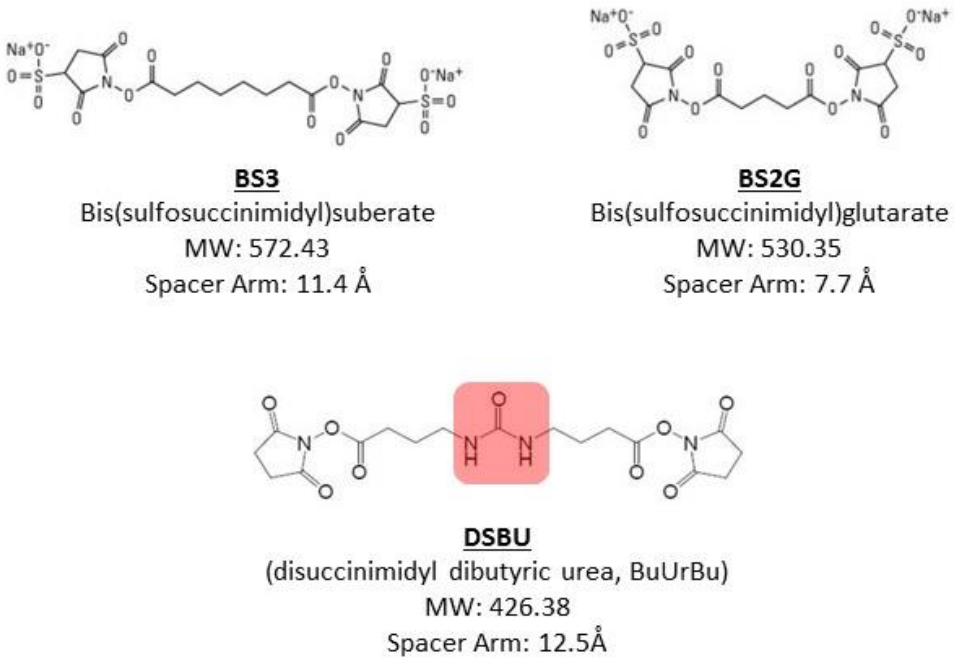


**Figure 20. Different crosslinkers molecules used.** The three different crosslinkers as well as their molecular weight (MW) and the spacer arm length, are represented in this image. The red symbol in DSBU crosslinker, remark the urea linker that could be cleaved during LC-MS/MS analysis.

## 2.1.- Crosslinking reaction between Ppz1-C-ter and Hal3

The protein complex was generated by co-expression in *E. coli* from the pET-Duet-1-Ppz1Cter+Hal3 plasmid followed by co-purification as in (Molero *et al*, 2017). The Hal3 protein was expressed without any tag (native version), and the C-terminal catalytic half of Ppz1 *(Δ1-344*) was expressed with a 6xHis tag at the C-terminus for nickel affinity chromatography purification. It is known that the Ppz1 C-terminal interacts in a much stronger way with Hal3 that the full-length phosphatase(De Nadal *et al*, 1998). For this reason, the untagged Hal3 could be only recovered if efficiently bound to the phosphatase. Figure 21.A shows a typical product of the purification procedure. Exchange of the buffer was required in order to eliminate the imidazole, which would quench the crosslinking reaction.

Once the proteins were purified and quantified, the cross-linking reaction was carried out using 20 µg of Ppz1-C-ter/Hal3 complex and different amounts of each crosslinker (BS2G, BS3 and DBSU) as it was described in the material and methods (point 10) part. Then, samples were run in a 6% acrylamide gel and stained. The result of the

BS3 reaction is shown in Figure 21.B and the result of DSBU treatment in Figure 21.C. The BS2G reaction was similar to that of the BS3 reaction (not shown). As it can be observed when the different crosslinking reactions were carried out, a protein band appear over 250 kDa, and part of this protein complex could not enter the stacking gel, indicating that very large complexes are formed. In the case of DSBU, a weak but evident band is observed with a size of ~170 kDa. However, the expected band from the cross-linked complex should have been approximately 110 kDa, the size of the sum of Ppz1-Cter (42 kDa) and Hal3 (62.5 kDa).

Then, the different bands were cut from the acrylamide gel and send to Dr. Peter Højrup (University of Southern Denmark) for LC-MS/MS analysis

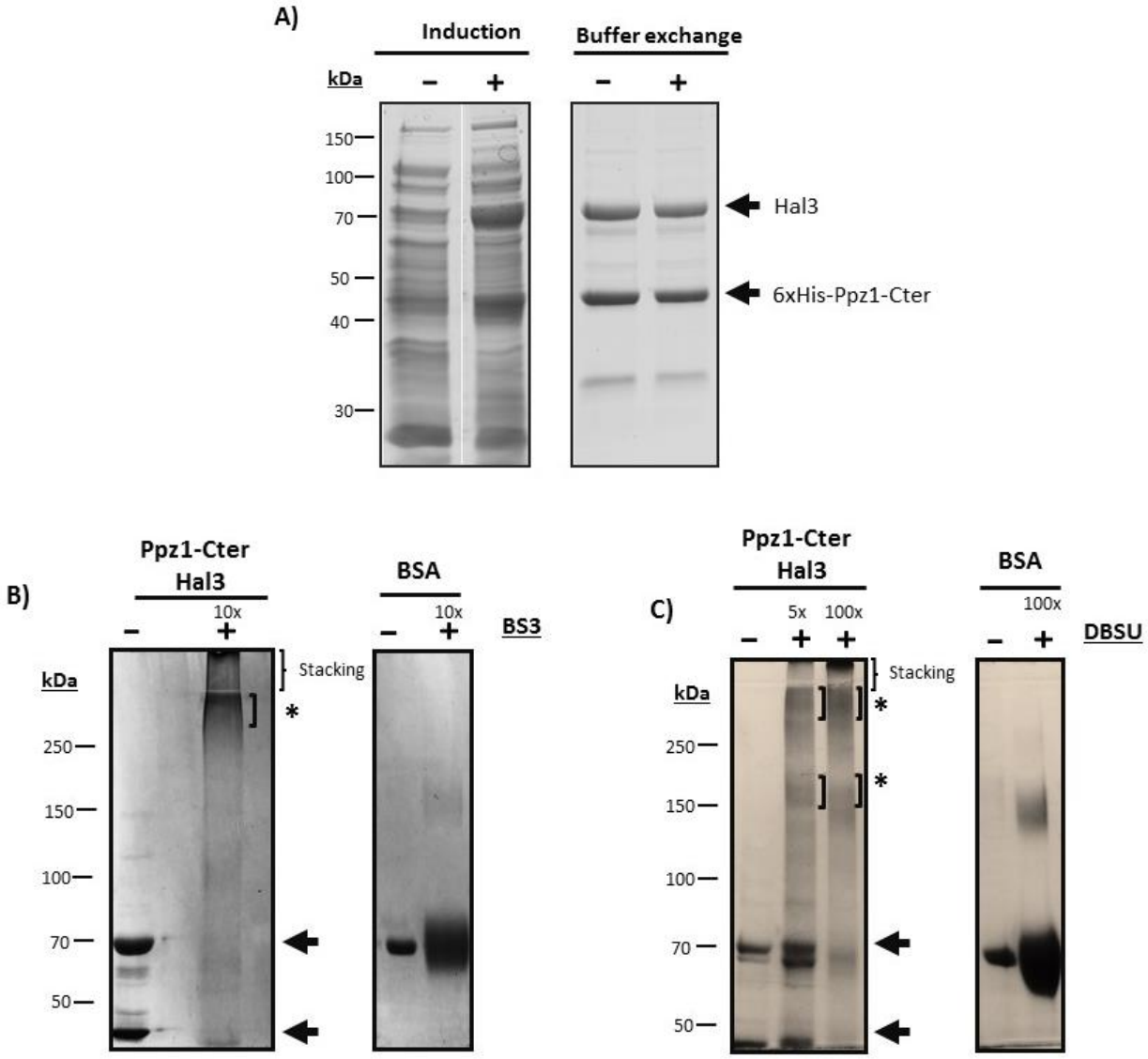


**Figure 21**. **A)** Co-expression and co-purification of Ppz1-Cter and Hal3 in *E. coli*. The left panel shows SDS-PAGE analysis of bacterial extracts before and after induction by IPTG. The right panel shows the elution of 6xHis-tagged Ppz1-Cter from Ni-NTA agarose affinity chromatography using 150 mM of imidazole, before and after buffer exchange (to eliminate the imidazole to carry out the crosslinking reaction). Samples were analyzed by 10% SDS-PAGE and stained with Coomassie Blue. **B)** BS3 crosslinking reaction. Forty µg of the protein complex were crosslinked with 10x weight excess of BS3. A 6% acrylamide SDS-PAGE gel was run and stained with Coomassie Blue. Arrows shows the Hal3 and the Ppz1-Cter size (62.5 and 42 kDa respectively) and the asterisk show the most abundant band of the crosslinking reaction. BSA was used as negative control of the crosslinking reaction. **C)** Shows the DSBU reaction, where 40 µg of protein complex were crosslinked with 5x and 100x of molar excess of DSBU. The procedures to run and stain the gel were as in **B)**.

## 2.2.- LC-MS/MS analysis of the cross-linked Ppz1-Cter/Hal3 complex

Finally, the results from the LC-MS/MS were analyzed using bioinformatics tools and allowed the identification of different peptides that are crosslinked by Lys residues. We can differentiate three kind of crosslinks: Hal3-Hal3, Ppz1-Ppz1 and Ppz1-Hal3. As can be observed in Figure 22.A, the most abundant crosslinks are Hal3-Hal3 (more than the 50% of identified crosslinks). This is result was expected due to the known capacity of Hal3 to trimerize *in vitro*. Crosslinks between Ppz1-Hal3 represented approximately 30% of the total. A summary of the best quality identified interactions and with which crosslinker was performed, is shown in Figure 22.B. Most experiments were carried out with BS3, which likely explains why the majority of crosslinks have been identified with this crosslinker. In the Table we can observe that lysines 120 and 210 interact with different residues of Ppz1 depending of the crosslinker, as it happens with K378 of Ppz1.

**A)**

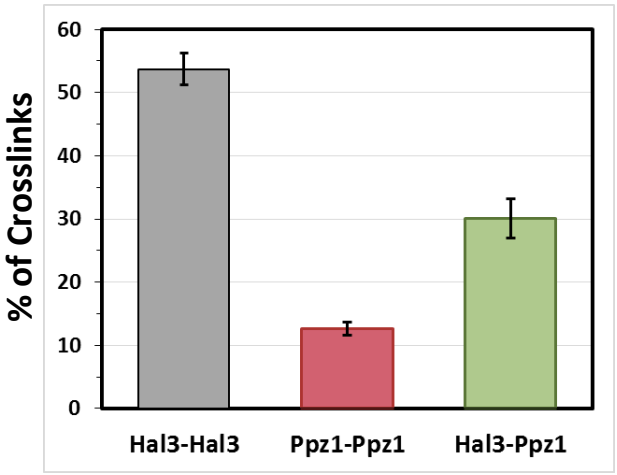


**B)**

| Hal3 lysine | Ppz1 lysine | Crosslinker |
|---|---|---|
| 90 | 593 | BS3 |
| 90 | 584 | BS3 |
| 90 | 589 | BS3 |
| 113 | 396 | DBSU |
| 120 | 356 | DBSU |
| 120 | 593 | BS3 |
| 120 | 584 | BS3 |
| 180 | 468 | BS3 |
| 197 | 468 | BS3 |
| 210 | 378 | Bs2G |
| 210 | 381 | BS3 |
| 210 | 502 | BS3 |
| 210 | 468 | BS3 |
| 236 | 378 | BS3 |
| 251 | 381 | BS3 |
| 285 | 378 | BS3 |
| 315 | 378 | BS3 |
| 315 | 502 | BS3 |
| 316 | 378 | BS3 |
| 323 | 378 | BS3 |
| 323 | 584 | BS3 |

**Figure 22.- Ppz1-Hal3 crosslinks results. A)** Percentage of the different types of identified crosslinks Data are mean ± SEM from three experiments with BS3. **B)** Table showing the main interactions between Ppz1-Hal3 found in crosslinks experiments.

In Figure 23, a bidimensional map of the cross-linked Lys is represented. Figure 23.A presents an overview of the inter-protein covalent bonds, showing that the C-terminal region of Ppz1 interacts mostly with the N-terminal half of Hal3 and the beginning of the PD-domain. Figure 23 shows a zoomed vision of such interactions, suggesting that certain regions of Hal3 seem to be frequently involved in the interaction with Ppz1. These regions correspond to Hal3 positions 90-120, 210-251 and 315-323. Besides, one of the Hal3 residue that appear in more peptide identifications is K90. In fact, this position interact specifically with a single region in Ppz1, around positions K584/K593 of Ppz1.

On the other hand, three regions of Ppz1 has been identified as possible candidates to be important for interaction with Hal3; they correspond to positions 378-381, 468-502 and 584-589. According to these results, Ppz1 K378 shows a large number of bonds with different parts of Hal3.

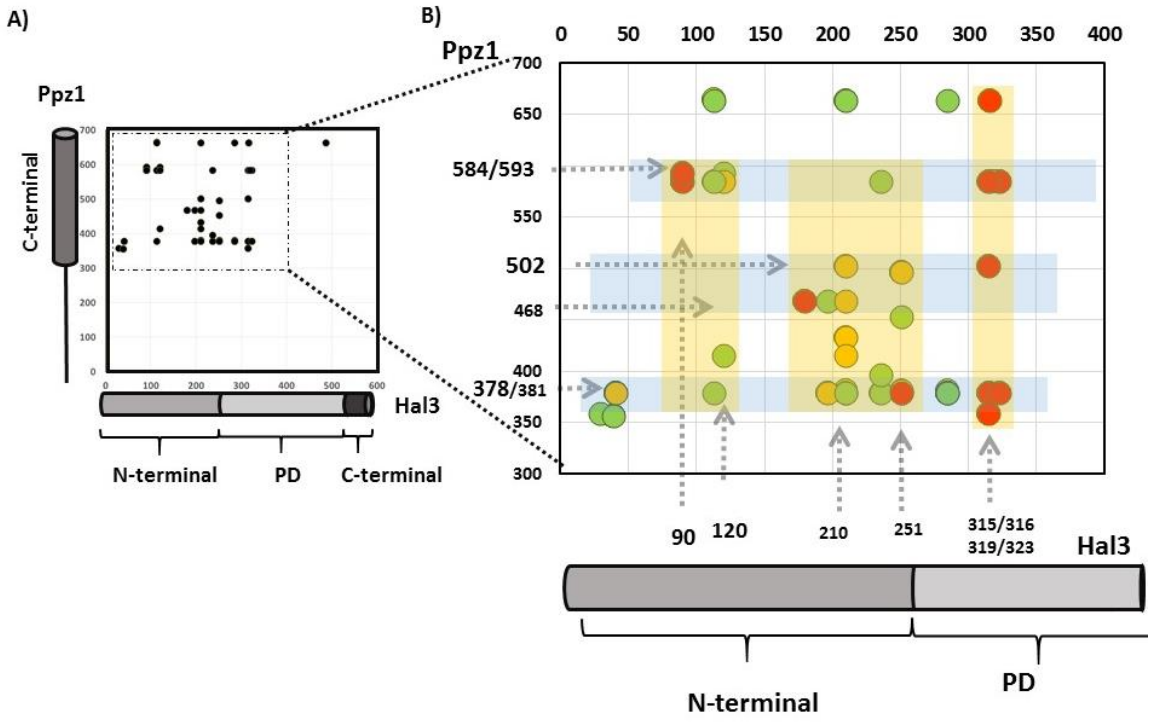


**Figure 23. Inter-protein crosslink identifications. A)** Coordinate map where each dot represents a crosslink between one lysine of Hal3 (x axis) and Ppz1 (y axis). **B)** Zoomed representation of panel A, where the points are color-coded: green, a crosslink identified once; yellow, twice; and red, thrice or more.

Figure 24 shows, using a model of the C-terminal domain of Ppz1, the mentioned lysines (marked in red), as well as the peptides containing those lysine (in raspberry). As it can be observed, the six lysines (378, 381, 468, 502, 584 and 593) are located at the two cluster in two different sections of the protein. No internal interactions have been identified.

Finally, it is important to remark that these results are preliminary.Nowadays new sample sets are being analyzed by the group of Dr Peter Højrup, with the expectation of improving resolution of the interaction map.

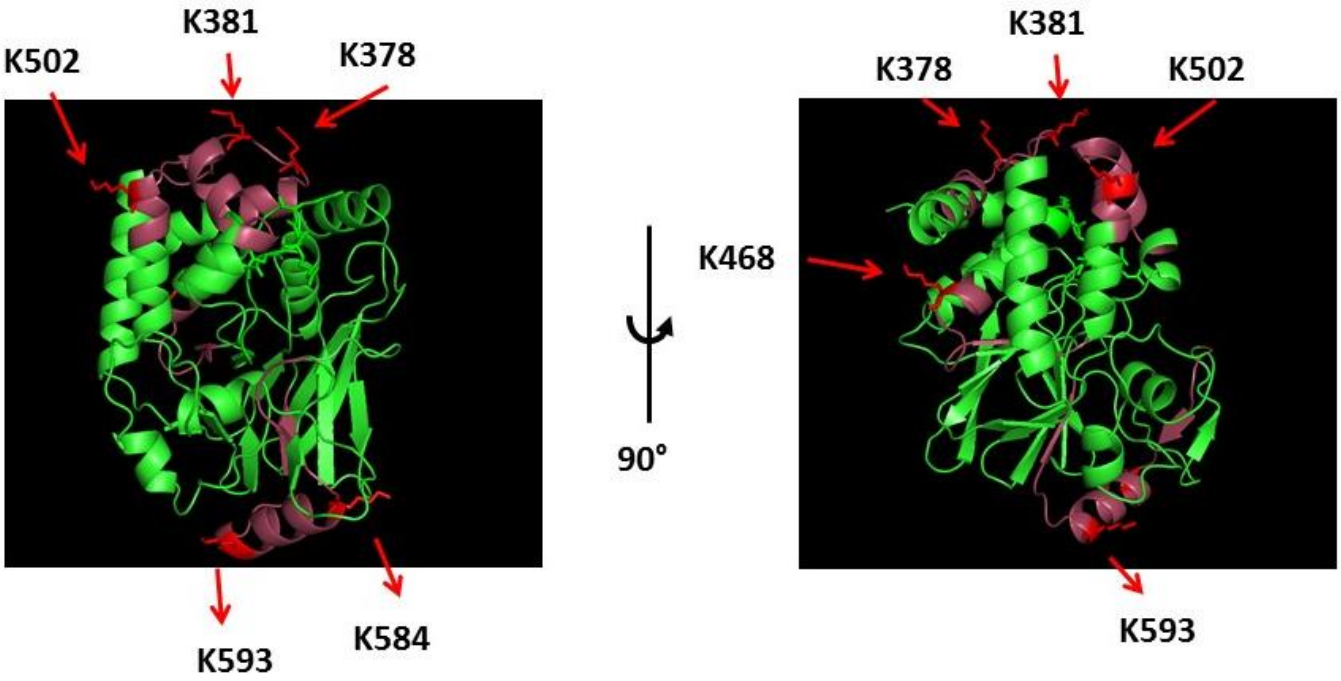


**Figure 24.- 3D localization of Ppz1 lysines bound to Hal3 by crosslink.** 3D-Structural mode of the C-terminal domain of Ppz1, in red are marked crosslinked lysines and in raspberry colour, the peptides identified that contain these lysines.

# CHAPTER2

## The regulation of Ppz1 and Hal3 by phosphorylation

# Chapter 2.- The regulation of Ppz1 and Hal3 by phosphorylation

## 1.-Study of the Ppz1 N-terminal region

In this chapter we describe our investigation about how different changes in the phosphorylation state in the N-terminal region of Ppz1 could affect its activity and binding to Hal3.

The N-terminal ends of Ppz1 and Ppz2 are very disordered regions, but both present domains of "folding upon binding", that is, domains that upon interaction with other molecules, ligands, proteins, membrane… could assume an ordered secondary structure. Therefore, Ppz1 sequence was analyzed by IUPred2A (https://iupred2a.elte.hu), a combined web interface that identifies protein binding sites located in disordered regions. To do so, the server runs two different algorithms upon the primary sequence of a given protein. IUPred2 scans for protein disorder and ANCHOR2 spots amino acid clusters for predicting protein binding regions in disordered proteins, capable to establish protein-protein interactions (Dosztányi *et al*, 2009). As predicted by IUPred2A, Ppz1 possesses two different structural domains, dividing the protein in a highly disordered N-terminal region and an ordered C-terminal region (Figure 25). ANCHOR uncovers up to four significant binding clusters within the disordered N-terminal region (showed in figure 25 from A to D), which may be involved in a Hal3-Ppz1 interaction or in transient stabilization contacts with the inner membrane moiety. It has been proposed that conformational transitions from unfolded to folded structures might provide regulatory functions to specific interactions, thus modulating from catalytic activation to protein stabilization (Csizmok *et al*, 2016).

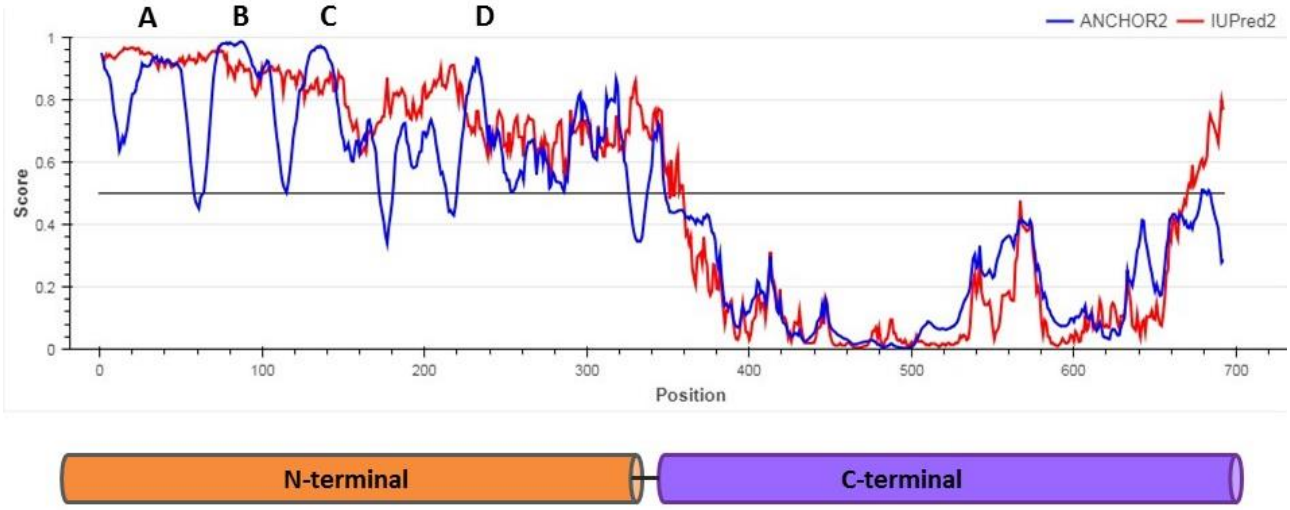


**Figure 25. Prediction of disordered regions and "folding upon binding" domains of Ppz1.** Using the tool https://iupred2a.elte.hu/ the evaluation of Ppz1 by the IUPred2A algorithm revealed that the N-terminal domain is highly disordered and comprises up to four significant binding sites. Normalized IUPred2 (red) and ANCHOR (blue) scores are plotted for each amino acid and the threshold, score of 0.5, highlighted.

The bioinformatics assessment of Ppz1 support the hypothesis that its N-terminal domain may play a critical role in the overall activity of the protein through the establishment of genuine interactions with several moieties, including Hal3 globular surface.

As was explained before, the N-terminal region of Ppz1 is very rich in positively charged (Arginine and Lysine) and phosphorylatable residues (Serine and Threonine). Therefore, phosphorylation in the N-terminus could change the net charge of this region, thus leading to modifications in the structure and the function. Thus, phosphorylation in the N-terminal region could be a mechanism for Ppz1 regulation.

The Ppz1 phosphatase can be phosphorylated by different kinases *in vivo* and *in vitro*, as described in the literature (Posas *et al*, 1995b; Swaney *et al*, 2013; Holt *et al*, 2009). One kinase that could participate in the regulation of Ppz1 is Hog1. This MAP kinase plays an important role in cation homeostasis. Hog1 is believed, on the one hand, to activate the efflux of $Na^+$ in response to salt stress by phosphorylating the Nha1 $H^+/Na^+$ antiporter (Kinclova-Zimmermannova *et al*, 2006). On the other hand, the Hog1 kinase pathway positively modulates the transcription of the gen *ENA1*, among other

pathways (Márquez & Serrano, 1996). We were advised by Dr. F. Posas (UPF-Barcelona) about the identification of two residues in Ppz1 (T261 and S265) that could be phosphorylated *in vivo* in a Hog1-dependent manner (recently reported in (Romanov *et al*, 2017)). We considered these findings as a starting point to investigate whether phosphorylation could regulate Ppz1 function. A further reason to focus on these residues was that the region comprising T261 and S265 in Ppz1 ($^{261}$TPLNS$^{265}$) is rather conserved in Ppz2 ($^{271}$TPLHS$^{275}$).

# 2.-*In vitro* phosphorylation of Ppz1 by Hog1

## 2.1.- Heterologous expression of Ppz1 variants

To analyze which residue of Ppz1 (T261 or S265) is phosphorylated by Hog1, we changed each or both residues to alanine (non-phosphorylatable residue) in a pGEX-6P1 PPZ1 construct to allow heterologous expression in *E. coli*. The same changes were introduced in a version of Ppz1 with a replacement of R451 to Leu, a change that produces a Ppz1 without phosphatase activity (Clotet *et al*, 1996). In this way, we can compare the *in vitro* phosphorylation of Ppz1 by Hog1 in the presence or the absence of phosphatase activity.

The eight versions of Ppz1, four with phosphatase activity and four without, were expressed in *E. coli* as GST-fusions to allow purification by affinity chromatography. After purification, the GST-tag was cleaved with PreScission protease. Small aliquots of each protein were analyzed by SDS-PAGE to quantify the concentration of each sample, as shown in Figure 26. The 70 kDa band is a contaminant, DnaK, as deduced by MALDI-TOF analysis. DnaK is one of the *E. coli* Hsp70 chaperones and its appearance is very typical in GST purifications (Morales *et al*, 2019).

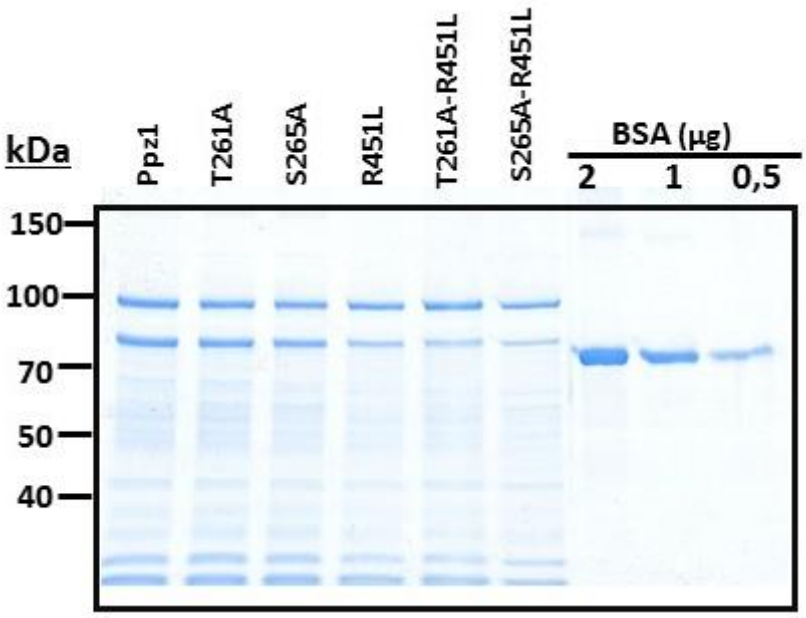


**Figure 26.-** SDS-PAGE of different affinity-purified Ppz1 variants after cleavage of the GST tag with preScission protease. Different quantities of BSA were used to quantify each protein**.**

## 2.2.- *In vitro* phosphorylation assay

After quantification, proteins were sent to Dr. Posas's lab (UPF), were a Hog1 *in vitro* phosphorylation assay with radioactive [γ-32P] ATP was carried out.

To perform this experiment it is necessary to activate Hog1 *in vitro*. This is accomplished by addition of a hyperactive version of the Hog1 kinase Pbs2 (Pbs2EE), carrying a double phosphomimetic mutation in the position of Ser514 and Thr518 (Warmka *et al*, 2001).

The experiment was performed thrice, with three different preparations of proteins, and very similar results. Six Ppz versions were analyzed in this case: native Ppz1, Ppz1 T261A, Ppz1 S265A and the same three versions with the inactivating R451L mutation. In some experiments, Ppz1 was inactivated by boiling of the enzyme sample prior the phosphorylation assay.

Figure 27 shows the result of a typical experiment. As shown in panel A, where the Ppz1 variants were not boiled, it can be observed phosphorylation of native Ppz1, proving that Ppz1 is a substrate of Hog1. On the contrary, neither Ppz1 T261A nor Ppz1

S265A were phosphorylated. This result was considered surprising, because one would expect that only mutation of the phoshorylatable residue would abolish phosphorylation. For example, if S265 would be the Hog1 target, Hog1 should phosphorylate the T261A variant (where S265 is present). The same reasoning would apply if T261 would be the Hog1 target.

In contrast, when Ppz1 versions without phosphatase activity (R451L) were used as substrate, native Ppz1 as well as the T261A version were phosphorylated, whereas the S265A variant was not. The phosphorylation pattern using Ppz1 versions lacking phosphatase activity was very similar to that observed using boiled Ppz1 versions (Figure27.B). This suggest that Ser265 of Ppz1 could be a target of phosphorylation by Hog1. On the other hand, the lack of phosphorylation of the T261A version, observed only when Ppz1 is active, could be interpreted if it is assumed that Ppz1 could autodephosphorylate at Ser265.

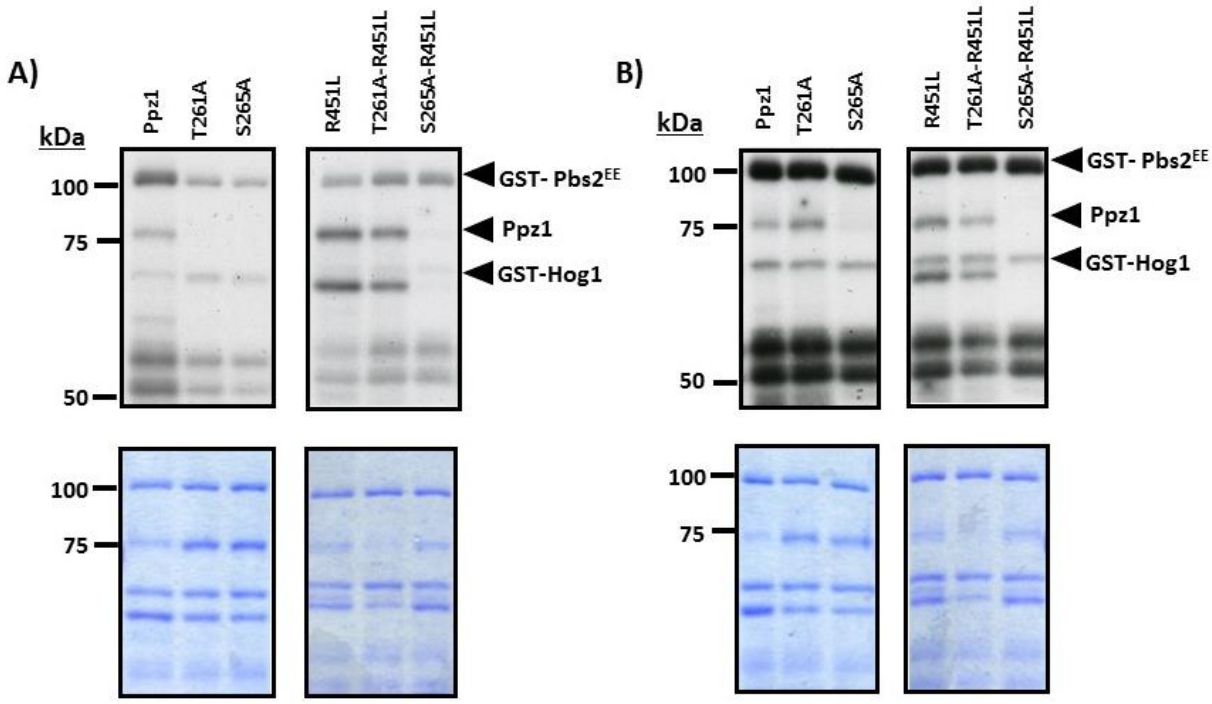


**Figure 27.- Hog1 *in vitro* phosphorylation.** GST-Pbs2EE and GST-Hog1 were preincubated in order to phosphorylate and activate Hog1 with [γ-32P] ATP. After that, the different versions of Ppz1 were added as Hog1 substrate either untreated **(A)** or boiled **(B)**. Top panels show autoradiographies. The bottom panels show the gel stained by Coomassie blue. This experiment was repeated thrice and a representative experiment is shown.

## 3.- *In vitro* inhibition of the phosphatase activity of the diverse Ppz1 versions by Hal3

Given the ability of S265 to be phosphorylated by Hog1, we considered the possibility that phosphorylation of this residue could affect the capacity of the phosphatase to be inhibited by Hal3. In this experiment, two versions of Ppz1 with double mutations, T261A/S265A and T261E/S265D were expressed in *E. coli* using pGEX-6P-1 plasmid (GST-fusion). The T261E/S265D version mimics Ppz1 constitutively phosphorylated in both residues. These Ppz1 versions, together with native Ppz1 and Hal3 were expressed and purified as described in the Material and Methods section (8.1), and the purified proteins were analyzed by SDS-PAGE (Figure 28.A).

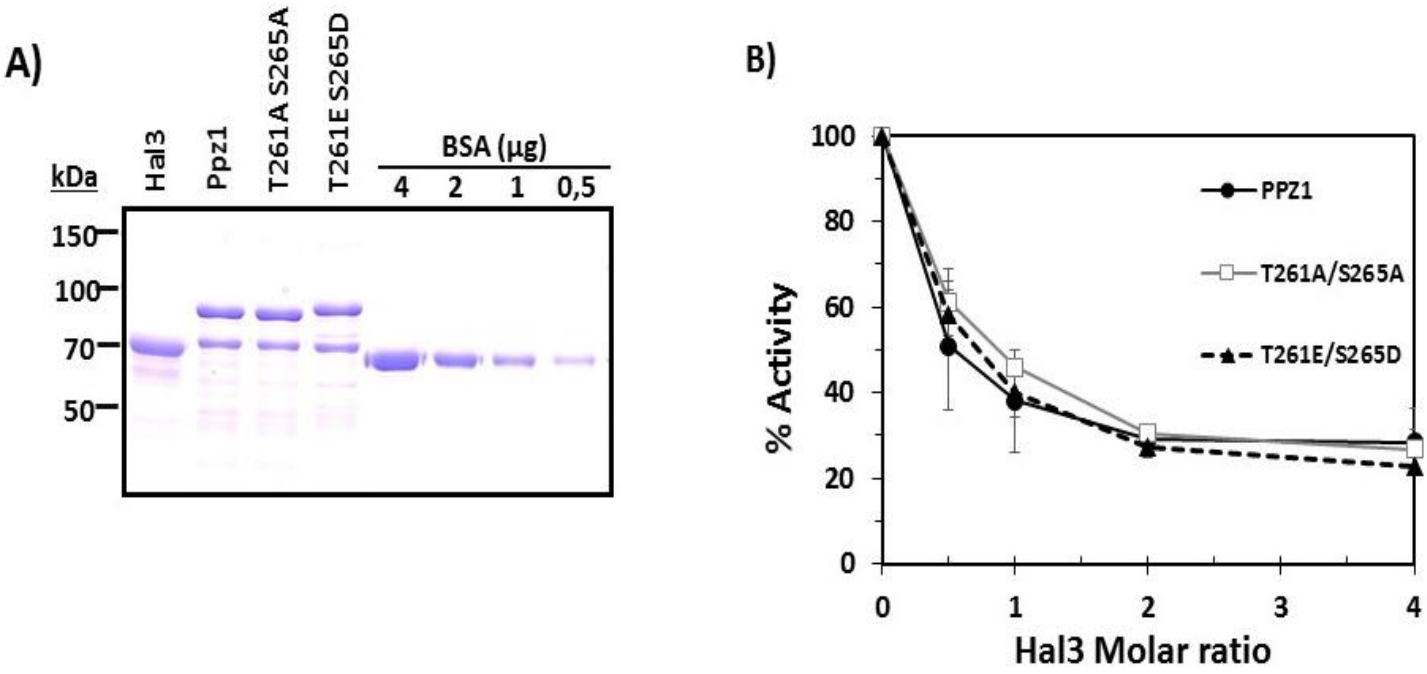


**Figure 28.-Phosphomimetic mutations of T261 and S265 do not affect inhibition of Ppz1 phosphatase activity by Hal3. A)** SDS-PAGE image showing the results of heterologous expression in *E. coli* of Hal3, Ppz1 and both mutated versions. BSA was used as reference to quantify protein concentrations **B)** One µg of the recombinant Ppz1 versions were incubated in the presence of increasing concentrations of Hal3, and the phosphatase activity was tested using *p*-nitrophenyl phosphate (pNPP).

The ability of Hal3 to inhibit the different versions of Ppz1 was tested by incubating stoichiometric amounts of the inhibitor with the phosphatase prior initiating the assay. As shown in Figure 28.B, native and mutated Ppz1 versions were inhibited by Hal3 in the same way. Therefore, the transformation of T261 and S265 in phosphomimetic residues does not preclude inhibition of Ppz1 by Hal3 and, likely, does not affect interaction of the phosphatase with its regulatory subunit.

## 4.-Phenotypic assays of Ppz1 N-terminal versions

To evaluate if phosphorylation changes in these residues could affect Ppz1 function, the different mutated versions were expressed in yeast from a centromeric plasmid (pRS316).

Two salts stress conditions (LiCl and NaCl) and caffeine were used to analyze the functionality of the different Ppz1 versions. As mentioned, a *ppz1* mutant shows increased tolerance to $Li^+$ and $Na^+$. The opposite happens in the presence of caffeine, where lack of *PPZ1* leads to a lytic phenotype. Therefore, the centromeric plasmids bearing the Ppz1 variants were introduced in *ppz1Δ* and *ppzΔ1 ppz2Δ* double mutant strains and then, mutants were grown in plates with the different compounds, with the objective to evaluate if the phosphatase variants were able to substitute for the native enzyme.

As it can be observed in Figure 29, none of the different mutations in the N-terminus of Ppz1, either to alanine or aspartic/glutamic acid, had any effect in the function of Ppz1. The levels of expression of each Ppz1 variant were analyzed by western blot (data shown in figure 37) and, in all cases, they were found to be equal to native Ppz1. This experiment was replicated in the same conditions in two other different genetic backgrounds, DBY746 and JA100, with similar results to those found in strain BY4741 (data not shown).

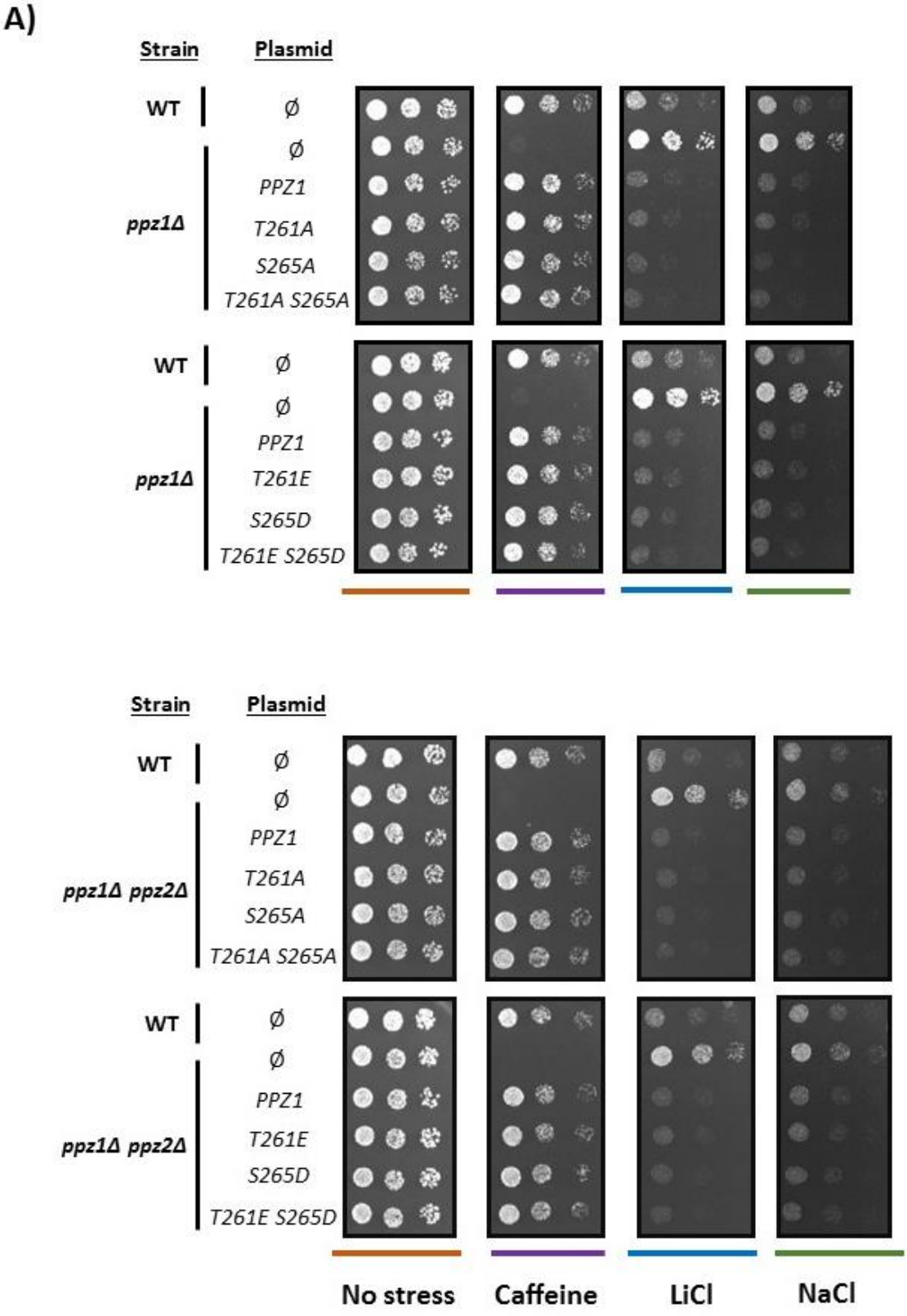


**Figure 29. Phenotypic analysis of Ppz1 variants**. BY4741 wild type (WT) or *ppz1*Δ **(A)** or *ppz1*Δ *ppz2*Δ **(B)** strains containing the indicated plasmids were spotted at OD600 0.05 and 1/5 dilutions on synthetic medium plates lacking uracil and containing either caffeine (8 mM), LiCl (400 mM) or NaCl (1.2 M). Plates were grown at 28°C for 72 h.

Due to the absence of functional effect of the mutations described above, we devised another strategy to elucidate whether phosphorylation could be involved in the regulation of Ppz1. This approach consisted in the over-expression of a GST-tagged Ppz1 version in yeast cells and then to expose these cells to diverse stress conditions that supposedly might induce changes in the functional properties of Ppz1. It was expected that these changes might be caused by changes in the phosphorylation state of the phosphatase. To this end, we grew cells with low concentrations of potassium or high concentration of $Na^+$ (NaCl), both conditions in which Ppz1 activity should be inhibited. After that, cells were harvested and lysed. Ppz1-GST was affinity-purified from crude protein extracts and Ppz1 phosphorylation was assessed using mass spectrometry. A schematic representation of this strategy is shown in Figure 30.

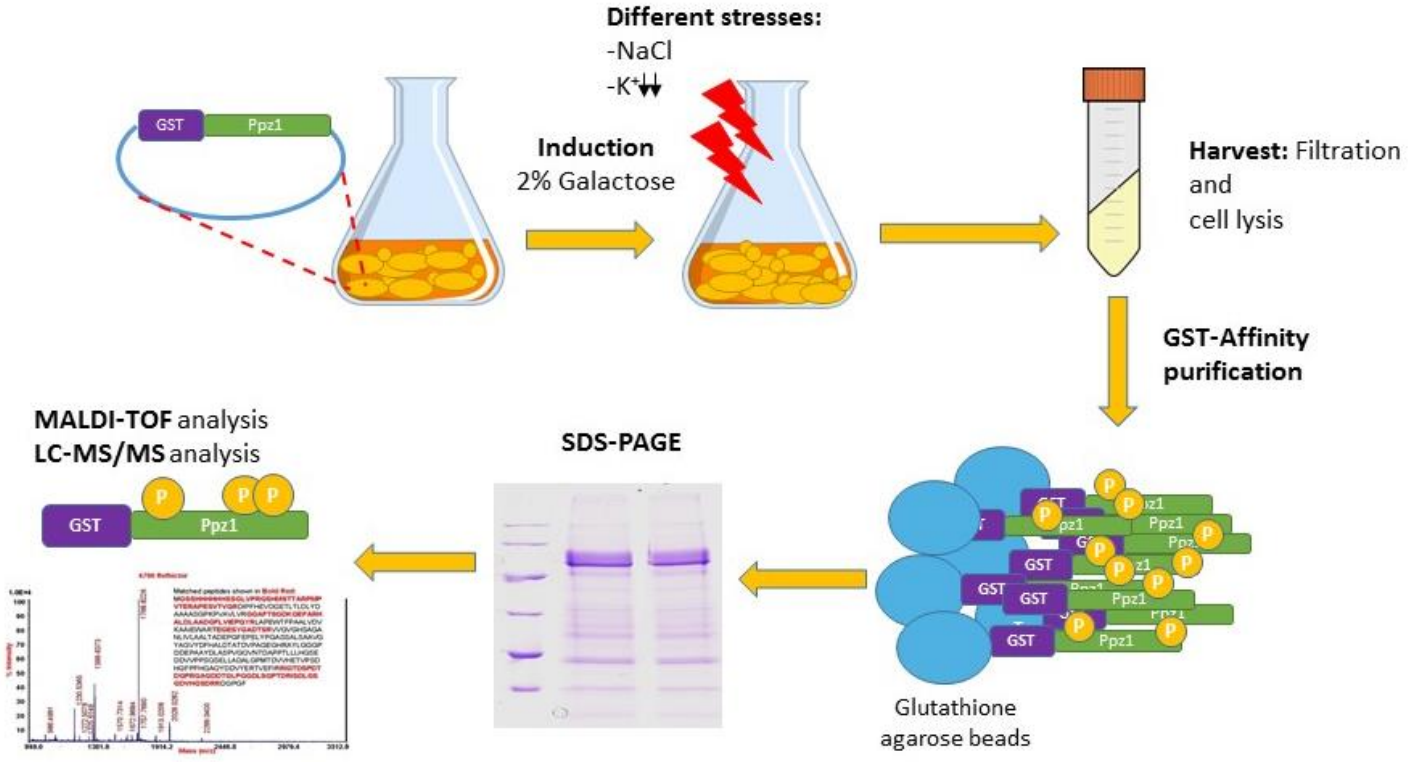


**Figure 30.- GST-Ppz1 purification and phosphorylation analysis workflow.**

## 4.1.- Over-expression of GST-Ppz1 in *S. cerevisiae* and sample collection

The first problem that we experienced was to overexpress Ppz1 from the *GAL1-10* promoter. Ppz1 is one of the most toxic protein when is over-expressed in *S. cerevisiae* and the amount of protein copies that the yeast cell can tolerate is very low (Makanae *et al*, 2013). This fact makes difficult to obtain sufficient quantities of purified Ppz1 for MS analysis. For this reason, Arg451 in the pEGH-Ppz1 plasmid (Zhu *et al*, 2008) was mutated to Leu, in order to overexpress the inactive version of the phosphatase(Clotet *et al*, 1996). Immunoblotting analysis of cell extracts expressing both versions from the pEGH plasmid (Ppz1 and Ppz1$^{R451L}$) showed (Figure 31) that conversion to the non-catalytic version of the phosphatase results in a substantial increase in the amount of expressed protein, thus allowing purification of enough amounts of Ppz1 for MS analysis.

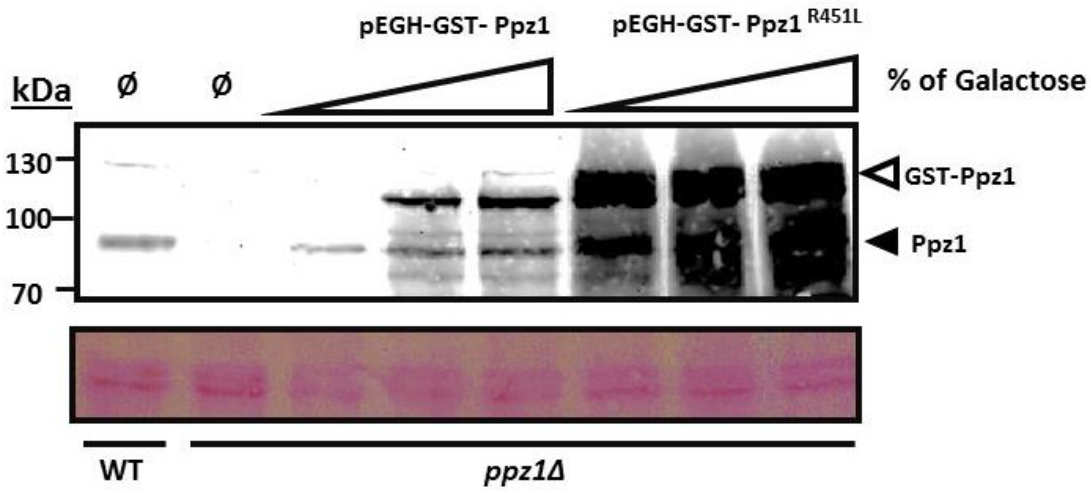


**Figure 31.-Expression levels of native Ppz1 vs Ppz1$^{R451L}$ overexpression.** Protein extracts (40 µg) prepared from the indicated strains transformed with the different plasmids were resolved by SDS-PAGE (10% polyacrylamide gel), transferred to membranes and proteins were probed with a polyclonal anti GST-Ppz1 antibody. BY4741 wild type (WT) and *ppz1Δ* were transformed with the empty plasmid. Strains transformed with pEGH-GST-Ppz1 and pEGH-GST-Ppz1$^{R451L}$, were treated with different concentrations of galactose (0.1, 1.0 and 2.0 % respectively) for 1 hour to induce Ppz1 overexpression from the *GAL1-10* promoter. Black arrowhead denotes the mobility of native Ppz1

Therefore, a *ppz1Δ* strain transformed with pEGH Ppz1$^{R451L}$ was used to continue with this approach. After the exponential phase in synthetic medium lacking uracil with 2% Raffinose as carbon source the over-expression of Ppz1 was induced by galactose at 2% and one hour later the cells were filtered to change the medium. Then, three different media were used: a standard one (with 50 mM KCl, as reference), one with low concentration of $K^+$ (50 µM KCl) and a third one with high concentration of salt (0.8 M NaCl). Samples were collected at two different times: 5 and 20 minutes. A schematic figure of this process is represented in Figure 32.

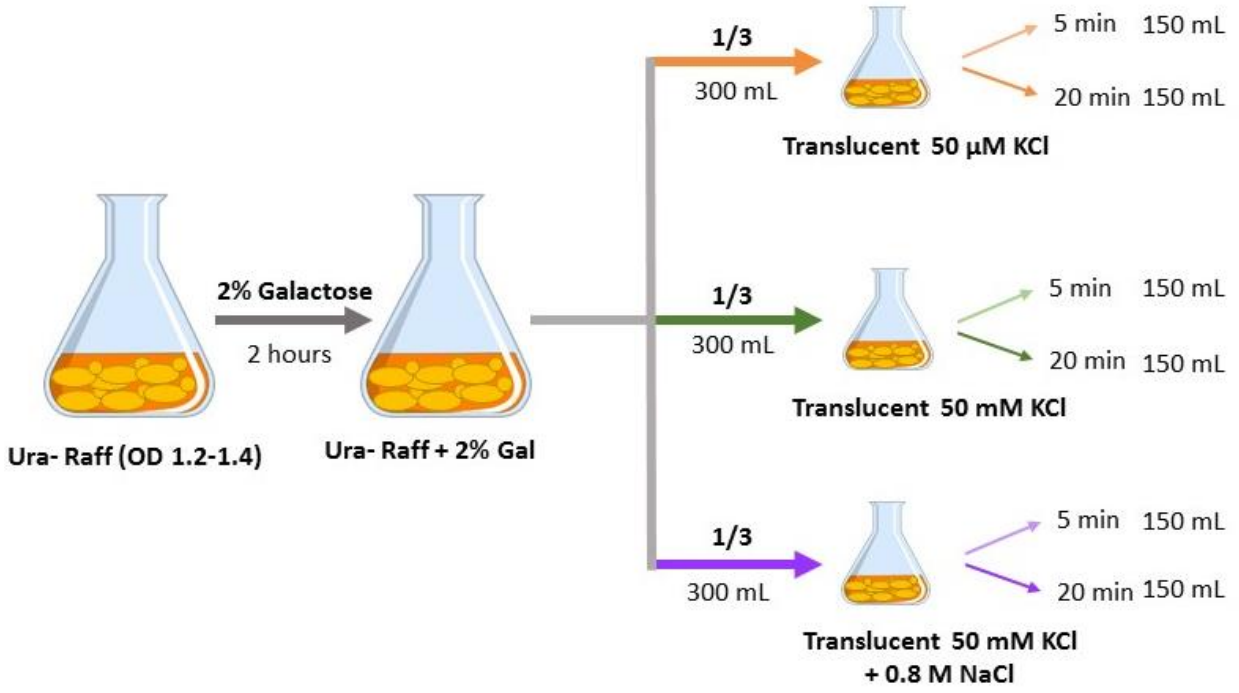


**Figure 32.- Schematic representation of the experimental procedure to overexpress Ppz1 upon the exposure of cells to different stresses.**

## 4.2.- GST-Ppz1 purification and analysis

Upon cell lysis and affinity purification of GST-Ppz1, samples were analyzed by SDS-PAGE, as shown in Figure 33. The gel showed a ~120kDa band, which approximately corresponds to the mass of the GST-Ppz1 fusion (theoretical mass: 107 kDa). These bands were cut out of the gel and analyzed by MALDI-TOF for identification. Afterwards, the GST-Ppz1 samples were digested by trypsin, and after that the samples were enriched in phosphopeptides by $TiO_2$ chromatography. We analyzed the tryptic peptides using MALDI-TOF. Although some differences between the different stresses could be observed, difficulties in the identification of the phosphorylated residues aroused. These problems were due to peptides containing large number of phosphorylatable residues (especially Ser or Thr). In fact, some identified peptides contained more than 6 serine, making it difficult, due to the limitations of the MALDI-TOF approach, to identify which

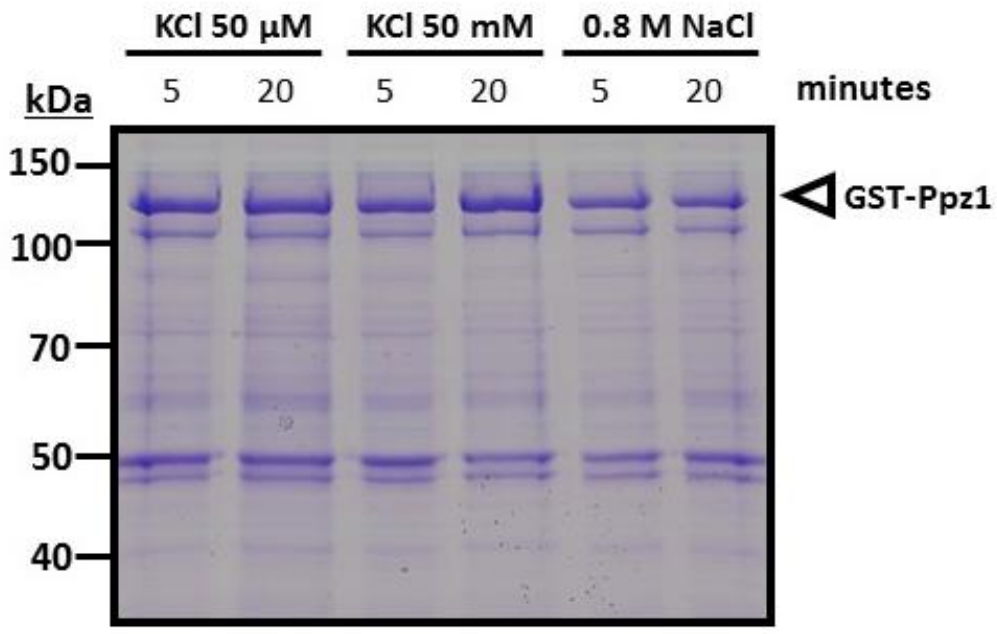


**Figure 33.- Purification of GST-Ppz1 from *S. cerevisiae* to analyze by Mass Spectrometry.** SDS-PAGE (10% acrylamide) stained with Coomassie Blue. GST-Ppz1 was purified from cells growing in different conditions to analyze how the specific stress affects Ppz1 phosphorylation.

residue was phosphorylated. Therefore, we resorted to the LC-MS/MS methodology, which is more sensitive, and allows very high confidence identifications.

## 4.3.- LC-MS/MS results of Ppz1 phosphorylation.

Analysis of purified GST-Ppz1 by LC-MS/MS was done in collaboration with Dr. Jensen's Group in the University of Southern Denmark. Two sets of experiments were analyzed, and the coverage of Ppz1 that we obtained after the phospho-enrichment was approximately 40% (Figure 34). We can observe that the coverage of the N-terminal region is quite extensive, although some Ser-rich segments are not covered. This could


**Figure 34.-Ppz1 coverage after LC-MS/MS analysis.** In orange appear identified regions of the N-terminal region and in purple that of the C-terminal one. Green rectangle indicates the rich serine-arginine region described in (Minhas *et al*, 2012)

be due to the fact that these residues are not phosphorylated, and for this reason are not selected by after of $TiO_2$ enrichment, or to the high number of lysine and arginine residues, yielding too small peptides that would escape purification.

As a summary of the results obtained, Figure 35, shows an overview of the phosphorylation state of different residues of Ppz1 in the different conditions described above. Positions appearing more than once denote that this residue was identified as phosphorylated in different peptides.

To note, Ser49 with a high score of identification, appear phosphorylated in normal and low potassium conditions, but, in the case of salt stress, peptides containing this residue are not identified, suggesting that they could be dephosphorylated in this condition and therefore would not be purified during the enrichment procedure. This is also the case for Ser81, Thr171 or the double phosphorylated peptide containing Ser239 and Ser242. On the other hand, we can identify a triphosphorylated peptide encompassing positions Ser239, Ser242 and Ser243 only in low potassium conditions.

Also, comparing our results with different databases as BioGRID (https://thebiogrid.org/) or SGD (Saccharomyces Genome Database https://www.yeastgenome.org) we can find new 9 positions of Ppz1 that can be phosphorylated *in vivo*, not described so far. These positions are S19, S81, S82, S97, S152, S189, S191, S209 and S242 and are marked in red in Figure 35.

| | | KCl 50 µM | | KCl 50 mM | | 0.8 M NaCl | | |
|---|---|---|---|---|---|---|---|---|
| | | 5 | 20 | 5 | 20 | 5 | 20 | minutes |
| Position | PEP | Xcorr | XCorr | XCorr | XCorr | XCorr | Xcorr | |
| S19 | 3.12E-02 | - | - | - | * | - | - | |
| S49 | 5.30E-16 | ***** | ***** | ***** | ***** | - | - | |
| S81 | 1.59E-05 | ** | ** | *** | *** | - | - | |
| S81, S82 | 7.04E-02 | * | * | - | - | - | - | |
| S97, S99 | 4.54E-07 | **** | *** | **** | **** | ** | - | |
| S99 | 8.90E-04 | **** | **** | **** | **** | **** | **** | |
| S152 | 3.01E-02 | *** | *** | *** | *** | *** | *** | |
| T171 | 1.16E-15 | **** | **** | **** | **** | - | - | |
| S189, S191 | 1.88E-02 | ** | ** | *** | *** | - | - | |
| S191 | 2.25E-02 | ** | ** | ** | ** | - | ** | |
| S191, S192, S194 | 1.82E-02 | - | ** | - | - | - | - | |
| S192, S194 | 1.74E-03 | - | - | - | ** | - | - | |
| S209 | 9.06E-16 | ***** | ***** | ***** | ***** | **** | **** | |
| S209 | 5.20E-03 | - | - | ** | - | - | - | |
| S239, S242 | 1.96E-04 | ** | ** | * | ** | - | - | |
| S239, S242, S243 | 3.69E-02 | ** | ** | - | - | - | - | |
| S243 | 5.30E-04 | *** | *** | *** | *** | *** | *** | |
| S250 | 1.42E-13 | ***** | ***** | ***** | ***** | ***** | ***** | |
| S250 | 7.12E-07 | *** | *** | *** | *** | ** | ** | |
| S250, S253 | 6.25E-16 | **** | **** | **** | ***** | **** | *** | |
| S253,S260, S265 | 9.44E-03 | - | - | - | * | - | - | |
| S275 | 3.57E-13 | **** | **** | **** | **** | *** | ** | |
| S319 | 2.68E-14 | - | - | **** | ***** | - | - | |
| S319 | 4.30E-14 | ***** | **** | ***** | ***** | ***** | ***** | |
| T682 | 2.95E-02 | ** | - | - | - | * | - | |
| S690 | 8.85E-03 | **** | *** | **** | **** | **** | **** | |

**Figure 35.- Ppz1 phosphorylated sites**. This figure show the results from LC-MS/MS of Ppz1; PEP (posterior error probability), is the probability that the observed PSM (number of identified peptide spectra) would be incorrect. XCorr (cross correlation) is a measure of the goodness of fit of experimental peptide fragments to theoretical spectra created from the sequence and ions. (*) represent 0.1-1.9 value of XCorr, (**) 2-3.9, (***) 4-5.9, (****) 6-7.9, (*****) 8 or more value of Xcorr.

## 4.4.- Generation and phenotypic analysis of Ppz1 versions based in the LC-MS/MS results

Once LC-MS/MS data was analyzed, we made the decision to study Ser49 as a possible Ppz1 regulatory site by phosphorylation and its impact in the phenotype.

The experimental procedure to study the implications of this residue in the regulation of Ppz1 was similar to that carried out for T261 and S265. This residue was mutated to Ala and Asp in the pRS316 *PPZ1* plasmid by QuickChange PCR. These vectors were introduced in *ppz1Δ* and *ppz1Δ ppz2Δ* cells for phenotypic analysis in LiCl, NaCl and caffeine plates. As it can be observed in Figure 36, the behavior of the S49 Ppz1 versions is the same than those of T261 and S265, and therefore, that is, indistinguishable from the native Ppz1 version. Immunoblot analysis showed that the level of expression of each version is virtually identical to that of native Ppz1 (Figure 37) in concordance with their behavior, alike to that of the native version of the phosphatase.

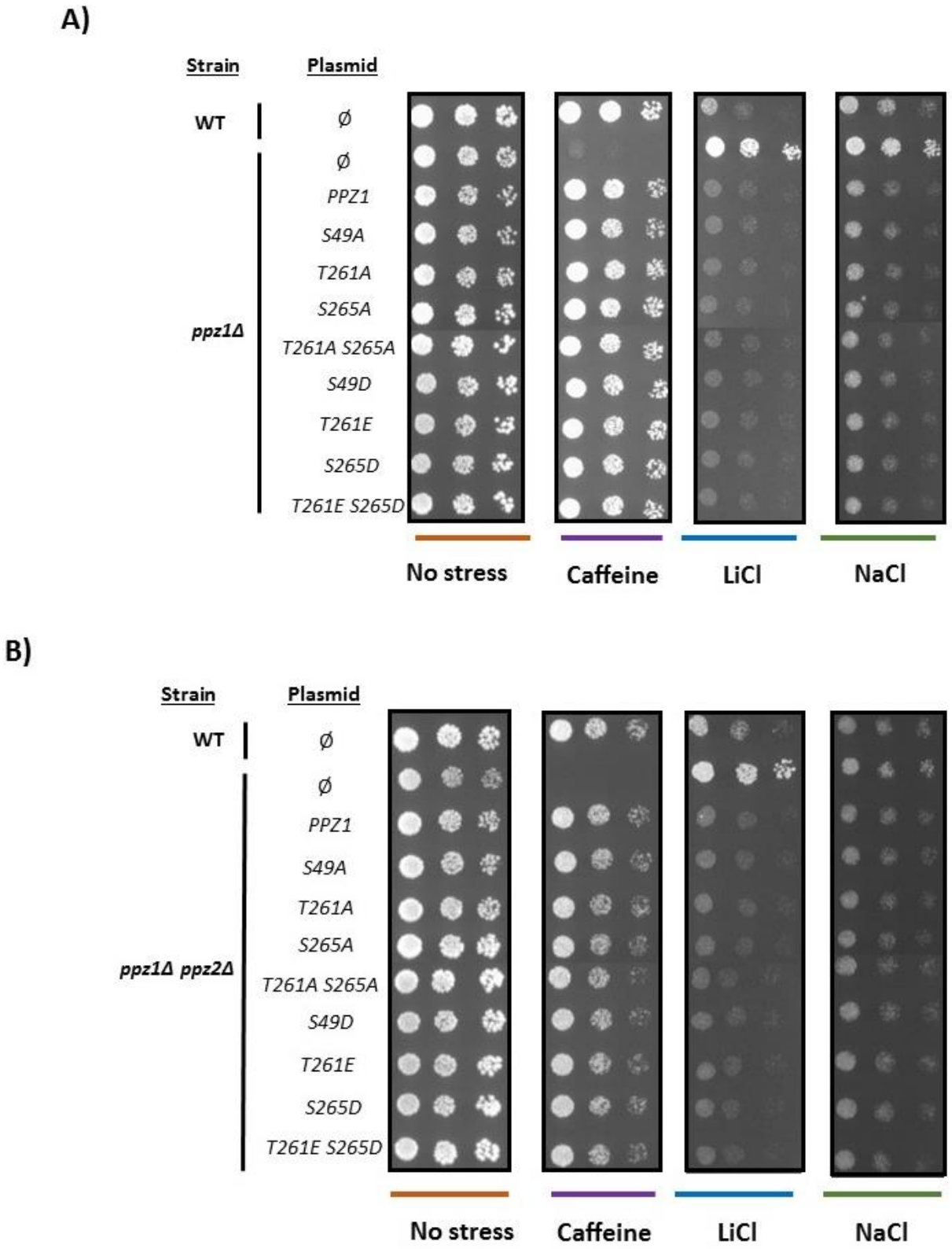


**Figure 36.- Phenotypic analysis of Ppz1 variants.** Wild type (WT) or *ppz1Δ* **(A)** *or ppz1Δ ppz2Δ* **(B)** strains containing the indicated plasmids were spotted at $OD_{600}$ =0.05 and 1/5 dilutions on synthetic medium plates lacking uracil and containing either caffeine (8 mM), LiCl (400 mM) or NaCl (1.2 M). Plates were grown at 28°C for 72 h.

Furthermore, mutations in S49 were combined, thus creating double and triple mutants, with the ones previously obtained for T261 and Ser265, and the phenotype cells expressing these mutants was analyzed in the same way. Figure 38 shows that even cells expressing the triple mutation to Ala or Asp/Glu were indistinguishable from those expressing the native phosphatase. Therefore, it must be concluded that the phosphorylation of S49, T261 and S265, by themselves, is not relevant for regulation of Ppz1 function.

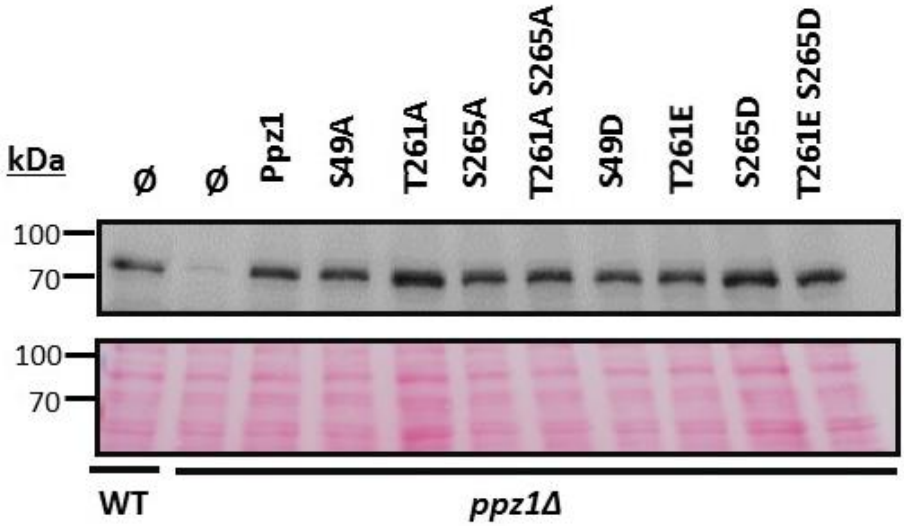


**Figure 37.- Immunodetection of Ppz1 variants.** Strain BY4741, and its derivative *ppz1*Δ were transformed with the indicate plasmids. Cells were collected in exponential phase. Protein extracts were prepared and subjected to SDS-PAGE. Proteins were transferred to PVDF membranes and the different Ppz1 versions were detected with anti GST-Ppz1 polyclonal antibodies [14].

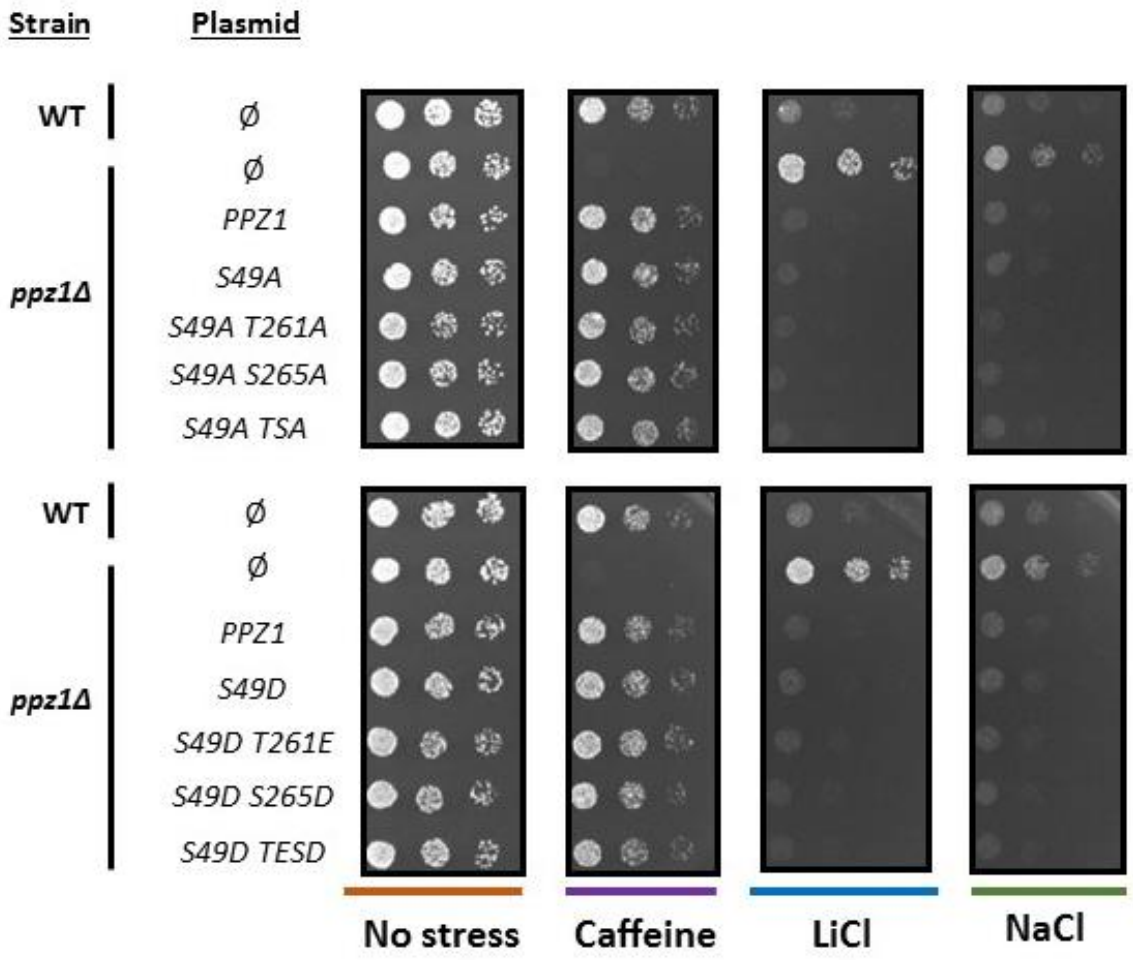


**Figure 38.- Phenotypic analysis of Ppz1 variants.** Wild type (WT) or *ppz1*Δ strains containing the indicated plasmids were spotted at $OD_{600}$=0.05 and 1/5 dilutions on synthetic medium plates lacking uracil and containing either caffeine (8 mM), LiCl (400 mM) or NaCl (1.2 M). Plates were grown at 28ºC for 72 h. TSA represents the double change T261A S265A and TESD denotes the double change T261E S265D.

## 5.- Study of a phosphorylatable region of Hal3 as a possible modulator of Ppz1-Hal3 interaction

As explained in the introduction of this work, Hal3 is the main negative regulator of Ppz1, by binding to the C-terminal domain of the phosphatase and inhibiting its activity (De Nadal *et al*, 1998). We hypothesized that changes in the phosphorylation state of Hal3 could affect the interaction between Ppz1-Hal3, thus regulating of Ppz1 activity. Recent work described that a region of Hal3 (residues 47-60, , containing five Ser), is dephosphorylated as a response to acetic acid stress (I. Sa Correia, personal communication and (Guerreiro *et al*, 2017)).

We analyzed this region of Hal3 with a bioinformatic tool for prediction of kinase-specific phosphorylation sites called Musite (http://musite.net/) (Gao *et al*, 2010) and found that this region could be phosphorylated by CDK1, CDK2, MAPKs and PKA.

To analyze a possible phosphoregulation of Hal3 and how this could affect to the Ppz1-Hal3 interaction we created different versions of Hal3 in the 47-60 region. Thus, Ser 47, 50, 54, 56 and 60 were changed to alanine and aspartic acid. Also, a double mutation in positions 54 and 56 (to alanine and aspartic acid), and a deletion of these thirteen residues were created. These Hal3 variants were cloned in the YEplac195 plasmid, introduced in BY4741 and its *hal3Δ* derivative strain, and grown in plates containing NaCl, LiCl or caffeine. Due to its inhibitory role on Ppz1, over-expression of Hal3 confers salt tolerance (Ferrando *et al*, 1995), and provoques a lytic phenotype in the presence of caffeine (de Nadal *et al*, 1998).

The results from this experiment are summarized in Figure 39. As it can be observed, the behavior of these Hal3 variants are the same than that of native Hal3, indicating that these region is not relevant to the functional interaction between Ppz1 and Hal3.

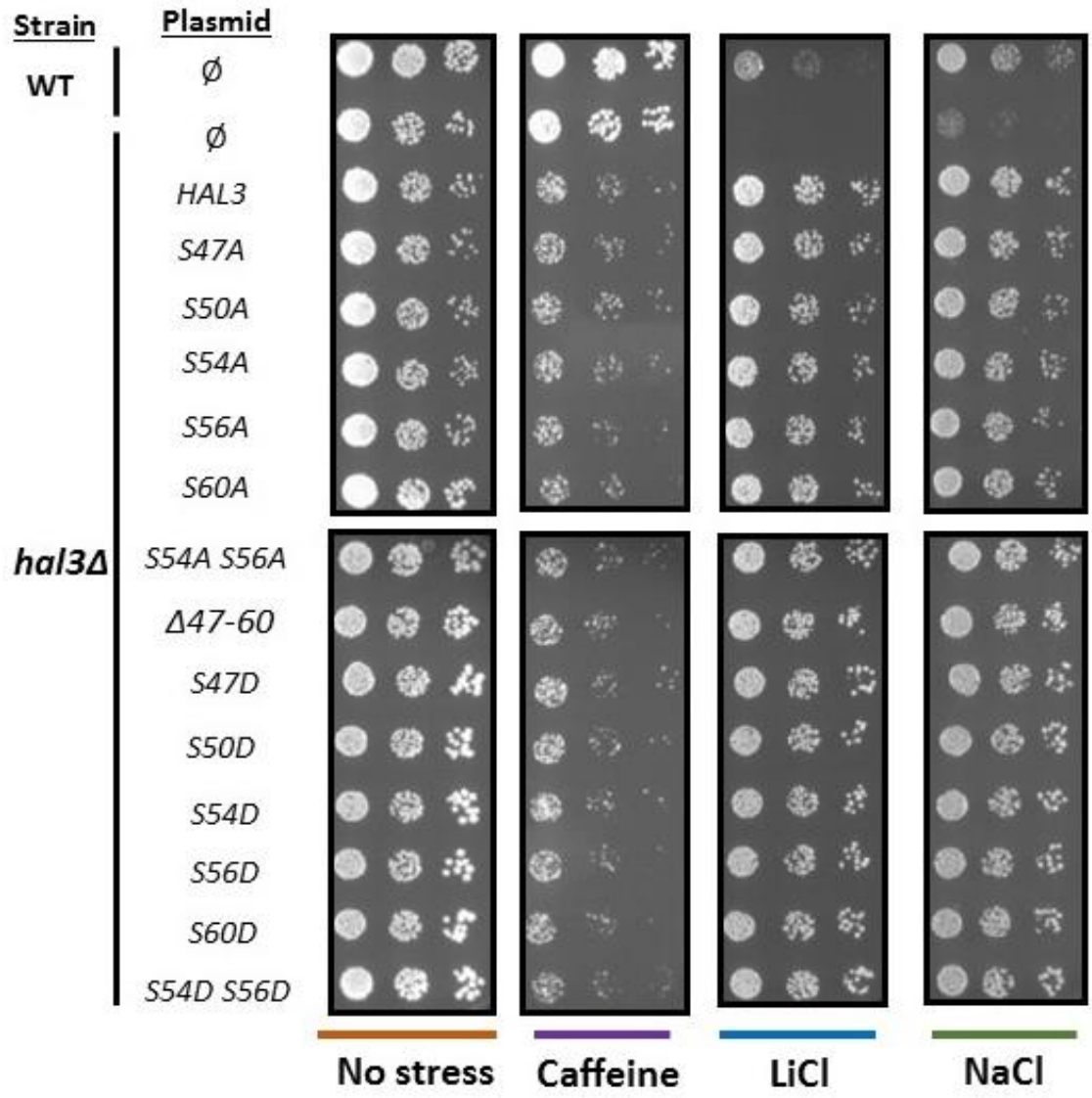


**Figure 39.- Phenotypic analysis of Hal3 variants**. Wild type (WT) or *hal3Δ* strains containing the indicated plasmids were spotted at $OD_{600}$ 0.05 and 1/5 dilutions on synthetic medium plates lacking uracil and containing either caffeine (8 mM), LiCl (400 mM) or NaCl (1.2 M). Plates were grown at 28°C for 72 h.

# CHAPTER3

## Understanding the molecular basis of Ppz1 toxicity

# Chapter 3.- Understanding the molecular basis of Ppz1 toxicity

## 1.- Over-expression of Ppz1 induces numerous changes in the protein phosphorylation profile

As it was explained in the introductory section, the over-expression of Ppz1 is deleterious for yeast cells. Recent studies in our laboratory demonstrated that the over-expression of a catalytically impaired version of Ppz1 ($Ppz1^{R451L}$) is not toxic, suggesting that the excess of Ppz1 phosphatase activity was responsible for toxicity, possibly due to changes in yeast phosphoproteome [1]. Because the molecular basis of this toxicity are still unknown, a global yeast phosphoproteomic assay was designed to gain insight into this phenomenon.

This assay was performed in parallel using two different strains, the wild type BY4741 and its derivative ZCZ01, developed in our laboratory. ZCZ01 is a yeast strain that overexpress *PPZ1* under the control of the *GAL1-10* promoter. Both strains were grown in raffinose as a carbon source, and after $OD_{600}$ 0.6 was reached, galactose was added to induce the expression of *PPZ1*. Cells were harvested before adding galactose and at different times after the shift, to analyze the samples by LC-MS/MS. Samples were collected at short and mid times after shift (30, 60, 120 and 240 minutes), in part based on our previous transcriptomics results showing changes in the transcriptional profile after 1-2 hours of over-expression.

As it can be observed in figure 40.A, when 2% of galactose was added to both cultures, growth of strain ZCZ01 was strongly affected. In figure 40.B we can observe by immunoblot that even at the shortest time (30 min) we can already detect significant amounts of Ppz1, which greatly increase after 2 h of induction. Four hours after shift, the differences in growth ($OD_{600}$) are significant, and the level of Ppz1 over-expression is substantial.

To perform the LC-MS/MS analysis the samples were treated as described in section 12 of Material and Methods. Four biological replicates were carried out. The main difference between sample preparation was the methodology for phosphopeptide enrichment; one replicate was performed by the $TiO_2$ method (Jørgensen *et al*, 2005) and the others by the IMAC method (Thingholm *et al*, 2007).

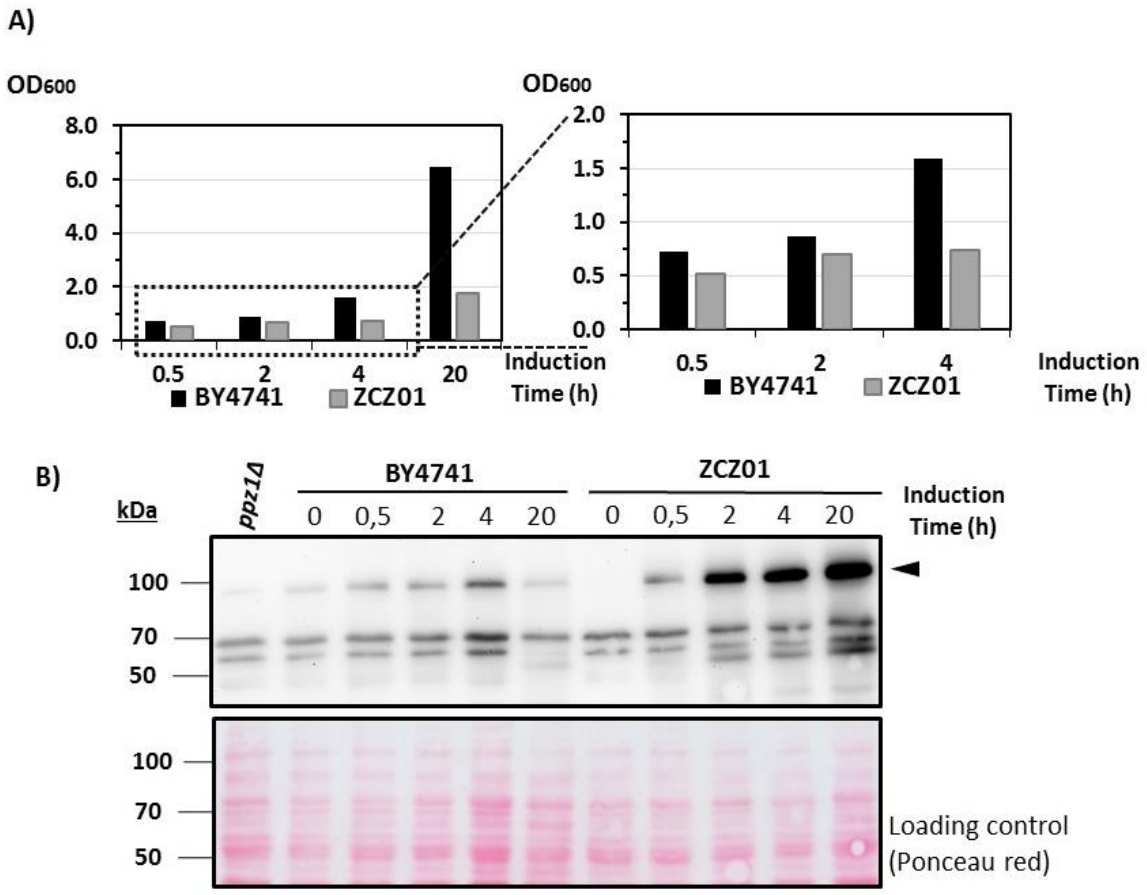


**Figure 40.-Time-course of the over-expression of Ppz1. A)** Optical density of ZCZ01 cells over-expressing Ppz1 versus BY4741 by using 2% of galactose. Cultures were grown in YPRaff until $OD_{600}$ 0.5, and then galactose was added. Samples were taken and the $OD_{600}$ measured. **B)** Ten mL of the same cultures was processed for immunoblotting analysis. Forty 40 µg of protein were used in all cases. Ppz1 was detected with polyclonal anti Ppz1-antibodies. Ponceau staining of the membrane is shown.

Analysis of the proteome allowed the identification of 4041 proteins. Changes in abundance were very limited in number and relatively modest: only 10 proteins were found to increase at least 2-fold (Yro2, Ser3, Ssa4, Nqm1, Gnd2, Rtc3, Rse1, Ald3, Ygp1, and Ypr1). All of them, with the only exception of Rtc3, also displayed consistent increases in expression at the mRNA level (Zhang, 2019). Gene Ontology analysis revealed a slight predominance (2.63E-4) of genes encoding oxido-reductases acting on alcohol groups (*SER3*, *GND2* and *YPR1*).

Analysis of phospho-proteomic data provided a total number of 8701 phosphopeptides identified in at least one experiment. Further analysis yielded 5705 unique peptides corresponding to 1435 different proteins. When filtered for localization

probability equal or greater than 0.5 the list was only slightly reduced to 5676 phosphopeptides (1430 proteins). Evaluation of changes in the phosphorylation level yielded 304 unique sites with at least 2-fold consistent decrease ($p<0.05$) in phosphorylation in cells overexpressing Ppz1, corresponding to 134 different proteins. On the other hand, only 80 phosphosites, corresponding to 37 different proteins, showed at least 2-fold increase in phosphorylation.

Examination of kinetics of changes in phosphorylation (Figure 41A and B) shows that overall a clear-cut increase in phosphorylated peptides is only detected after 60 min of Ppz1 over-expression, and that relatively minor changes occur after 120 min. In contrast, a slight modification in the overall profile of dephosphorylated peptides is already seen after 30 min, becoming very evident at 60 min, and showing a further shift towards dephosphorylated forms at 120 and 240 min. When the number of different proteins affected in their phosphorylation state is plotted it is observed that both phosphor and dephosphorylation events initiate between min 30 and 60. At 60 min the figures are not too different (18 phosphorylated and 25 dephosphorylated). However, after 60 min the number of phosphorylated proteins is stabilized, whereas that of dephoshorylated proteins increases over 4-fold at 240 min (Figure 41B). It must be noted that over-expression of Ppz1 caused dephosphorylation of certain residues and phosphorylation of others in six specific proteins, Gdc6, Rtg1, Cdc3, Seg1, Tpo3, and Ppz1 itself, which appears dephoshorylated at Thr171 at the initial stages of the experiments and becomes phosphorylated at Ser265 at 60 min. A summary of phosphorylation and dephosphorylation by the type of residue affected is shown in Table 2.

| | Phosphorylated | | Dephosphorylated | |
|---|---|---|---|---|
| Residue | number | % | number | % |
| S | 57 | 71.25 | 251 | 82.57 |
| T | 22 | 27.50 | 48 | 15.79 |
| Y | 1 | 1.25 | 5 | 1.64 |
| Total | 80 | 100.00 | 304 | 100.00 |

**Table 2.- Percentage of phosphorylation and dephosphorylation by type of amino acid.**

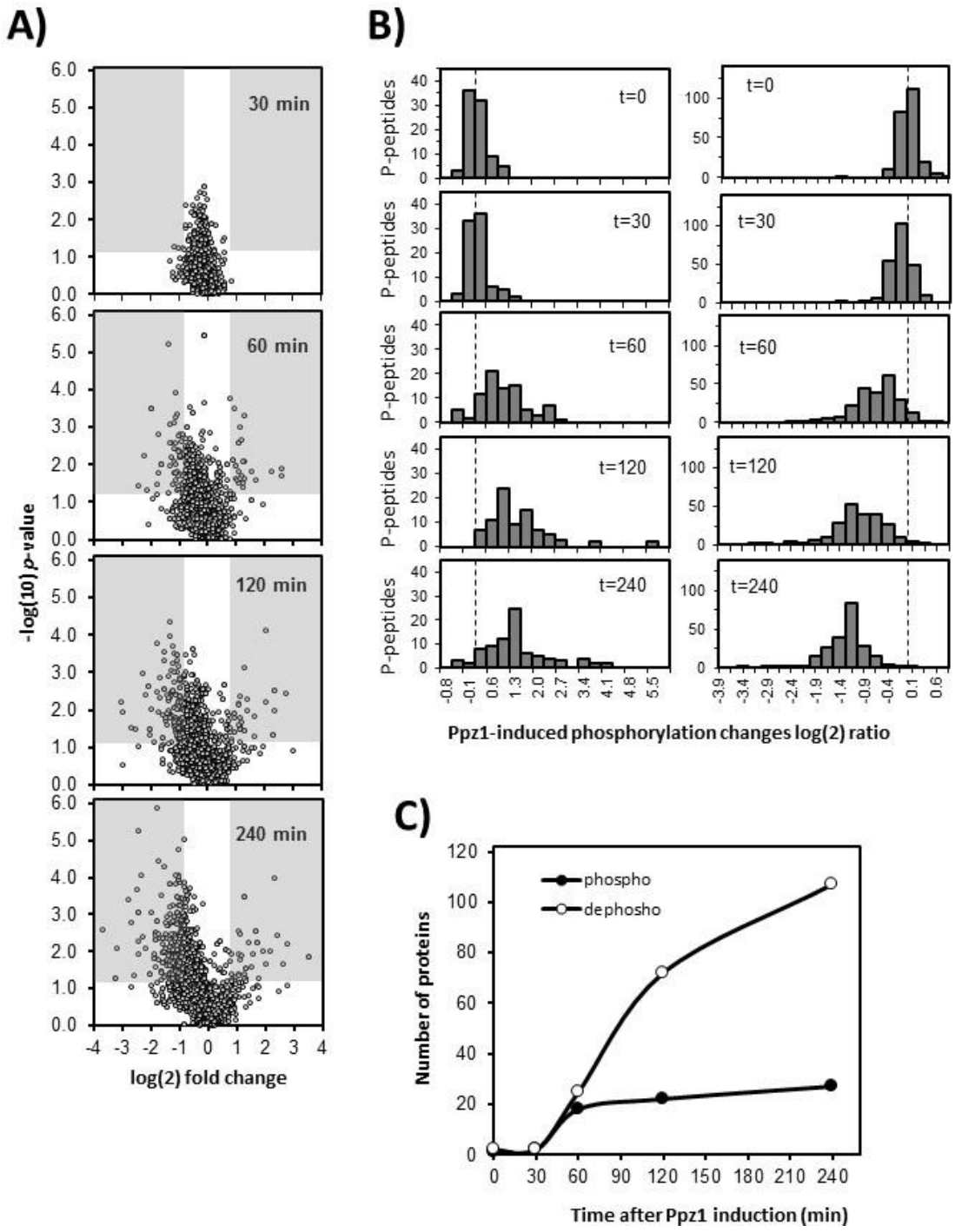


**Figure 41.- Time-course of changes in phosphorylation profile upon over-expression of Ppz1**. **A)** Volcano plot of the 6008 unique phosphosites identified in this work and their variation along time with overexpression of Ppz1. Fold-change is calculated as the ratio of Ppz1 overexpressing cells *vs* control cells, for each time, and in comparison with t=0. Shadows denote regions in which log (2) value of the change is ≥1 (phosphorylated) or ≤ -1 (dephosphorylated) and p-value ≤ 0.05. **B)** Data for a total number of 230 dephosphorylated (right panel) and 85 phosphorylated phosphopeptides (left panel) showing statistically significant changes at least at one time-point was log(2) transformed and plotted. The discontinuous line marks the zero point in the X axis. **C)** Variation of the number of phosphor- (●) and dephosphorylated (○) proteins along the experiment.

Time-course evaluation of the dephosphorylated proteins revealed only two proteins showing dephosphorylated sites after 30 min of Ppz1 induction: Rpp1A, the ribosomal stalk protein P1 alpha, involved in the interaction between translational elongation factors and the ribosome, and Rnr1, the major isoform of the large subunit of ribonucleotide-diphosphate reductase. After 60 min, 25 proteins suffered dephophorylation at least at one site, five of them showing functional links with the bud neck (Hsl7, Shs1, Gnp1, Rts1 and Sec8). This tendency was intensified after 120 min of Ppz1 over-expression, when 72 proteins were found. Among them, 14 proteins (7.5E-5) were related to the bud neck (including the six ones dephosphorylated at 60 min), of which five (Kcc4, Shs1, Rga2, Gin4, Cdc3, and Rts1) are involved in the organization of the septin ring. Interestingly, at this time all three glucose phosphorylating enzymes (Hxk1, Hxk2 and Glk1), plus the β-subunit of phosphofructokinase Pfk2, Mig1 and Reg1 (the last two involved in the glucose repression mechanism), were also dephosphorylated. The number of dephosphorylated proteins after 240 min raised to 107. Twenty-nine of them (6.7E-09) were related to the mitotic cell cycle, of which 21 are specifically involved in cytoskeleton organization (mostly actin cytoskeleton), whereas other 7 (9.5E-04) are implicated in the regulation of transcription involved in the G1/S cell cycle transition (Yph1, Spt6, Stb1, Whi5, Swi4, Swi5, and Swi6). Gene Ontology analysis of the total set of 134 proteins dephosphorylated at least at one time-point confirmed a strong incidence of proteins involved in mitotic cell cycle (6.19E-10) and located in sites of polarized growth (7.8E-16), particularly in the bud neck (2.3E-12).

Gene Ontology analysis of the 37 proteins in which over-expression of Ppz1 induced increased phosphorylation of at least one site showed common traits from min 60 onwards. Thus, six proteins related to the cytoplasmic ribonucleoprotein granules (Hek2, Ksp1, Tif4631, Rie1, Bre5 and Ded1) were identified. Interestingly, four phosphorylated proteins were related to translation initiation, such as Sui3 and Gcd6 (corresponding to the β-subunit and the catalytic ε subunit of the translation initiation factor eIF2, respectively), the translation initiation factor eIF4G (Tif4631), and Ded1, an ATP-dependent -box RNA helicase required for translation.

Hierarchic clustering of the data corresponding to the proteins whose phosphorylation state changed upon over-expression of Ppz1 is shown as a heat-map in Figure 42, together with Gene Ontology annotation of the predominant categories in

the main clusters. As it can be observed, cluster 1 and 2 corresponded to proteins with hyperphosphorylated sites, whereas clusters 3, 4a, 4b, 4c, and 5 correspond to proteins dephosphorylated at least in one site. Notable, clusters 3, 4b and 5 are enriched in proteins involved in mitotic cell cycle (p-values of 8.3E-06, 4.24E-09, and 2.3E-06, respectively). However, proteins in cluster 3 showed a tendency to be functionally associated with the cytoskeleton, whereas those belonging to clusters 4b and 5 are related to sites of polarized growth and, in particular, with the bud neck (p-value of 7.5E-13 and 4.1E-09, respectively). Cluster 4c, however, was enriched in plasma membrane proteins (p-value 9.4E-07) and in proteins functionally related to metabolism of carbohydrates (8.6E-05, including Glk1, Hxk2, Pfk2, Mig1, Reg1 and Gpd2). A complete list of the phosphoproteomic results is shown in Annex 3.

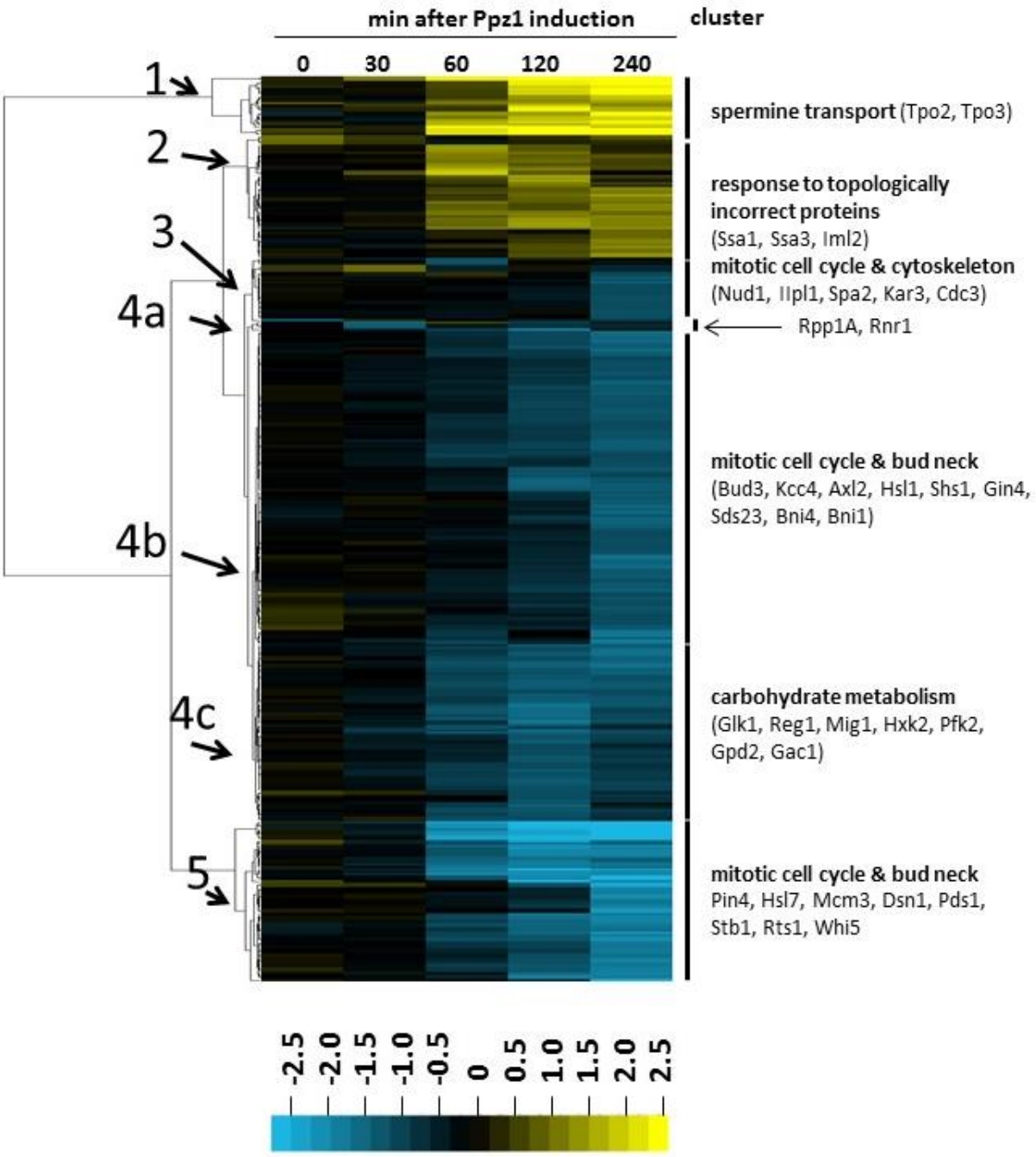


**Figure 42.- Cluster analysis of phosphoproteome changes upon Ppz1 over-expression**. Data from a total of 384 phosphosites (phospho or dephosphorylated) was calculated as the ratio between Ppz1-overexpressing cells and control cells. Log(2) transformed data was clustered with the Cluster software (Euclidean distance / complete linkage) and the result was visualized with Java Tree View (v. 1.145). The intensity of the phosphorylation change can be deduced by comparison with the enclosed scale (log(2) values). Data is presented for all time-points even if in some cases the *p*-value between experiments is >0.05.

## 2.-Identification of new phosphorylation sites in the *S. cerevisiae* phosphoproteome.

Our phosphoproteome results were crossed and compared with different databases as phosphoGrid (https://thebiogrid.org/) or YeastMine (https://yeastmine.yeastgenome.org/) and with data from a recent publication (Bai *et al*, 2017). We can identify, appearing in at least one experiment, **466** residues not yet described as phosphorylatable, corresponding to **317** different proteins. Only 15 of these residues, corresponding to 13 proteins (Table 3), undergo significant phosphorylation change ($p<0.05$) when Ppz1 is over-expressed. Two of these 15 residues are detected as hyperphosphorylated (Hpc2 in S229 and T231 and Sap155 in Y63) while the rest appear as dephosphorylated.

| Gene | Uniprot ID | Aa | Position |
|---|---|---|---|
| *HPC2* | Q01448 | S | 229 |
| *HPC2* | Q01448 | T | 231 |
| *LRE1* | P25579 | S | 37 |
| *FIR1* | P40020 | S | 2 |
| *FIR1* | P40020 | T | 6 |
| *SAP155* | P43612 | Y | 63 |
| *FYV8* | P46949 | S | 301 |
| *AXL2* | P38928 | T | 688 |
| *YOX1* | P34161 | S | 356 |
| *EIS1* | Q05050 | S | 781 |
| *SLM2* | P53955 | Y | 643 |
| *BNI4* | P53858 | S | 49 |
| *GAC1* | P28006 | T | 65 |
| *GDS1* | P41913 | T | 374 |
| *SEC8* | P32855 | T | 1015 |

**Table 3.- Identification of new sites of phosphorylation in the *S. cerevisiae* proteome affected by over-expression of Ppz1.**

## 3.- Ppz1 over-expression causes dephosphorylation of Rps6A

Rps6A is a protein component of the small ribosomal subunit (40S) and it can be phosphorylated at Ser-232 and Ser-233 (corresponding to Ser235 and Ser-236 of mammals) by the AGC kinase Ypk3 in response different stresses. Both TORC1 and TORC2 complexes can regulate indirectly this protein and, in fact, such phosphorylation is used as readout for activation of the TOR pathway (González *et al*, 2015; Yerlikaya *et al*, 2016). Our phosphoproteomic results show a strong dephosphorylation of this protein in these specific residues (Figure 33.A) already at 1 hour after the shift to galactose. To confirm this, an anti-phospho-S6 Ribosomal Protein (Ser235/236) antibody was used to check by immunoblot the effect of over-expression of Ppz1 in the phosphorylation state of Rps6A. As can be observed in figure 33.B, over-expression of Ppz1 results in rapid dephosphorylation of Rps6a. The phosphorylated form is almost undetectable by immunoblot after 1 hour of Ppz1 over-expression, thus confirming the dephosphorylation kinetics deduced from the phosphoproteomic data.

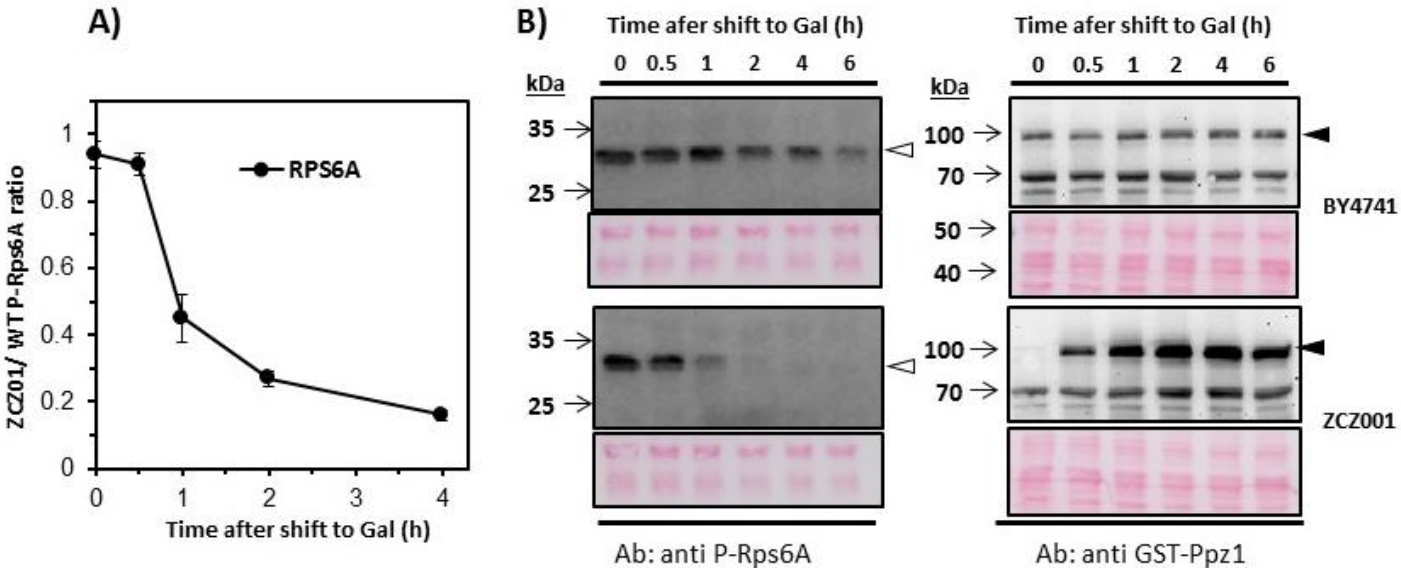


**Figure 43.- Overexpression of Ppz1 results in dephosphorylation of Rps6A**. A) The ratio between the phosphorylation signal for Rps6A Ser232, 233 in the ZCZ01 strain vs BY4741 is plotted against time after induction of Ppz1. Data are the mean ± SEM from 4 experiments B) Time-course of the dephosphorylation of Rps6A evaluated by immunoblot. All samples contained 25 µg of protein and Rps6A-P was detected using anti-phospho-S6 Ribosomal Protein (Ser235/236) (Cell Signaling). Ponceau staining of the membranes is shown.

## 4.- Ppz1 over-expression induces dephosphorylation of Mig1

Mig1 is a transcription factor involved in glucose repression, regulated by the Snf1 kinase and the Glc7 phosphatase. In conditions of low glucose, Mig1 is phosphorylated by Snf1 and this results in a change in Mig1 localization from the nucleus to cytoplasm (Rubenstein *et al*, 2008). When yeast is grown in the presence of high concentrations of glucose Glc7, bound to its Reg1 regulatory subunit, dephosphorylate Mig1 promoting its return to the nucleus in order to repress the transcription of genes whose expression is not necessary when glucose is present, such as those encoding transporters and enzymes for utilization of maltose or galactose (Carlson, 1999). Our phosphoproteomic results show a dephosphorylation of Mig1 compared to BY4741 in positions S311 and S314 from after 1 hour of galactose shift (Figure 44A). Both residues are the phosphorylation target for Snf1 (Ahuatzi *et al*, 2007) Dephosphorylation was confirmed by immunoblot experiments, in which a change in the electrophoretic mobility of Mig1 can be detected depending of its phosphorylation state. As shown in Figure 44B, a shift to rapidly migrating species is observed 2 h after the shift to galactose. This is congruent with a dephosphorylation of Mig1. It is remarkable that the phosphorylation status of Mig1 in strain ZCZ01 grown on galactose resembles that of wild type cells grown on glucose.

To evaluate if the observed dephosphorylation of Mig1 could affect its subcellular localization, a study was carried out using a Mig1-GFP plasmid and fluorescence microscopy. Figure 44.C shows representative images of cells after 2 hours of galactose shift, showing intense nuclear staining in ZCZ01 cells. Quantitative determinations (Figure 44D) showed that Mig1 was localized in the nucleus in about one third of ZCZ01 cells, whereas it was virtually absent in the nucleus of control cells. It must be noted that nuclear localization and dephosphorylation events exhibit similar kinetics.

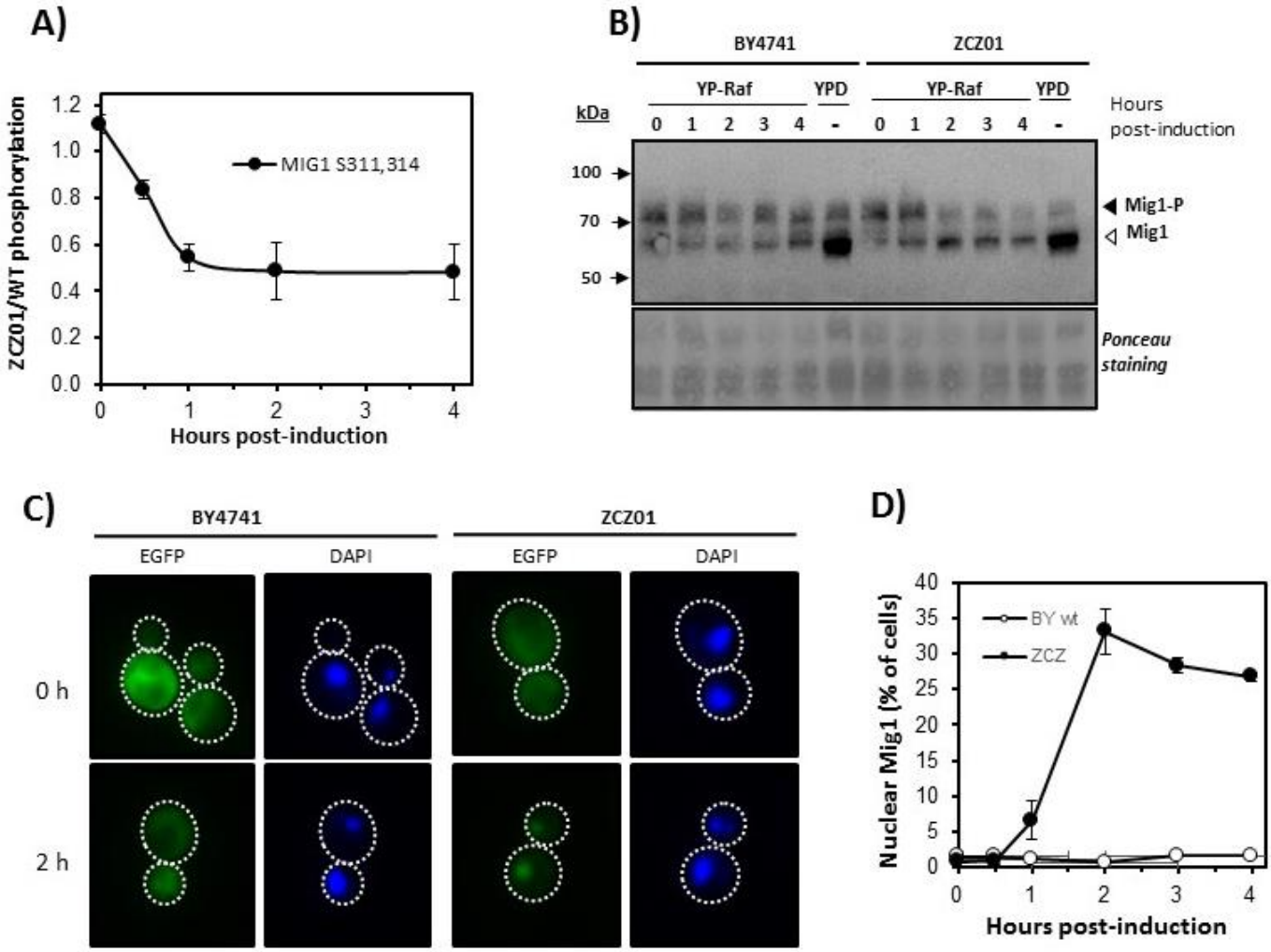


**Figure 44.- Dephosphorylation of Mig1 induced by Ppz1 over-expression. A)** Graph of Mig1 phosphorylation in S311 and S314 in ZCZ01 vs BY4741 at different times of Ppz1 overexpression. **B)** Strains BY4741 and ZCZ01 transformed with plasmid p-HA-Mig1 were shifted to galactose and protein extracts were prepared. Forty µg of proteins were resolved by SDS-PAGE (10% polyacrylamide gels) followed by immunoblot using anti-HA antibodies to reveal HA-tagged Mig1. Slower migrating bands correspond to the dephosphorylated forms. Cells grown on YPD were used as reference for dephosphorylated Mig1. **C)** Strains BY4741 and ZCZ01 were transformed with plasmid YEp195 Mig1-GFP and grown in YPRaff. Pictures were taken before and after 2 hours of galactose shift. Nuclei were stained with DAPI to illustrate nuclear co-localization. **D)** Quantification of nuclear localization of Mig1 in BY4741 and ZCZ01 strains. Data are mean ± SEM from 3 experiments (167-423 average cells per time-point).

## 5.-Over-expression of Ppz1 results in Npl3 delocalization

Preliminary data from the first biological phosphoproteomic replicate suggested that over-expression of Ppz1 results in the strong dephosphorylation of Npl3 specifically at Ser-411 (Figure 45A), whereas other residues as S349 and S413 shows little change in its phosphorylation state. This was interesting, because Npl3 is a SR-like RNA-binding protein involved in regulation of different processes, including translation. Although Npl3 shuttles from the nucleus to the cytosol, it is usually visualized in the nucleus. Interestingly, a non-phosphorylatable version, Npl3-S411A, was described as found also in the cytosol (Madrid *et al*, 2006) probably because its cytoplasmic accumulation bound to mRNA. To test whether the excess of Ppz1 activity could be affecting the function of Npl3, we analyzed the intracellular localization of a functional GFP-tagged version of Npl3 (Gilbert *et al*, 2001). As expected, we found Npl3 localized in the nucleus of wild type cells with no detectable cytoplasmic signal (Fig 45B). However, when ZCZ01 cells were analyzed, while Npl3 was also detectable in the nucleus, it was also evident in the cytosol after 2h and 4h of induction of *PPZ1* over-expression. This was not an artefactual effect caused by an increase in the total amount of the Npl3 protein, since Npl3 levels were unchanged when *PPZ1* was over-expressed (Fig 45C). These results suggested that over-expression of Ppz1 causes dephosphorylation of Npl3 in Ser411 and that this leads to an abnormal Npl3 subcellular distribution.

As shown in Figure 45D, over-expression of Npl3 by itself barely affected cell growth of wild type cell but it had a negative effect, already noticeable in medium containing 2% glucose, when Ppz1 was also over-expressed. Over-expression of Sky1, a reported Npl3 kinase (Gilbert *et al*, 2001), had not effect on cell growth, suggesting that it could not counteract Ppz1 toxicity. We then considered if abnormal dephosphorylation of Npl3 could contribute to the growth defect observed in the MLM04 strain. In this strain, the *PPZ1* ORF is placed under the control of a doxycycline-repressive $tetO_{(7)}$ promoter. The growth of MLM04 in synthetic solid medium was not affected by the presence of doxycycline. Moreover Ppz1 expression in this strain is lower of than ZCZ01.

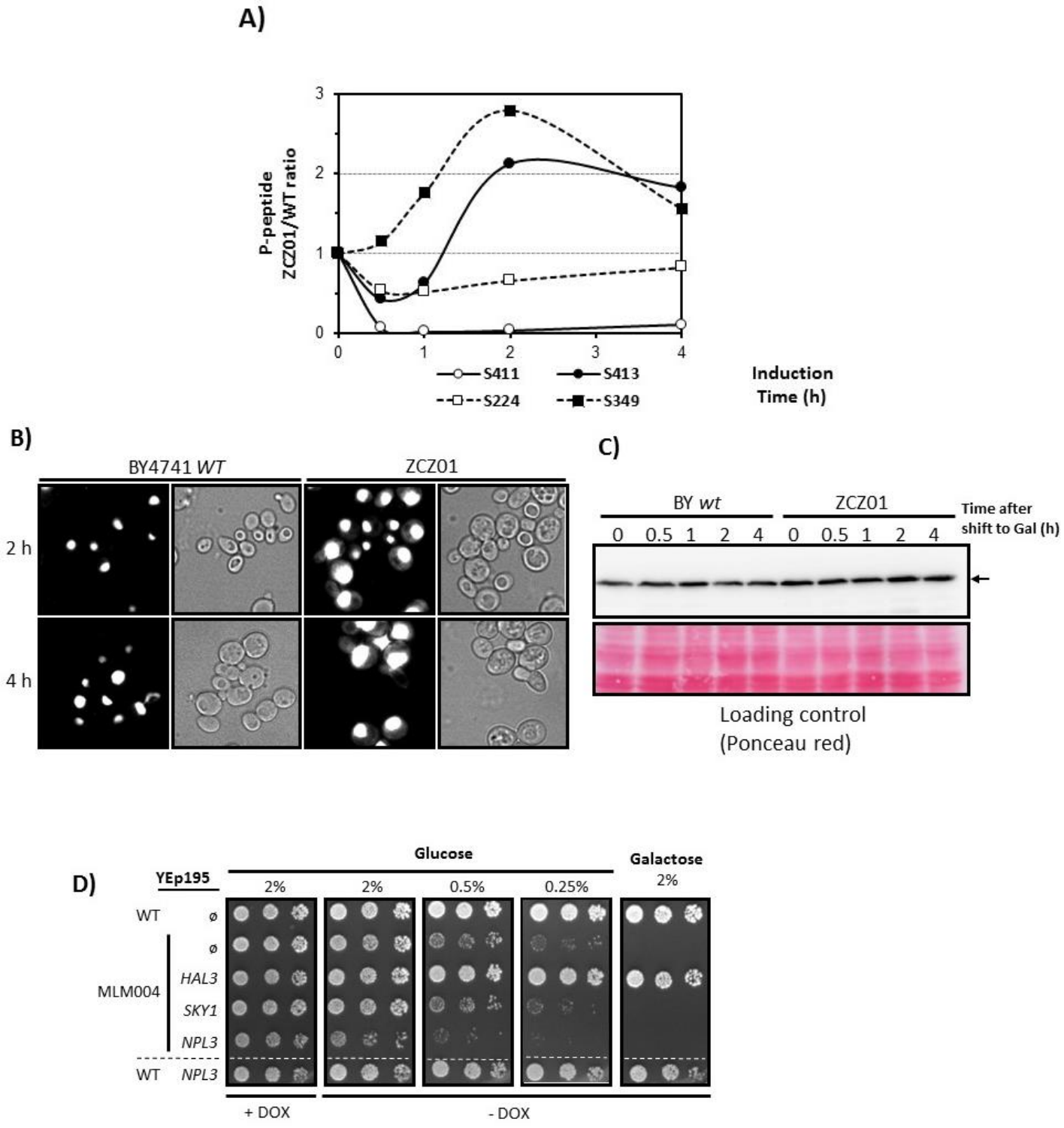


**Figure 45.- Overexpression of Ppz1 results in dephosphorylation and abnormal localization of Npl3. A)** Ratio of Npl3 phosphorylation in diverse residues in ZCZ01 versus BY4741 strains. **B)** Strains BY4741 and ZCZ01 were transformed with a vector carrying a Npl3-GFP fusion. Cultures grown on raffinose were shifted to galactose (2%) for the indicated times and cells processed for fluorescence microscopy (x1000). **C)** Protein extracts were prepared from cultures grown as above and processed for immunoblot using an anti-GFP antibody. **D)** Strain BY4741 (WT) and MLM04 were transformed with the indicated YEp195-based plasmids. Cultures cells were spotted in the presence or absence of doxycycline on synthetic medium plates lacking uracil and the indicated carbon sources. Pictures were taken after 4 days of incubation.

## 6.- Vhs2 is dephosphorylated in Ppz1 over-expressing cells

Other interesting protein that appeared hyperdephosphorylated in the first replicate was Vhs2. *VHS2* was identified in our laboratory as a high-copy suppressor of the synthetic lethality of the double mutation *sit4Δ hal3Δ* (**v**iable in **h**al3 **s**it4 background). Recently, it has been described that Vhs2 is in involved in the regulation of septin dynamics at the bud neck after mitotic entry. It has been demonstrated that Vhs2 can be phosphorylated in multiple sites during S phase until nuclear division, and is dephosphorylated just before cell division (Cassani *et al*, 2014). We identified a specific dephosphorylation in S314 (Figure 36.A), and we considered that investigation of the relevance of this residue, which had not been described as phosphorylatable, could be interesting. Vhs2 has a paralog, Mlf3 that also appeared dephosphorylated in our experiment in the equivalent residue (S315), as shown in Figure 46B.

In order to understand the relevance of Vhs2, and its phosphorylation in S314, we created a native Vhs2 version and two mutated S314A and S314D versions that were cloned in multicopy plasmids. Our results show that Vhs2 acts as a modest high-copy suppressor of the lack of growth caused by over-expression of *PPZ1*, an effect that can be observed in both ZCZ01 (46.C) and MLM04 (46.D) strains. However, this effect occurs independently of the phosphorylation state of S314.

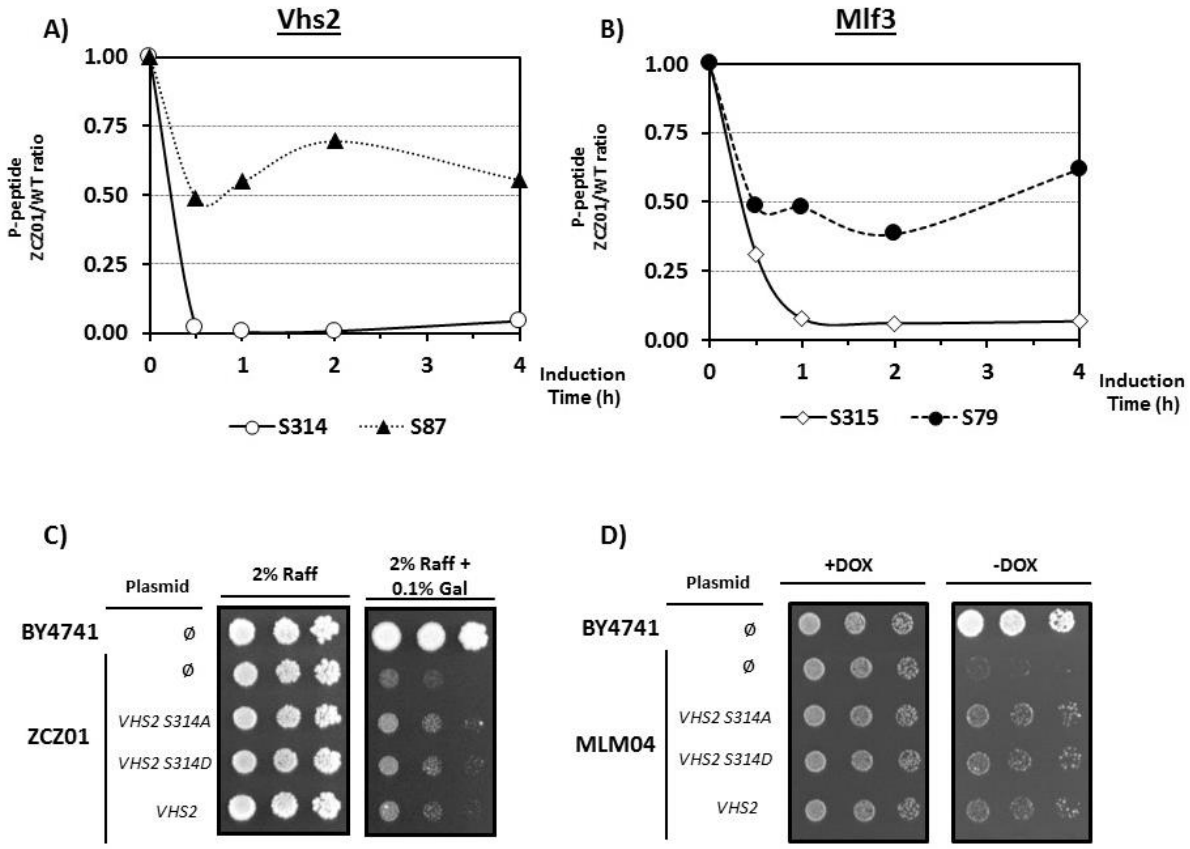


**Figure 46.- Vhs2 is dephosphorylated upon Ppz1 over-expression**. Ratio of Vhs2 **(A)** and Mlf3 phosphorylation in ZCZ01 vs BY4741 cells after galactose shift. **C)** Strains BY4741 and ZCZ01 were transformed with the indicated YEp195-based plasmids, and growth in plates with 2% of Raffinose and with or without 0.1% of galactose as inductor of Ppz1 overexpression. **D)** Strains BY4741 (WT) and MLM04 were transformed with the indicated YEp195-based plasmids. Cultures were spotted on synthetic plates lacking uracil as in Figure 45D. Growth was monitored after 4 days.

## 7.- Identification of GST-Ppz1-interacting proteins.

A parallel approach to identify new possible physical interactions of Ppz1 was to determine the set of proteins co-purifying with the GST-Ppz1 fusion protein. For this purpose, GST and the catalytically inactive mutant version GST-Ppz1$^{R451L}$, were purified from yeast cells (this variant was used to allow sufficient level of Ppz1 expression) and the identity of the tryptic fragments from co-purified proteins discerned by MALDI-TOF. As shown in the Figure 47, several proteins co-purified with GST-Ppz1 that did not bind to GST. The tryptic peptides identified from these proteins corresponded to Yef3 (elongation factor eEF3), the translational elongation factor EF-1 alpha proteins Tef1/Tef2 (the identified peptides were identical in both proteins), and four (or five) ribosomal 60S subunit proteins: Rpl3, Rpl13b, Rpl10 and Rpl2a/b (the identified peptides were identical in these last two proteins). The detected interactions of Ppz1 with elongation factors and ribosomal proteins together with the phospohoproteomic results suggest that the over-expression of this phosphatase might have an impact in the

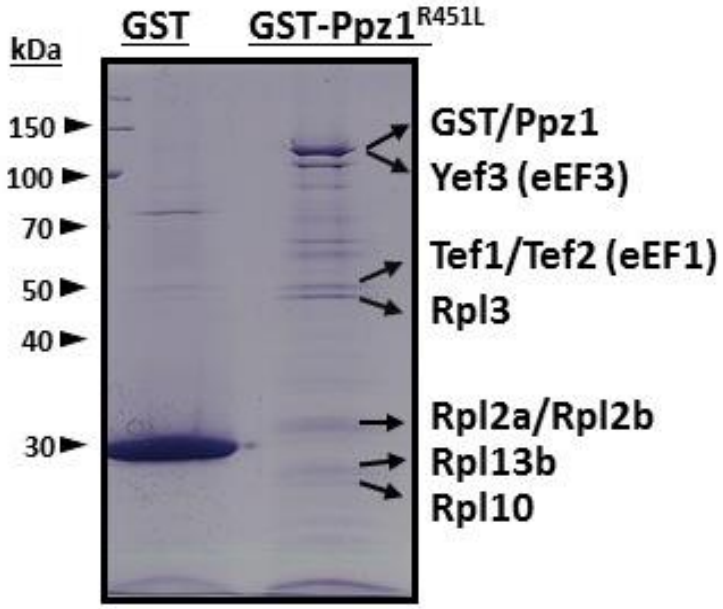


**Figure 47.- Ribosomal proteins and translational elongation factors co-purify with Ppz1.** Yeast cells harboring the *PPZ1*$^{R451L}$ variant fused to GST and expressed under control of the *GAL1-10* promoter in the pEGH plasmid were grown in presence of 2% galactose 2 hours and protein extracts were prepared. Proteins that were pulled-down together with the affinity-purified catalytically inactive phosphatase were resolved by SDS-PAGE, and relevant bands excised and identified by MS.

translation process. In the Annex 4, the identification of different peptides of each interactor protein is shown.

## 8.-Over-expression of Ppz1 results in eIF2α phosphorylation

eIF2 is a conserved heterotrimer that, when bound to GTP, delivers the $tRNA_i^{Met}$ to the P site in the ribosome. Phosphorylation of eIF2α at Ser51 is considered a major step in halting translation initiation in response diverse forms of stress. The evidences described above linking Ppz1 overexpression and the translation process prompted us to investigate the phosphorylation state of eIF2α when *PPZ1* was over-expressed by using a phospho-specific antibody again the phosphorylated Ser-51.

As shown in Figure 48, over-expression of Ppz1 in strain ZCZ01 led to a long-term (4h and 6h) hyperphosphorylation of eIF2α in Ser51. This indicates that the over-expression of Ppz1 is likely affecting protein translation, in keeping with phosphoproteomic data.

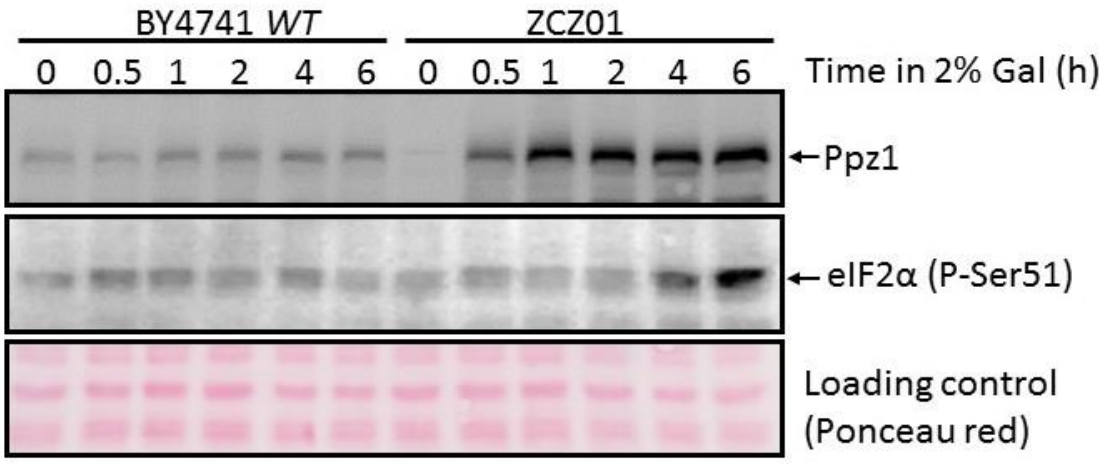


**Figure 48.- Overexpression of Ppz1 increases phosphorylation of eIF2α at Ser51**. Strain BY4741 (WT) and ZCZ01 were grown on raffinose and galactose (2%) was added. Protein extracts were prepared at the indicated times after induction and electrophoresed. The levels of Ppz1 were determined with an anti-Ppz1 antibody and the phosphorylation state of eIF2α was monitored with an antibody that recognizes the protein when phosphorylated at Ser51 (mAb #3597, Cell Signalling).

# DISCUSSION

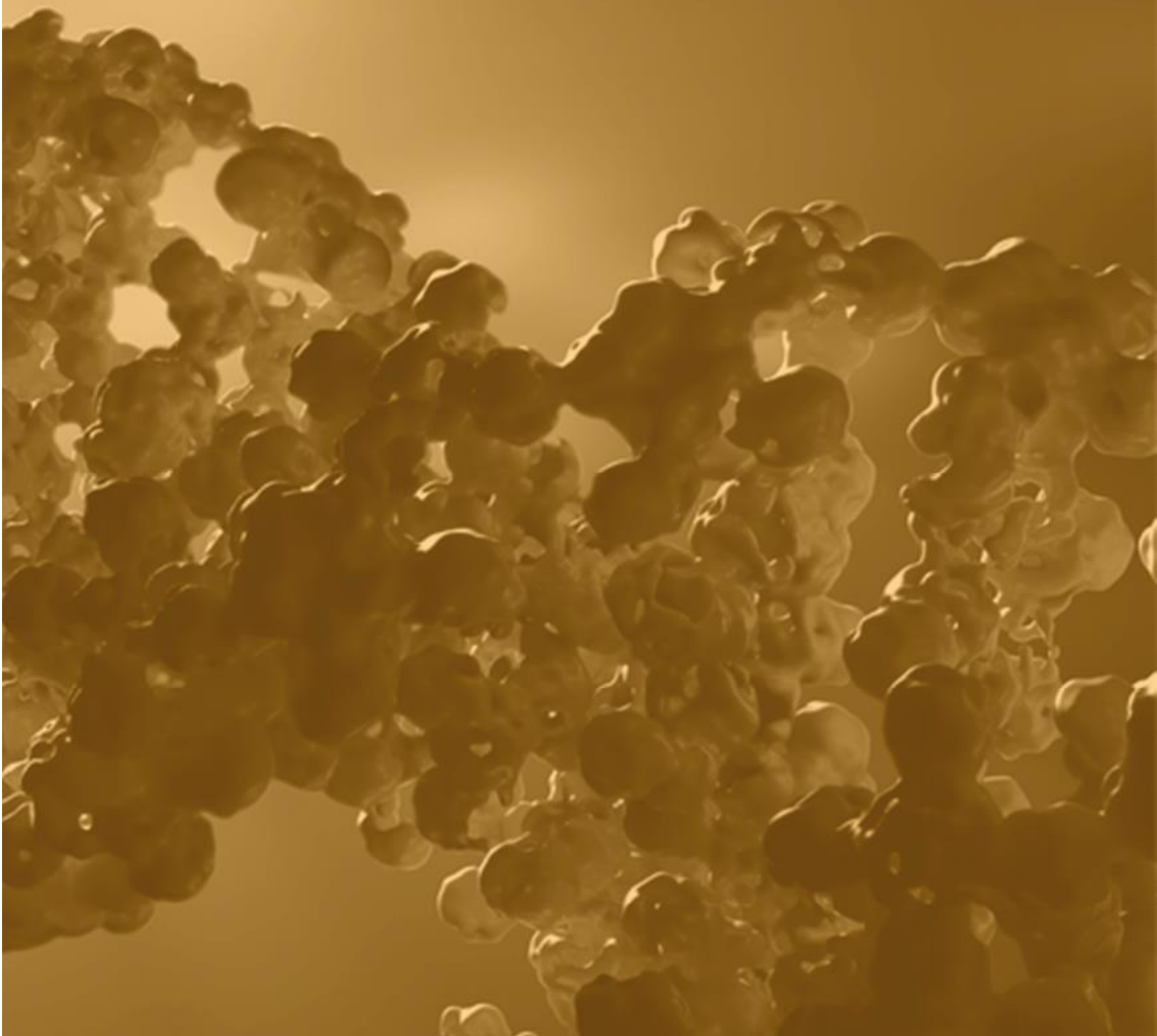

# Discussion

## Chapter 1. Study of the interaction between Ppz1 and Hal3.

Our results demonstrate that different tagged versions at the C-terminus of Hal3 and Ppz1 can be expressed at levels similar to those found for the wild type protein. Cells expressing these tagged versions show a normal behavior in phenotypic assays in presence of LiCl or caffeine, restoring the wild type phenotypes of the corresponding deletion mutants. This indicates that these fusion protein can be expressed correctly in the yeast cell, and that they are stable and functionally competent (i.e., the tag does not interfere with the function). Therefore, they are good candidates to be used in FRET-based experimental approaches. In addition, our results show an increase in signal in the FRET channel when the DVS009 strain (expressing both Ppz1-GFP and Hal3-mCherry) is analyzed by flow cytometry, physically confirming the *in vivo* interaction between Ppz1 and Hal3. It is worth noting that this interaction was only demonstrated years ago by *in vitro* methods for the *S. cerevisiae* proteins (Muñoz *et al*, 2004; Abrie *et al*, 2012; De Nadal *et al*, 1998; Yenush *et al*, 2005) and, in the case of *Debaryomyces hansenii* by an indirect *in vivo* method, such as 2H-hybrid assays (Minhas *et al*, 2012). Therefore, the strains created in this work represent a tool to follow *in vivo* dynamically the interaction between Ppz1 and Hal3.

One of the great challenges that we face is the relatively poor level of expression of both proteins, and consequently the low signal level in the FRET channel. For this reason we designed a strategy based on multicopy plasmids tagging in this case Ppz1 with GFP either at the C-terminus or at the N-terminus and maintaining the native Ppz1 and Hal3 promoters. Our results suggest that the best combination to carry out a FRET approach is to have both proteins (Ppz1 and Hal3) tagged at the C-terminus. We also reached the conclusion that the best combination to perform FRET was the use of tagged Ppz1 as receptor (GFP) and Hal3 as emitter (mCherry). This combination of plasmids produced a detectable and reproducible FRET signal and could be used in subsequent experiments to investigate changes in the interaction under different environmental conditions.

Thus, the work done in this section establishes the basis for using FRET as a tool to analyze the interaction between Ppz1 and Hal3 *in vivo*.

Crosslinking studies between Ppz1-Cter and Hal3 required the co-expression of both proteins in *E. coli.* We observed that they co-purify roughly in equimolecular proportions. Since Hal3 has not tags, and the only way to purify it is through binding with Ppz1, it is confirmed that the stoichiometry of this purification process is 1:1, as previously described by Molero and coworkers (Molero *et al*, 2017).

When the crosslinking reactions between the C-terminal of Ppz1 and Hal3 were performed and analyzed by SDS-PAGE we expected band at ~110 kDa, as the sum of both proteins (42 kDa Ppz1-Cter and 62.5 kDa of Hal3). Instead, high molecular weight bands of more than 300 kDa appeared in the gel in all crosslinking reactions. It is known that Hal3 is a moonlighting protein, acting as inhibitor of Ppz1 (de Nadal *et al*, 1998) in its monomeric form, and also involved in the formation of an heterotrimeric PPCDC complex (Ruiz *et al*, 2009). This suggests that Hal3 must be able to actively switch between its oligomeric states.

It has been also observed that Hal3 retains the ability to form homotrimers *in vitro* (Abrie *et al*, 2015). Thus, it is conceivable that Hal3 could trimerize and form a homotrimer *in vitro* (3xHal3) and then each Hal3 could bind to Ppz1. Such multimeric structure could explain why we obtain these high molecular weight bands when the crosslinking reaction is resolved by SDS-PAGE, since its molecular mass would be around 330 kDa. This notion fits with previous results from our laboratory in which purification by gel-filtration chromatography of the Ppz1-C-terminal/Hal3 complex results in forms with apparent size of around 400 kDa. In addition, the existence of Hal3 trimeric structures in our crosslink products would explain the large number of Hal3-Hal3 crosslinks detected (>50% when BS3 is used). Indeed, the generation of mutated forms of Hal3 with lesser tendency to trimerize without compromising the interaction with Ppz1 could be a good tool for more precise interaction mapping.

One of the results that raised our interest was that although some crosslinks were detected between Ppz1 and a region corresponding to the initial sequence of the PD region (315 to 323) the majority of the identified bonds occurred between the N-

terminal half of Hal3 and the catalytic Ppz1-Cter. It was known that while the Hal3 PD domain is necessary for the interaction, the Hal3 N-terminal region alone cannot bind *in vitro* to Ppz1 (neither full-length nor C-terminal version) (Abrie *et al*, 2012). These evidences could seem contradictory with our current results. However, in the same publication it is shown that Hal3 and a mutated version lacking the acidic C-terminal domain can bind with higher affinity to the C-terminal Ppz1 domain that to the full length, whereas PD and the combination of PD and the acidic C-terminal tail shows preferential binding with the full length version of Ppz1. These evidences suggest that the N-terminal region of Hal3 is necessary to provide the protein with its constitutive properties and that, in spite of not being sufficient, it likely contributes to the physical interaction

The identification of the crosslinked Lys in a 3D model of the C-terminal domain of Ppz1 indicates that all lysines are located near the protein surface and they are mostly clustered in two regions that are almost in opposite sides of the molecule. For instance, Hal3 K90 was identified in different experiments interacting with a specific region of Ppz1 (K584 and K593), similarly as Hal3 K120 does. This Ppz1 region is located in a α-helix that is completely opposite from the 468-502 and 378-381 regions of Ppz1, which are crosslinked with Hal3 regions 210-251 and 315-323. These Hal3 regions are rather close in sequence, the first one very near to the PD-domain and the second one located at the beginning of this domain. This could suggest that Hal3 would interact with the C-terminal domain of Ppz1 in diverse points, blocking a large part of the Ppz1 surface and likely preventing the active site of Ppz1 being in contact with the substrate. In a recent publication in our laboratory, diverse residues of Ppz1 are identified as important in Ppz1 inhibition by Hal3 (Molero *et al*, 2017). These residues are located very near to our identified cluster (468-502 and 378-381) and close to the active site of Ppz1. These results jointly suggest the importance of this Ppz1 region to regulate Hal3.

Moreover, a bionformatic study performed by Carlos Santolaria in our laboratory reveals that the Hal3 region including residues 67-110 is conserved in Vhs3 but not in Cab3. These proteins have the ability to bind Ppz1, but only Vhs3 is able to inhibit its phosphatase activity (Ruiz *et al*, 2009). This could suggest that this region of Hal3 could play a role in Ppz1 inhibition. On the other hand we identified by crosslink analysis a

second region of Hal3 around positions 210-251. This region is conserved in Hal3-like proteins of different organisms, as *Candida albicans.* Nowadays, Carlos Santolaria is studying the interaction of Ppz1-Hal3 and deleted regions 67-110 and 210-251 in Hal3, based in our crosslinks results and bionformatic analysis. Preliminary results demonstrate that the 67-110 region is relevant for the role of Hal3 in regulating Ppz1 *in vivo*.

Unfortunately, the present set of data is relatively limited and we are currently waiting for additional crosslinking data from samples treated with DBSU with the expectation to improve peptide identification. In the long run, with the help of different 3D-models of Hal3 and Ppz1, and with more experimental results from the crosslinking approach, maybe the coarse 3D-structure of this interaction could be elucidated. As reported in recent works, this technical approach has been shown able to predict the structure of different proteins (Yu & Huang, 2018; De Graaf *et al*, 2019).

## Chapter 2.- The regulation of Ppz1 and Hal3 by phosphorylation

Regarding the study of the phosphoregulation of Ppz1, it is known that the N-terminal region of Ppz1 is unstructured but plays an important role in Ppz1 function. In fact, deletion of specific segments in this region causes changes in the behavior of Ppz1 including the interaction with Hal3 (Minhas *et al*, 2012; Clotet *et al*, 1996; De Nadal *et al*, 1998; Szabó *et al*, 2019). One out of three amino acids of the Ppz1 N-terminal region are phosphorylable residues (serine or threonine mainly), including multiple potential phosphorylation sites for a number of known protein kinases, such as PKA, PKC and Cdk-2, so this fact confers to the Ppz1 N-terminus the possibility to be phosphorylated at multiple sites. In fact, Ppz1 could be phosphorylated *in vitro* by different kinases at the N-terminal region (Posas *et al*, 1995b). In addition, different high-throughput phosphoproteomic analyses have revealed multiple phosphorylated residues (Swaney *et al*, 2013; Holt *et al*, 2009). Also, it was demonstrated that Ppz1 is a substrate for Cdk1 (*CDC28*) (Holt *et al*, 2009). Recent studies show that the phosphorylation state of Ppz1 could change in response to osmostress (Romanov *et al*, 2017), being phosphorylated directly by the MAPK Hog1, although some residues of Ppz1 could be also

phosphorylated in a Hog1-independent way. Therefore, the possibility that Ppz1 could be regulated by phosphorylation was tempting and founded in significant experimental evidence.

Our results of the *in vitro* phosphorylation assays of Ppz1 by Hog1 demonstrate that Ser265, but not Thr261, is a direct phosphorylation target of Hog1. This finding is consistent with what was published by Romanov and coworkers (Romanov *et al*, 2017), where it was described that a peptide encompassing residues 260 and 265 of Ppz1 could be phosphorylated by Hog1 after the yeast cells were exposed to 0.5 M of NaCl. Moreover, our results suggest that Ppz1 itself could dephosphorylate its Ser265. One might speculate that this ability could contribute to the hypothetical regulatory switch. However, the results of the phenotypic analysis (see below) do not support this hypothesis.

In order to test if phosphorylation of T261 and S265 might affect the inhibition of Ppz1 by Hal3, an *in vitro* enzymatic assay was performed. This experiment was done with two versions of Ppz1, one version carrying T261A and S265A changes and the other with the T261E and S265D modifications. However, the inhibition profile by Hal3 of native Ppz1 and its variants was identical. In conclusion, whereas we demonstrate that Hog1 can directly phosphorylate, at least *in vitro*, Ppz1 at serine 265, this phosphorylation by itself does not modify the ability of Ppz1 to be inhibited *in vitro* by Hal3. In agreement with the *in vitro* data, the mentioned mutations did not alter the ability of Ppz1 in complementing the chromosomal deletion in any of the three genetic background tested. Therefore, we must conclude that the phosphorylation in these residues is not enough to modify the activity of Ppz1. Because the large number of phosphorylatable residues within the N-terminus of Ppz1, it is conceivable that additional sites must be modify to regulate the activity of this phosphatase.

Exploring this hypothesis, the phosphorylation pattern of Ppz1 was determined by over-expression of an inactive GST-Ppz1 version from cells subjected to change in the ionic conditions (low potassium or high NaCl), followed by affinity-purification and MALDI-TOF and LC-MS/MS analysis. This was done in collaboration with the University of Southern Denmark.

These experiments confirmed the notion that the phosphorylation pattern of the N-terminus of Ppz1 can change depending of the environment. In our case, Ppz1 phosphorylation was altered when yeast cells were exposed to high concentrations of salt (0.8 M of NaCl) and when potassium in the media was limiting. Specifically, several phophoresidues (S49, T171, S81, S97 and S99 or S239 and S242) were identified in standard growth conditions but they were not present in salt-treated cells, indicating dephosphorylation of Ppz1. On the other hand, we observed a specific phosphorylation in low potassium stress in six serines distributed in two triphosphopeptides (S191, S192 and S194 in one peptide, and S239, S242 and S243 in the other). Moreover, some phosphorylation sites maintain their phosphorylation state independently of the different stresses (i.e. S250).

In a recent phosphoproteomic study it was shown that in the presence of NaCl the phosphorylation of Ppz1 can change in two manners: Hog1-dependent and Hog1-independent (Romanov *et al*, 2017). One residue that change its phosphorylation state in Hog1-independent manner in presence of NaCl is Ser49. This phosphoresidue also appeared in our proteomic results, showing a dephosphorylation in the presence of high salt levels. Unfortunately, the phenotypic assays showed that neither change of S49 to alanine or aspartic acid, nor the combination of these mutations with the T261 and S265 ones caused alterations in the Ppz1 function.

Although coverage of the N-terminal region of Ppz1 was relatively good (85% approximately), the set of phosphopeptides obtained could not cover the entire N-terminal region. For instance, some portions of Ppz1, described as important for its function, were not totally covered. One of these regions corresponds to residues 43-52. This region, which contains several Ser and is represented in our experiments only from position 49 onwards, seems important for Ppz1 behavior, as deduced from the fact that its renders the phosphatase unable to complement the salt tolerant phenotype of the deletion mutant (Minhas *et al*, 2012). It is conceivable that, in addition of S49, changes in phosphorylation of diverse Ser residues in the vicinity (such as S43, S44 or S46) could be necessary to alter Ppz1 function. The relatively poor coverage of some regions of the N-terminal region of Ppz1 is likely due to its very high content of positive residues (lysine and arginine), which are the target for trypsin activity. It is plausible that trypsinization

of this region produces too small peptides, difficult to purify by $TiO_2$ and/or to identify by LC-MS/MS. A possible solution to this problem would be to obtain a different set of peptides by employing a protease with different amino acid recognition to cleave the protein.

An interesting output of our LC-MS/MS results in the identification of several novel phosphorylatable positions of Ppz1. In some cases, this identification has a high level of confidence, because the residues are identified with low error probability, in almost all samples analyzed, and in different peptides, as it is the case of S209 or S242. One explanation why these residues have not yet been identified as phosphorylatable is that in our case the experiment has been carried out with an inactive version of Ppz1 in a *ppz1Δ* background and that galactose and raffinose have been used as a carbon source. Both factors could alter the phosphorylation status of the phosphatase.

As described previously, Hal3 is the main regulator of Ppz1 and binds to the phosphatase to prevent its activity. In this work, we tried to identify if some changes in the phosphorylation status of Hal3 could affect the ability of this protein to inhibit Ppz1 and, consequently, to alter its regulatory properties. We focused in a short region comprising Hal3 positions 47 to 60 based on data indicating that phosphorylation of this region was decreased is some stresses, such as exposure to acetic acid (Guerreiro *et al*, 2017). This region includes five serine susceptible of being phosphorylated and, in fact, they have been identified as such in different databases and studies (Holt *et al*, 2009; Swaney *et al*, 2013; Guerreiro *et al*, 2017). However, our results indicate that different mutations of these residues or even the complete deletion of the region did not alter the inhibitory properties of the protein, as deduced from *in vitro* and *in vivo* experiments. Thus, it must be concluded that this part of Hal3 is not relevant for its function on the regulation of Ppz1. Given the ability of the Hal3 PD region to behave as a functional PPCDC (Abrie *et al*, 2015), it does not seem plausible that changes in the N-terminal section of Hal3 might affect its PPCDC function.

## Chapter 3. Understanding the molecular basis of Ppz1 toxicity

The toxic effect of Ppz1 overexpression was known long time ago (Clotet *et al*, 1996). In fact, evidences for negative effect of overexpression of protein phosphatases have been obtained in the past. Thus, it has been demonstrated for calcineurin, whose overexpression causes altered budding pattern and cell morphology (Mendoza *et al*, 1996). Similarly, Glc7 overexpression induces cell death (Ghosh & Cannon, 2013). It must be noted that this does not occur in the case of Ppz1, since its overexpression results in a halt in cell cycle progression but cells remain alive (unpublished results of our laboratory). It was also known that the over-expression of the full-length phosphatase and that of the C-terminal part is toxic, but not that the N-terminus (Clotet *et al*, 1996). Recently our laboratory demonstrated that the phosphatase activity of Ppz1 is a requirement for toxicity (Zhang, 2019). Therefore, it was conceivable that the increase in phosphatase activity would result in alterations in the phosphorylation pattern of diverse proteins, which might lead to the toxic effect. Based on seminal work in our laboratory, describing that cells overexpressing Ppz1 show a delay in G1/S transition, delayed expression of *CLN2* and *CLB5* and increased number of unbudded cells (Clotet *et al*, 1999), it was expected that toxicity in strain ZCZ01 would be related to a halt in the G1 to S cell cycle transition.

Our phosphoproteomic study aimed to analyze the changes in the phosphorylation pattern in the cell caused by overexpression of Ppz1 in order to identify: 1) possible cellular targets of Ppz1, and 2) the molecular basis of the toxic effect of Ppz1 overexpression. Our results indicate that Ppz1 overexpression has a wide impact in protein phosphorylation, since 134 different proteins show a consistent decrease in their phosphorylation state, and 37 proteins increase its phosphorylation.

Changes in the phosphorylation pattern fit well with the timing of expression of Ppz1. Thus, after 30 min of induction, the level of Ppz1 in the ZCZ01 strain is roughly that observed in a wild type strain, and at this moment, the alterations in the phosphoproteome profile are marginal. In contrast, most of changes in phosphorylation appear from 120 minutes of Ppz1-overexpression onward, in concordance with the

accumulation of high levels of the phosphatase, as deduced by Western-blot experiments, and a perceptible halt in the growth of the culture.

Although most of residues affected in their phosphorylation state suffered a dephosphorylation event, they were a significant number of residues (mostly Ser and Thr) that resulted hyperphosphorylated. It seems clear that these changes are secondary to the direct impact of increased Ppz1 activity. It is conceivable that Ppz1 could dephosphorylate proteins that would alter the activity of specific protein kinases or the catalytic kinase polypeptide itself. However, such events must occur rather rapidly, since most proteins result hyperphosphorylated between 30 and 60 minutes of Ppz1 overexpression.

Our results highlight a major impact of Ppz1 in the dephosphorylation of proteins related with mitotic cell division (cell cycle, bud neck, polarized growth), carbohydrate metabolism and translation initiation. These processes are of vital importance, and their missregulation is likely to have deleterious effects for cell growth.

Regarding cell cycle, diverse proteins implicated in the regulation of transcription involved in G1/S transition were identified as dephosphorylated 4 hours after the shift to galactose. These protein are **Yph1,** necessary for maturation of the large ribosomal subunit and important for exit from G0 (Oeffinger *et al*, 2002), **Spt6** (a nucleosome remodeling protein), and **Stb1,** a regulator of MBF-specific transcription at Start. Stb1 is phosphorylated by Cln-Cdc28 kinases (Ubersax *et al*, 2003), and this phosphorylation mediates dissociation of the Stb1-MBF complex, resulting in termination of MBF-specific transcription (Costanzo *et al*, 2003). **Swi4** and **Swi6** (also dephosphorylated in our experiments) form the SBF transcription factor involved in the transcription of necessary genes for G1/S transition. The main inhibitor of SBF is **Whi5,** functionally equivalent to the Retinoblastoma (Rb) tumor suppressor protein in mammals. Whi5 is phosphorylated in diverse residues by the Cln3/Cdc28 kinase (Costanzo *et al*, 2004; de Bruin *et al*, 2004), and phosphorylation of Whi5 promotes its dissociation from Swi6 and its exit from the nucleus, thus releasing its inhibitory effect on G1 specific transcription. Our results show that Whi5 is dephosphorylated in positions S88, S154, S156 and S161 when Ppz1 is over-expressed. These are some of the residues phosphorylated by the Cln3/Cdc28 kinase (Wagner *et al*, 2009). This suggests that in Ppz1 overexpressing cells Whi5 is not properly

phosphorylated and might remain might bound to the SBF transcription factor, thus inhibiting the G1/S transition.

Two proteins identified in our phosphoproteomic experiments were **Vhs2** and its paralog **Mlf3**. Both proteins show dephosphorylation in the equivalent residue (S314 in Vhs2 and S315 in Mlf3). These residues have not reported as phosphorylatable in the databases. Vhs2 was identified in our laboratory as a multicopy suppressor of the synthetically lethal phenotype of a conditional *sit4Δ hal3Δ* mutant, a strain that suffers an arrest in G1 phase (Muñoz *et al*, 2003). Previous studies from our laboratory demonstrated that mutation of *PPZ1* eliminated the lethal phenotype, suggesting that Ppz1 and Sit4 play and opposite roles in G1/S transition (Clotet *et al*, 1999). Our current results demonstrate that the over-expression of Vhs2 partially suppresses the growth defect produced by Ppz1 over-expression observed in strains ZCZ01 and MLM04. This could suggest that Vhs2 is playing an opposite role to Ppz1 in G1/S transition, similar to that observed in the *sit4Δ hal3Δ* background. However, our data suggest that phosphorylation of S314 is not important for the ability of Vhs2 to rescue the growth defect in Ppz1 overexpressing cells. It has been reported that Vhs2 is involved in the regulation of septin dynamics (Cassani *et al*, 2014), and it is tempting to speculate that over-expression of Vhs2 in ZCZ01 cells could be attenuating the problems at the bud neck level caused by Ppz1 over-expression.

It could be suggested that the dephosphorylation effects described above could be the trigger of the halt in G1/S transition observed upon Ppz1 overexpression (Clotet *et al*, 1999; Zhang, 2019). However, it must be noted that the effect of overexpression of Ppz1 on cell cycle are already patent after 2 h of induction, as deduced from growth rate and the index of budding of the culture induction (Zhang, 2019). In contrast, our data shows that many of the cell-cycle related proteins appear dephosphorylated only after 4 hours of Ppz1. This would be the case of Whi5. Therefore, the change in the phosphorylation of Whi5 is likely a consequence of the halt in cell cycle, and not a cause. In contrast, Vhs2 is dephoshorylated already after 30 min of Ppz1 expression. This kinetics supports the possibility of Vhs2 being a primary target for Ppz1 and a trigger of the cell cycle blockage induced by high levels of Ppz1.

Our phosphoproteomic data shows a dephosphorylation in several proteins related with carbohydrate metabolism. A striking example is Mig1, a transcriptional repressor that is dephosphorylated at S311 and S314 already after 60 min of Ppz1 induction. Mig1 is a transcription factor involved in glucose repression, phosphorylated by Snf1, precisely at S311 and S314 (Ahuatzi *et al*, 2007), in low glucose conditions to trigger its exit from the nucleus to cytosol, and consequently activate the transcription of glucose-repressed genes. Mig1 is dephosphorylated by Reg1-Glc7 in high glucose conditions and returns to the nucleus to repress the transcription of these genes (De Vit *et al*, 1997; Treitel *et al*, 1998). We have confirmed the dephosphorylation of Mig1 by a shift assay and demonstrated that, in Ppz1 overexpressing cells, Mig1 is retained in the nucleus in the absence of glucose in a significant number of cells. Remarkably, work in our laboratory has shown that, even though we did not identified the relevant Snf1 peptides in our phosphoproteomic data, Snf1 is rapidly dephosphorylated at T210, a key residue for activation of the Snf1 kinase (Marcel Albacar, personal communication). Therefore, although the possibility that Mig1 could be a direct substrate for Ppz1 cannot be ruled out, it seems evident that high levels of Ppz1 negatively influence the Snf1 pathway upstream of the Snf1 kinase. This is highly relevant because, in addition of its role in the control of carbohydrate metabolism, a role for Snf1 in the activation of SBF and MBF-dependent transcription, thus promoting G1/S transition has been reported (Busnelli *et al*, 2013). Therefore, dephosphorylation of Snf1 induced by excessive ppz1 activity could be at the basis of the observed cell cycle effects.

### 3.1 Ppz1 over-expression affects protein translation

As explained above, other proteins whose phosphorylation status appears affected in our results are related with protein translation, as it is the case of initiation factors (Sui3 and Gcd6) or ribosomal protein (Rps6A and Rpp1A). This fits well with the kind of proteins identified in the interatomic experiments, that is, different elongation factors (eEF3 and eEF1) or ribosomal proteins (Rpl2, Rpl3, Rpl13b and Rpl10). Taken together, this results suggests that Ppz1 over-expression would be affecting protein translation.

We demonstrate in our phosphoproteomic approach and by immunoblot that overexpression of Ppz1 causes dephosphorylation of Rps6A in residues S232 and S233 (corresponding to S235 and S236 in mammals). In mammals, it is known that S6K phosphorylates ribosomal protein S6 (S6) at five Ser residues (Ser235/236/240/244/247) to promote transcription of genes required for ribosome biogenesis. In *S. cerevisiae* Rps6 is phosphorylated by Ypk3 solely at S232 and S233, and it is dephosphorylated by Shp1-Glc7 (González *et al*, 2015; Yerlikaya *et al*, 2016). Although commonly used as a read-out of the TORC activation pathway, the function of the phosphorylation in these residues in yeast is unknown. In any case, our results suggest that over-expressed Ppz1 plays an opposite role to TORC1 and TORC2 in Rps6A phosphorylation.

Another protein related with translation is Npl3. We identified a strong dephosphorylation of S411, whereas other phosphoresidues were not affected by ppz1 overexpresion. Although Npl3 data was obtained only in our first experiment, we considered interesting to further investigate this issue. Npl3 is SR-like RNA-binding protein involved in regulation of different processes related with translation, such as exporting from the nucleus mRNA and ribosomal pre-60S subunit (Baierlein *et al*, 2013). Usually this protein is found in the nucleus in exponential cultures (Lund *et al*, 2008), and it is phosphorylated in cytosol by Sky1 in S411, causing its dissociation from the mRNA and its return into the nucleus. In fact, a non-phosphorylable version of Npl3 (S411A) accumulates in the cytosol (Gilbert *et al*, 2001; Madrid *et al*, 2006). Our results demonstrate that dephosphorylation of Npl3 at S411 is accompanied by delocalization of the protein from the nucleus to cytoplasm. This should negatively affect translation due to the interference with mRNA and ribosomal pre-60s transport. Besides, Npl3 can bind to eIF4G to repress translation, and only upon Sky1-mediated phosphorylation it dissociates from the mRNA and translation can continue (Rajyaguru *et al*, 2012). Interestingly, when we co-overexpressed Npl3 together with Ppz1 we observed a negative effect, aggravating the toxic phenotype of Ppz1. Previous studies demonstrate that the accumulation of Npl3 in the cytoplasm induce an important decrease in the amount of polysomes and the protein can be find bound to this polysome by immunoblotting (Baierlein *et al*, 2013; Windgassen *et al*, 2004). In this regard,

experiments performed in our laboratory in parallel by Carlos Calafí, show a decrease in the polysome profile when Ppz1 is over-expressed in strain MLM04. It is plausible that dephosphorylation of Npl3 induced by Ppz1 overexpression and its consequent cytosolic accumulation might retain an excess of mRNA bound to Npl3, thus inhibiting polysome formation and translation, and that this could be further aggravated by an excess of Npl3.

Taken together, our results corroborate that Ppz1 is affecting translation initiation. Because of its crucial role in translation initiation, we decided to analyze the phosphorylation state of Ser-51 of eIF2α (Sui2), an event that has been demonstrated to cause inhibition of protein translation (Gordiyenko *et al*, 2019). Our results demonstrate a hyperphosphoylation of this residue after 4 hours of Ppz1 over-expression. It has been described that eIF2α is phosphorylated exclusively by the Gcn2 kinase (Dever *et al*, 1992; Zaborske *et al*, 2009). Recently Ppz1 has been over-expressed in a *gcn2Δ* background in our laboratory. In this background eIF2α was not phosphorylated upon Ppz1 overexpression, but lack of Gcn2 did not rescue the toxic phenotype of Ppz1 over-expression, indicating that eiF2α phosphorylation is not a cause of Ppz1 toxicity but a consequence.

Different proteins that appear as dephosphorylated in our phosphoproteomic data are substrates of Glc7 as Mig1, Npl3, Rps6A, or the Glc7 regulatory subunit Reg1 (Cannon, 2010). As mentioned above, over-expression of Gl7 is also toxic for yeast cells. However, Ghosh and coworkers demonstrated that for Glc7 over-expression to be toxic, it was required the presence of specific PP1c regulatory subunits, such as Ypi1, Sds22 (likely to import the phosphatase inside the nucleus), or Glc8 (Ghosh & Cannon, 2013). In addition, in this publication it is described that over-expression of Glc7 caused cell death. However, Ppz1 over-expression does not affect cell viability, as demonstrated in our laboratory by plating arrested ZCZ01 cells after 20 hours in galactose, and recent work in our laboratory shows that deletion of Glc8 does not attenuate Ppz1 toxicity Carlos Calafí, personal communication). Therefore, although it cannot be excluded that in overexpression Ppz1 might dephosphorylate specific targets of Glc7, it is unlikely that this spurious dephosphorylation events are the cause for Ppz1 toxicity.

# CONCLUSIONS

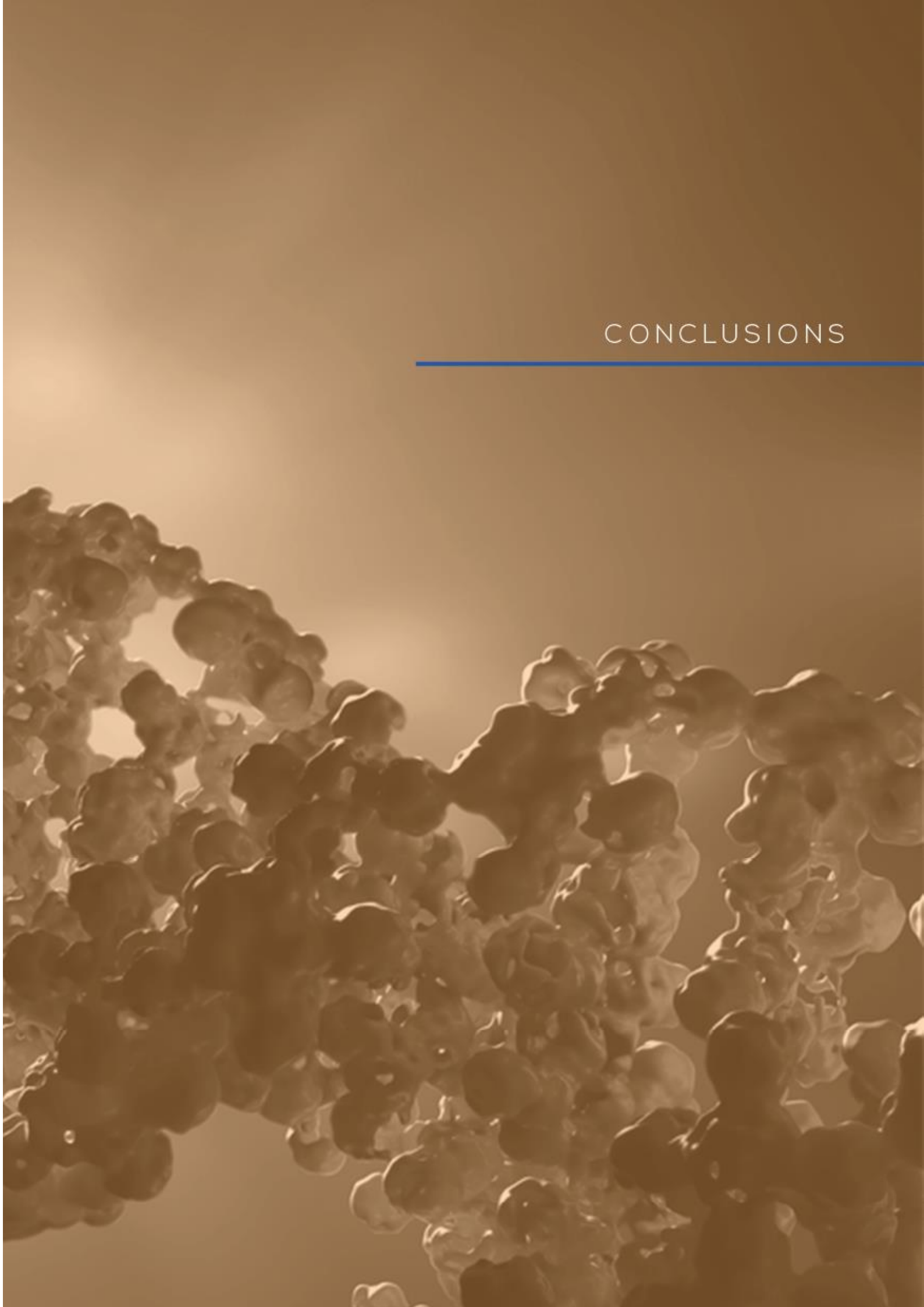

# Conclusions

1.- Fluorescent C-terminally tagged versions of Ppz1 and Hal3 maintain the functionality of their native versions.

2.- Expression of Ppz1-GFP and Hal3-mCherry allow detection of FRET, thus demonstrating the interaction of Ppz1 and Hal3 *in vivo* and leading the way for future studies no the likely dynamic interaction between these proteins.

3.- Chemical crosslinking assays between the C-terminal half of Ppz1 and Hal3 copurified from E. coli as an apparent 1:1 complex yield high molecular weight species, suggesting the formation of higher order structures (perhaps in a 3:3 ratio).

4.- Chemical crosslinking assays show numerous links between the N-terminal half of Hal3 and the catalytic domain of Ppz1, in spite that reported data indicates that this Hal3 region alone does not bind with Ppz1.

5.- Ppz1 is phosphorylated *in vitro* by Hog1 in Ser-265, and this residue can be dephosphorylated by Ppz1 itself. However, mutation of this residue to Ala or Asp does not alter Ppz1 function.

6.- The Ppz1 phosphorylation state changes depending on the environment. Specific dephosphorylation events have been found in cells exposed to high salt or low potassium conditions.

7.- Nine new residues of Ppz1 (S19, S81, S82, S97, S152, S189, S191, S209 and S242) have been identified as phosphorylatable.

8.- Ppz1 is dephosphorylated at S49 in cells exposed to salt stress. However, mutation to ala or Asp does not affect Ppz1 function. In fact, a version combining mutation at S49, T261 and S265 positions is indistinguishable from native Ppz1.

9.- Point mutation in specific Ser residues in the serine-rich Hal3 47-60 region, where phosphorylation changes have been reported in the presence of acetic acid, or deletion of the entire region, it does not have an impact in Hasl3 function as Ppz1 inhibitor.

10.- LC-MS/MS studies reveals that Ppz1 overexpression causes important changes in the phosphoproteome of *S. cerevisiae*, affecting mainly proteins related with cell division, carbohydrate metabolism and protein translation.

11.- These studies allowed the identification of 466 new phosphoresidues that correspond to 317 different proteins.

12.- Rps6A is dephosphorylated in cells that overexpress Ppz1, whereas eIF2α results hyperphosphorylated, suggesting that the excess of Ppz1 impinges in the translation process.

13.- Ppz1 over-expression induces rapid Mig1 dephosphorylation, and triggers nuclear localization of the repressor even in the absence of glucose.

14.- Ppz1 overexpression produces dephosphorylation of Npl3 at S411 and delocalization of Npl3 from the nucleus to cytoplasm.

15.- Vhs2 and its paralog Mlf3 are dephosphorylated upon overexpression of Ppz1 in the equivalent residue (S314 and S315, respectively). Vhs2 overexpression attenuates the growth defect of strains ZCZ01 and MLM04, but this occur independently of the phosphorylation state of Vhs2.

16.- We are confident that careful analysis of phosphoproteomic data followed by experimental confirmation will allow to the identification of the relevant changes leading to the characteristic G1/S blockage due to high levels of Ppz1.

# BIBLIOGRAPHY

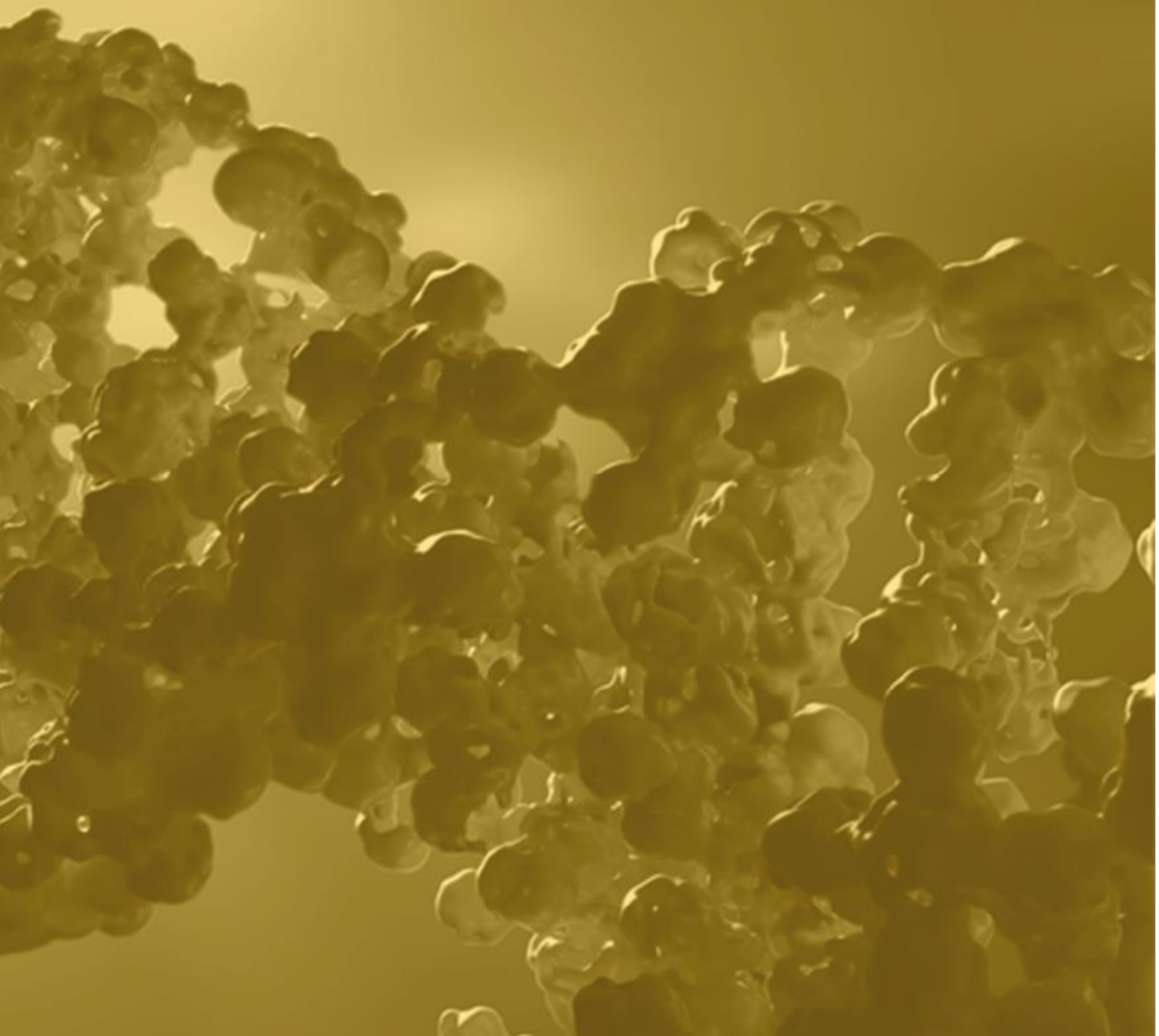

# Bibliography


Abrie JA, González A, Strauss E & Ariño J (2012) Functional mapping of the disparate activities of the yeast moonlighting protein Hal3. *Biochem. J.* **442:** 357–368

Abrie JA, Molero C, Ariño J & Strauss E (2015) Complex stability and dynamic subunit interchange modulates the disparate activities of the yeast moonlighting proteins Hal3 and Vhs3. *Sci. Rep.* **5:** 1–17

Ádám C, Erdei É, Casado C, Kovács L, González A, Majoros L, Petrényi K, Bagossi P, Farkas I, Molnar M, Pócsi I, Ariño J & Dombrádi V (2012) Protein phosphatase CaPpz1 is involved in cation homeostasis, cell wall integrity and virulence of Candida albicans. *Microbiology* **158:** 1258–1267

Adams, A., gottschling, D.E.; Kaiser, C.A., and Stearns T (1997) Methods in Yeast Genomics Cold Spring Harbor, NY: Cold Spring Harbor Laboratory Press, NY

Aguilar-Uscanga B & François JM (2003) A study of the yeast cell wall composition and structure in response to growth conditions and mode of cultivation. *Lett. Appl. Microbiol.* **37:** 268–274

Ahuatzi D, Riera A, Peláez R, Herrero P & Moreno F (2007) Hxk2 regulates the phosphorylation state of Mig1 and therefore its nucleocytoplasmic distribution. *J. Biol. Chem.* **282:** 4485–4493

Aksenova A, Munoz I, Volkov K, Arino J & Mironova L (2007) The HAL3-PPZ1 dependent regulation of nonsense suppression efficiency in yeast and its influence on manifestation of the yeast prion-like determinant [ISP(+)]. *Genes Cells* **12:** 435–445

Alepuz PM, Cunningham KW & Estruch F (1997) Glucose repression affects ion homeostasis in yeast through the regulation of the stress-activated ENA1 gene. *Mol. Microbiol.* **26:** 91–98

Alms GR, Sanz P, Carlson M & Haystead TAJ (1999) Reg1p targets protein phosphatase 1 to dephosphorylate hexokinase II in Saccharomyces cerevisiae: Characterizing the effects of a phosphatase subunit on the yeast proteome. *EMBO J.* **18:** 4157–4168

Ariño J (2002) Novel protein phosphatases in yeast. *Eur. J. Biochem.* **269:** 1072–1077

Ariño J, Casamayor A & González A (2011) Type 2C protein phosphatases in fungi. *Eukaryot. Cell* **10:** 21–33

Ariño J, Ramos J & Sychrová H (2010) Alkali metal cation transport and homeostasis in yeasts. *Microbiol. Mol. Biol. Rev.* **74:** 95–120:

Arndt KT, Styles CA & Fink GR (1989) A suppressor of a HIS4 transcriptional defect encodes a protein with homology to the catalytic subunit of protein phosphatases. *Cell* **56:** 527–537

Bai Y, Chen B, Li M, Zhou Y, Ren S, Xu Q, Chen M & Wang S (2017) FPD: A comprehensive phosphorylation database in fungi. *Fungal Biol.* **121:** 869–875

Baierlein C, Hackmann A, Gross T, Henker L, Hinz F & Krebber H (2013) Monosome formation during translation initiation requires the serine/arginine-rich protein Npl3. *Mol. Cell. Biol.* **33:** 4811–4823

Bajar BT, Wang ES, Zhang S, Lin MZ & Chu J (2016) A Guide to Fluorescent Protein FRET Pairs. *Sensors (Basel).* **16:** 1488

Balcells L, Gómez N, Casamayor a, Clotet J & Ariño J (1997) Regulation of salt tolerance in fission yeast by a protein-phosphatase-2-like Ser/Thr protein phosphatase. *Eur. J. Biochem.* **250:** 476–483

Bilsland-Marchesan E, Ariño J, Saito H, Sunnerhagen P & Posas F (2000) Rck2 kinase is a substrate for the osmotic stress-activated mitogen-activated protein kinase Hog1. *Mol. Cell. Biol.* **20:** 3887–3895

Bloecher A & Tatchell K (2000) Dynamic Localization of Protein Phosphatase Type 1 in the Mitotic Cell Cycle of Saccharomyces cerevisiae . *J. Cell Biol.* **149:** 125–140

Böhm S & Buchberger A (2013) The Budding Yeast Cdc48Shp1 Complex Promotes Cell Cycle Progression by Positive Regulation of Protein Phosphatase 1 (Glc7). *PLoS One* **8:** e56486

Bollen M, Peti W, Ragusa MJ & Beullens M (2010) The extended PP1 toolkit: designed to create specificity. *Trends Biochem.* **35:** 450–458

Botstein D & Fink GR (2011) Yeast: An experimental organism for 21st century biology. *Genetics* **189:** 695–704

Brachmann CB, Davies A, Cost GJ, Caputo E, Li J, Hieter P & Boeke JD (1998) Designer deletion strains derived from Saccharomyces cerevisiae S288C: A useful set of strains and plasmids for PCR-mediated gene disruption and other applications. *Yeast* **14:** 115–132

de Bruin RAM, McDonald WH, Kalashnikova TI, Yates J & Wittenberg C (2004) Cln3 Activates G1-Specific Transcription via Phosphorylation of the SBF Bound Repressor Whi5. *Cell* **117:** 887–898

Busnelli S, Tripodi F, Nicastro R, Cirulli C, Tedeschi G, Pagliarin R, Alberghina L & Coccetti P (2013) Snf1/AMPK promotes SBF and MBF-dependent transcription in budding yeast. *Biochim. Biophys. Acta - Mol. Cell Res.* **1833:** 3254–3264

Cannon JF (2010) Function of protein phosphatase-1, Glc7, in Saccharomyces cerevisiae. *Adv.Appl.Microbiol.* **73:** 27–59

Cannon JF, Pringle JR, Fiechter A & Khalil M (1994) Characterization of Glycogen-Deficient Glc Mutants of Saccharomyces Cerevisiae. *Genetics* **136:** 485–503

Carlson M (1999) Glucose repression in yeast. *Curr. Opin. Microbiol.* **2:** 202–207

Cassani C, Raspelli E, Chiroli E & Fraschini R (2014) Vhs2 is a novel regulator of septin dynamics in budding yeast. *Cell Cycle* **13:** 1590–1601

Ceulemans H & Bollen M (2004) Functional Diversity of Protein Phosphatase-1, a Cellular Economizer and Reset Button. *Physiol. Rev.* **84:** 1–39

Ceulemans H, Vulsteke V, De Maeyer M, Tatchell K, Stalmans W & Bollen M (2002) Binding of the concave surface of the Sds22 superhelix to the alpha 4/alpha 5/alpha 6-triangle of protein phosphatase-1. *J. Biol. Chem.* **277:** 47331–47337

Chang JS, Henry K, Wolf BL, Geli M & Lemmon SK (2002) Protein Phosphatase-1 Binding to Scd5p Is Important for Regulation of Actin Organization and Endocytosis in Yeast. *J. Biol. Chem.* **277:** 48002–48008

Chen E, Choy MS, Petrényi K, Kónya Z, Erdődi F, Dombrádi V, Peti W & Page R (2016a) Molecular Insights into the Fungus-Specific Serine/Threonine Protein Phosphatase Z1 in

Candida albicans. *MBio* **7:** e00872-16

Chen E, Choy MS, Petrényi K, Kónya Z, Erdődi F, Dombrádi V, Peti W & Page R (2016b) Molecular Insights into the Fungus-Specific Serine/Threonine Protein Phosphatase Z1 in Candida albicans. *MBio* **7:** e00872-16

Cheng Y-L & Chen R-H (2010) The AAA-ATPase Cdc48 and cofactor Shp1 promote chromosome bi-orientation by balancing Aurora B activity. *J. Cell Sci.* **123:** 2025 LP – 2034

Cheng Y-L & Chen R-H (2015) Assembly and quality control of the protein phosphatase 1 holoenzyme involves the Cdc48-Shp1 chaperone. *J. Cell Sci.* **128:** 1180–1192

Clotet J, Garí E, Aldea M & Ariño J (1999) The yeast Ser/Thr phosphatases sit4 and ppz1 play opposite roles in regulation of the cell cycle. *Mol. Cell. Biol.* **19:** 2408–2415

Clotet J, Posas F, Casamayor A, Schaaff-Gerstenschlager I & Arino J (1991) The gene DIS2S1 is essential in Saccharomyces cerevisiae and is involved in glycogen phosphorylase activation. *Curr. Genet.* **19:** 339–342

Clotet J, Posas F, De Nadal E & Arino J (1996) The NH2-terminal extension of protein phosphatase PPZ1 has an essential functional role. *J. Biol. Chem.* **271:** 26349–26355

Cohen P (1989) The Structure and Regulation of Protein Phosphatases. *Annu. Rev. Biochem.* **58:** 453–508

Cohen P (1991) Classification of Protein- Serine/Threonine Phosphatases: Identification and Quantitation in Cell Extracts. In *Methods in Enzymology* pp 389–398. Academic Press

Cohen P (1997) Novel protein serine/threonine phosphatases: Variety is the spice of life. *Trends Biochem. Sci.* **22:** 245–251

Cohen P (2002) Protein phosphatase 1--targeted in many directions. *J. Cell Sci.* **115:** 241–256

Di Como CJ, Bose R & Arndt KT (1995) Overexpression of SIS2, which contains an extremely acidic region, increases the expression of SWI4, CLN1 and CLN2 in sit4 mutants. *Genetics* **139:** 95–107

Costanzo M, Nishikawa JL, Tang X, Millman JS, Schub O, Breitkreuz K, Dewar D, Rupes I, Andrews B & Tyers M (2004) CDK Activity Antagonizes Whi5, an Inhibitor of G1/S Transcription in Yeast. *Cell* **117:** 899–913

Costanzo M, Schub O & Andrews B (2003) G1 Transcription Factors Are Differentially Regulated in Saccharomyces cerevisiae by the Swi6-Binding Protein Stb1. *Mol. Cell. Biol.* **23:** 5064–5077

Csizmok V, Follis AV, Kriwacki RW & Forman-Kay JD (2016) Dynamic Protein Interaction Networks and New Structural Paradigms in Signaling. *Chem. Rev.* **116:** 6424–6462

Dever TE, Feng L, Wek RC, Cigan AM, Donahue TF & Hinnebusch AG (1992) Phosphorylation of initiation factor 2α by protein kinase GCN2 mediates gene-specific translational control of GCN4 in yeast. *Cell* **68:** 585–596

Dey M, Velyvis A, Li JJ, Chiu E, Chiovitti D, Kay LE, Sicheri F & Dever TE (2011) Requirement for kinase-induced conformational change in eukaryotic initiation factor 2alpha (eIF2alpha) restricts phosphorylation of Ser51. *Proc. Natl. Acad. Sci. U. S. A.* **108:** 4316–4321 A

Doseff AI & Arndt KT (1995) LAS1 is an essential nuclear protein involved in cell morphogenesis and cell surface growth. *Genetics* **141:** 857–71

Dosztányi Z, Mészáros B & Simon I (2009) ANCHOR: Web server for predicting protein binding regions in disordered proteins. *Bioinformatics* **25:** 2745–2746

Dye BT, Schell K, Miller DJ & Ahlquist P (2005) Detecting protein–protein interaction in live yeast by flow cytometry. *Cytom. Part A* **63A:** 77–86

Egloff M-P, Cohen PTW, Reinemer P & Barford D (1995) Crystal Structure of the Catalytic Subunit of Human Protein Phosphatase 1 and its Complex with Tungstate. *J. Mol. Biol.* **254:** 942–959

Egloff MP, Johnson DF, Moorhead G, Cohen PT, Cohen P & Barford D (1997) Structural basis for the recognition of regulatory subunits by the catalytic subunit of protein phosphatase 1. *EMBO J.* **16:** 1876–1887 A

Erez O & Kahana C (2001) Screening for modulators of spermine tolerance identifies Sky1, the SR protein kinase of Saccharomyces cerevisiae, as a regulator of polyamine transport and ion homeostasis. *Mol. Cell Biol.* **21:** 175–184

Ewald H, Bart L, Janina G, Monique B, Luc VM & Mathieu B (2012) The PP1 binding code: a molecular-lego strategy that governs specificity. *FEBS J.* **280:** 584–595

Feng ZH, Wilson SE, Peng ZY, Schlender KK, Reimann EM & Trumbly RJ (1991) The yeast GLC7 gene required for glycogen accumulation encodes a type 1 protein phosphatase. *J. Biol. Chem.* **266:** 23796–23801

Fernandez-Sarabia MJ, Sutton A, Zhong T & Arndt KT (1992) SIT4 protein phosphatase is required for the normal accumulation of SWI4, CLN1, CLN2, and HCS26 RNAs during late G1. *Genes Dev.* **6:** 2417–2428

Ferrando A, Kron SJ, Rios G, Fink GR & Serrano R (1995) Regulation of cation transport in Saccharomyces cerevisiae by the salt tolerance gene HAL3. *Mol. Cell Biol.* **15:** 5470–5481

Ferrer-Dalmau J, González A, Platara M, Navarrete C, Martínez JL, Barreto L, Ramos J, Ariño J & Casamayor A (2010) Ref2, a regulatory subunit of the yeast protein phosphatase 1, is a novel component of cation homoeostasis. *Biochem. J.* **426:** 355 LP – 364

Ferrer-Dalmau J, Randez-Gil F, Marquina M, Prieto JA & Casamayor A (2015) Protein kinase Snf1 is involved in the proper regulation of the unfolded protein response in <em>Saccharomyces cerevisiae</em> *Biochem. J.* **468:** 33 LP – 47

Francisco L, Wang W & Chan CS (1994) Type 1 protein phosphatase acts in opposition to IpL1 protein kinase in regulating yeast chromosome segregation. *Mol. Cell. Biol.* **14:** 4731–4740

Friedman DB (2007) Quantitative Proteomics for Two-Dimensional Gels Using Difference Gel Electrophoresis BT - Mass Spectrometry Data Analysis in Proteomics. In, Matthiesen R (ed) pp 219–239. Totowa, NJ: Humana Press

Gaber RF, Styles CA & Fink GR (1988) TRK1 encodes a plasma membrane protein required for high-affinity potassium transport in Saccharomyces cerevisiae. *Mol. Cell. Biol.* **8:** 2848–2859

Gancedo JM (2008) The early steps of glucose signalling in yeast. *FEMS Microbiol. Rev.* **32:** 673–704

Gao J, Thelen JJ, Dunker AK & Xu D (2010) Musite, a Tool for Global Prediction of General and Kinase-specific Phosphorylation Sites. *Mol. Cell. Proteomics* **9:** 2586–2600

Garcia-Gimeno MA, Munoz I, Arino J & Sanz P (2003) Molecular characterization of Ypi1, a novel Saccharomyces cerevisiae type 1 protein phosphatase inhibitor. *J.Biol.Chem.* **278:** 47744–47752

Garciadeblas B, Rubio F, Quintero FJ, Bañuelos MA, Haro R & Rodríguez-Navarro A (1993) Differential expression of two genes encoding isoforms of the ATPase involved in sodium efflux in Saccharomyces cerevisiae. *Mol. Gen. Genet. MGG* **236:** 363–368

Ghosh A & Cannon JF (2013) Analysis of protein phosphatase-1 and aurora protein kinase suppressors reveals new aspects of regulatory protein function in Saccharomyces cerevisiae. *PLoS One* **8:** e69133

Ghosh A, Shuman S & Lima CD (2008) The structure of Fcp1, an essential RNA polymerase II CTD phosphatase. *Mol. Cell* **32:** 478–490

Gibbons J, Kozubowski L, Tatchell K & Shenolikar S (2007) Expression of human protein phosphatase-1 in Saccharomyces cerevisiae highlights the role of phosphatase isoforms in regulating eukaryotic functions. *J. Biol. Chem.* **282:** 21838–21847

Gietz RD & Akio S (1988) New yeast-Escherichia coli shuttle vectors constructed with in vitro mutagenized yeast genes lacking six-base pair restriction sites. *Gene* **74:** 527–534

Gilbert W, Siebel CW & Guthrie C (2001) Phosphorylation by Sky1p promotes Npl3p shuttling and mRNA dissociation. *RNA* **7:** 302–313

Goldberg J, Huang H, Kwon Y, Greengard P, Nairn AC & Kuriyan J (1995) Three-dimensional structure of the catalytic subunit of protein serine/threonine phosphatase-1. *Nature* **376:** 745

Goldstein AL & McCusker JH (1999) Three new dominant drug resistance cassettes for gene disruption in Saccharomyces cerevisiae. *Yeast* **15:** 1541–1553

González A, Shimobayashi M, Eisenberg T, Merle DA, Pendl T, Hall MN & Moustafa T (2015) TORC1 promotes phosphorylation of ribosomal protein S6 via the AGC kinase Ypk3 in Saccharomyces cerevisiae. *PLoS One* **10:** e0120250–e0120250

Gordiyenko Y, Llácer JL & Ramakrishnan V (2019) Structural basis for the inhibition of translation through eIF2α phosphorylation. *Nat. Commun.* **10:** 2640

Gordon GW, Berry G, Liang XH, Levine B & Herman B (1998) Quantitative fluorescence resonance energy transfer measurements using fluorescence microscopy. *Biophys. J.* **74:** 2702–2713

De Graaf SC, Klykov O, Van Den Toorn H & Scheltema RA (2019) Cross-ID: Analysis and Visualization of Complex XL-MS-Driven Protein Interaction Networks. *J. Proteome Res.* **18:** 642–651

Gressner AM & Wool IG (1974) The phosphorylation of liver ribosomal proteins in vivo. *J. Biol. Chem.* **249:** 6917–6925

Guerreiro JF, Mira NP, Santos AXS, Riezman H & Sá-Correia I (2017) Membrane Phosphoproteomics of Yeast Early Response to Acetic Acid: Role of Hrk1 Kinase and Lipid Biosynthetic Pathways, in Particular Sphingolipids. *Front. Microbiol.* **8:** 1302

Hackmann A, Gross T, Baierlein C & Krebber H (2011) The mRNA export factor Npl3 mediates the nuclear export of large ribosomal subunits. *EMBO Rep.* **12:** 1024 LP – 1031

Haro R, Garciadeblas B & Rodriguez-Navarro A (1991) A novel P-type ATPase from yeast

involved in sodium transport. *FEBS Lett.* **291:** 189–191

He L, Bradrick TD, Karpova TS, Wu X, Fox MH, Fischer R, McNally JG, Knutson JR, Grammer AC & Lipsky PE (2003) Flow cytometric measurement of fluorescence (Förster) resonance energy transfer from cyan fluorescent protein to yellow fluorescent protein using single-laser excitation at 458 nm. *Cytom. Part A* **53A:** 39–54

He X & Moore C (2005) Regulation of Yeast mRNA 3' End Processing by Phosphorylation. *Mol. Cell* **19:** 619–629

Hinnebusch AG (2005) Translational regulation of GCN4 and the general amino acid control of yeast. *Annu. Rev. Microbiol.* **59:** 407–50

Hofmann T, Fischer AW, Meiler J & Kalkhof S (2015) Protein structure prediction guided by crosslinking restraints - A systematic evaluation of the impact of the crosslinking spacer length. *Methods* **89:** 79–90

Holt LJ, Tuch BB, Villén J, Johnson AD, Gygi SP & Morgan DO (2009) Global analysis of Cdk1 substrate phosphorylation sites provides insights into evolution. *Science* **325:** 1682–6

Hughes V, Müller a, Stark MJ & Cohen PT (1993) Both isoforms of protein phosphatase Z are essential for the maintenance of cell size and integrity in Saccharomyces cerevisiae in response to osmotic stress. *Eur. J. Biochem.* **216:** 269–79

Illuxley C, Green ED & Dunbam I (1990) Rapid assessment of S. cerevisiae mating type by PCR. *Trends Genet.* **6:** 236

Ingebritsen TS & Cohen P (1983) The protein phosphatases involved in cellular regulation. 1. Classification and substrate specificities. *Eur. J. Biochem.* **132:** 255–61

Ito H, Fukuda Y, Murata K & Kimura A (1983) Transformation of intact yeast cells treated with alkali cations. *J. Bacteriol.* **153:** 163–168

Ivanov MS, Aksenova AI, Burdaeva I V, Radchenko EA & Mironova LN (2008) [Overexpression of gene PPZ1 in the yeast Saccharomyces cerevisiae affects the efficiency of nonsense suppression]. *Genetika* **44:** 177–84

Ivanov MS, Radchenko EA & Mironova LN (2010) [The protein complex Ppz1p/Hal3p and nonsense suppression efficiency in the yeast Saccharomyces cerevisiae]. *Mol. Biol. (Mosk).* **44:** 1018–26

Jackson RJ, Hellen CUT & Pestova T V (2010) The mechanism of eukaryotic translation initiation and principles of its regulation. *Nat. Rev. Mol. Cell Biol.* **11:** 113–127

Janke C, Magiera MM, Rathfelder N, Taxis C, Reber S, Maekawa H, Moreno-Borchart A, Doenges G, Schwob E, Schiebel E & Knop M (2004) A versatile toolbox for PCR-based tagging of yeast genes: new fluorescent proteins, more markers and promoter substitution cassettes. *Yeast* **21:** 947–962

Jenner L, Melnikov S, de Loubresse NG, Ben-Shem A, Iskakova M, Urzhumtsev A, Meskauskas A, Dinman J, Yusupova G & Yusupov M (2012) Crystal structure of the 80S yeast ribosome. *Curr. Opin. Struct. Biol.* **22:** 759–767

Jimenez A & Davies J (1980) Expression of a transposable antibiotic resistance element in Saccharomyces. *Nature* **287:** 869–871

Johnson DR, Cok SJ, Feldmann H & Gordon JI (1994) Suppressors of nmtl-181, a conditional

lethal allele of the Saccharomyces cerevisiae myristoyl-CoA:protein N-myristoyltransferase gene, reveal proteins involved in regulating protein N-myristoylation. *Proc. Natl. Acad. Sci. U. S. A.* **91:** 10158–62

Johnson SA & Hunter T (2004) Kinomics: methods for deciphering the kinome. *Nat. Methods* **2:** 17

Jørgensen TJD, Jensen ON, Larsen MR, Thingholm TE & Roepstorff P (2005) Highly Selective Enrichment of Phosphorylated Peptides from Peptide Mixtures Using Titanium Dioxide Microcolumns. *Mol. Cell. Proteomics* **4:** 873–886

Kimura Y, Irie K & Mizuno T (2017) Expression control of the AMPK regulatory subunit and its functional significance in yeast ER stress response. *Sci. Rep.* **7:** 46713

Kinclova-Zimmermannova O, Gaskova D & Sychrova H (2006) The Na+,K+/H+-antiporter Nha1 influences the plasma membrane potential of Saccharomyces cerevisiae. *FEMS Yeast Res.* **6:** 792–800

Klis FM, Boorsma A & De Groot PWJ (2006) Cell wall construction in Saccharomyces cerevisiae. *Yeast* **23:** 185–202

Ko CH, Buckley AM & Gaber RF (1990) TRK2 is required for low affinity K+ transport in Saccharomyces cerevisiae. *Genetics* **125:** 305–312

Ko CH & Gaber RF (1991) TRK1 and TRK2 encode structurally related K+ transporters in Saccharomyces cerevisiae. *Mol. Cell. Biol.* **11:** 4266–4273

Kozubowski L, Panek H, Rosenthal A, Bloecher A, DeMarini DJ, Tatchell K & Stearns T (2002) A Bni4-Glc7 Phosphatase Complex That Recruits Chitin Synthase to the Site of Bud Emergence. *Mol. Biol. Cell* **14:** 26–39

Kress TL, Krogan NJ & Guthrie C (2008) A Single SR-like Protein, Npl3, Promotes Pre-mRNA Splicing in Budding Yeast. *Mol. Cell* **32:** 727–734

Krügel H, Fiedler G, Haupt I, Sarfert E & Simon H (1988) Analysis of the nourseothricin-resistance gene (nat) of Streptomyces noursei. *Gene* **62:** 209–217

Laemmli UK (1970) Cleavage of structural proteins during the assembly of the head of bacteriophage T4. *Nature* **227:** 680–685

Lammers T & Lavi S (2007) Role of Type 2C Protein Phosphatases in Growth Regulation and in Cellular Stress Signaling. *Crit. Rev. Biochem. Mol. Biol.* **42:** 437–461

Lee KS, Hines LK & Levin DE (1993) A pair of functionally redundant yeast genes (PPZ1 and PPZ2) encoding type 1-related protein phosphatases function within the PKC1-mediated pathway. *Mol. Cell. Biol.* **13:** 5843–53

Leiter É, González A, Erdei É, Casado C, Kovács L, ádám C, Oláh J, Miskei M, Molnar M, Farkas I, Hamari Z, Ariño J, Pócsi I & Dombrádi V (2012) Protein phosphatase Z modulates oxidative stress response in fungi. *Fungal Genet. Biol.* **49:** 708–716

Leitner A, Faini M, Stengel F & Aebersold R (2016) Crosslinking and Mass Spectrometry: An Integrated Technology to Understand the Structure and Function of Molecular Machines. *Trends Biochem. Sci.* **41:** 20–32

Leitner A, Walzthoeni T, Kahraman A, Herzog F, Rinner O, Beck M & Aebersold R (2010) Probing Native Protein Structures by Chemical Cross-linking, Mass Spectrometry, and Bioinformatics. *Mol. & Cell. Proteomics* **9:** 1634 LP – 1649

Levin DE (2005) Cell wall integrity signaling in Saccharomyces cerevisiae. *Microbiol. Mol. Biol. Rev.* **69:** 262–291

Li B, Nierras CR & Warner JR (1999) Transcriptional Elements Involved in the Repression of Ribosomal Protein Synthesis. *Mol. Cell. Biol.* **19:** 5393 LP – 5404

Liu H, Krizek J & Bretscher A (1992) Construction of a GAL1-regulated yeast cDNA expression library and its application to the identification of genes whose overexpression causes lethality in yeast. *Genetics* **132:** 665–673

Liu H & Naismith JH (2008) An efficient one-step site-directed deletion, insertion, single and multiple-site plasmid mutagenesis protocol. *BMC Biotechnol.* **8:** 91

Loewith R & Hall MN (2011) Target of rapamycin (TOR) in nutrient signaling and growth control. *Genetics* **189:** 1177–1201

Lund MK, Kress TL & Guthrie C (2008) Autoregulation of Npl3, a Yeast SR Protein, Requires a Novel Downstream Region and Serine Phosphorylation. *Mol. Cell. Biol.* **28:** 3873–3881

Madrid AS, Mancuso J, Cande WZ & Weis K (2006) The role of the integral membrane nucleoporins Ndc1p and Pom152p in nuclear pore complex assembly and function. *J. Cell Biol.* **173:** 361–71

Makanae K, Kintaka R, Makino T, Kitano H & Moriya H (2013) Identification of dosage-sensitive genes in Saccharomyces cerevisiae using the genetic tug-of-war method. *Genome Res.* **23:** 300–311

Manning G, Plowman GD, Hunter T & Sudarsanam S (2002) Evolution of protein kinase signaling from yeast to man. *Trends Biochem. Sci.* **27:** 514–520

Márquez JA & Serrano R (1996) Multiple transduction pathways regulate the sodium-extrusion gene PMR2/ENA1 during salt stress in yeast. *FEBS Lett.* **382:** 89–92

Marquina M, González A, Barreto L, Gelis S, Muñoz I, Ruiz A, Álvarez MC, Ramos J & Ariño J (2012a) Modulation of Yeast Alkaline Cation Tolerance by Ypi1 Requires Calcineurin. *Genetics* **190:** 1355–1364

Marquina M, Queralt E, Casamayor A & Ariño J (2012b) Lack of the Glc7 phosphatase regulatory subunit Ypi1 activates the morphogenetic checkpoint. *Int. J. Biochem. Cell Biol.* **44:** 1862–1871

Martinez R, Latreille M-T & Mirande M (1991) APMR2 tandem repeat with a modified C-terminus is located downstream from theKRS1 gene encoding lysyl-tRNA synthetase inSaccharomyces cerevisiae. *Mol. Gen. Genet. MGG* **227:** 149

Maziarz M, Shevade A, Barrett L & Kuchin S (2016) Springing into Action: Reg2 Negatively Regulates Snf1 Protein Kinase and Facilitates Recovery from Prolonged Glucose Starvation in Saccharomyces cerevisiae . *Appl. Environ. Microbiol.* **82:** 3875–3885

Mendoza I, Quintero FJ, Bressan RA, Hasegawa PM & Pardo JM (1996) Activated calcineurin confers high tolerance to ion stress and alters the budding pattern and cell morphology of yeast cells. *J. Biol. Chem.* **271:** 23061–23067

Mendoza I, Rubio F, Rodriguez-Navarro A & Pardo JM (1994) The protein phosphatase calcineurin is essential for NaCl tolerance of Saccharomyces cerevisiae. *J.Biol.Chem.* **269:** 8792–8796

Merchan S, Bernal D, Serrano R & Yenush L (2004) Response of the Saccharomyces cerevisiae

Mpk1 Mitogen-Activated Protein Kinase Pathway to Increases in Internal Turgor Pressure Caused by Loss of Ppz Protein Phosphatases. *Eukaryot. Cell* **3:** 100–107

Meyuhas O (2008) Chapter 1 Physiological Roles of Ribosomal Protein S6: One of Its Kind. In *International Review of Cell and Molecular Biology* pp 1–37. Academic Press

Milgrom E, Diab H, Middleton F & Kane PM (2007) Loss of Vacuolar Proton-translocating ATPase Activity in Yeast Results in Chronic Oxidative Stress. *J. Biol. Chem.* **282:** 7125–7136

Minhas A, Sharma A, Kaur H, Fnu Y, Ganesan K & Mondal AK (2012) A conserved Ser/Arg rich motif in PPZ orthologs from fungi is important for its role in cation tolerance. *J. Biol. Chem.* **287:** 7301–7312

Molero C, Casado C & Ariño J (2017) The inhibitory mechanism of Hal3 on the yeast Ppz1 phosphatase: A mutagenesis analysis. *Sci. Rep.* **7:**

Molero C, Petrényi K, González A, Carmona M, Gelis S, Abrie JA, Strauss E, Ramos J, Dombradi V, Hidalgo E & Ariño J (2013) The Schizosaccharomyces pombe fusion gene hal3 encodes three distinct activities. *Mol. Microbiol.* **90:** 367–382

Moorhead GBG, De Wever V, Templeton G & Kerk D (2009) Evolution of protein phosphatases in plants and animals. *Biochem. J.* **417:** 401 LP – 409

Moorhead GBG, Trinkle-Mulcahy L & Ulke-Lemée A (2007) Emerging roles of nuclear protein phosphatases. *Nat. Rev. Mol. Cell Biol.* **8:** 234

Morales ES, Parcerisa IL & Ceccarelli EA (2019) A novel method for removing contaminant Hsp70 molecular chaperones from recombinant proteins. *Protein Sci.* **28:** 800–807

Moritz M, Paulovich AG, Tsay YF & Woolford JL (1990) Depletion of yeast ribosomal proteins L16 or rp59 disrupts ribosome assembly. *J. Cell Biol.* **111:** 2261 LP – 2274

Morrison DK, Murakami MS & Cleghon V (2000) Protein kinases and phosphatases in the Drosophila genome. *J. Cell Biol.* **150:** F57 LP-F62

Munoz I, Ruiz A, Marquina M, Barcelo A, Albert A & Arino J (2004) Functional characterization of the yeast Ppz1 phosphatase inhibitory subunit Hal3: a mutagenesis study. *J.Biol.Chem.* **279:** 42619–42627

Muñoz I, Simón E, Casals N, Clotet J & Ariño J (2003) Identification of multicopy suppressors of cell cycle arrest at the G1 - S transition in Saccharomyces cerevisiae. *Yeast* **20:** 157–169

de Nadal E, Clotet J, Posas F, Serrano R, Gomez N & Ariño J (1998) The yeast halotolerance determinant Hal3p is an inhibitory subunit of the Ppz1p Ser/Thr protein phosphatase. *Proc. Natl. Acad. Sci. U. S. A.* **95:** 7357–62

De Nadal E, Clotet J, Posas F, Serrano R, Gomez N & Ariño J (1998) The yeast halotolerance determinant Hal3p is an inhibitory subunit of the Ppz1p Ser/Thr protein phosphatase. *Proc. Natl. Acad. Sci. U. S. A.* **95:** 7357

De Nadal E, Fadden RPP, Ruiz A, Haystead T, Ariño J & Arino J (2001) A role for the Ppz Ser/Thr protein phosphatases in the regulation of translation elongation factor 1Balpha. *J.Biol.Chem.* **276:** 14829–14834

Nakamura TS, Numajiri Y, Okumura Y, Hidaka J, Tanaka T, Inoue I, Suda Y, Takahashi T, Nakanishi H, Gao X-D, Neiman AM, Tachikawa H & Brennwald PJ (2017) Dynamic localization of a yeast development–specific PP1 complex during prospore membrane

formation is dependent on multiple localization signals and complex formation. *Mol. Biol. Cell* **28:** 3881–3895

Oeffinger M, Lueng A, Lamond A & Tollervey D (2002) Yeast Pescadillo is required for multiple activities during 60s ribosomal subunit synthesis. *Rna* **8:** 626–636

Offley SR & Schmidt MC (2018) Protein phosphatases of Saccharomyces cerevisiae. *Curr. Genet.*

Offley SR & Schmidt MC (2019) Protein phosphatases of Saccharomyces cerevisiae. *Curr. Genet.* **65:** 41–55

Ohkura H, Kinoshita N, Miyatani S, Toda T & Yanagida M (1989) The fission yeast dis2+ gene required for chromosome disjoining encodes one of two putative type 1 protein phosphatases. *Cell* **57:** 997–1007

Olsen J V., Blagoev B, Gnad F, Macek B, Kumar C, Mortensen P & Mann M (2006) Global, In Vivo, and Site-Specific Phosphorylation Dynamics in Signaling Networks. *Cell* **127:** 635–648

Orii M, Kono K, Wen H-I & Nakanishi M (2016) PP1-Dependent Formin Bnr1 Dephosphorylation and Delocalization from a Cell Division Site. *PLoS One* **11:** e0146941

Palmer BR & Marinus MG (1994) The dam and dcm strains of Escherichia coli--a review. *Gene* **143:** 1–12

Pedelini L, Marquina Rodríguez M, Ariño J, Casamayor A, Sanz L, Bollen M, Sanz P & García-Gimeno A (2007) YPI1 and SDS22 Proteins Regulate the Nuclear Localization and Function of Yeast Type 1 Phosphatase Glc7

Petrényi K, Molero C, Kónya Z, Erdődi F, Ariño J & Dombrádi V (2016) Analysis of Two Putative Candida albicans Phosphopantothenoylcysteine Decarboxylase / Protein Phosphatase Z Regulatory Subunits Reveals an Unexpected Distribution of Functional Roles. *PLoS One* **11:** e0160965

Phizicky EM & Fields S (1995) Protein-protein interactions: methods for detection and analysis. *Microbiol. Rev.* **59:** 94–123

Posas F, Bollen M, Stalmans W & Arino J (1995a) Biochemical characterization of recombinant yeast PPZ1, a protein phosphatase involved in salt tolerance. *FEBS Lett* **368:** 39–44

Posas F, Camps M & Arino J (1995b) The PPZ protein phosphatases are important determinants of salt tolerance in yeast cells. *J. Biol. Chem.* **270:** 13036–13041

Posas F, Casamayor A & Ariño J (1993) The PPZ protein phosphatases are involved in the maintenance of osmotic stability of yeast cells. *FEBS Lett.* **318:** 282–286

Posas F, Casamayor A, Morral N & Ariño J (1992) Molecular cloning and analysis of a yeast protein phosphatase with an unusual amino-terminal region. *J. Biol. Chem.* **267:** 11734–11740

Prior C, Potier S, Souciet J-L & Sychrova H (1996) Characterization of the NHA1 gene encoding a Na+/H+-antiporter of the yeast Saccharomyces cerevisiae. *FEBS Lett.* **387:** 89–93

Rajyaguru P, She M & Parker R (2012) Scd6 Targets eIF4G to Repress Translation: RGG Motif Proteins as a Class of eIF4G-Binding Proteins. *Mol. Cell* **45:** 244–254

Ramos J, Ariño J & Sychrová H (2011) Alkali-metal-cation influx and efflux systems in nonconventional yeast species. *FEMS Microbiol. Lett.* **317:** 1–8

Rodríguez-Navarro A, Quintero FJ & Garciadeblás B (1994) Na+-ATPases and Na+/H+ antiporters in fungi. *Biochim. Biophys. Acta - Bioenerg.* **1187:** 203–205 A

Rodríguez-Navarro A & Ramos J (1984) Dual system for potassium transport in Saccharomyces cerevisiae. *J. Bacteriol.* **159:** 940–9457

Rojas M, Gingras A-C & Dever TE (2014) Protein phosphatase PP1/GLC7 interaction domain in yeast eIF2γ bypasses targeting subunit requirement for eIF2α dephosphorylation. *Proc. Natl. Acad. Sci.* **111:** E1344–E1353

Romanov N, Hollenstein DM, Janschitz M, Ammerer G, Anrather D & Reiter W (2017) Identifying protein kinase–specific effectors of the osmostress response in yeast. *Sci. Signal.* **10:** eaag2435

Rubenstein EM, McCartney RR, Zhang C, Shokat KM, Shirra MK, Arndt KM & Schmidt MC (2008) Access Denied: Snf1 Activation Loop Phosphorylation Is Controlled by Availability of the Phosphorylated Threonine 210 to the PP1 Phosphatase. *J. Biol. Chem.* **283:** 222–230

Ruiz A, Gonzalez A, Munoz I, Serrano R, Abrie JA, Strauss E & Arino J (2009) Moonlighting proteins Hal3 and Vhs3 form a heteromeric PPCDC with Ykl088w in yeast CoA biosynthesis. *Nat. Chem. Biol.* **5:** 920–928

Ruiz A, Muñoz I, Serrano R, Gonzalez A, Simon E & Arino J (2004a) Functional characterization of the Saccharomyces cerevisiae VHS3 gene: a regulatory subunit of the Ppz1 protein phosphatase with novel, phosphatase-unrelated functions. *J. Biol. Chem.* **279:** 34421–34430

Ruiz A, Ruiz MC, Sanchez-Garrido MA, Arino J & Ramos J (2004b) The Ppz protein phosphatases regulate Trk-independent potassium influx in yeast. *FEBS Lett.* **578:** 58–62

Ruiz A, Xu X & Carlson M (2011) Roles of two protein phosphatases, Reg1-Glc7 and Sit4, and glycogen synthesis in regulation of SNF1 protein kinase. *Proc. Natl. Acad. Sci. U.S.A* **108:** 6349–6354

Ruiz A, Xu X & Carlson M (2013) Ptc1 Protein Phosphatase 2C Contributes to Glucose Regulation of SNF1/AMP-activated Protein Kinase (AMPK) in Saccharomyces cerevisiae . *J. Biol. Chem.* **288:** 31052–31058

Ruiz A, Yenush L & Ariño J (2003) Regulation of ENA1 Na+-ATPase gene expression by the Ppz1 protein phosphatase is mediated by the calcineurin pathway. *Eukaryot. Cell* **2:** 937–948

Russell ID & Tollervey D (1992) NOP3 is an essential yeast protein which is required for pre-rRNA processing. *J. Cell Biol.* **119:** 737 LP – 747

Sadowski I, Breitkreutz BJ, Stark C, Su TC, Dahabieh M, Raithatha S, Bernhard W, Oughtred R, Dolinski K, Barreto K & Tyers M (2013) The PhosphoGRID Saccharomyces cerevisiae protein phosphorylation site database: Version 2.0 update. *Database* **2013:** bat026–bat026

Sambrook J, Fritsch EF & Maniatis T (1989) Molecular cloning: a laboratory manual. Cold Spring Harbor, NY: Cold Spring Harbor Laboratory Press

Santolaria C, Velázquez D, Strauss E & Ariño J (2018a) Mutations at the hydrophobic core affect Hal3 trimer stability, reducing its Ppz1 inhibitory capacity but not its PPCDC moonlighting function. *Sci. Rep.* **8:** 14701

Sanz P, Alms GR, Haystead TAJ & Carlson M (2000) Regulatory Interactions between the Reg1-

Glc7 Protein Phosphatase and the Snf1 Protein Kinase. *Mol. Cell. Biol.* **20:** 1321–1328

Serrano R (1996) Salt tolerance in plants and microorganisms: Toxicity targets and defense responses. *Int. Rev. Cytol.* **165:** 1–52

Shashkova S, Wollman AJM, Leake MC & Hohmann S (2017) The yeast Mig1 transcriptional repressor is dephosphorylated by glucose-dependent and -independent mechanisms. *FEMS Microbiol. Lett.* **364:** fnx133–fnx133

Shi Y (2009a) Assembly and structure of protein phosphatase 2A. *Sci. China Ser. C Life Sci.* **52:** 135–146

Shi Y (2009b) Serine/Threonine Phosphatases: Mechanism through Structure. *Cell* **139:** 468–484

Sikorski RS & Hieter P (1989) A system of shuttle vectors and yeast host strains designed for efficient manipulation of DNA in Saccharomyces cerevisiae. *Genetics* **122:** 19–27

Simon E, Clotet J, Calero F, Ramos J & Arino J (2001) A screening for high copy suppressors of the sit4 hal3 synthetically lethal phenotype reveals a role for the yeast Nha1 antiporter in cell cycle regulation. *J. Biol. Chem.* **276:** 29740–29747

Simpson CE & Ashe MP (2012) Adaptation to stress in yeast: to translate or not? *Biochem. Soc. Trans.* **40:** 794 LP – 799

Sonenberg N & Hinnebusch AG (2009) Regulation of Translation Initiation in Eukaryotes: Mechanisms and Biological Targets. *Cell* **136:** 731–745

Stark MJR (1996) Yeast protein serine/threonine phosphatases: Multiple roles and diverse regulation. *Yeast* **12:** 1647–1675

Sutton A, Immanuel D & Arndt KT (1991) The SIT4 protein phosphatase functions in late G1 for progression into S phase. *Mol.Cell Biol.* **11:** 2133–2148

Swaney DL, Beltrao P, Starita L, Guo A, Rush J, Fields S, Krogan NJ & Villén J (2013) Global analysis of phosphorylation and ubiquitylation cross-talk in protein degradation. *Nat. Methods* **10:** 676–682

Szabó K, Kónya Z, Erdődi F, Farkas I & Dombrádi V (2019) Dissection of the regulatory role for the N-terminal domain in Candida albicans protein phosphatase Z1. *PLoS One* **14:** e0211426

Szöőr B, Fehér Z, Zeke T, Gergely P, Yatzkan E, Yarden O & Dombrádi V (1998) pzl-1 encodes a novel protein phosphatase-Z-like Ser/Thr protein phosphatase in Neurospora crassa1 The DNA sequences reported in this publication have been deposited in the EMBL database and have been given the accession numbers AF071751 and AF071752.1. *Biochim. Biophys. Acta - Protein Struct. Mol. Enzymol.* **1388:** 260–266

Tartof K & Hobbs C (1987) Improved media for growing plasmid and cosmid clones. *Focus (Madison).* **9:** 11

Terrak M, Kerff F, Langsetmo K, Tao T & Dominguez R (2004) Structural basis of protein phosphatase 1 regulation. *Nature* **429:** 780

Thingholm TE, Jensen ON, Robinson PJ & Larsen MR (2007) SIMAC (Sequential Elution from IMAC), a Phosphoproteomics Strategy for the Rapid Separation of Monophosphorylated from Multiply Phosphorylated Peptides. *Mol. Cell. Proteomics* **7:** 661–671

Tomek W & Wollenhaupt K (2012) The “closed loop model” in controlling mRNA translation

during development. *Anim. Reprod. Sci.* **134:** 2–8

Treitel MA, Kuchin S & Carlson M (1998) Snf1 protein kinase regulates phosphorylation of the Mig1 repressor in Saccharomyces cerevisiae. *Mol. Cell. Biol.* **18:** 6273–6280

Tsien RY (1998) the Green Fluorescent Protein. *Annu. Rev. Biochem.* **67:** 509–544

Tyanova S, Temu T, Carlson A, Sinitcyn P, Mann M & Cox J (2015) Visualization of LC-MS/MS proteomics data in MaxQuant. *Proteomics* **15:** 1453–1456

Tyanova S, Temu T & Cox J (2016a) The MaxQuant computational platform for mass spectrometry-based shotgun proteomics. *Nat. Protoc.* **11:** 2301–2319

Tyanova S, Temu T, Sinitcyn P, Carlson A, Hein MY, Geiger T, Mann M & Cox J (2016b) The Perseus computational platform for comprehensive analysis of (prote)omics data. *Nat. Methods* **13:** 731–740

Tyson JJ, Csikasz-Nagy A & Novak B (2002) The dynamics of cell cycle regulation. *BioEssays* **24:** 1095–1109

Ubersax JA, Woodbury EL, Quang PN, Paraz M, Blethrow JD, Shah K, Shokat KM & Morgan DO (2003) Targets of the cyclin-dependent kinase Cdk1. *Nature* **425:** 859–864

Vasicek EM, Berkow EL, Bruno VM, Mitchell AP, Wiederhold NP, Barker KS & Rogers PD (2014) Disruption of the Transcriptional Regulator Cas5 Results in Enhanced Killing of Candida albicans by Fluconazole. *Antimicrob. Agents Chemother.* **58:** 6807–6818

Venema J & Tollervey D (1999) Ribosome Synthesis in Saccharomyces cerevisiae. *Annu. Rev. Genet.* **33:** 261–311

Venturi GM, Bloecher A, Williams-Hart T & Tatchell K (2000) Genetic interactions between GLC7, PPZ1 and PPZ2 in Saccharomyces cerevisiae. *Genetics* **155:** 69–83

Vissi E, Clotet J, de Nadal E, Barcelo A, Bako E, Gergely P, Dombradi V & Arino J (2001) Functional analysis of the Neurospora crassa PZL-I protein phosphatase by expression in budding and fission yeast. *Yeast* **18:** 115–124

De Vit MJ, Waddle JA & Johnston M (1997) Regulated nuclear translocation of the Mig1 glucose repressor. *Mol. Biol. Cell* **8:** 1603–1618

Wagner M V, Smolka MB, de Bruin RAM, Zhou H, Wittenberg C & Dowdy SF (2009) Whi5 Regulation by Site Specific CDK-Phosphorylation in Saccharomyces cerevisiae. *PLoS One* **4:** e4300

Wakula P, Beullens M, Ceulemans H, Stalmans W & Bollen M (2003) Degeneracy and function of the ubiquitous RVXF motif that mediates binding to protein phosphatase-1. *J.Biol.Chem.* **278:** 18817–18823

Warmka J, Hanneman J, Lee J, Amin D & Ota I (2001) Ptc1, a type 2C Ser/Thr phosphatase, inactivates the HOG pathway by dephosphorylating the mitogen-activated protein kinase Hog1. *Mol. Cell. Biol.* **21:** 51–60

Wieland J, Nitsche AM, Strayle J, Steiner H & Rudolph HK (1995) The PMR2 gene cluster encodes functionally distinct isoforms of a putative Na+ pump in the yeast plasma membrane. *EMBO J.* **14:** 3870–3882

Williams-Hart T, Wu X & Tatchell K (2002) Protein phosphatase type 1 regulates ion homeostasis in Saccharomyces cerevisiae. *Genetics* **160:** 1423–1437

Windgassen M, Sturm D, Cajigas IJ, González CI, Seedorf M, Bastians H & Krebber H (2004) Yeast Shuttling SR Proteins Npl3p, Gbp2p, and Hrb1p Are Part of the Translating mRNPs, and Npl3p Can Function as a Translational Repressor. *Mol. Cell. Biol.* **24:** 10479–10491

Wu X & Tatchell K (2001) Mutations in Yeast Protein Phosphatase Type 1 that Affect Targeting Subunit Binding. *Biochemistry* **40:** 7410–7420

Yenush L, Merchan S, Holmes J & Serrano R (2005) pH-Responsive, posttranslational regulation of the Trk1 potassium transporter by the type 1-related Ppz1 phosphatase. *Mol. Cell. Biol.* **25:** 8683–92

Yenush L, Mulet JM, Ariño J & Serrano R (2002) The Ppz protein phosphatases are key regulators of $K^+$ and pH homeostasis: implications for salt tolerance, cell wall integrity and cell cycle progression. *EMBO J* **21:** 920–929

Yerlikaya S, Meusburger M, Kumari R, Huber A, Anrather D, Costanzo M, Boone C, Ammerer G, Baranov P V & Loewith R (2016) TORC1 and TORC2 work together to regulate ribosomal protein S6 phosphorylation in Saccharomyces cerevisiae. *Mol. Biol. Cell* **27:** 397–409

Yonemoto W, L McGlone M & S Taylor S (1993) N-Myristylation of the catalytic subunit of cAMP-dependent protein kinase conveys structural stability

Yu C & Huang L (2018) Cross-Linking Mass Spectrometry: An Emerging Technology for Interactomics and Structural Biology. *Anal. Chem.* **90:** 144–165

Zaborske JM, Narasimhan J, Jiang L, Wek SA, Dittmar KA, Freimoser F, Pan T & Wek RC (2009) Genome-wide analysis of tRNA charging and activation of the eIF2 kinase Gcn2p. *J. Biol. Chem.* **284:** 25254–25267

Zhang C (2019) The Ppz1 protein phosphatase as a potential antifungal target.

Zhang Y, McCartney RR, Chandrashekarappa DG, Mangat S & Schmidt MC (2011) Reg1 Protein Regulates Phosphorylation of All Three Snf1 Isoforms but Preferentially Associates with the Gal83 Isoform. *Eukaryot. Cell* **10:** 1628–1636

Zhao Y, Sohn J-H & Warner JR (2003) Autoregulation in the Biosynthesis of Ribosomes. *Mol. Cell. Biol.* **23:** 699 LP – 707

Zhu H, Bilgin M, Bangham R, Hall D, Bertone P, Lan N, Jansen R, Houfek T, Mitchell T, Miller P, Ralph A, Gerstein M, Snyder M, Casamayor A, Bidlingmaier S & Dean RA (2008) Global Analysis of Protein Activities Using Proteome Chips -- Zhu et al ... *Science (80-. ).* **2101:** 8–10

# ANNEXES

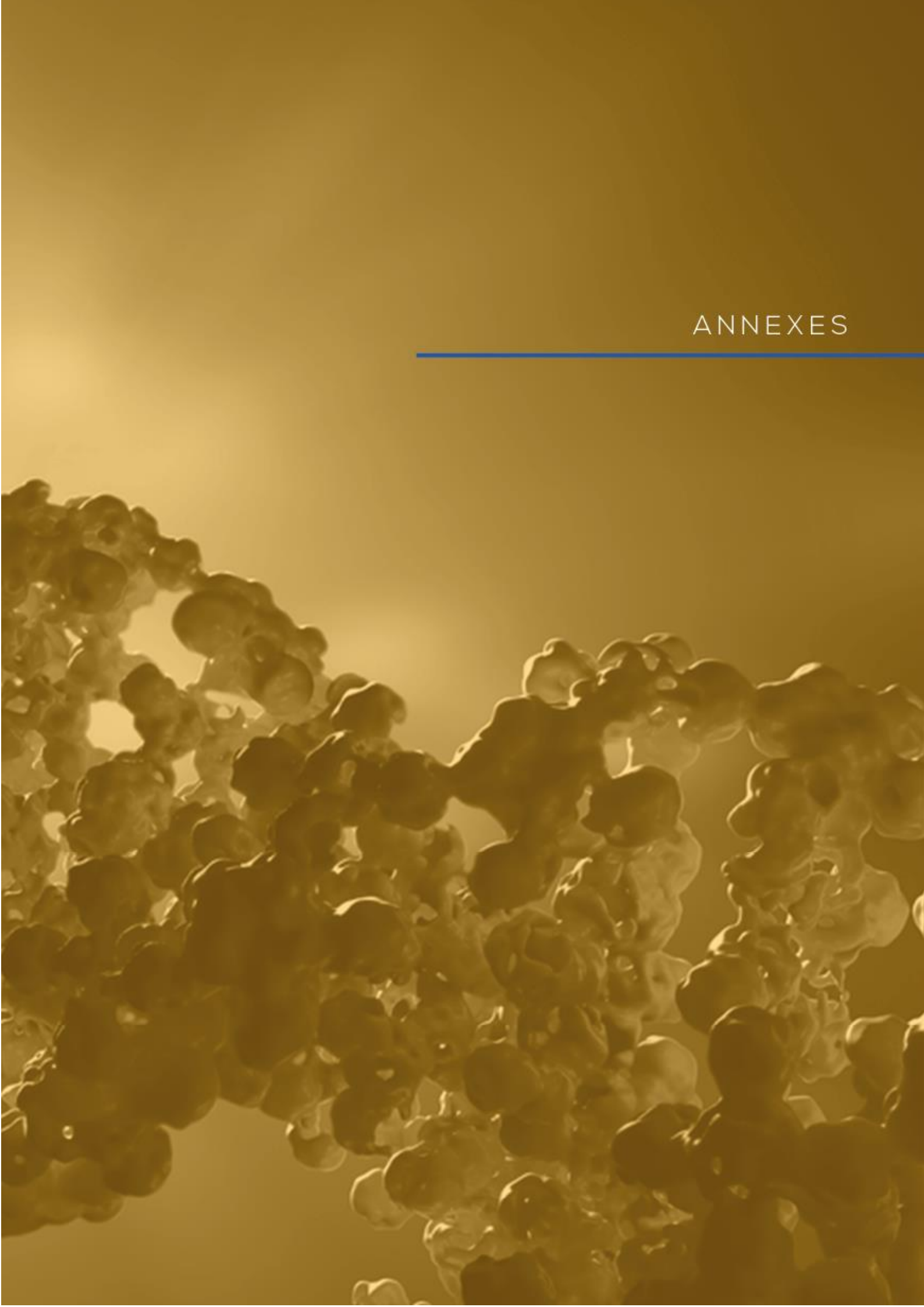

# Annex 1:

## Strains used in this work

| Strain | Genotype | Source of reference |
|---|---|---|
| **DBY746** | *MATα his3-1 leu2-3,112 trp1-289 ura3-52* | D. Botstein |
| **RSC52** | DBY746 *ppz1::LEU2* | Raquel Serrano |
| **EDN4** | DBY746 *hal3::LEU2* | (De Nadal *et al*, 1998) |
| **DVS001** | DBY746 *PPZ1-EGFP-HIS3MX6* | This work |
| **DVS002** | DBY746 *PPZ1-CFP-HIS3MX6* | This work |
| **DVS003** | DBY746 *PPZ1-YFP-kanMX4* | This work |
| **DVS004** | DBY746 *HAL3-EGFP-HIS3MX6* | This work |
| **DVS005** | DBY746 *HAL3-CFP-HIS3MX6* | This work |
| **DVS006** | DBY746 *HAL3-YFP-kanMX4* | This work |
| **DVS007** | DBY746 *PPZ1-mCherry-kanMX4* | This work |
| **DVS008** | DBY746 *HAL3-mCherry-kanMX4* | This work |
| **DVS009** | DBY746 *PPZ1-EGFP-HIS3MX6 HAL3-mCherry-kanMX4* | This work |
| **DVS010** | DBY746 *PPZ1-mCherry-kanMX4 HAL3-EGFP-HIS3MX6* | This work |
| **DVS011** | DBY746 *PPZ1-YFP-kanMX4 HAL3-CFP-HIS3MX6* | This work |
| **DVS012** | DBY746 *PPZ1-CFP-HIS3MX6 HAL3-YFP-kanMX4* | This work |
| **DVS013** | DBY746 *NAT1-pGAL-GFP-PPZ1* | This work |
| **DVS014** | DBY746 *NAT1-pGAL-GFP-HAL3* | This work |
| **BY4741** | *MATa his3Δ1 leu2Δ0 met15Δ0 ura3Δ0* | (Brachmann *et al*, 1998) |
| ***ppz1Δ*** | BY4741 *ppz1::KanMX4* | Eursocarf |
| ***hal3Δ*** | BY4741 *hal3::KanMX4* | Euroscarf |
| **AGS19** | BY4741 *ppz1::KAN ppz2::HIS3* | (Leiter *et al*, 2012) |
| **DVS015** | BY4741 *PPZ1-YFP-kanMX4* | This work |
| **DVS016** | BY4741 *HAL3-YFP-kanMX4* | This work |
| **DVS017** | BY4741 *PPZ1-CFP-HIS3MX6* | This work |
| **DVS018** | BY4741 *HAL3-CFP-HIS3MX6* | This work |
| **DVS019** | BY4741 *PPZ1-YFP-kanMX4 HAL3-CFP-HIS3MX6* | This work |
| **DVS020** | BY4741 *PPZ1-CFP-HIS3MX6 HAL3-YFP-kanMX4* | This work |
| **MLM04** | BY4741 *promoter ppz1::tetOFF7 promoter::kanMX4* | María López Malo |
| **ZCZ01** | BY4741 *promoter ppz1::pGAL:: kanMX6* | (Zhang, 2019) |
| **RF1668** | W303-1A *VHS2-6HA::KanMX* | (Cassani *et al*, 2014) |

# Annex 2:

## Primers used in this work

| Primer Name | Sequence |
|---|---|
| **3-Hal3-S47D** | TTGCCTCCCTGACACGGGATCGTTGATTATTGAATCCTTC |
| **3-Hal3-S50D** | GCTTATTGATTGCCTCCCATCCACGGGGGAGTTGATTATTG |
| **3-Hal3-S54+56D** | GCATTCGACAAAGTAGGATCTATATCTTGCCTCCCTGACACGG |
| **3-Hal3-S56D** | GCATTCGACAAAGTAGGATCTATTGATTGCCTCCCTGACACGG |
| **3-Hal3-S60D** | GTCGTGGTAGTAGCATTATCCAAAGTAGGGCTTATTGATT |
| **5-Hal3-S47D** | GAAGGATTCAATAATCAACGATCCCGTGTCAGGGAGGCAA |
| **5-Hal3-S50D** | CAATAATCAACTCCCCCGTGGATGGGAGGCAATCAATAAGC |
| **5-Hal3-S54+56D** | CCGTGTCAGGGAGGCAAGATATAGATCCTACTTTGTCGAATGC |
| **5-Hal3-S54D** | CCCCGTGTCAGGGAGGCAAGATATAAGCCCTACTTTGTCG |
| **5-Hal3-S54D** | CGACAAAGTAGGGCTTATATCTTGCCTCCCTGACACGGGG |
| **5-Hal3-S56D** | CCGTGTCAGGGAGGCAATCAATAGATCCTACTTTGTCGAATGC |
| **5-Hal3-S60D** | AATCAATAAGCCCTACTTTGGATAATGCTACTACCACGAC |
| **Ppz1Fluo_Fw** | CAAATGATGGAAACAAGCATCACAAATGATAACGAATCTCAACAGCTTCGTACGCTGCAGGTCGA |
| **Ppz1Fluo_Rev** | ATGAAATAATGAATATAATACTTCTGGATTTTTTAGTCAGTAAATCACTATAGGGAGACCGGCAG |
| **Hal3Fluo_Fw** | GACGAGGACGAAGCAGAAACCCCAGGTATAATAGATAAGCATCAACTTCGTACGCTGCAGGTCGA |
| **Hal3Fluo_Rev** | ACAAATAAGTAGAATGTGTTTAGTGTATTTGTAATTCATAGACTACACTATAGGGAGACCGGCAG |
| **Ppz1 S49A Fw** | TCTTCAAGATCAAGGCGAGCTCTTCCTTCTTCGTCCA |
| **Ppz1 S49A Rev** | TGGACGAAGAAGGAAGAGCTCGCCTTGATCTTGAAGA |
| **Ppz1 S49D Fw** | TCTTCAAGATCAAGGCGAGATCTTCCTTCTTCGTCCAC |
| **Ppz1 S49D Rev** | GTGGACGAAGAAGGAAGATCTCGCCTTGATCTTGAAGA |
| **Ppz1_BspEI_3** | TTGTTTCCGGAAGATTGCA |
| **Ppz1_HpaI_5** | GAATTGTTAACTACTCCTTC |
| **Ppz1_S265D 3** | CCTGGATCGTTTAATGGGGTGCTG |
| **Ppz1_S265D 5** | ATTAAACGATCCAGGCTTGTCCAAG |
| **Ppz1_T261A_3** | GTAATACCGCATACAGCGCCCCATT |
| **Ppz1_T261A_5** | CATACAGCGCCCCATTAAACTCTCCAG |
| **Ppz1_T261A_S265A** | CCTGGAGCGTTTAATGGGGCGCTG |
| **Ppz1_T261E 3** | AATGGTTCGCTGTATGCGGTATTAC |
| **Ppz1_T261E 5** | CATACAGCGAACCATTAAACTCTCCAG |
| **Ppz1_T261E_S265D 3** | CCTGGATCGTTTAATGGTTCGCTG |
| **Ppz1_S265A_3** | CCTGGAGCGTTTAATGGGGTGCTG |
| **Ppz1_S265A_5** | ATTAAACGCTCCAGGCTTGTCCAAG |
| **SacI Npl3 term Rev** | AGCGAGCTCTCCTGCCCGTATGTTGAAGA |
| **BamHI Npl3 prom Fw** | AGCGGATCCTCTCAGCTCCGGAACCGGTA |
| **Vhs2 S314A Fw** | ACTTAAACAACAAAGGGCACCTTCAGGGAGCGCCC |
| **Vhs2 S314A Rev** | GGGCGCTCCCTGAAGGTGGCCTTTGTTGTTTAAGT |

| | |
|---|---|
| **Vhs2 S314D Fw** | ACTTAAACAACAAAGGGATCCTTCAGGGAGCGCCC |
| **Vhs2 S314D Rev** | GGGCGCTCCCTGAAGGATCCCTTTGTTGTTTAAGT |
| **KpnI Rev vhs2HA term** | ACCGGTACCGTCAAGACTGTCAAGGAG |
| **SacI Fw vhs2 prom** | ACCGAGCTCGCATGTCACAAGATACTTGA |
| **Sky1_Fw** | ACGCGTCGACCTACCAAATGACCCAGGGA |
| **Sky_Rev** | CGGGATCCATCATCCTTCACCAGGACAA |

# ANNEX 3:

Proteins are listed according to the relative fold change log(2) values, before and after 30, 60, 120 and 240 Ppz1 induction.

| ORF | UniprotID | Gene | Description | | | | | | | | | | | | |
|---|---|---|---|---|---|---|---|---|---|---|---|---|---|---|---|
| | | | | AA | Pos | T0 | T30 | p-30 | T60 | p-60 | T120 | p-120 | T240 | p-240 | Multiplicity |
| **YBL051C** | **P34217** | **PIN4** | Protein involved in G2/M phase progression and response to DNA damage. | | | | | | | | | | | | |
| | | | | S | 191 | 1.13±0.11 | 0.92±0.035 | | 0.38±0.01 | * | 0.25±0.02 | * | 0.27±0.04 | * | 3 |
| | | | | S | 194 | 1.04±0.06 | 0.94±0.09 | | 0.49±0.08 | * | 0.32±0.03 | * | 0.43±0.07 | * | 3 |
| | | | | S | 197 | 1.01±0.07 | 0.99±0.15 | | 0.55±0.09 | * | 0.32±0.05 | * | 0.32±0.04 | * | 3 |
| | | | | S | 199 | 0.93±0.06 | 1.15±0.21 | | 0.65±0.133 | | 0.48±0.0536 | ** | 0.39±0.04 | ** | 2 |
| | | | | S | 653 | 1.69±0.37 | 0.71±0.04 | * | 0.42±0.056 | * | 0.21±0.0366 | ** | 0.34±0.05 | * | 2 |
| | | | | S | 655 | 1.53±0.30 | 0.78±0.04 | | 0.50±0.07 | * | 0.32±0.073 | * | 0.44±0.07 | * | 2 |
| **YBL085W** | **P38041** | **BOI1** | Protein implicated in polar growth; | | | | | | | | | | | | |
| | | | | T | 647 | 0.87±0.11 | 0.92±0.0709 | | 0.84±0.0987 | | 0.77±0.1274 | | 0.36±0.07 | * | 2 |
| | | | | S | 648 | 0.97±0.06 | 0.87±0.026 | | 0.83±0.1041 | | 0.67±0.0726 | * | 0.48±0.12 | * | 2 |
| **YBR023C** | **P29465** | **CHS3** | Chitin synthase III; catalyzes the transfer of N-acetylglucosamine (GlcNAc) to chitin | | | | | | | | | | | | |
| | | | | S | 32 | 0.91±0.05 | 0.77±0.112 | | 0.52±0.0481 | ** | 0.49±0.2136 | | 0.39±0.22 | | 2 |
| **YBR086C** | **P38250** | **IST2** | Cortical ER protein involved in ER-plasma membrane tethering. | | | | | | | | | | | | |
| | | | | S | 867 | 1.02±0.055 | 0.82±0.01 | | 0.3±0.015 | ** | 0.26±0.085 | * | 0.27±0.12 | * | 2 |
| **YBR133C** | **P38274** | **HSL7** | Protein arginine N-methyltransferase | | | | | | | | | | | | |
| | | | | S | 702 | 0.81±0.08 | 0.71±0.025 | | 0.31±0.1 | | 0.18±0 | * | 0.24±0.07 | * | 2 |
| **YBR200W** | **P29366** | **BEM1** | Protein containing SH3-domains; involved in establishing cell polarity and morphogenesis | | | | | | | | | | | | |
| | | | | S | 67 | 0.96±0.11 | 1.1±0.0463 | | 0.95±0.044 | | 0.6±0.1697 | | 0.46±0.10 | * | 2 |
| | | | | S | 72 | 0.99±0.13 | 1.01±0.0643 | | 1.05±0.12 | | 0.65±0.2001 | | 0.42±0.08 | * | 2 |
| **YCL012C** | **Q8J0M4** | **YCL012C** | Protein of unknown function | | | | | | | | | | | | |
| | | | | S | 71 | 1.12±0.11 | 0.79±0.0722 | | 0.69±0.13 | | 0.45±0.08 | ** | 0.54±0.07 | * | 2 |
| | | | | S | 74 | 1.12±0.11 | 0.79±0.0722 | | 0.69±0.13 | | 0.45±0.08 | ** | 0.54±0.07 | * | 2 |
| **YCL014W** | **P25558** | **BUD3** | Guanine nucleotide exchange factor (GEF) for Cdc42p. | | | | | | | | | | | | |
| | | | | S | 1075 | 1.31±0.05 | 0.81±0.05 | * | 0.82±0.28 | | 0.69±0.295 | | 0.49±0.015 | ** | 2 |
| | | | | S | 1085 | 1.31±0.05 | 0.81±0.05 | * | 0.82±0.28 | | 0.69±0.295 | | 0.49±0.015 | ** | 2 |
| | | | | S | 1515 | 1.1±0.09 | 0.87±0.19 | | 0.72±0.27 | | 0.57±0.235 | | 0.44±0.025 | * | 2 |
| | | | | S | 1527 | 1.13±0.1301 | 0.86±0.1323 | | 0.82±0.2146 | | 0.64±0.1889 | | 0.44±0.06 | ** | 2 |
| **YCL024W** | **P25389** | **KCC4** | Protein kinase of the bud neck involved in the septin checkpoint | | | | | | | | | | | | |

| | | | | | | | | | | | | | | | |
|---|---|---|---|---|---|---|---|---|---|---|---|---|---|---|---|
| | | | | S | 892 | 0.94±0.06 | 1±0.09 | | 0.88±0.02 | | 0.45±0.06 | * | 0.43±0.045 | * | 2 |
| | | | | S | 894 | 0.85±0.025 | 1±0.09 | | 0.88±0.02 | | 0.57±0.185 | | 0.38±0.015 | ** | 2 |
| **YCL040W** | **P17709** | **GLK1** | Glucokinase | | | | | | | | | | | | |
| | | | | S | 2 | 0.99±0.0467 | 0.76±0.1519 | | 0.59±0.0982 | * | 0.43±0.0153 | *** | 0.44±0.024 | *** | 1 |
| **YCL051W** | **P25579** | **LRE1** | Protein involved in control of cell wall structure and stress response | | | | | | | | | | | | |
| | | | | S | 33 | 0.94±0.08 | 1.01±0.10 | | 0.61±0.06 | * | 0.53±0.102 | * | 0.32±0.0786 | ** | 2 |
| | | | | S | 37 | 0.94±0.0809 | 1.01±0.1035 | | 0.61±0.0674 | * | 0.53±0.102 | * | 0.32±0.0786 | ** | 2 |
| **YCR065W** | **P25364** | **HCM1** | Forkhead transcription factor | | | | | | | | | | | | |
| | | | | S | 61 | 1.07±0.1916 | 0.75±0.1894 | | 0.63±0.235 | | 0.58±0.2 | | 0.42±0.1004 | * | 2 |
| | | | | T | 447 | 0.98±0.055 | 1.07±0.02 | | 0.77±0.01 | | 0.71±0.11 | | 0.3±0.065 | * | 2 |
| | | | | S | 453 | 1±0.0338 | 1.06±0.0176 | | 0.84±0.0736 | | 0.67±0.0769 | * | 0.33±0.0433 | *** | 2 |
| **YDL022W** | **Q00055** | **GPD1** | NAD-dependent glycerol-3-phosphate dehydrogenase | | | | | | | | | | | | |
| | | | | S | 22 | 0.86±0.08 | 0.75±0.075 | | 0.47±0.035 | * | 1.26±0.435 | | 0.99±0.115 | | 2 |
| | | | | S | 24 | 0.95±0.0801 | 0.96±0.0879 | | 0.46±0.0634 | ** | 0.91±0.121 | | 0.8±0.0552 | | 2 |
| | | | | S | 27 | 0.9±0.0786 | 0.83±0.0549 | | 0.45±0.0404 | ** | 1.02±0.1506 | | 0.89±0.0376 | | 2 |
| **YDL081C** | **P05318** | **RPP1A** | Ribosomal stalk protein P1 alpha | | | | | | | | | | | | |
| | | | | S | 96 | 1.02±0.1756 | 0.37±0.094 | * | 1.61±0.776 | | 0.56±0.2001 | | 0.76±0.1021 | | 1 |
| **YDL161W** | **Q12518** | **ENT1** | Epsin-like protein involved in endocytosis and actin patch assembly | | | | | | | | | | | | |
| | | | | S | 177 | 0.97±0.08 | 0.99±0 | | 0.64±0.06 | | 0.5±0.11 | | 0.36±0.055 | * | 2 |
| | | | | T | 180 | 0.97±0.08 | 0.99±0 | | 0.64±0.06 | | 0.5±0.11 | | 0.36±0.055 | * | 2 |
| **YDL225W** | **Q07657** | **SHS1** | Component of the septin ring that is required for cytokinesis | | | | | | | | | | | | |
| | | | | S | 440 | 1.11±0.07 | 1.14±0.08 | | 0.5±0.015 | * | 0.35±0.01 | ** | 0.28±0.025 | ** | 3 |
| | | | | S | 441 | 1.11±0.07 | 1.14±0.08 | | 0.5±0.015 | * | 0.35±0.01 | ** | 0.28±0.025 | ** | 3 |
| | | | | T | 541 | 1.06±0.025 | 0.92±0.07 | | 0.91±0.025 | | 0.82±0.15 | | 0.41±0.135 | * | 3 |
| **YDR028C** | **Q00816** | **REG1** | Regulatory subunit of type 1 protein phosphatase Glc7p | | | | | | | | | | | | |
| | | | | S | 346 | 1.08±0.0404 | 0.92±0.0784 | | 0.52±0.0666 | ** | 0.45±0.132 | ** | 0.67±0.1337 | * | 2 |
| | | | | S | 349 | 0.98±0.0929 | 0.96±0.0536 | | 0.47±0.041 | ** | 0.43±0.1384 | * | 0.55±0.0808 | * | 2 |
| **YDR087C** | **P35178** | **RRP1** | Essential evolutionarily conserved nucleolar protein | | | | | | | | | | | | |
| | | | | S | 263 | 1.05±0.03 | 1.14±0.0788 | | 1.02±0.0819 | | 0.66±0.047 | ** | 0.44±0.0971 | ** | 2 |
| | | | | S | 267 | 1.05±0.03 | 1.14±0.0788 | | 1.02±0.0819 | | 0.66±0.047 | ** | 0.44±0.0971 | ** | 2 |
| **YDR113C** | **P40316** | **PDS1** | Securin; inhibits anaphase by binding separin Esp1p | | | | | | | | | | | | |
| | | | | S | 185 | 1.5±0.125 | 1.4±0.32 | | 1.09±0.27 | | 0.47±0.1 | * | 0.2±0.02 | ** | 2 |
| | | | | S | 186 | 1.5±0.125 | 1.4±0.32 | | 1.09±0.27 | | 0.47±0.1 | * | 0.2±0.02 | ** | 2 |

| | | | | | | | | | | | | | | | | |
|---|---|---|---|---|---|---|---|---|---|---|---|---|---|---|---|---|
| **YDR146C** | **P08153** | **SWI5** | Transcription factor that recruits Mediator and Swi/Snf complexes | | | | | | | | | | | | | |
| | | | | S | 660 | 1.01±0.1354 | 0.8±0.196 | | 0.75±0.1955 | | 0.67±0.0984 | | 0.44±0.0788 | * | 2 |
| | | | | S | 663 | 1.11±0.1097 | 0.89±0.1855 | | 0.7±0.1737 | | 0.55±0.1452 | * | 0.41±0.0265 | ** | 2 |
| | | | | S | 664 | 1.02±0.1188 | 0.83±0.1449 | | 0.77±0.1431 | | 0.58±0.1079 | * | 0.45±0.0419 | ** | 2 |
| **YDR150W** | **Q00402** | **NUM1** | Protein required for nuclear migration; component of the mitochondria-ER-cortex-ancor (MECA) | | | | | | | | | | | | | |
| | | | | S | 2542 | 0.9±0.05 | 1±0.11 | | 0.51±0.09 | | 0.45±0.115 | | 0.4±0.09 | * | 2 |
| | | | | S | 2545 | 0.9±0.05 | 1±0.11 | | 0.51±0.09 | | 0.45±0.115 | | 0.4±0.09 | * | 2 |
| **YDR182W** | **P40986** | **CDC1** | Putative mannose-ethanolamine phosphate phosphodiesterase | | | | | | | | | | | | | |
| | | | | S | 12 | 0.96±0.0841 | 0.77±0.1114 | | 0.39±0.024 | ** | 0.35±0.026 | ** | 0.36±0.04 | ** | 2 |
| | | | | T | 13 | 1±0.047 | 0.79±0.0961 | | 0.46±0.0233 | *** | 0.41±0.0426 | *** | 0.38±0.0328 | *** | 2 |
| | | | | S | 15 | 0.88±0.13 | 0.66±0.17 | | 0.27±0.005 | * | 0.25±0.005 | * | 0.28±0.005 | * | 2 |
| **YDR211W** | **P32501** | **GCD6** | Catalytic epsilon subunit of the translation initiation factor eIF2B | | | | | | | | | | | | | |
| | | | | S | 478 | 0.88±0.045 | 1.13±0.005 | * | 1.1±0.04 | | 0.76±0.11 | | 0.41±0.025 | * | 2 |
| | | | | S | 481 | 0.91±0.035 | 1.15±0.04 | * | 1.1±0.12 | | 0.76±0.135 | | 0.43±0.06 | * | 2 |
| **YDR239C** | **Q03780** | **YDR239C** | Protein of unknown function; may interact with ribosomes, based on co-purification experiments | | | | | | | | | | | | | |
| | | | | S | 257 | 1.06±0.0145 | 0.99±0.0265 | | 0.67±0.0584 | ** | 0.53±0.0233 | *** | 0.45±0.0698 | *** | 3 |
| | | | | S | 260 | 1.06±0.0145 | 0.99±0.0265 | | 0.67±0.0584 | ** | 0.53±0.0233 | *** | 0.45±0.0698 | *** | 3 |
| | | | | Y | 261 | 1.06±0.0145 | 0.99±0.0265 | | 0.67±0.0584 | ** | 0.53±0.0233 | *** | 0.45±0.0698 | *** | 3 |
| **YDR284C** | **Q05521** | **DPP1** | Diacylglycerol pyrophosphate (DGPP) phosphatase | | | | | | | | | | | | | |
| | | | | S | 285 | 0.95±0.01 | 1.1±0.32 | | 0.96±0.27 | | 0.94±0.285 | | 0.5±0.105 | * | 1 |
| **YDR293C** | **P24276** | **SSD1** | Translational repressor with a role in polar growth and wall integrity | | | | | | | | | | | | | |
| | | | | S | 152 | 1.15±0.1179 | 0.98±0.1644 | | 0.64±0.0657 | * | 0.56±0.1466 | * | 0.49±0.0361 | ** | 2 |
| | | | | S | 154 | 1.07±0.015 | 1.06±0.05 | | 0.75±0.04 | * | 0.71±0.035 | ** | 0.49±0.07 | * | 2 |
| | | | | T | 482 | 1.07±0.02 | 0.84±0.265 | | 0.65±0.215 | | 0.66±0.205 | | 0.49±0.015 | ** | 2 |
| **YDR326C** | **Q06681** | **YSP2** | Sterol-binding protein | | | | | | | | | | | | | |
| | | | | S | 574 | 1.01±0.0924 | 0.93±0.1906 | | 0.58±0.1429 | | 0.57±0.1002 | * | 0.43±0.1733 | * | 2 |
| **YDR333C** | **Q05468** | **RQC1** | Component of the ribosome quality control complex (RQC) | | | | | | | | | | | | | |
| | | | | T | 158 | 1±0.0643 | 1.19±0.122 | | 0.88±0.03 | | 0.77±0.1364 | | 0.48±0.0498 | ** | 2 |
| | | | | S | 160 | 1±0.0617 | 1.19±0.122 | | 0.88±0.0318 | | 0.77±0.1375 | | 0.48±0.0561 | ** | 2 |
| | | | | S | 166 | 0.94±0.02 | 1.19±0.135 | | 0.77±0.02 | * | 0.69±0.165 | | 0.44±0.175 | | 2 |
| **YDR348C** | **Q05518** | **PAL1** | Protein of unknown function thought to be involved in endocytosis | | | | | | | | | | | | | |
| | | | | T | 436 | 1±0.005 | 0.92±0.08 | | 0.72±0.105 | | 0.58±0.12 | | 0.31±0.035 | ** | 2 |

| | | | | | | | | | | | | | | | |
|---|---|---|---|---|---|---|---|---|---|---|---|---|---|---|---|
| | | | | S | 439 | 1±0.005 | 0.92±0.08 | | 0.72±0.105 | | 0.58±0.12 | | 0.31±0.035 | ** | 2 |
| **YDR379W** | **Q06407** | **RGA2** | GTPase-activating protein for polarity-establishment protein Cdc42p | | | | | | | | | | | | |
| | | | | S | 702 | 1.06±0.1007 | 0.91±0.0945 | | 0.69±0.1473 | | 0.59±0.07 | * | 0.45±0.0933 | * | 2 |
| | | | | S | 763 | 1±0.1501 | 0.86±0.1884 | | 0.79±0.2875 | | 0.66±0.1671 | | 0.47±0.0698 | * | 3 |
| | | | | S | 770 | 1±0.1501 | 0.86±0.1884 | | 0.79±0.2875 | | 0.66±0.1671 | | 0.47±0.0698 | * | 3 |
| | | | | S | 772 | 1.04±0.08 | 0.85±0.12 | | 0.77±0.21 | | 0.598±0.11 | | 0.53±0.05 | * | 3 |
| **YDR451C** | **Q04116** | **YDR451C** | Homeobox transcriptional repressor | | | | | | | | | | | | |
| | | | | S | 315 | 1.15±0.117 | 0.88±0.0406 | | 1.11±0.0971 | | 0.99±0.102 | | 0.42±0.0067 | ** | 2 |
| | | | | S | 325 | 1.1±0.1431 | 0.88±0.0406 | | 1.02±0.0754 | | 0.85±0.117 | | 0.47±0.04 | * | 2 |
| **YDR475C** | **Q03361** | **JIP4** | Protein of unknown function | | | | | | | | | | | | |
| | | | | S | 48 | 1.2±0.0214 | 0.79±0.1198 | * | 0.32±0.0595 | *** | 0.19±0.0465 | *** | 0.17±0.0202 | *** | 2 |
| | | | | S | 55 | 1.27±0.105 | 0.61±0.025 | * | 0.22±0.065 | * | 0.13±0.03 | ** | 0.1±0.03 | ** | 2 |
| | | | | S | 804 | 1.15±0.0633 | 0.73±0.1642 | | 0.25±0.0291 | *** | 0.21±0.05 | *** | 0.17±0.0338 | *** | 2 |
| | | | | S | 807 | 1.15±0.0633 | 0.73±0.1642 | | 0.25±0.0291 | *** | 0.21±0.05 | *** | 0.17±0.0338 | *** | 2 |
| **YDR505C** | **P50896** | **PSP1** | Asn and gln rich protein of unknown function | | | | | | | | | | | | |
| | | | | S | 31 | 1.1±0.095 | 0.77±0.085 | | 0.37±0.05 | * | 0.3±0.025 | * | 0.36±0.085 | * | 2 |
| | | | | S | 34 | 1.1±0.095 | 0.77±0.085 | | 0.39±0.025 | * | 0.33±0.015 | * | 0.45±0 | * | 2 |
| **YDR507C** | **Q12263** | **GIN4** | Protein kinase involved in bud growth and assembly of the septin ring | | | | | | | | | | | | |
| | | | | S | 384 | 0.98±0.0219 | 0.96±0.0674 | | 0.83±0.0677 | | 0.61±0.0651 | ** | 0.33±0.0088 | *** | 3 |
| | | | | S | 385 | 1.1±0.02 | 0.98±0.055 | | 0.84±0.035 | * | 0.66±0.155 | | 0.39±0.08 | * | 2 |
| | | | | S | 483 | 0.88±0.0694 | 0.91±0.0474 | | 0.7±0.0337 | | 0.52±0.0196 | ** | 0.41±0.0805 | ** | 2 |
| | | | | S | 486 | 1±0.04 | 0.97±0.1 | | 0.69±0.11 | | 0.49±0.04 | * | 0.38±0.19 | | 2 |
| **YDR508C** | **P48813** | **GNP1** | High-affinity glutamine permease | | | | | | | | | | | | |
| | | | | S | 124 | 0.75±0.0287 | 0.87±0.1415 | | 0.48±0.0286 | *** | 0.37±0.0598 | ** | 0.3±0.0745 | ** | 2 |
| | | | | Y | 125 | 0.78±0.0536 | 0.93±0.1729 | | 0.51±0.0267 | * | 0.37±0.0318 | ** | 0.24±0.0633 | ** | 2 |
| | | | | T | 127 | 0.74±0.033 | 0.87±0.1329 | | 0.49±0.016 | *** | 0.39±0.0248 | *** | 0.32±0.0531 | *** | 2 |
| **YEL032W** | **P24279** | **MCM3** | Protein involved in DNA replication | | | | | | | | | | | | |
| | | | | S | 761 | 0.95±0.0296 | 0.97±0.0318 | | 1.01±0.0617 | | 0.72±0.0481 | * | 0.29±0.0481 | *** | 2 |
| | | | | S | 765 | 0.95±0.0296 | 0.97±0.0318 | | 1.01±0.0617 | | 0.72±0.0481 | * | 0.29±0.0481 | *** | 2 |
| | | | | S | 777 | 0.93±0.0176 | 0.92±0.1626 | | 0.85±0.167 | | 0.71±0.1255 | | 0.49±0.085 | ** | 2 |
| **YER024W** | **P40017** | **YAT2** | Carnitine acetyltransferase; has similarity to Yat1p | | | | | | | | | | | | |
| | | | | S | 813 | 0.78±0.0821 | 0.77±0.2255 | | 0.48±0.0826 | * | 0.45±0.0563 | * | 0.7±0.031 | | 2 |
| **YER032W** | **P40020** | **FIR1** | Protein involved in 3' mRNA processing | | | | | | | | | | | | |

| | | | | | | | | | | | | | | | | |
|---|---|---|---|---|---|---|---|---|---|---|---|---|---|---|---|---|
| | | | | S | 2 | 1.19±0.09 | 0.94±0.175 | | 0.9±0.03 | | 0.7±0.02 | * | 0.34±0.08 | * | 2 |
| | | | | T | 6 | 1.19±0.09 | 0.94±0.175 | | 0.9±0.03 | | 0.7±0.02 | * | 0.34±0.08 | * | 2 |
| **YER070W** | **P21524** | **RNR1** | Major isoform of large subunit of ribonucleotide-diphosphate reductase | | | | | | | | | | | | | |
| | | | | S | 816 | 0.96±0.025 | 0.41±0.095 | * | 0.8±0.255 | | 0.62±0.075 | * | 0.68±0.115 | | 2 |
| | | | | S | 824 | 0.96±0.025 | 0.41±0.095 | * | 0.8±0.255 | | 0.62±0.075 | * | 0.68±0.115 | | 2 |
| **YER111C** | **P25302** | **SWI4** | DNA binding component of the SBF complex (Swi4p-Swi6p) | | | | | | | | | | | | | |
| | | | | T | 798 | 0.93±0.0328 | 0.85±0.0498 | | 0.79±0.0829 | | 0.78±0.0874 | | 0.48±0.0869 | ** | 2 |
| **YFL004W** | **P43585** | **VTC2** | Regulatory subunit of the vacuolar transporter chaperone (VTC) complex | | | | | | | | | | | | | |
| | | | | S | 193 | 1.17±0.0448 | 0.98±0.0586 | | 0.78±0.0231 | ** | 0.48±0.0426 | *** | 0.34±0.0406 | *** | 2 |
| | | | | S | 196 | 1.17±0.0448 | 0.98±0.0586 | | 0.78±0.0231 | ** | 0.48±0.0426 | *** | 0.34±0.0406 | *** | 2 |
| **YFL005W** | **P07560** | **SEC4** | Rab family GTPase | | | | | | | | | | | | | |
| | | | | S | 8 | 1.21±0.14 | 0.96±0.16 | | 0.51±0.06 | * | 0.49±0.025 | * | 0.4±0.11 | * | 2 |
| | | | | S | 11 | 1.21±0.14 | 0.96±0.16 | | 0.51±0.06 | * | 0.49±0.025 | * | 0.4±0.11 | * | 2 |
| | | | | S | 201 | 0.96±0.05 | 0.96±0.09 | | 0.78±0.02 | | 0.41±0.065 | * | 0.46±0.085 | * | 2 |
| | | | | S | 204 | 0.96±0.05 | 0.93±0.055 | | 0.78±0.02 | | 0.38±0.04 | * | 0.44±0.065 | * | 2 |
| | | | | S | 206 | 0.98±0.075 | 0.91±0.075 | | 0.81±0.045 | | 0.38±0.035 | * | 0.44±0.06 | * | 2 |
| **YFL026W** | **D6VTK4** | **STE2** | Receptor for alpha-factor pheromone | | | | | | | | | | | | | |
| | | | | S | 339 | 0.95±0.04 | 0.92±0.1 | | 0.67±0.01 | * | 0.6±0.07 | * | 0.48±0.025 | ** | 2 |
| | | | | S | 360 | 0.89±0.0551 | 1.02±0.3381 | | 0.53±0.0115 | ** | 0.44±0.0851 | * | 0.47±0.1168 | * | 3 |
| | | | | S | 366 | 0.89±0.0551 | 1.02±0.3381 | | 0.53±0.0115 | ** | 0.44±0.0851 | * | 0.47±0.1168 | * | 3 |
| | | | | T | 368 | 0.91±0.0351 | 1.03±0.3494 | | 0.52±0.0208 | *** | 0.41±0.0529 | ** | 0.46±0.1192 | * | 3 |
| **YFL042C** | **P43560** | **LAM5** | Putative sterol transfer protein | | | | | | | | | | | | | |
| | | | | S | 140 | 1.07±0.06 | 1.03±0.05 | | 0.79±0.04 | ** | 0.68±0.05 | * | 0.46±0.05 | *** | 3 |
| | | | | T | 143 | 1.06±0.0606 | 1.06±0.0669 | | 0.75±0.0088 | ** | 0.59±0.0874 | * | 0.44±0.0186 | *** | 3 |
| | | | | S | 149 | 1.02±0.06 | 1.00±0.04 | | 0.79±0.06 | ** | 0.64±0.05 | * | 0.43±0.03 | *** | 3 |
| **YFR053C** | **P04806** | **HXK1** | Hexokinase isoenzyme 1 | | | | | | | | | | | | | |
| | | | | S | 15 | 0.92±0.0465 | 0.99±0.2527 | | 0.83±0.1234 | | 0.44±0.0657 | *** | 0.51±0.07 | ** | 1 |
| **YGL008C** | **P05030** | **PMA1** | Plasma membrane P2-type H+-ATPase | | | | | | | | | | | | | |
| | | | | S | 911 | 1.24±0.09 | 0.75±0.105 | | 0.58±0.25 | | 0.49±0.22 | | 0.61±0.065 | * | 1 |
| **YGL021W** | **P43633** | **ALK1** | Protein kinase; along with its paralog, ALK2 | | | | | | | | | | | | | |
| | | | | S | 354 | 0.95±0.08 | 0.89±0.06 | | 0.69±0.045 | | 0.6±0.05 | | 0.39±0.005 | * | 2 |
| **YGL023C** | **P53191** | **PIB2** | Protein of unknown function; contains FYVE domain; similar to Fab1 and Vps27 | | | | | | | | | | | | | |
| | | | | T | 52 | 1.14±0.026 | 0.82±0.1784 | | 0.76±0.2624 | | 0.52±0.1931 | * | 0.45±0.0694 | *** | 2 |

| | | | | | | | | | | | | | | | |
|---|---|---|---|---|---|---|---|---|---|---|---|---|---|---|---|
| | | | | T | 56 | 1.13±0.0318 | 0.82±0.1774 | | 0.77±0.2663 | | 0.5±0.1828 | * | 0.43±0.0524 | *** | 2 |
| **YGL035C** | **P27705** | **MIG1** | Transcription factor involved in glucose repression | | | | | | | | | | | | |
| | | | | S | 311 | 1.12±0.0392 | 0.84±0.0413 | ** | 0.54±0.0566 | *** | 0.48±0.1237 | ** | 0.48±0.1184 | ** | 2 |
| | | | | S | 314 | 1.13±0.0349 | 0.84±0.043 | ** | 0.55±0.0585 | *** | 0.49±0.1223 | ** | 0.49±0.1167 | ** | 2 |
| **YGL056C** | **P53172** | **SDS23** | Protein involved in cell separation during budding | | | | | | | | | | | | |
| | | | | S | 46 | 1.09±0.1788 | 0.9±0.1633 | | 0.87±0.3353 | | 0.47±0.2036 | | 0.45±0.0931 | * | 2 |
| **YGL197W** | **P53094** | **MDS3** | Putative component of the TOR regulatory pathway | | | | | | | | | | | | |
| | | | | S | 693 | 1.1±0.0721 | 0.75±0.1338 | | 0.74±0.2034 | | 0.49±0.057 | ** | 0.72±0.0722 | * | 2 |
| | | | | S | 698 | 1.1±0.0721 | 0.75±0.1338 | | 0.74±0.2034 | | 0.49±0.057 | ** | 0.72±0.0722 | * | 2 |
| **YGL253W** | **P04807** | **HXK2** | Hexokinase isoenzyme 2 | | | | | | | | | | | | |
| | | | | S | 15 | 1±0.0938 | 0.78±0.0601 | | 0.73±0.1158 | | 0.44±0.0405 | ** | 0.56±0.0414 | ** | 1 |
| **YGR116W** | **P23615** | **SPT6** | Nucleosome remodeling protein | | | | | | | | | | | | |
| | | | | S | 148 | 1.1±0.09 | 0.96±0.01 | | 0.88±0.115 | | 0.81±0.075 | | 0.49±0.1 | * | 3 |
| | | | | S | 155 | 1.12±0.07 | 0.98±0.005 | | 0.86±0.1 | | 0.81±0.07 | | 0.49±0.1 | * | 3 |
| **YGR130C** | **P53278** | **YGR130C** | Component of the eisosome with unknown function | | | | | | | | | | | | |
| | | | | S | 347 | 0.85±0.05 | 0.8±0.175 | | 0.64±0.085 | | 0.41±0.02 | * | 0.43±0.01 | * | 2 |
| **YGR196C** | **P46949** | **FYV8** | Protein of unknown function; required for survival upon exposure to K1 killer toxin | | | | | | | | | | | | |
| | | | | S | 92 | 1.05±0.0866 | 1.03±0.0603 | | 0.66±0.1266 | | 0.51±0.1311 | * | 0.37±0.0463 | ** | 2 |
| | | | | Y | 98 | 1.07±0.0437 | 1.02±0.0176 | | 0.62±0.0808 | ** | 0.52±0.0784 | ** | 0.33±0.024 | *** | 2 |
| | | | | S | 100 | 1.13±0.0436 | 1.05±0.0513 | | 0.58±0.0463 | *** | 0.4±0.024 | *** | 0.28±0.0463 | *** | 2 |
| | | | | S | 301 | 1.12±0.085 | 0.9±0.515 | | 0.45±0.235 | | 0.24±0.145 | * | 0.3±0.04 | * | 2 |
| **YGR202C** | **P13259** | **PCT1** | Cholinephosphate cytidylyltransferase | | | | | | | | | | | | |
| | | | | S | 16 | 1.46±0.02 | 1.31±0.135 | | 0.71±0.24 | | 0.47±0 | *** | 0.66±0.065 | ** | 2 |
| | | | | S | 21 | 1.46±0.02 | 1.31±0.135 | | 0.71±0.24 | | 0.47±0 | *** | 0.66±0.065 | ** | 2 |
| **YGR229C** | **P32566** | **SMI1** | Protein involved in the regulation of cell wall synthesis | | | | | | | | | | | | |
| | | | | S | 394 | 1.07±0.0058 | 1.05±0.1533 | | 0.64±0.0981 | * | 0.53±0.1299 | * | 0.48±0.0551 | *** | 3 |
| **YGR237C** | **P50089** | **YGR237C** | Putative protein of unknown function | | | | | | | | | | | | |
| | | | | S | 123 | 0.92±0.0393 | 0.85±0.2689 | | 0.57±0.1245 | | 0.46±0.0338 | *** | 0.85±0.1317 | | 2 |
| | | | | S | 708 | 0.74±0.06 | 0.83±0.23 | | 0.25±0.07 | * | 0.12±0.04 | * | 0.09±0.01 | ** | 2 |
| | | | | S | 712 | 0.74±0.06 | 0.83±0.23 | | 0.25±0.07 | * | 0.12±0.04 | * | 0.09±0.01 | ** | 2 |
| **YHL007C** | **Q03497** | **STE20** | Cdc42p-activated signal transducing kinase | | | | | | | | | | | | |
| | | | | S | 226 | 1.02±0.03 | 0.85±0.085 | | 0.66±0.025 | * | 0.52±0.01 | ** | 0.41±0.005 | ** | 2 |
| | | | | S | 228 | 0.98±0.0467 | 0.89±0.0584 | | 0.68±0.026 | ** | 0.5±0.024 | *** | 0.35±0.0551 | *** | 2 |

| | | | | | | | | | | | | | | | |
|---|---|---|---|---|---|---|---|---|---|---|---|---|---|---|---|
| | | | | S | 289 | 0.82±0.02 | 1.03±0.02 | * | 0.62±0.045 | | 0.58±0.04 | * | 0.36±0.015 | ** | 1 |
| **YHR016C** | **P32793** | **YSC84** | Actin-binding protein; involved in bundling of actin filaments and endocytosis of actin cortical patches | | | | | | | | | | | | |
| | | | | S | 274 | 0.93±0.0935 | 0.79±0.0176 | | 0.61±0.0321 | * | 0.49±0.0895 | * | 0.34±0.085 | ** | 1 |
| **YHR052W** | **P38779** | **CIC1** | Essential protein that interacts with proteasome components | | | | | | | | | | | | |
| | | | | S | 7 | 1.04±0.0273 | 1.01±0.3995 | | 0.59±0.2596 | | 1±0.3884 | | 0.32±0.0448 | *** | 3 |
| | | | | T | 11 | 1.04±0.0273 | 1.01±0.3995 | | 0.59±0.2596 | | 1±0.3884 | | 0.32±0.0448 | *** | 3 |
| | | | | S | 14 | 0.99±0.015 | 0.65±0.3 | | 0.54±0.44 | | 0.73±0.47 | | 0.29±0.01 | *** | 3 |
| | | | | T | 15 | 1.08±0.0736 | 1.01±0.4023 | | 0.59±0.2627 | | 1±0.3916 | | 0.32±0.0498 | *** | 3 |
| **YHR154W** | **P38850** | **RTT107** | Protein implicated in Mms22-dependent DNA repair during S phase | | | | | | | | | | | | |
| | | | | S | 593 | 0.91±0.105 | 0.99±0.035 | | 0.91±0.085 | | 0.81±0.07 | | 0.42±0.02 | * | 2 |
| | | | | S | 596 | 0.74±0.01 | 1.11±0.065 | * | 0.94±0.12 | | 0.64±0.085 | | 0.45±0.125 | | 2 |
| | | | | T | 599 | 0.83±0.0717 | 1.05±0.0636 | | 0.92±0.0536 | | 0.69±0.0698 | | 0.42±0.0493 | ** | 2 |
| **YHR159W** | **P38854** | **TDA11** | Putative protein of unknown function | | | | | | | | | | | | |
| | | | | S | 263 | 1.06±0.0306 | 0.98±0.0684 | | 1±0.1472 | | 0.77±0.07 | * | 0.49±0.1041 | ** | 2 |
| | | | | S | 266 | 1.16±0.035 | 1.03±0.015 | | 0.99±0.015 | * | 0.92±0.085 | | 0.4±0.11 | * | 2 |
| **YHR164C** | **P38859** | **DNA2** | Tripartite DNA replication factor | | | | | | | | | | | | |
| | | | | S | 236 | 1.08±0.1117 | 1.02±0.0285 | | 0.97±0.0549 | | 0.78±0.0441 | | 0.47±0.0451 | ** | 2 |
| | | | | S | 237 | 1.08±0.1117 | 1.02±0.0285 | | 0.97±0.0549 | | 0.78±0.0441 | | 0.47±0.0451 | ** | 2 |
| **YHR182W** | **P38870** | **YHR182W** | Protein of unknown function | | | | | | | | | | | | |
| | | | | T | 763 | 0.96±0.045 | 0.78±0.115 | | 0.75±0.255 | | 0.62±0.13 | | 0.39±0.12 | * | 2 |
| **YIL105C** | **P40485** | **SLM1** | Phosphoinositide PI4,5P(2) binding protein, forms a complex with Slm2p | | | | | | | | | | | | |
| | | | | T | 149 | 0.91±0 | 0.93±0.17 | | 0.45±0.015 | ** | 0.28±0.01 | *** | 0.28±0 | | 3 |
| | | | | S | 150 | 0.91±0 | 0.93±0.17 | | 0.45±0.015 | ** | 0.28±0.01 | *** | 0.28±0 | | 3 |
| | | | | S | 153 | 0.91±0 | 0.94±0.165 | | 0.46±0.01 | *** | 0.28±0.01 | *** | 0.28±0.005 | *** | 3 |
| | | | | T | 642 | 1.05±0.1 | 0.97±0.09 | | 0.88±0.065 | | 0.71±0.02 | | 0.39±0.075 | * | 2 |
| **YIL115C** | **P40477** | **NUP159** | FG-nucleoporin component of central core of the nuclear pore complex | | | | | | | | | | | | |
| | | | | S | 940 | 1.2±0.09 | 0.81±0.055 | | 0.57±0.05 | * | 0.49±0.075 | * | 0.63±0.075 | * | 2 |
| | | | | S | 945 | 1.2±0.09 | 0.81±0.055 | | 0.57±0.05 | * | 0.49±0.075 | * | 0.63±0.075 | * | 2 |
| **YIL140W** | **P38928** | **AXL2** | Integral plasma membrane protein | | | | | | | | | | | | |
| | | | | S | 685 | 0.95±0.06 | 0.81±0.04 | | 0.82±0.02 | | 0.51±0.1 | | 0.46±0.09 | * | 3 |
| | | | | T | 688 | 0.95±0.06 | 0.81±0.04 | | 0.82±0.02 | | 0.51±0.1 | | 0.46±0.09 | * | 3 |
| | | | | T | 691 | 0.95±0.06 | 0.81±0.04 | | 0.82±0.02 | | 0.51±0.1 | | 0.46±0.09 | * | 3 |
| **YIR010W** | **P40568** | **DSN1** | | | | | | | | | | | | | |

| | | | | | | | | | | | | | | | |
|---|---|---|---|---|---|---|---|---|---|---|---|---|---|---|---|
| | | | | T | 380 | 1.13±0.085 | 0.94±0.225 | | 0.7±0.01 | * | 0.47±0.04 | * | 0.29±0.045 | * | 2 |
| | | | | T | 386 | 1.13±0.085 | 0.94±0.225 | | 0.7±0.01 | * | 0.47±0.04 | * | 0.29±0.045 | * | 2 |
| **YJL112W** | **P47025** | **MDV1** | Peripheral protein of cytosolic face of mitochondrial outer membrane; required for mitochondrial fission | | | | | | | | | | | | |
| | | | | S | 337 | 1.23±0.185 | 0.88±0.155 | | 0.93±0.06 | | 0.66±0.175 | | 0.09±0.09 | * | 2 |
| **YJR060W** | **P17106** | **CBF1** | Basic helix-loop-helix (bHLH) protein | | | | | | | | | | | | |
| | | | | S | 45 | 1.04±0.1446 | 1.11±0.0628 | | 1±0.1061 | | 0.67±0.0446 | * | 0.36±0.0761 | ** | 2 |
| | | | | S | 48 | 1.04±0.1407 | 1.1±0.0652 | | 1.01±0.0999 | | 0.66±0.0466 | * | 0.36±0.0761 | ** | 2 |
| | | | | S | 140 | 1.13±0.0289 | 1.04±0.0696 | | 0.93±0.0561 | * | 0.81±0.0346 | ** | 0.5±0.0524 | *** | 3 |
| **YKL038W** | **P32862** | **RGT1** | Glucose-responsive transcription factor | | | | | | | | | | | | |
| | | | | S | 202 | 1.1±0.065 | 0.88±0.2 | | 0.64±0.295 | | 0.58±0.255 | | 0.49±0.095 | * | 2 |
| **YKL101W** | **P34244** | **HSL1** | Nim1p-related protein kinase | | | | | | | | | | | | |
| | | | | S | 1284 | 0.81±0.08 | 1.08±0 | | 0.92±0.025 | | 0.78±0.11 | | 0.38±0.035 | * | 2 |
| | | | | S | 1287 | 0.81±0.08 | 1.08±0 | | 0.92±0.025 | | 0.78±0.11 | | 0.38±0.035 | * | 2 |
| **YKL124W** | **P32343** | **SSH4** | Specificity factor required for Rsp5p-dependent ubiquitination | | | | | | | | | | | | |
| | | | | S | 95 | 1.24±0.07 | 0.9±0.12 | | 0.79±0.07 | * | 0.57±0.005 | * | 0.49±0.085 | * | 2 |
| **YKL204W** | **P36041** | **EAP1** | eIF4E-associated protein, competes with eIF4G for binding to eIF4E | | | | | | | | | | | | |
| | | | | T | 284 | 1.23±0.015 | 0.91±0.165 | | 0.46±0.06 | ** | 0.36±0.045 | ** | 0.51±0.02 | ** | 2 |
| **YKL217W** | **P36035** | **JEN1** | Monocarboxylate/proton symporter of the plasma membrane | | | | | | | | | | | | |
| | | | | S | 11 | 1.57±0.27 | 1±0.04 | | 0.82±0.01 | | 0.14±0.025 | * | 0.29±0.295 | | 2 |
| **YKR093W** | **P32901** | **PTR2** | Integral membrane peptide transporter | | | | | | | | | | | | |
| | | | | S | 594 | 1±0.0371 | 0.84±0.0956 | | 0.79±0.0984 | | 0.64±0.0779 | ** | 0.47±0.0544 | *** | 2 |
| | | | | S | 597 | 0.99±0.0394 | 0.82±0.077 | | 0.79±0.0984 | | 0.62±0.0613 | ** | 0.48±0.0569 | *** | 2 |
| **YLL013C** | **Q07807** | **PUF3** | Protein of the mitochondrial outer surface | | | | | | | | | | | | |
| | | | | S | 86 | 1.02±0.0323 | 0.91±0.0588 | | 0.74±0.0643 | ** | 0.39±0.0338 | *** | 0.41±0.0601 | *** | 2 |
| | | | | T | 89 | 1.02±0.0317 | 0.91±0.0581 | | 0.76±0.0703 | * | 0.4±0.0423 | *** | 0.43±0.0826 | *** | 2 |
| | | | | S | 210 | 1.12±0.025 | 0.97±0.015 | * | 0.77±0.05 | * | 0.54±0.02 | ** | 0.45±0.11 | * | 3 |
| | | | | T | 213 | 1.12±0.025 | 0.97±0.015 | * | 0.77±0.05 | * | 0.54±0.02 | ** | 0.45±0.11 | * | 3 |
| | | | | T | 216 | 1.12±0.025 | 0.97±0.015 | * | 0.77±0.05 | * | 0.54±0.02 | ** | 0.45±0.11 | * | 3 |
| **YLL021W** | **P23201** | **SPA2** | Component of the polarisome; functions in actin cytoskeletal organization during polarized growth; | | | | | | | | | | | | |
| | | | | S | 575 | 0.96±0.02 | 1.19±0.215 | | 1.38±0.06 | * | 0.93±0.08 | | 0.5±0.005 | ** | 2 |
| | | | | S | 585 | 0.96±0.02 | 1.19±0.215 | | 1.38±0.06 | * | 0.93±0.08 | | 0.5±0.005 | ** | 2 |
| **YLL048C** | **P32386** | **YBT1** | Transporter of the ATP-binding cassette (ABC) family | | | | | | | | | | | | |

| | | | | | | | | | | | | | | | |
|---|---|---|---|---|---|---|---|---|---|---|---|---|---|---|---|
| | | | | S | 952 | 1.07±0.0352 | 0.86±0.0342 | ** | 0.55±0.0202 | *** | 0.44±0.0492 | *** | 0.58±0.0622 | *** | 2 |
| | | | | S | 955 | 1.11±0.0573 | 0.86±0.0342 | ** | 0.53±0.0352 | *** | 0.42±0.0652 | *** | 0.58±0.0684 | *** | 2 |
| | | | | S | 957 | 1.13±0.01 | 0.83±0.025 | ** | 0.5±0.015 | *** | 0.35±0.03 | ** | 0.5±0.085 | * | 2 |
| **YLR138W** | **Q99271** | **NHA1** | Na+/H+ antiporter | | | | | | | | | | | | |
| | | | | T | 765 | 0.98±0.0733 | 0.93±0.1982 | | 0.47±0.0381 | *** | 0.42±0.0491 | *** | 0.42±0.0256 | *** | 2 |
| | | | | T | 767 | 0.97±0.0685 | 0.94±0.1942 | | 0.48±0.0522 | ** | 0.41±0.0613 | *** | 0.42±0.0357 | *** | 2 |
| | | | | S | 768 | 1.01±0.07 | 0.83±0.06 | | 0.58±0.025 | * | 0.53±0.02 | * | 0.47±0.035 | * | 2 |
| **YLR177W** | **Q06251** | **YLR177W** | Putative protein of unknown function | | | | | | | | | | | | |
| | | | | S | 31 | 0.88±0.035 | 0.89±0.4 | | 0.43±0.095 | * | 0.36±0.055 | * | 0.54±0.045 | * | 2 |
| | | | | S | 34 | 0.88±0.035 | 0.89±0.4 | | 0.43±0.095 | * | 0.36±0.055 | * | 0.54±0.045 | * | 2 |
| **YLR182W** | **P09959** | **SWI6** | Transcription cofactor | | | | | | | | | | | | |
| | | | | S | 170 | 1.38±0.075 | 0.88±0.05 | * | 0.8±0.06 | * | 0.86±0.235 | | 0.49±0.13 | * | 2 |
| **YLR187W** | **Q06315** | **SKG3** | Protein of unknown function | | | | | | | | | | | | |
| | | | | S | 6 | 0.9±0.0657 | 0.88±0.0674 | | 0.84±0.1397 | | 1.1±0.2926 | | 0.46±0.0681 | ** | 2 |
| | | | | S | 10 | 0.9±0.0657 | 0.88±0.0674 | | 0.84±0.1397 | | 1.1±0.2926 | | 0.46±0.0681 | ** | 2 |
| | | | | S | 694 | 0.92±0.07 | 0.97±0.02 | | 0.53±0.03 | * | 0.44±0.04 | *** | 0.31±0.02 | ** | 3 |
| | | | | S | 701 | 0.91±0.09 | 0.99±0.03 | | 0.61±0.08 | * | 0.56±0.13 | *** | 0.42±0.05 | ** | 3 |
| | | | | S | 709 | 0.97±0.06 | 0.98±0.016 | | 0.56±0.05 | * | 0.46±0.06 | *** | 0.39±0.06 | ** | 3 |
| **YLR206W** | **Q05785** | **ENT2** | Epsin-like protein required for endocytosis and actin patch assembly | | | | | | | | | | | | |
| | | | | S | 167 | 1.08±0.03 | 0.83±0.13 | | 0.53±0.08 | * | 0.55±0.12 | | 0.51±0.08 | * | 3 |
| | | | | S | 172 | 1.11±0.055 | 0.84±0.2 | | 0.58±0.1 | * | 0.52±0.13 | | 0.41±0.14 | * | 3 |
| | | | | S | 173 | 1.11±0.055 | 0.84±0.2 | | 0.58±0.1 | * | 0.52±0.13 | | 0.41±0.14 | * | 3 |
| **YLR248W** | **P38623** | **RCK2** | Protein kinase involved in response to oxidative and osmotic stress | | | | | | | | | | | | |
| | | | | S | 46 | 1.13±0.115 | 1±0.05 | | 1.04±0.07 | | 0.48±0.035 | * | 0.59±0.145 | | 2 |
| **YLR257W** | **Q06146** | **YLR257W** | Protein of unknown function | | | | | | | | | | | | |
| | | | | S | 66 | 1.15±0.057 | 0.83±0.1986 | | 0.42±0.0524 | *** | 0.39±0.0839 | ** | 0.51±0.0698 | ** | 2 |
| | | | | Y | 67 | 1.23±0.17 | 1.07±0.445 | | 0.31±0.07 | * | 0.31±0.09 | * | 0.36±0.08 | * | 2 |
| | | | | T | 68 | 1.09±0.0167 | 0.71±0.085 | * | 0.55±0.0971 | ** | 0.41±0.0788 | ** | 0.58±0.0581 | ** | 2 |
| | | | | S | 69 | 1.06±0.045 | 0.66±0.005 | * | 0.44±0.025 | ** | 0.56±0.045 | * | 0.72±0.025 | * | 2 |
| **YLR314C** | **P32457** | **CDC3** | Component of the septin ring that is required for cytokinesis | | | | | | | | | | | | |
| | | | | S | 2 | 1.06±0.055 | 0.71±0.25 | | 0.57±0.285 | | 0.47±0.18 | | 0.56±0.065 | * | 2 |
| | | | | S | 9 | 1.06±0.055 | 0.71±0.25 | | 0.57±0.285 | | 0.47±0.18 | | 0.56±0.065 | * | 2 |
| **YLR413W** | **Q06689** | **INA1** | Protein of unknown function; not an essential gene | | | | | | | | | | | | |

| | | | | | | | | | | | | | | | |
|---|---|---|---|---|---|---|---|---|---|---|---|---|---|---|---|
| | | | | S | 657 | 0.94±0.1189 | 1.11±0.2987 | | 0.59±0.1466 | | 0.59±0.0433 | | 0.42±0.115 | * | 2 |
| **YML016C** | **P26570** | **PPZ1** | Serine/threonine protein phosphatase Z, isoform of Ppz2p | | | | | | | | | | | | |
| | | | | T | 171 | 0.4±0.0878 | 1.36±0.3722 | * | 1.02±0.1703 | * | 0.71±0.1383 | | 0.57±0.0944 | | 2 |
| **YML027W** | **P34161** | **YOX1** | Homeobox transcriptional repressor | | | | | | | | | | | | |
| | | | | S | 356 | 1.05±0.02 | 0.54±0.135 | | 0.56±0.25 | | 0.36±0.005 | *** | 0.51±0.155 | | 2 |
| **YML052W** | **P54003** | **SUR7** | Plasma membrane protein | | | | | | | | | | | | |
| | | | | S | 293 | 1.14±0.1374 | 0.86±0.0528 | | 0.47±0.0633 | ** | 0.4±0.0697 | ** | 0.34±0.072 | ** | 2 |
| | | | | S | 301 | 1.14±0.1374 | 0.86±0.0528 | | 0.47±0.0633 | ** | 0.4±0.0697 | ** | 0.34±0.072 | ** | 2 |
| **YML123C** | **P25297** | **PHO84** | High-affinity inorganic phosphate (Pi) transporter | | | | | | | | | | | | |
| | | | | S | 3 | 0.9±0.1557 | 0.88±0.3312 | | 0.51±0.0869 | | 0.41±0.0689 | * | 0.43±0.0953 | | 2 |
| **YMR031C** | **Q05050** | **EIS1** | Component of the eisosome required for proper eisosome assembly | | | | | | | | | | | | |
| | | | | T | 18 | 1.01±0.075 | 0.68±0.135 | | 0.53±0.265 | | 0.29±0.095 | * | 1.16±0.675 | | 3 |
| | | | | S | 781 | 1.03±0.07 | 0.92±0.035 | | 0.84±0.165 | | 0.47±0.17 | | 0.53±0.075 | * | 2 |
| | | | | S | 791 | 0.88±0.055 | 0.79±0.03 | | 0.72±0.21 | | 0.5±0.115 | | 0.61±0.01 | * | 1 |
| **YMR086W** | **Q04279** | **SEG1** | Component of eisosome required for proper eisosome assembly | | | | | | | | | | | | |
| | | | | S | 895 | 0.94±0.0594 | 0.79±0.111 | | 0.59±0.1023 | * | 0.43±0.0384 | *** | 0.34±0.0212 | *** | 2 |
| | | | | S | 898 | 0.94±0.0594 | 0.79±0.111 | | 0.59±0.1023 | * | 0.43±0.0384 | *** | 0.34±0.0212 | *** | 2 |
| **YMR102C** | **Q03177** | **YMR102C** | Protein of unknown function | | | | | | | | | | | | |
| | | | | S | 531 | 0.9±0.07 | 0.99±0.1 | | 0.7±0.04 | | 0.46±0.04 | * | 0.42±0.045 | * | 2 |
| **YMR124W** | **P39523** | **EPO1** | Protein involved in septin-ER tethering | | | | | | | | | | | | |
| | | | | S | 649 | 1.03±0.0689 | 1±0.0557 | | 0.91±0.0722 | | 0.71±0.1002 | | 0.48±0.1179 | * | 2 |
| | | | | S | 653 | 1.03±0.0689 | 1±0.0557 | | 0.91±0.0722 | | 0.71±0.1002 | | 0.48±0.1179 | * | 2 |
| **YMR205C** | **P16862** | **PFK2** | Beta subunit of heterooctameric phosphofructokinase | | | | | | | | | | | | |
| | | | | S | 160 | 1.08±0.0492 | 0.84±0.1369 | | 0.56±0.0912 | ** | 0.41±0.0673 | *** | 0.53±0.0287 | *** | 3 |
| | | | | S | 163 | 1.06±0.03 | 0.87±0.10 | | 0.56±0.05 | ** | 0.44±0.04 | *** | 0.51±0.03 | *** | 3 |
| | | | | S | 166 | 1.10±0.04 | 0.80±0.10 | | 0.52±0.06 | ** | 0.41±0.04 | *** | 0.48±0.05 | *** | 3 |
| | | | | S | 167 | 1.08±0.04 | 0.98±0.19 | | 0.46±0.06 | *** | 0.33±0.02 | *** | 0.45±0.04 | *** | 3 |
| | | | | S | 171 | 1.02±0.05 | 0.65±0.12 | | 0.42±0.09 | * | 0.39±0.023 | ** | 0.48±0.031 | ** | 3 |
| **YMR221C** | **Q04991** | **FMP42** | Putative protein of unknown function | | | | | | | | | | | | |
| | | | | S | 238 | 1.12±0.1162 | 0.93±0.1705 | | 0.58±0.0696 | * | 0.45±0.0491 | ** | 0.32±0.0551 | ** | 2 |
| | | | | S | 249 | 1.11±0.0825 | 0.92±0.1213 | | 0.55±0.0609 | ** | 0.43±0.0418 | *** | 0.32±0.0389 | *** | 2 |
| **YMR291W** | **Q03533** | **TDA1** | Protein kinase of unknown cellular role | | | | | | | | | | | | |
| | | | | S | 380 | 1.07±0.1781 | 0.79±0.1571 | | 0.81±0.2668 | | 0.4±0.0335 | ** | 0.59±0.1153 | | 2 |

| | | | | | | | | | | | | | | | |
|---|---|---|---|---|---|---|---|---|---|---|---|---|---|---|---|
| | | | | S | 383 | 0.97±0.1068 | 1±0.0567 | | 1±0.223 | | 0.47±0.0252 | ** | 0.67±0.1102 | | 2 |
| | | | | S | 523 | 0.96±0.065 | 0.78±0.075 | | 0.6±0.035 | * | 0.31±0.075 | * | 0.45±0.105 | | 2 |
| | | | | T | 524 | 1.05±0.0669 | 0.82±0.0644 | | 0.66±0.0581 | * | 0.34±0.0393 | *** | 0.52±0.0929 | ** | 2 |
| **YMR295C** | **Q03559** | **YMR295C** | Protein of unknown function that associates with ribosomes | | | | | | | | | | | | |
| | | | | S | 11 | 0.89±0.03 | 1.03±0.10 | | 0.78±0.12 | | 0.61±0.07 | | 0.41±0.06 | * | 3 |
| | | | | T | 13 | 1.00±0.05 | 1.05±0.07 | | 0.76±0.06 | | 0.65±0.05 | | 0.42±0.05 | ** | 3 |
| | | | | S | 14 | 0.98±0.04 | 1.056±0.07 | | 0.75±0.06 | | 0.62±0.05 | | 0.41±0.04 | ** | 3 |
| **YNL047C** | **P53955** | **SLM2** | Phosphoinositide PI4,5P(2) binding protein | | | | | | | | | | | | |
| | | | | Y | 643 | 1.07±0.0874 | 0.96±0.0173 | | 0.69±0.0889 | * | 0.59±0.0176 | ** | 0.46±0.0033 | ** | 2 |
| | | | | S | 649 | 1.07±0.0874 | 0.96±0.0173 | | 0.69±0.0889 | * | 0.59±0.0176 | ** | 0.46±0.0033 | ** | 2 |
| **YNL098C** | **P01120** | **RAS2** | GTP-binding protein | | | | | | | | | | | | |
| | | | | T | 307 | 0.91±0.0416 | 0.87±0.0265 | | 0.81±0.0513 | | 0.54±0.0954 | * | 0.43±0.0513 | ** | 2 |
| | | | | S | 308 | 0.9±0.07 | 0.9±0.015 | | 0.76±0.02 | | 0.6±0.135 | | 0.48±0.02 | * | 2 |
| | | | | S | 311 | 0.91±0.0416 | 0.87±0.0265 | | 0.81±0.0513 | | 0.54±0.0954 | * | 0.43±0.0513 | ** | 2 |
| **YNL183C** | **P22211** | **NPR1** | Protein kinase | | | | | | | | | | | | |
| | | | | S | 353 | 1.01±0.0392 | 0.95±0.0928 | | 0.71±0.0829 | * | 0.47±0.0287 | *** | 0.57±0.0766 | ** | 2 |
| | | | | S | 356 | 1.09±0.02 | 0.96±0.045 | | 0.59±0.015 | ** | 0.38±0.035 | ** | 0.8±0.33 | | 2 |
| | | | | S | 357 | 1.02±0.0405 | 0.88±0.1171 | | 0.75±0.0726 | * | 0.5±0.0523 | *** | 0.57±0.0595 | *** | 2 |
| **YNL233W** | **P53858** | **BNI4** | Targeting subunit for Glc7p protein phosphatase | | | | | | | | | | | | |
| | | | | S | 46 | 1.21±0.06 | 1.13±0.02 | | 1.02±0.075 | | 0.84±0.09 | | 0.23±0.025 | ** | 2 |
| | | | | S | 49 | 1.21±0.06 | 1.13±0.02 | | 1.02±0.075 | | 0.84±0.09 | | 0.23±0.025 | ** | 2 |
| | | | | S | 500 | 0.94±0.0464 | 1.03±0.0452 | | 0.76±0.0629 | | 0.65±0.0901 | * | 0.47±0.099 | ** | 2 |
| | | | | S | 503 | 0.94±0.0464 | 1.03±0.0452 | | 0.76±0.0629 | | 0.65±0.0901 | * | 0.47±0.099 | ** | 2 |
| **YNL254C** | **P53850** | **RTC4** | protein of unknown function | | | | | | | | | | | | |
| | | | | S | 47 | 1.34±0.18 | 1.05±0.12 | | 0.74±0.015 | | 0.69±0.105 | | 0.49±0.02 | * | 2 |
| | | | | S | 53 | 1.34±0.18 | 1.05±0.12 | | 0.74±0.015 | | 0.69±0.105 | | 0.49±0.02 | * | 2 |
| **YNL271C** | **P41832** | **BNI1** | Formin; polarisome component | | | | | | | | | | | | |
| | | | | S | 75 | 1.04±0.0731 | 0.81±0.2928 | | 0.54±0.2325 | | 0.62±0.2542 | | 0.49±0.1193 | * | 2 |
| **YNL278W** | **P53836** | **CAF120** | Part of the CCR4-NOT transcriptional regulatory complex | | | | | | | | | | | | |
| | | | | S | 637 | 0.77±0.025 | 0.93±0.185 | | 0.61±0.04 | | 0.39±0.06 | * | 0.34±0.025 | ** | 3 |
| | | | | S | 640 | 0.77±0.025 | 0.93±0.185 | | 0.61±0.04 | | 0.39±0.06 | * | 0.34±0.025 | ** | 3 |
| **YNL297C** | **P48563** | **MON2** | Protein with a role in endocytosis and vacuole integrity | | | | | | | | | | | | |
| | | | | S | 567 | 0.93±0.09 | 0.95±0.05 | | 0.67±0.04 | | 0.57±0.09 | | 0.47±0.05 | * | 2 |

| | | | | | | | | | | | | | | | | |
|---|---|---|---|---|---|---|---|---|---|---|---|---|---|---|---|---|
| **YNL309W** | **P42845** | **STB1** | Protein with role in regulation of MBF-specific transcription at Start | | | | | | | | | | | | | |
| | | | | T | 99 | 0.89±0.07 | 1.18±0.27 | | 0.92±0.33 | | 0.38±0.06 | * | 0.29±0.14 | | | 2 |
| **YOL019W** | **Q08157** | **YOL019W** | Protein of unknown function | | | | | | | | | | | | | |
| | | | | S | 224 | 1.13±0.09 | 1.12±0.085 | | 0.75±0.11 | | 0.56±0.02 | * | 0.41±0.065 | * | | 2 |
| | | | | S | 232 | 1.13±0.09 | 1.12±0.085 | | 0.75±0.11 | | 0.56±0.02 | * | 0.41±0.065 | * | | 2 |
| **YOL059W** | **P41911** | **GPD2** | NAD-dependent glycerol 3-phosphate dehydrogenase | | | | | | | | | | | | | |
| | | | | S | 72 | 1.06±0.0334 | 0.89±0.0765 | | 0.61±0.0403 | *** | 0.47±0.032 | *** | 0.54±0.0524 | *** | | 2 |
| | | | | S | 75 | 1.04±0.0287 | 0.87±0.0477 | * | 0.62±0.0275 | *** | 0.47±0.0259 | *** | 0.52±0.0771 | *** | | 2 |
| **YOL109W** | **Q08245** | **ZEO1** | Peripheral membrane protein of the plasma membrane; interacts with Mid2p | | | | | | | | | | | | | |
| | | | | S | 85 | 1.29±0.2404 | 0.9±0.1138 | | 0.61±0.0547 | * | 0.45±0.1309 | * | 0.3±0.0478 | ** | | 2 |
| | | | | S | 89 | 1.29±0.2404 | 0.9±0.1138 | | 0.61±0.0547 | * | 0.45±0.1309 | * | 0.3±0.0478 | ** | | 2 |
| **YOR014W** | **P38903** | **RTS1** | B-type regulatory subunit of protein phosphatase 2A (PP2A) | | | | | | | | | | | | | |
| | | | | S | 263 | 1.19±0.115 | 1.07±0.505 | | 0.21±0.09 | * | 0.18±0.07 | * | 0.13±0.01 | * | | 2 |
| | | | | S | 264 | 1.19±0.115 | 1.07±0.505 | | 0.21±0.09 | * | 0.18±0.07 | * | 0.13±0.01 | * | | 2 |
| **YOR083W** | **Q12416** | **WHI5** | Repressor of G1 transcription; binds to SCB binding factor (SBF) at SCB target promoters in early G1 | | | | | | | | | | | | | |
| | | | | S | 88 | 1±0.06 | 0.94±0.2 | | 0.84±0.2 | | 0.73±0.29 | | 0.49±0.015 | * | | 2 |
| | | | | S | 154 | 1.14±0.0694 | 0.91±0.1411 | | 0.88±0.1044 | | 0.69±0.0924 | * | 0.48±0.0467 | ** | | 2 |
| | | | | S | 156 | 1.14±0.0694 | 0.91±0.1411 | | 0.88±0.1044 | | 0.69±0.0924 | * | 0.48±0.0467 | ** | | 2 |
| | | | | S | 161 | 1.06±0.045 | 1.15±0.115 | | 0.84±0.025 | | 0.74±0.015 | * | 0.26±0.075 | * | | 2 |
| | | | | T | 164 | 1.06±0.045 | 1.15±0.115 | | 0.84±0.025 | | 0.74±0.015 | * | 0.26±0.075 | * | | 2 |
| **YOR174W** | **Q12343** | **MED4** | Subunit of the RNA polymerase II mediator complex | | | | | | | | | | | | | |
| | | | | T | 237 | 0.99±0.0433 | 1.03±0.1 | | 0.97±0.0418 | | 0.7±0.0551 | * | 0.47±0.1 | ** | | 2 |
| | | | | S | 242 | 0.99±0.047 | 1.08±0.15 | | 0.92±0.0033 | | 0.69±0.0484 | * | 0.45±0.08 | ** | | 2 |
| **YOR178C** | **P28006** | **GAC1** | Regulatory subunit for Glc7p type-1 protein phosphatase (PP1) | | | | | | | | | | | | | |
| | | | | T | 65 | 0.98±0.005 | 0.92±0.275 | | 0.91±0.045 | | 0.44±0.09 | * | 0.61±0.16 | | | 2 |
| **YOR239W** | **Q08641** | **ABP140** | AdoMet-dependent tRNA methyltransferase and actin binding protein | | | | | | | | | | | | | |
| | | | | S | 321 | 1.12±0.0321 | 0.78±0.1659 | | 0.59±0.0517 | *** | 0.41±0.0713 | *** | 0.44±0.0593 | *** | | 2 |
| | | | | S | 326 | 1.12±0.0321 | 0.78±0.1659 | | 0.59±0.0517 | *** | 0.41±0.0713 | *** | 0.44±0.0593 | *** | | 2 |
| **YOR355W** | **P41913** | **GDS1** | Protein of unknown function; required for growth on glycerol as a carbon source | | | | | | | | | | | | | |
| | | | | T | 374 | 1.03±0.045 | 0.87±0.11 | | 0.73±0.03 | * | 0.44±0.04 | ** | 0.63±0.03 | * | | 2 |
| **YOR373W** | **P32336** | **NUD1** | Component of the spindle pole body outer plaque | | | | | | | | | | | | | |
| | | | | S | 140 | 0.93±0.02 | 0.89±0.085 | | 0.84±0.095 | | 0.97±0.065 | | 0.48±0.1 | * | | 2 |
| | | | | T | 147 | 0.93±0.02 | 0.89±0.085 | | 0.84±0.095 | | 0.97±0.065 | | 0.48±0.1 | * | | 2 |

| | | | | | | | | | | | | | | | | |
|---|---|---|---|---|---|---|---|---|---|---|---|---|---|---|---|---|
| **YPL019C** | **Q02725** | **VTC3** | Regulatory subunit of the vacuolar transporter chaperone (VTC) complex | | | | | | | | | | | | | |
| | | | | S | 195 | 1.39±0.1157 | 1.25±0.2429 | | 0.96±0.0731 | * | 0.72±0.0872 | ** | 0.47±0.1212 | ** | 2 |
| | | | | S | 198 | 1.39±0.1157 | 1.25±0.2429 | | 0.96±0.0731 | * | 0.72±0.0872 | ** | 0.47±0.1212 | ** | 2 |
| | | | | S | 589 | 0.96±0.0598 | 0.89±0.1024 | | 0.48±0.0598 | ** | 0.44±0.0404 | *** | 0.26±0.0615 | *** | 2 |
| | | | | S | 592 | 0.96±0.0598 | 0.89±0.1024 | | 0.48±0.0598 | ** | 0.44±0.0404 | *** | 0.26±0.0615 | *** | 2 |
| **YPL090C** | **P0CX37** | **RPS6A** | Protein component of the small (40S) ribosomal subunit | | | | | | | | | | | | | |
| | | | | S | 232 | 0.94±0.0412 | 0.91±0.0324 | | 0.45±0.0705 | *** | 0.27±0.0239 | *** | 0.16±0.0155 | *** | 2 |
| | | | | S | 233 | 0.94±0.0412 | 0.91±0.0324 | | 0.45±0.0705 | *** | 0.27±0.0239 | *** | 0.16±0.0155 | *** | 2 |
| **YPL115C** | **P32873** | **BEM3** | Rho GTPase activating protein (RhoGAP) | | | | | | | | | | | | | |
| | | | | S | 206 | 0.99±0.01 | 0.86±0.175 | | 0.67±0.125 | | 0.62±0.14 | | 0.47±0.07 | * | 2 |
| | | | | S | 324 | 0.87±0.0623 | 0.91±0.0186 | | 0.98±0.1568 | | 0.66±0.0418 | | 0.39±0.0462 | ** | 2 |
| | | | | S | 327 | 0.87±0.0623 | 0.91±0.0186 | | 0.98±0.1568 | | 0.66±0.0418 | | 0.39±0.0462 | ** | 2 |
| **YPL124W** | **P33419** | **SPC29** | Inner plaque spindle pole body (SPB) component | | | | | | | | | | | | | |
| | | | | S | 58 | 1.03±0.015 | 1.06±0.32 | | 0.84±0.245 | | 0.6±0.18 | | 0.31±0.155 | * | 2 |
| | | | | S | 59 | 1.01±0.04 | 1.09±0.295 | | 0.88±0.2 | | 0.57±0.21 | | 0.28±0.125 | * | 2 |
| **YPL180W** | **Q08921** | **TCO89** | Subunit of TORC1 (Tor1p or Tor2p-Kog1p-Lst8p-Tco89p) | | | | | | | | | | | | | |
| | | | | S | 40 | 0.88±0.1139 | 0.93±0.0473 | | 0.53±0.1153 | | 0.46±0.0769 | * | 0.61±0.2367 | | 2 |
| | | | | S | 43 | 0.88±0.1139 | 0.93±0.0473 | | 0.53±0.1153 | | 0.46±0.0769 | * | 0.61±0.2367 | | 2 |
| **YPL186C** | **Q08926** | **UIP4** | Protein that interacts with Ulp1p | | | | | | | | | | | | | |
| | | | | S | 205 | 1.3±0.045 | 0.79±0.355 | | 1.02±0.13 | | 0.69±0.135 | * | 0.43±0.18 | * | 1 |
| **YPL209C** | **P38991** | **IPL1** | Aurora kinase of chromosomal passenger complex | | | | | | | | | | | | | |
| | | | | S | 36 | 1.03±0.0722 | 0.87±0.1762 | | 0.88±0.2194 | | 0.86±0.1484 | | 0.48±0.0252 | ** | 2 |
| | | | | S | 38 | 1.03±0.0722 | 0.87±0.1762 | | 0.88±0.2194 | | 0.86±0.1484 | | 0.48±0.0252 | ** | 2 |
| **YPR030W** | **Q12734** | **CSR2** | Nuclear ubiquitin protein ligase binding protein | | | | | | | | | | | | | |
| | | | | T | 43 | 1.31±0.02 | 1.12±0.325 | | 0.75±0.075 | * | 0.8±0.075 | * | 0.48±0.005 | *** | 2 |
| | | | | S | 46 | 1.31±0.02 | 1.12±0.325 | | 0.75±0.075 | * | 0.8±0.075 | * | 0.48±0.005 | *** | 2 |
| | | | | S | 525 | 1.48±0.035 | 0.95±0.18 | | 0.66±0.075 | ** | 0.72±0.045 | ** | 0.42±0.03 | ** | 2 |
| | | | | S | 528 | 1.48±0.035 | 0.95±0.18 | | 0.66±0.075 | ** | 0.72±0.045 | ** | 0.42±0.03 | ** | 2 |
| **YPR055W** | **P32855** | **SEC8** | Essential 121 kDa subunit of the exocyst complex | | | | | | | | | | | | | |
| | | | | T | 1015 | 1.03±0.025 | 0.67±0.22 | | 0.35±0.145 | * | 0.3±0.15 | * | 0.32±0.06 | ** | 2 |
| **YPR072W** | **Q12514** | **NOT5** | Component of the CCR4-NOT core complex, involved in mRNA decapping | | | | | | | | | | | | | |
| | | | | S | 245 | 0.93±0.065 | 0.85±0.31 | | 0.64±0.32 | | 0.85±0.03 | | 0.41±0.035 | * | 1 |

| | | | | | | | | | | | | | | | |
|---|---|---|---|---|---|---|---|---|---|---|---|---|---|---|---|
| | | | | S | 256 | 0.9±0.0462 | 0.86±0.1009 | | 0.5±0.0775 | * | 0.68±0.0233 | * | 0.34±0.0906 | ** | 1 |
| **YPR105C** | **Q06096** | **COG4** | Essential component of the conserved oligomeric Golgi complex | | | | | | | | | | | | |
| | | | | S | 352 | 0.93±0.09 | 0.89±0.13 | | 0.71±0.105 | | 0.44±0.05 | * | 0.56±0.125 | | 2 |
| | | | | T | 356 | 0.93±0.09 | 0.89±0.13 | | 0.71±0.105 | | 0.44±0.05 | * | 0.56±0.125 | | 2 |
| **YPR124W** | **P49573** | **CTR1** | High-affinity copper transporter of plasma membrane | | | | | | | | | | | | |
| | | | | S | 344 | 0.86±0.085 | 1.24±0.505 | | 0.48±0.01 | * | 0.49±0.01 | * | 0.66±0.155 | | 2 |
| | | | | S | 349 | 0.86±0.085 | 1.24±0.505 | | 0.48±0.01 | * | 0.49±0.01 | * | 0.66±0.155 | | 2 |
| **YPR141C** | **P17119** | **KAR3** | Minus-end-directed microtubule motor | | | | | | | | | | | | |
| | | | | T | 19 | 1.02±0.035 | 0.81±0.175 | | 0.63±0.145 | | 0.69±0.13 | | 0.48±0.045 | * | 2 |
| | | | | S | 21 | 1.02±0.035 | 0.81±0.175 | | 0.63±0.145 | | 0.69±0.13 | | 0.48±0.045 | * | 2 |
| | | | | T | 38 | 1±0.025 | 0.79±0.165 | | 0.8±0.195 | | 0.63±0.075 | * | 0.48±0.05 | * | 2 |
| | | | | S | 66 | 0.99±0.08 | 1±0.005 | | 0.88±0.055 | | 0.87±0.02 | | 0.48±0.085 | * | 2 |
| | | | | S | 68 | 0.99±0.08 | 1±0.005 | | 0.88±0.055 | | 0.87±0.02 | | 0.48±0.085 | * | 2 |
| **YPR156C** | **Q06451** | **TPO3** | Polyamine transporter of the major facilitator superfamily | | | | | | | | | | | | |
| | | | | S | 124 | 0.98±0.05 | 0.9±0.02 | | 0.72±0.045 | | 0.3±0.045 | ** | 0.3±0.12 | * | 2 |
| | | | | S | 125 | 0.98±0.05 | 0.9±0.02 | | 0.72±0.045 | | 0.3±0.045 | ** | 0.3±0.12 | * | 2 |
| | | | | S | 132 | 1.13±0.105 | 0.9±0.025 | | 0.7±0.06 | | 0.43±0.085 | * | 0.41±0.005 | * | 2 |

# Annex 4

Peptide identification by Mass Spectrometry of GST-Ppz1-interacting proteins. In bold and red letter are marked the identified tryptic peptides.

**Ppz1** (AJS96320.1). Serine/threonine protein phosphatase Z.

```
  1 MGNSSSKSSK KDSHSNSSSR NPRPQVSRTE TSHSVKSAKS NKSSRSRRSL
 51 PSSSTTNTNS NVPDPSTPSK PNLEVNHQRH SSHTNRYHFP SSSHSHSNSQ
101 NELLTTPSSS STKRPSTSRR SSYNTKAAAD LPPSMIQMEP KSPILKTNNS
151 STHVSKHKSS YSSTYYENAL TDDDNDDKDN DISHTKRFSR SSNSRPSSIR
201 SGSVSRRKSD VTHEEPNNGS YSSNNQENYL VQALTRSNSH ASSLHSRKSS
251 FGSDGNTAYS TPLNSPGLSK LTDHSGEYFT SNSTSSLNHH SSRDIYPSKH
301 ISNDDDIENS SQLSNIHASM ENVNDKNNNI TDSKKDPNEE FNDIMQSSGN
351 KNAPKKFKKP IDIDETIQKL LDAGYAAKRT KNVCLKNNEI LQICIKAREI
401 FLSQPSLLEL SPPVKIVGDV HGQYGDLLRL FTKCGFPPSS NYLFLGDYVD
451 RGKQSLETIL LLFCYKIKYP ENFFLLRGNH ECANVTRVYG FYDECKRRCN
501 IKIWKTFIDT FNTLPLAAIV AGKIFCVHGG LSPVLNSMDE IRHVVRPTDV
551 PDFGLINDLL WSDPTDSPNE WEDNERGVSY CYNKVAINKF LNKFGFDLVC
601 RAHMVVEDGY EFFNDRSLVT VFSAPNYCGE FDNWGAVMSV SEGLLCSFEL
651 LDPLDSAALK QVMKKGRQER KLANQQQQMM ETSITNDNES QQ
```

**Yef3** (NP_013350.1): Translation elongation factor 3

```
  1 MSDSQQSIKV LEELFQKLSV ATADNRHEIA SEVASFLNGN IIEHDVPEHF
 51 FGELAKGIKD KKTAANAMQA VAHIANQSNL SPSVEPYIVQ LVPAICTNAG
101 NKDKEIQSVA SETLISIVNA VNPVAIKALL PHLTNAIVET NKWQEKIAIL
151 AAISAMVDAA KDQVALRMPE LIPVLSETMW DTKKEVKAAA TAAMTKATET
201 VDNKDIERFI PSLIQCIADP TEVPETVHLL GATTFVAEVT PATLSIMVPL
251 LSRGLNERET GIKRKSAVII DNMCKLVEDP QVIAPFLGKL LPGLKSNFAT
```

**301** IADPEAREVT LRALKTLRRV GNVGEDDAIP EVSHAGDVST TLQVVNELLK

**351** DETVAPRFKI VVEYIAAIGA DLIDERIIDQ QAWFTHITPY MTIFLHEKKA

**401** KDILDEFRKR AVDNIPVGPN FDDEEDEGED LCNCEFSLAY GAKILLNKTQ

**451** LRLKRARRYG ICGPNGCGKS TLMRAIANGQ VDGFPTQEEC RTVYVEHDID

**501** GTHSDTSVLD FVFESGVGTK EAIKDKLIEF GFTDEMIAMP ISALSGGWKM

**551** KLALARAVLR NADILLLDEP TNHLDTVNVA WLVNYLNTCG ITSITISHDS

**601** VFLDNVCEYI INYEGLKLRK YKGNFTEFVK KCPAAKAYEE LSNTDLEFKF

**651** PEPGYLEGVK TKQKAIVKVT NMEFQYPGTS KPQITDINFQ CSLSSRIAVI

**701** GPNGAGKSTL INVLTGELLP TSGEVYTHEN CRIAYIKQHA FAHIESHLDK

**751** TPSEYIQWRF QTGEDRETMD RANR**QINEND AEAMNKIFKI** EGTPRRIAGI

**801** HSRRKFKNTY EYECSFLLGE NIGMKSERWV PMMSVDNAWI PRGELVESHS

**851** KMVAEVDMKE ALASGQFRPL TRKEIEEHCS MLGLDPEIVS HSRIRGLSGG

**901** QKVKLVLAAG TWQRPHLIVL DEPTNYLDRD SLGALSKALK EFEGGVIIIT

**951** HSAEFTKNLT EEVWAVKDGR MTPSGHNWVS GQGAGPRIEK KEDEEDKFDA

**1001** MGNKIAGGKK KKKLSSAELR KKKKERMKK**K KELGDAYVSS DEEF**

**eEF1α** (NP_009676.1) translation elongation factor EF-1α. Product of *TEF1* or *TEF2* genes.

**1** MGKEKSHINV VVIGHVDSGK **STTTGHLIYK CGGIDKRTIE KFEK**EAAELG

**51** KGSFKYAWVL DKLKAERERG ITIDIALWKF ETPK**YQVTVI DAPGHR**DFIK

**101** NMITGTSQAD CAILIIAGGV GEFEAGISKD GQTR**EHALLA FTLGVR**QLIV

**151** AVNKMDSVK**W DESRFQEIVK** ETSNFIKKVG YNPKTVPFVP ISGWNGDNMI

**201** EATTNAPWYK GWEKETKAGV VKGKTLLEAI DAIEQPSRPT DKPLRLPLQD

**251** VYK**IGGIGTV PVGRVETGVI KPGMVVTFAP AGVTTEVKSV EMHHEQLEQG**

**301** **VPGDNVGFNV K**NVSVKEIRR GNVCGDAKND PPKGCASFNA TVIVLNHPGQ

**351** ISAGYSPVLD CHTAHIACR**F DELLEKNDRR** SGKKLEDHPK FLK**SGDAALV**

**401** **KFVPSKPMCV EAFSEYPPLG RFAVRDMRQT VAVGVIK**SVD KTEKAAKVTK

**451** AAQKAAKK

**RPL2** (NP_012246.1) Ribosomal 60S subunit protein L2A and L2B. Product of *RPL2A* or *RPL2B* genes.

```
  1 MGRVIRNQRK GAGSIFTSHT RLRQGAAKLR TLDYAERHGY IRGIVKQIVH
 51 DSGRGAPLAK VVFRDPYKYR LREEIFIANE GVHTGQFIYA GKKASLNVGN
101 VLPLGSVPEG TIVSNVEEKP GDRGALARAS GNYVIIIGHN PDENKTRVRL
151 PSGAKKVISS DARGVIGVIA GGGRVDKPLL KAGRAFHKYR LKRNSWPKTR
201 GVAMNPVDHP HGGGNHQHIG KASTISRGAV SGQKAGLIAA RRTGLLRGSQ
251 KTQD
```

**RPL13B** (NP_013862.1) Ribosomal 60S subunit protein L13B. Product of *RPL13B* gene (and *RPL13A* gene).

```
  1 MAISKNLPIL KNHFRKHWQE RVKVHFDQAG KKVSRRNARA ARAAKIAPRP
 51 LDLLRPVVRA PTVKYNRKVR AGRGFTLAEV KAAGLTAAYA RTIGIAVDHR
101 RQNRNQEIFD ANVQRLKEYQ SKIIVFPRDG KAPEAEQVLS AAATFPIAQP
151 ATDVEARAVQ DNGESAFRTL RLARSEKKFR GIREKRAREK AEAEAEKKK
```

**YDL082W.** RPL13A. Ribosomal 60S subunit protein L13A;

```
  1 MAISKNLPIL KNHFRKHWQE RVKVHFDQAG KKVSRRNARA TRAAKIAPRP
 51 LDLLRPVVRA PTVKYNRKVR AGRGFTLAEV KAAGLTAAYA RTIGIAVDHR
101 RQNRNQEIFD ANVQRLKEYQ SKIIVFPRNG KAPEAEQVLS AAATFPIAQP
151 ATDVEARAVQ DNGESAFRTL RLARSEKKFR GIREKRAREK AEAEAEKKK
```

**RPL10** (NP_013862.1) ribosomal 60S subunit protein L10. Product of *RPL10* gene.

```
  1 MARRPARCYR YQKNKPYPKS RYNRAVPDSK IRIYDLGKKK ATVDEFPLCV
 51 HLVSNELEQL SSEALEAARI CANKYMTTVS GRDAFHLRVR VHPFHVLRIN
101 KMLSCAGADR LQQGMRGAWG KPHGLAARVD IGQIIFSVRT KDSNKDVVVE
151 GLRRARYKFP GQQKIILSKK WGFTNLDRPE YLKKREAGEV KDDGAFVKFL
201 SKKGSLENNI REFPEYFAAQ A
```

**Glutathione S-transferase of *Schistosoma Japonicum*** (1GNE_A)

```
  1 SPILGYWKIK GLVQPTRLLL EYLEEKYEEH LYERDEGDKW RNKKFELGLE
 51 FPNLPYYIDG DVKLTQSMAI IRYIADKHNM LGGCPKERAE ISMLEGAVLD
101 IRYGVSRIAY SKDFETLKVD FLSKLPEMLK MFEDRLCHKT YLNGDHVTHP
151 DFMLYDALDV VLYMDPMCLD AFPKLVCFKK RIEAIPQIDK YLKSSKYIAW
201 PLQGWQATFG GGDHPPKSDL VPRGSMELDK WA
```